FERMILAB-Conf-98/064

Contributions to the Mini-Workshop On Beam-Beam Compensation

Fermilab, 12-13 February 1998

Compilation, editing, preface and report
By Vladimir SHILTSEV

February 1998

Disclaimer

This report was prepared as an account of work sponsored by an agency of the United States Government. Neither the United States Government nor any agency thereof, nor any of their employees, makes any warranty, express or implied, or assumes any legal liability or responsibility for the accuracy, completeness, or usefulness of any information, apparatus, product, or process disclosed, or represents that its use would not infringe privately owned rights. Reference herein to any specific commercial product, process, or service by trade name, trademark, manufacturer, or otherwise, does not necessarily constitute or imply its endorsement, recommendation, or favoring by the United States Government or any agency thereof. The views and opinions of authors expressed herein do not necessarily state or reflect those of the United States Government or any agency thereof.

Distribution

Approved for public release; further dissemination unlimited.

Preface: Mini-Workshop on Beam-Beam Compensation in Tevatron.

Fermilab, 12-13 February 1998

V. Shiltsev, Organizer

February 24, 1998

A Mini-Workshop on Beam-Beam Compensation in the Tevatron was held at Fermilab on February 12-13, 1998. The purpose of the Workshop was to assay the current understanding of compensation of the beam-beam effects in Tevatron with use of low-energy high-current electron beam, relevant accelerator technology, along with other novel techniques of the compensation and previous attempts. About 30 scientists representing seven institutions from four countries – FNAL, SLAC, BNL, Novosibirsk, CERN, and Dubna were in attendance. Twenty one talks were presented. The event gave firm ground for wider collaboration on experimental test of the compensation at the Tevatron collider.

The Workshop organization had required efforts of very few persons and it took only two days - all of which is reflected in the prefix "Mini-". If there are any questions concerning the Workshop or these Proceedings which are published as FNAL-Conf-98/064, with very limited circulation, contact the Workshop organizer or secretary:

Vladimir Shiltsev	Marion Richardson
FNAL,MS221, PO Box 500	FNAL,MS323, PO Box 500
Batavia, IL 60510	Batavia, IL 60510
ph.(630)840 5241	ph.(630)840 2767
FAX (630)840 6311	FAX (630)840 8461
E-mail: shiltsev@fnal.gov	E-mail: mhr98@fnal.gov

The Workshop information also can be found at:

http://www-bd.fnal.gov/lug/tev33/ebeam_comp/ebeam_comp.html

We are indebted to John Marriner for making and keeping the Web page.

Following is the agenda of the Workshop:

Thur.,Feb.12

9:00-9:15	J.Marriner	FNAL	Opening Address
9:15-10:45	V.Shiltsev	FNAL	Beam-Beam Compensation with Electron Beam in Tevatron
	V.Danilov	INP/FNAL	Beam-Beam Tracking for Tevatron with "Electron Compressor"
11:15-12:45	R.Siemann	SLAC	Beam-Beam Interaction with Four Colliding Beams
	A.Zinchenko	Dubna	Compensation Proposals for SSC and LHC
1:45-3:30	H.Riege	CERN	What Could We Gain with Beam Neutralization in LHC?
	G.Stupakov	SLAC	Plasma Suppression of Beam-Beam Interaction
	M.Syphers	BNL	Issues of e-p Polarimetry in RHIC
4:00-5:45	F.Zimmerman	SLAC	Beam-Beam Effects in Linear Colliders
	D.Whittum	SLAC	Beam-Beam Compensation in Linear Colliders

Fri.,Feb.13

9:00-10:45	V.Danilov	INP/FNAL	TMCI of Tevatron p-bar Beam Interacting with Electron Current
	A.Burov	INP/FNAL	Impedance of Compensating Electron Beam
	V.Shiltsev	FNAL	Simulations of Head-Tail Instability in Tevatron with "Electron Compressor"
11:15-12:45	V.Shiltsev	FNAL	Requirements on Electron Beam for Beam-Beam Compensation in Tevatron
	A.Zinchenko	Dubna	Electron Beam Distortions due to
	and V.Shiltsev	FNAL	Interaction with (Anti)Protons
	A.Sery	INP/FNAL	Stability of Electron Beam with Ions
1:45-3:45	S.Nagaitsev	FNAL	Experience with Electron Guns for Medium Energy Electron Cooling and Possible e-Source for "Electron Compressor"
	I.Meshkov	Dubna	Generation of Intense Stationary Electron Beam with Controlled Parameters
	P.Wesolowsky	DESY	Electron Cooling in PETRA
4:15-5:45	V.Shiltsev	FNAL	Particle Loss Diagnostics for PACMAN-Effect in TEV'33
	A.Sery	INP/FNAL	Particle Losses due to Electron Beam

Besides this preface, this book follows the same order, and concludes with the report submitted to *The Beams Dynamics Newsletter*.

As indicated, the following papers are not the formal proceedings for the Mini-Workshop. Mostly they are copies of transparencies presented and compressed texts of already printed papers. The participants were very responsive and energetic in addressing the issues posed to them; nearly every concern was considered at some level and several points were largely resolved. Questions and answers were an essential part of the meeting and are placed in this book after each talk in a brief form.

There were no special working groups, and all talks were plenary, nevertheless, the informal format of the presentations and flexible schedule did allow enough time for discussions. The meeting started with a welcoming address by the FNAL Beams Division Deputy Head John Marriner, followed by talks which can be divided in several groups accordingly to the beam-beam compensation topics chosen by the organizer. These groups are presented below, together with relevant publications available up to date:

proposal and physics of beam-beam compensation in the Tevatron	[1, 2]
proposals and realization of similar ideas in storage rings, SSC-LHC,linear colliders	[3, 4, 5, 6, 7, 8, 9]
coherent effects due to electron beam	[10]
electron beam stability and distortions	[11]
electron beam sources and transport	[12]
beams diagnostics and other problems	[13]

In addition to reviewing the plausibility of the beam-beam compensation in the Tevatron, it was the goal of the Workshop to advance understanding of the general character of the challenges to be met and to make incremental progress on design issues. In this, the Workshop was very successful.

References

[1] V.Shiltsev, D.Finley, "Electron Compression" of Beam-Beam Tune Spread in the Tevatron", FERMILAB-TM-2008 (1997).

[2] V.Shiltsev, "Electron Lens" to Compensate Bunch-To-Bunch Tune Spread in TEV33", FERMILAB-TM-2031 (1997).

[3] J. Le Duff, *et. al,* "Space Charge Compensation with DCI", *Proc. 11th Int. Conf. on High Energy Accel.*, CERN (1980), p.707.

[4] B.Podobedov, R.Siemann, "Coherent Beam-Beam Interaction with Four Colliding Beams", *Phys.Rev.E, vol.52, No.3*, (1995).

[5] E.Tsyganov, A.Taratin, A.Zinchenko, "Innovations in Accelerator Technology", *Fizika Elementarnih Chistic i Atomnogo Yadra, vol.27, No.3*, (1996) p.675; see also SSCL-Preprint-519 (1993).

[6] H.Riege, "Beam Space Charge Neutralization in the Interaction Regions of LHC with Low-Energy DC Electron Beam", to appear as LHC Project Note (1998).

[7] G.Stupakov, P.Chen, "Plasma Suppression of Beam-Beam Interaction in Circular Colliders", *Phys.Rev.Lett., vol.76*, (1996), p.3715.

[8] D.Whittum, R.Siemann, "Neutral Beam Collisions at 5TeV", *Proc. 1997 IEEE PAC*, Vancouver (1997).

[9] D.Whittum, R.Siemann, "Neutral Beam Collisions at 5TeV", *Proc. 1997 IEEE PAC*, Vancouver (1997).

[10] A.Burov, "Electron Cooler Impedances", *Particle Accelerators, vol.57,* (1997), p.131.

[11] A.Burov, V.Kudelainen, V.Lebedev, V.Parkhomchuk, A.Sery, V.Shiltsev, "Experimental Studies of Compensated Electron Beam", Novosibirsk INP 89-116 (1989); translated in CERN PS 93-09 (1993).

[12] I.Meshkov, "Physics and Technique of Electron Cooling", RIKEN-AF-AC-2 (1997);
I.Meshkov, ed., *Proc. Workshop on Beam Cooling, NIM A 391, No.1* (1997).

[13] V.Shiltsev, "Fast PIN-Diode Beam Loss Monitors at Tevatron", FERMILAB-TM-2012 (1997).

List of participants:

Assadi, Saeed	FNAL, MS341	assadi@fnal.gov
Bagley, Peter	FNAL, MS341	ppb@fnal.gov
Blokland, Wim	FNAL, MS308	blokland@fnal.gov
Burov, Alexei	FNAL, MS221	burov@fnal.gov
Danilov, Slava	FNAL, MS221	danilov@fnal.gov
Drozhdin, Sasha	FNAL, MS220	drozhdin@fnal.gov
Edwards, Helen	FNAL, MS306	hedwards@fnal.gov
Finley, David	FNAL, MS221	finley@fnal.gov
Holmes, Steve	FNAL, MS306	holmes@fnal.gov
Jackson, Gerry	FNAL, MS306	gpj@fnal.gov
Jowett, John	CERN-SL	john.jowett@cern.ch
Malamud, Ernie	FNAL, MS318	malamud@fnal.gov
Marriner, John	FNAL, MS306	marriner@fnal.gov
McGinnis, David	FNAL, MS341	mcginnis@fnal.gov
Meshkov, Igor	JINR-LNP	meshkov@nusun.jinr.ru
Mironov, Sergei	JINR-LNP	mironov@jinr.ru
Nagaitsev, Sergei	FNAL, MS307	nsergei@fnal.gov
Neuffer, David	FNAL, MS220	neuffer@fnal.gov
Riege, Hans	CERN-PS	hans.riege@cern.ch
Sery, Andrei	FNAL, MS221	sery@fnal.gov
Siemann, Robert	SLAC, MS26	siemann@slac.stanford.edu
Sidorin, Anatoly	JINR-LNP	sao@nusun.jinr.ru
Stupakov, Gennadi	SLAC, MS26	stupakov@slac.stanford.edu
Shiltsev, Vladimir	FNAL, MS221	shiltsev@fnal.gov
Syphers, Mike	BNL-AGS	syphers@bnl.gov
Weselowsky, Pawel	DESY-MPY	wesolow@mail.desy.de
Whittum, David	SLAC, MS26	whittum@slac.stanford.edu
Wildman, David	FNAL, MS306	wildman@fnal.gov
Zimmerman, Frank	SLAC, MS26	frankz@slac.stanford.edu
Zinchenko, Alexander	JINR	alexandre.zintchenko@cern.ch

Full mail addresses:

FNAL, PO Box 500
Batavia, Il 60510, USA

BNL, 35 Lawrence Dr.,
Bldg. 911, Upton,
NY 11973-5000, USA

SLAC, PO Box 4349,
Stanford, CA 94309, USA

JINR, 141980 Dubna,
Moscow Region, Russia

DESY, Notkestrasse 85,
22607 Hamburg, Germany

Budker INP, 630090,
Novosibirsk, Russia

John Marriner (FNAL)

Beam-Beam Compensation Mini-Worksh

- Welcome to Fermilab
- Thank you for coming

Luminosity Formula

$$\mathcal{L} = \frac{3\gamma f_0}{\beta^*}\left(BN_{\bar{p}}\right)\left(\frac{N_p}{\varepsilon_p}\right)\frac{F\left(\beta^*, \theta_{x,y}, \varepsilon_{p,\bar{p}}, \sigma^L_{p,\bar{p}}\right)}{\left(1+\varepsilon_{\bar{p}}/\varepsilon_p\right)}$$

The major luminosity limitations are

- The number of antiprotons (BN_p)
- The proton beam brightness (N_p/ε_p)
- $F<1$

Beam-Beam Tune Footprint 140 p x 121 pbar

136 μrad crossing angle
14 cm bunch length

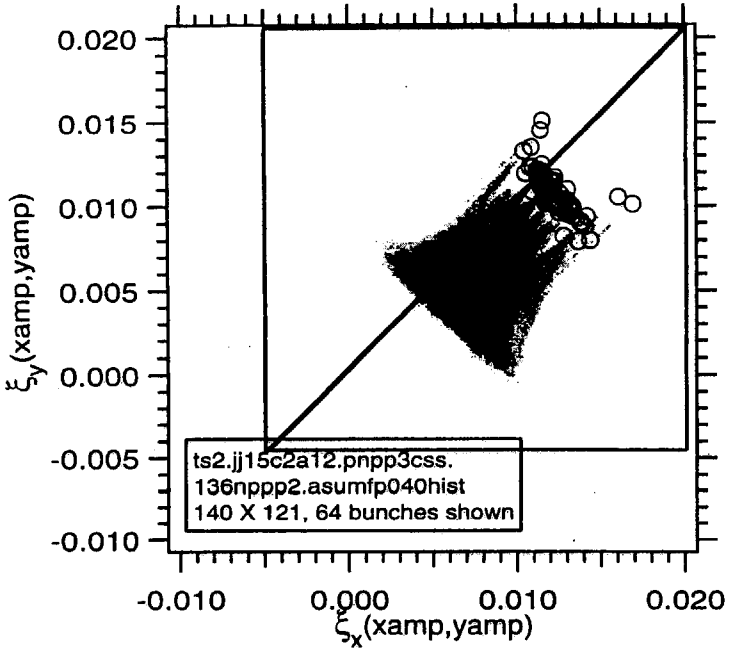

Possible Goal #1

- Eliminate bunch-by-bunch tune variations.
  - *An electron beam could provide the necessary focussing if the beam intensity were modulated by the proper amount*
  - *Tune correction in both planes could be obtained with two beams: an "F-like" lens and a "D-like" lens*

Possible Goal #2

- Eliminate the amplitude dependence of the tune
  - *a properly shaped electron beam can eliminate the tune spread*
  - *some tuneability of the electron beam shape might be necessary to accommodate a variety of beam conditions*

Complications

- Proton and antiproton beams occupy the same aperture.
- Electrons defocus antiprotons and focus protons.
- The Tevatron does not have any space for new devices

Does it Work?

- Are the parameters of the compensation system reasonable?
- Are the regulation requirements (electron beam intensity, position, shape) achievable?
- Does the addition of a non-linear lens (Goal #2) really reduce beam loss?

Conclusion

?

?

?

Beam-Beam Compensation Workshop
Fermilab, Feb. 12-13, 1998

Vladimir SHILTSEV

Compensation of Beam-Beam Effects in Tevatron with Use of Electron Beam

1. ***Introduction***
2. ***Brief Overview of Beam-Beam Effects in Tevatron***
3. ***Beam-Beam Compensation with Electron Beam***
4. ***Electron Beam Consideration***
5. ***Experimental Test***
6. ***Discussion and Summary***

Acknowledgements

Co-Authors: Alexei Burov
Slava Danilov
Dave Finley
Andrei Sery

Input and Comments: Peter Bagley
Weiren Chou
Sasha Drozhdin
John Marriner
Fred Mills
Sergei Nagaitsev
Vasily Parkhomchuk
Dave Ritson
Tolya Sharapa
Sasha Shemyakin
Sasha Zinchenko

Nov. 96

Table 1: Parameters of Fermilab Collider

Parameter	Run-IB	Run-II (MI)	RUN-II (MI+Recycler)	TeV33
Beam energy (TeV)	0.9	1.0	1.0	1.0
N_b	6	36	36	108 → 121×140
N_p, 10^{11} per bunch	2.3	2.7	2.7	2.7
$N_{\overline{p}}$, 10^{10} per bunch	5.5	3.0	7.0	variable
ϵ_p, π mm-mrad	23	20	20	20
$\epsilon_{\overline{p}}$, π mm-mrad	13	15	15	20
rms bunch length, m	0.60	0.43	0.38	0.18
β^*, m	0.35	0.35	0.35	0.35
θ_x=θ_y, μrad	0	0	0	$\pm$100
Bunch spacing, nsec	3500	396	396	132
Int/crossing	2.7	2.3	5.8	8.7
$\overline{p}$ tune shift	0.015	0.020	0.022	0.022
$\mathcal{L}$, cm^{-2} s^{-1}	2.1×10^{31}	8.1×10^{31}	2.0×10^{32}	1.2×10^{33}
$\mathcal{L}$, pb^{-1} week^{-1}	4.2	16.3	41.0	246

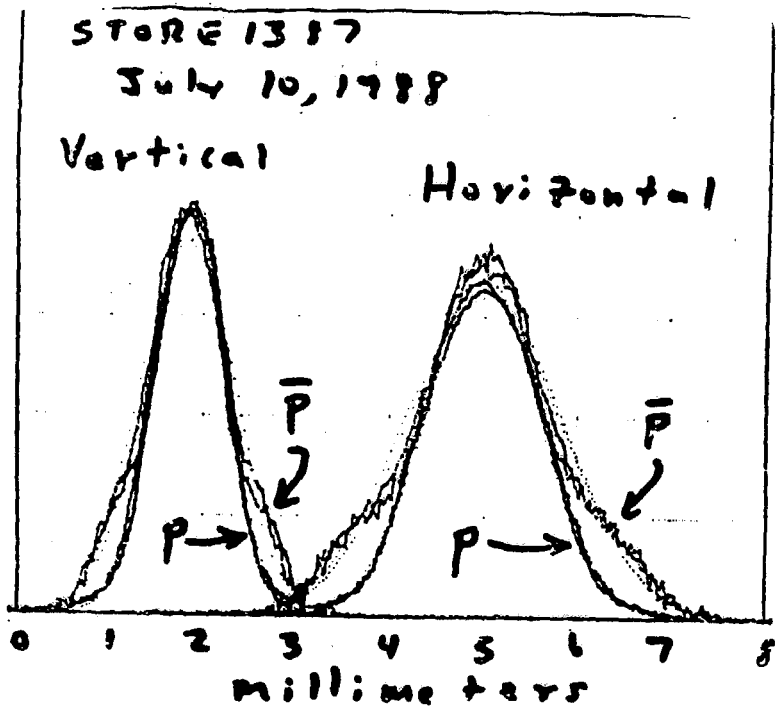

Figure 3. Transverse beam profiles demonstrating a problem encountered early in the Fermilab run. The bunch intensities were ~ 40E9 for the protons and ~8E9 for the antiprotons.

Run Ia

6x6 bunches, No separation

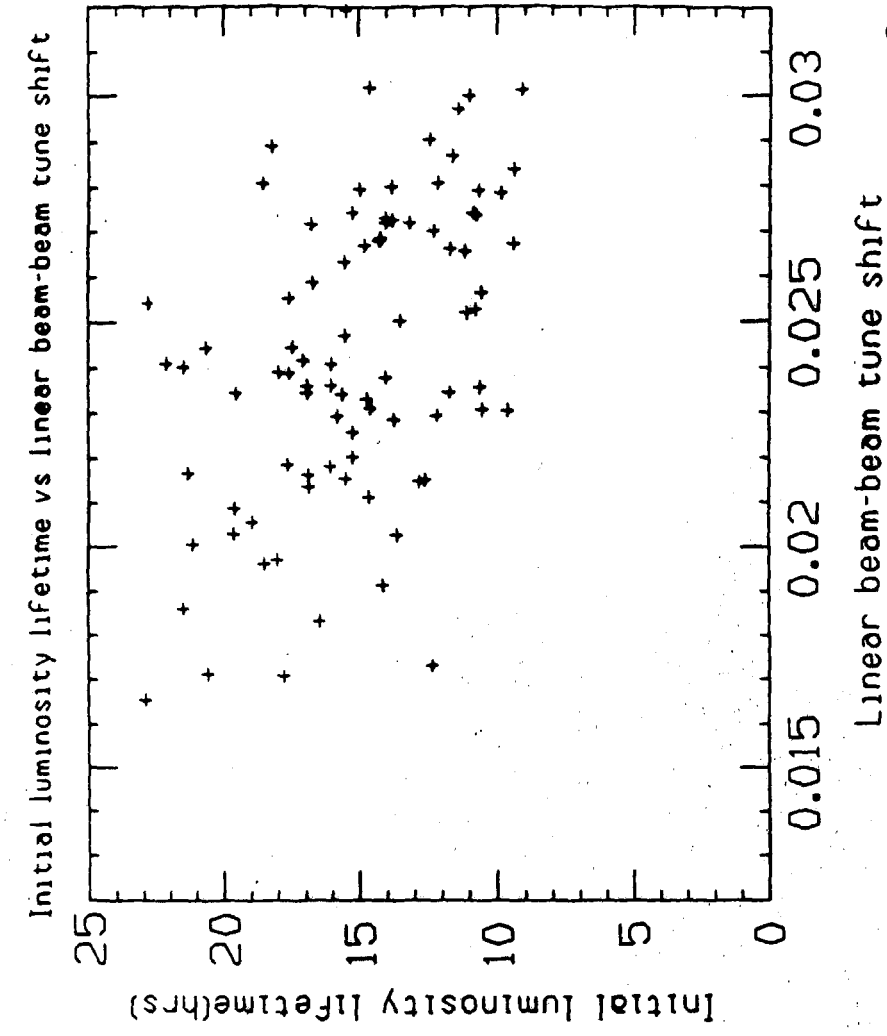

Run Ia

12 collisions/turn

6x6 bunches

Figure 3

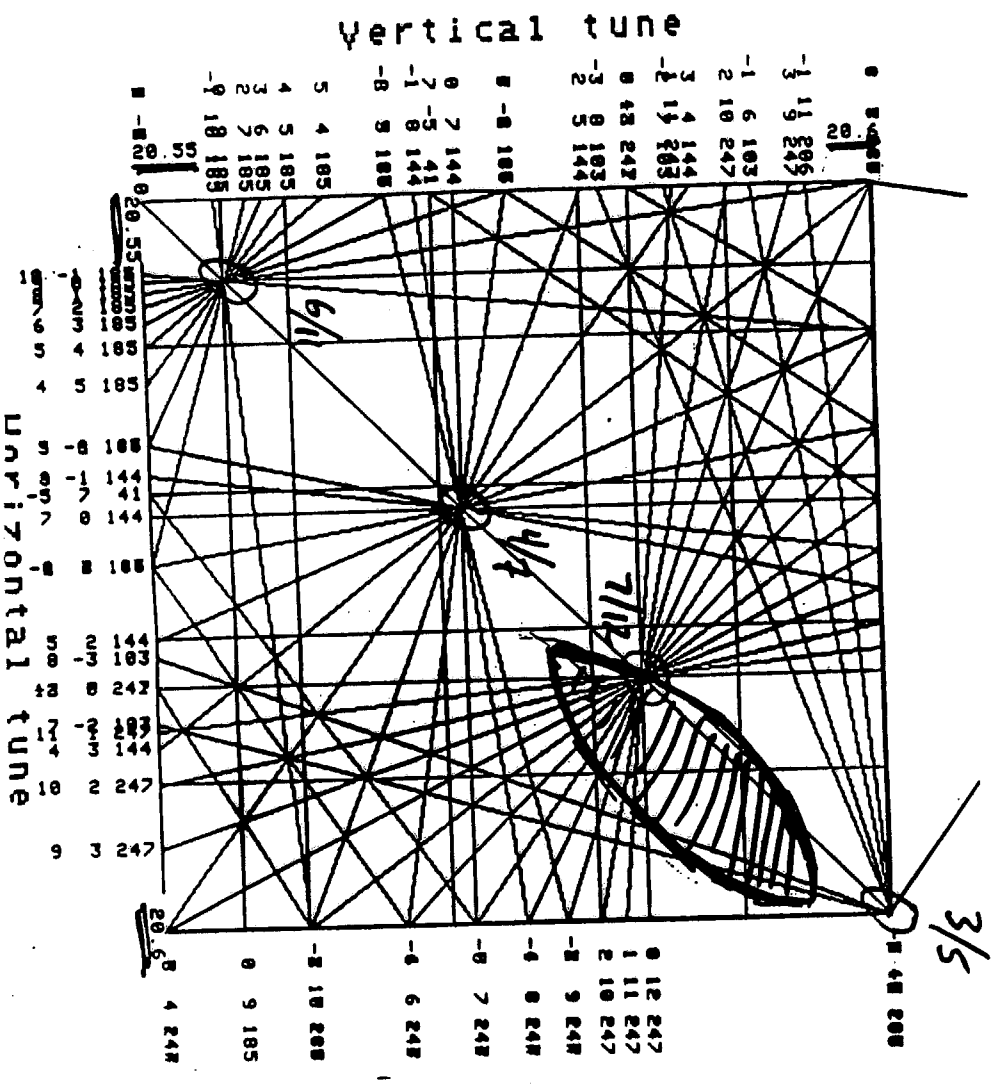

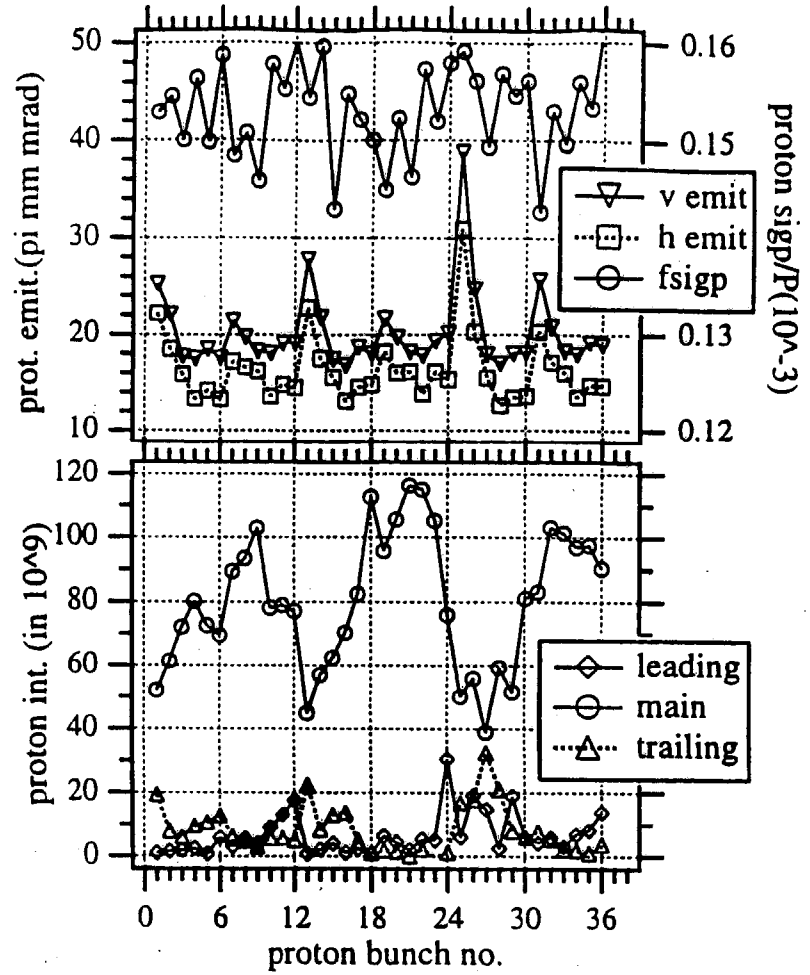

Figure 1 : Bunch by bunch proton intensities and emittances at 900 GeV in colliding beam conditions

36 bunch studies, fall 1995

36p × 1p̄ ·····→ Run II 36×36

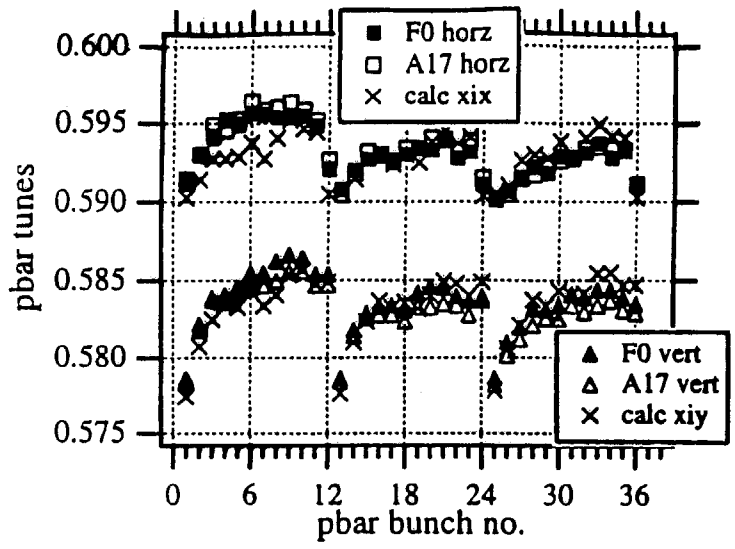

Figure 2 : Measured and Calculated Pbar Tunes for Colliding Beam Conditions. We assume base pbar horizontal and vertical tunes of 0.5855 and 0.5755, horizontal proton emittances equal to the vertical proton emittances, and we use a scale factor of 0.648 for the tune shifts from the head on beam beam interaction.

36 bunches studies, FALL 95

36 p × 1 p̄

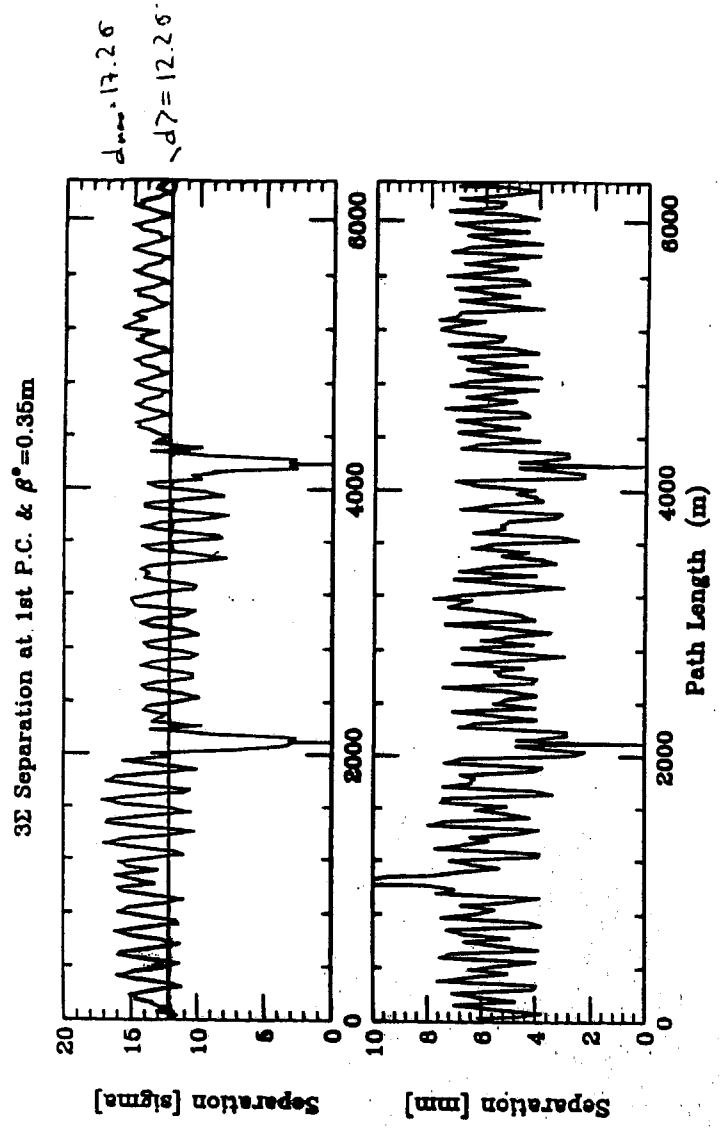

Figure 35. Beam-beam separation around the ring corresponding to 3σ separation at the first parasitic crossing.

Beam-Beam Tune Spread 100 μrad Crossing Angle

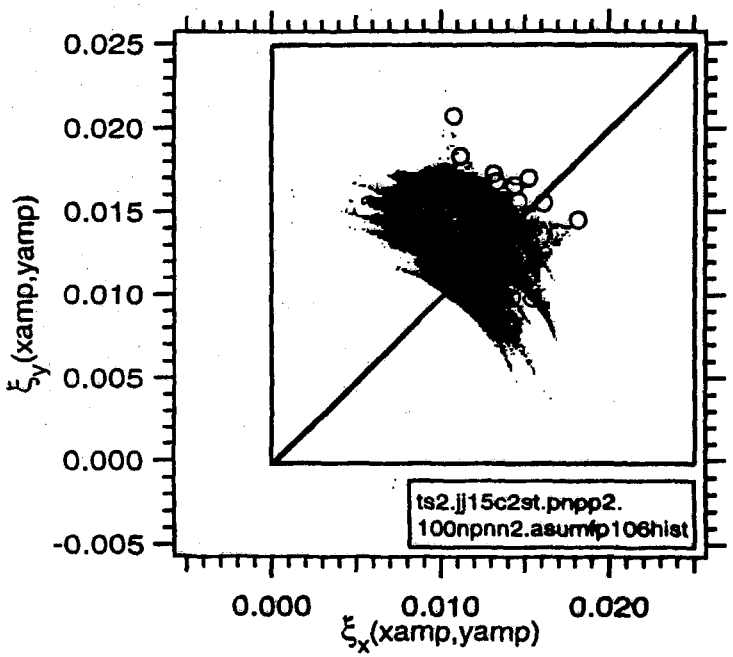

The Need for a Crossing Angle

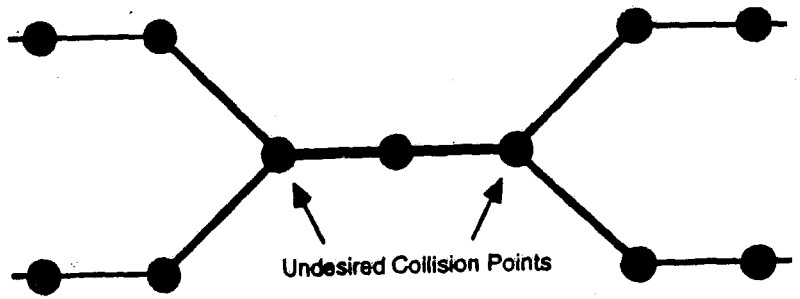

With a 7 rf bucket spacing a crossing angle is required

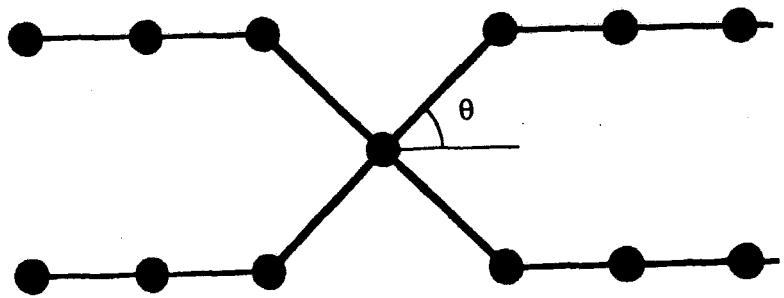

Luminosity vs Crossing Angle

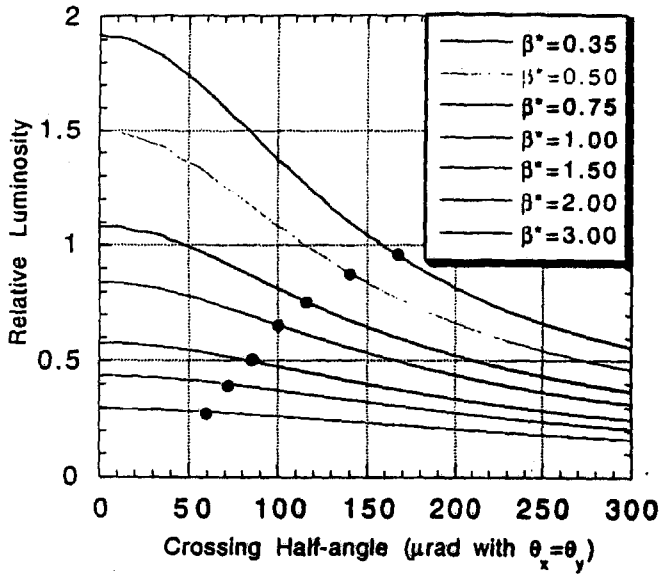

$\varepsilon_{H_p} = \varepsilon_{V_p} = \varepsilon_{H_{\bar{p}}} = \varepsilon_{V_{\bar{p}}} = 20\pi$ mm - mrad

$\sigma_{L_p} = \sigma_{L_{\bar{p}}} = 35$ cm

Units are 10^{33} cm^{-2}sec^{-1} if

$N_p = N_{\bar{p}} = 270\times10^9$ and $n_b = 100$

Linear Beam-Beam Tune Shift with Crossing Angle Effect

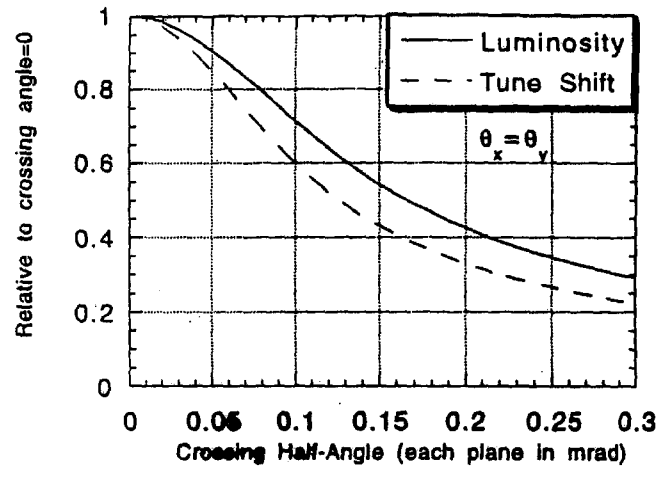

$N_p = 27\times10^{10}$

$\beta^* = 35$ cm

$\varepsilon_{H_p} = \varepsilon_{V_p} = \varepsilon_{H_{\bar{p}}} = \varepsilon_{V_{\bar{p}}} = 20\pi$ mm - mrad

$\sigma_{L_p} = \sigma_{L_{\bar{p}}} = 35$ cm

Tevatron Collider with "Electron Compression" Device

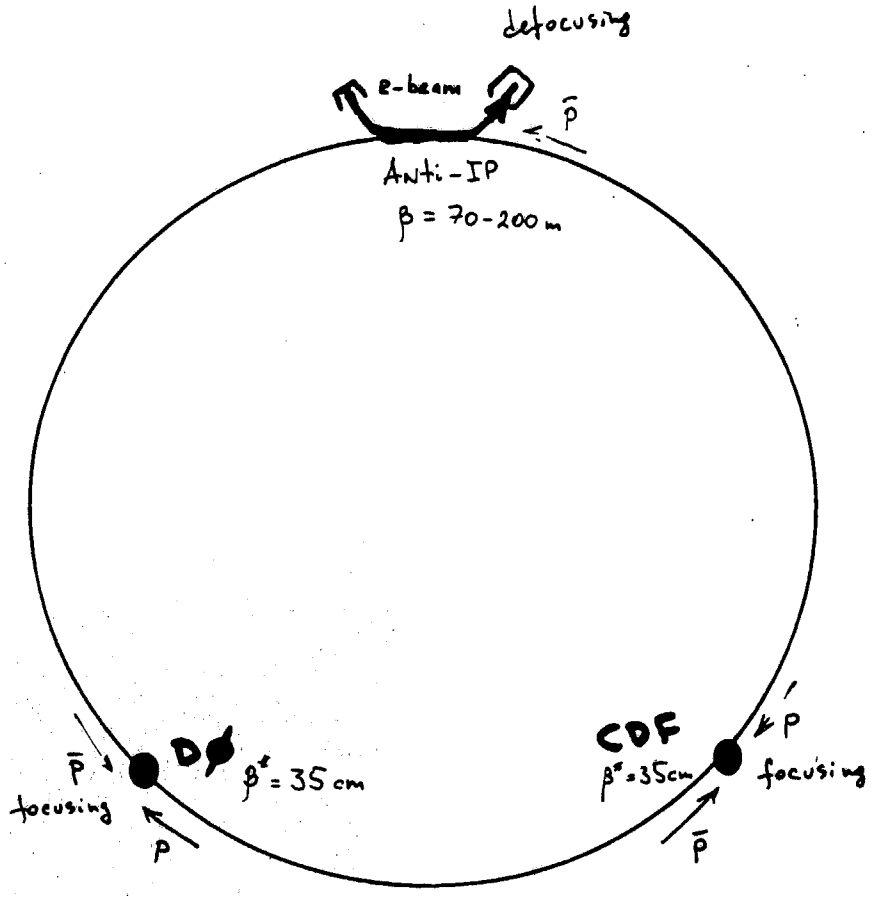

Possible Schemes for Electron Compressor

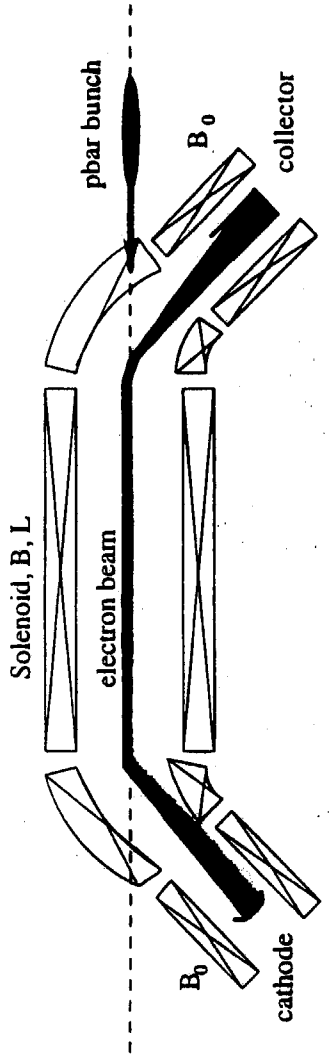

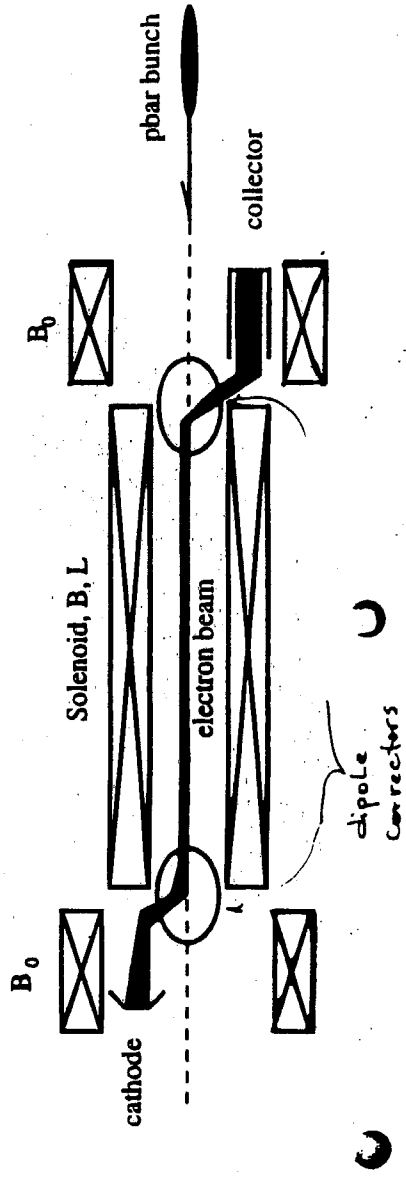

Basics of Electron Compensation

ck experienced by $\bar{p}$ particle at one of interaction oints due to proton bunch:

$$\Delta\vec{r}' = -8\pi\xi_p \epsilon\cdot\vec{r}\cdot\frac{1-e^{-\frac{r^2}{2\beta\epsilon}}}{r^2}$$

um-Beam parameter

$$\xi_p = \frac{\nu_p r_p}{4\pi\epsilon_n^{rms}} = \frac{N_p r_p}{\frac{2}{3}\epsilon_n^{FINAL}} = 0.007\cdot\frac{N_p[10^{11}]}{\epsilon_n^{FINAL}[\text{mm-mrad}]}$$

$\vec{r} = \vec{a}\cdot\sin\psi$

e.g. $\xi_p = 0.01$ $N_p = 2.7\cdot10^{11}$ $\epsilon_n = 20\pi$ mm·mrad

: Normalized variables $\left(\frac{\vec{r}}{\sqrt{\beta\epsilon}}; \sqrt{\frac{\beta}{\epsilon}}\vec{r}'\right)$

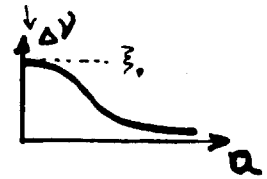

$$\Delta\vec{r}_n' = -8\pi\xi_p\cdot\frac{1-e^{-\frac{r_n^2}{2}}}{r_n^2}\cdot\vec{r}_n$$

$\to 0$ $\Delta\vec{r}_n' = -4\pi\xi_p\vec{r}_n \to \Delta\nu = \xi_p = -\frac{1}{4\pi}\frac{\partial\vec{r}'}{\partial r}$

$r\neq0 \to$ averaging over $\vec{r} = \vec{a}\sin\psi \longrightarrow \Delta\nu = \Delta\nu_0(a)$

dd electron beam $\longrightarrow$

t $\beta \gg \beta^*$; $\bar{p}$ size $\sigma = \sqrt{\beta\epsilon}$, e-beam – Gaussian with σ

Low energy $\beta_e = \frac{v_e}{c} \ll 1$

fter collision: $\Delta\vec{r}_n' = +8\pi\xi_e\vec{r}_n\cdot\frac{1-e^{-\frac{r_n^2}{2}}}{r_n^2}$

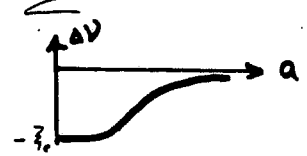

$$\xi_e = \frac{N_e\cdot r_p\cdot(1+\beta_e)}{8\pi\epsilon_n^{rms}}$$

otal Effect of 2 IPs and electron beam:

$$\Delta\nu(\vec{r}\ll1) = (2\xi_p - \xi_e) \longrightarrow \Delta\nu = 0$$

$$\Delta\nu(a) = \frac{\Delta\nu_0(a)}{\xi_p}\cdot(2\xi_p - \xi_e) \longrightarrow 0$$

if $\xi_e = 2\xi_p$ or $N_e = \frac{2}{1+\beta_e}N_p$

Beam-Beam Interaction Schemes:

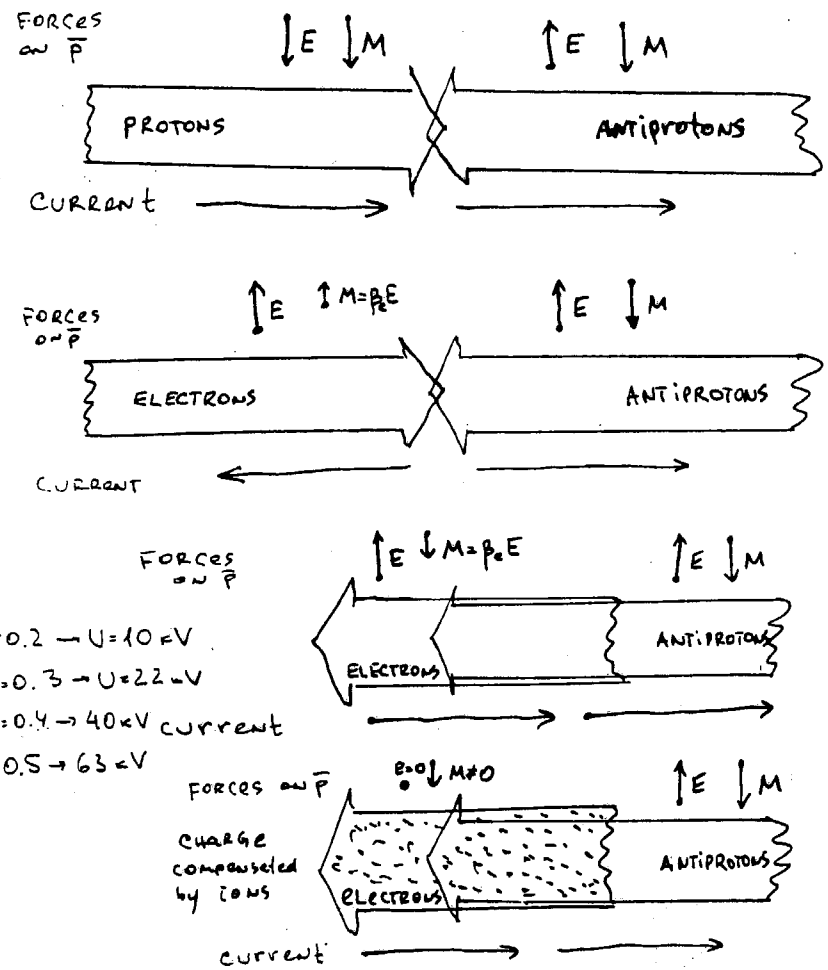

$\beta_e = 0.2 \to U = 10$ kV

$\beta_e = 0.3 \to U = 22$ kV

$\beta_e = 0.4 \to 40$ kV

$\beta_e = 0.5 \to 63$ kV

Numerical Example:

10-kV electron beam $\beta_e = 0.2$

2 Interaction points (DØ & BØ)

$N_p = 2.7 \cdot 10^{11}$ – Number protons / bunch

$\longrightarrow$ $N_e = 4.5 \cdot 10^{11}$ – Total Number of e's

Required e-beam size:

$\sigma_e = \sigma_p =$ 0.5 mm @ $\beta = 70$ m

0.7 mm @ $\beta = 150$ m

0.9 mm @ $\beta = 250$ m

If Length of e-beam $L = 3$ m then required current: $J_e = \frac{e N_e \beta_0 c}{L} = 1.4$ A

Maximum current density:

$$j_e^{max} = \frac{J_e}{2\pi\sigma^2} \simeq 50 \ A/cm^2$$

Knobs available for the "Electron Compressor":

1. **Intensity, Ne**
2. **Radius, a**
3. **Distribution function, $\rho(r)$**
4. **Time-variable current, Je(t)**
5. **Several E-compressors**

---

6. **Displacement, d**
7. **Tilt, $\varphi(z)$**
8. **Variable magnetic field, B(z)->r(z)**
9. **Ellipticity, ε**
10. **Energy of the beam, E**
11. **Solenoid Field or Beam direction**
11. **Pbar beta-functions, $\beta x \neq \beta y$**

Beam-Beam Interaction Issues in TEV'33

	How can E-compressor possibly help?
Bunch-by-Bunch Tune Shift	***equalize***
Tune Spread (footprints)	***shrink***
Unequal Emittances and Bunch Intensities	***compensate***
Crossing Angle	***eliminate***
Bunch-by-Bunch Coupling	***?***
Bunch-by-Bunch Closed Orbit Distortions	***-***

GAUSSIAN CHARGE distribution $\rho_G = const. e^{-\frac{r^2}{2\sigma^2}}$

$$\rho_1 = \frac{const_1}{\left(1+\left(\frac{r}{\sigma}\right)^2\right)^2} \; ; \; const_1 = 0.93$$

$$\rho_2 = \frac{const_2}{1+\left(\frac{r}{\sigma}\right)^8} \; ; \; const_2 = 0.83$$

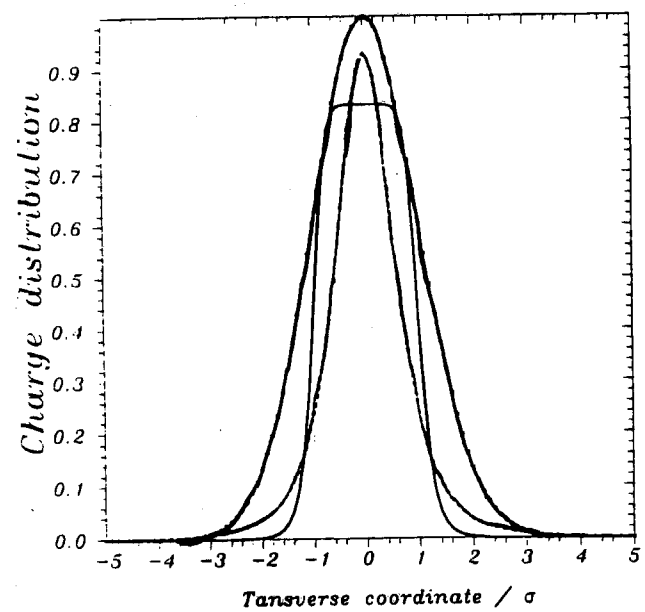

$\rho_0 = const \cdot e^{-\frac{r^2}{2\sigma^2}}$ – initial, due to protons

$\rho_1 = \frac{const_1}{\left(1+\left(\frac{r}{\sigma}\right)^2\right)^2}$ – "compressor 1"

$\rho_2 = \frac{const_2}{1+\left(\frac{0.9r}{\sigma}\right)^8}$ – "compressor 2"

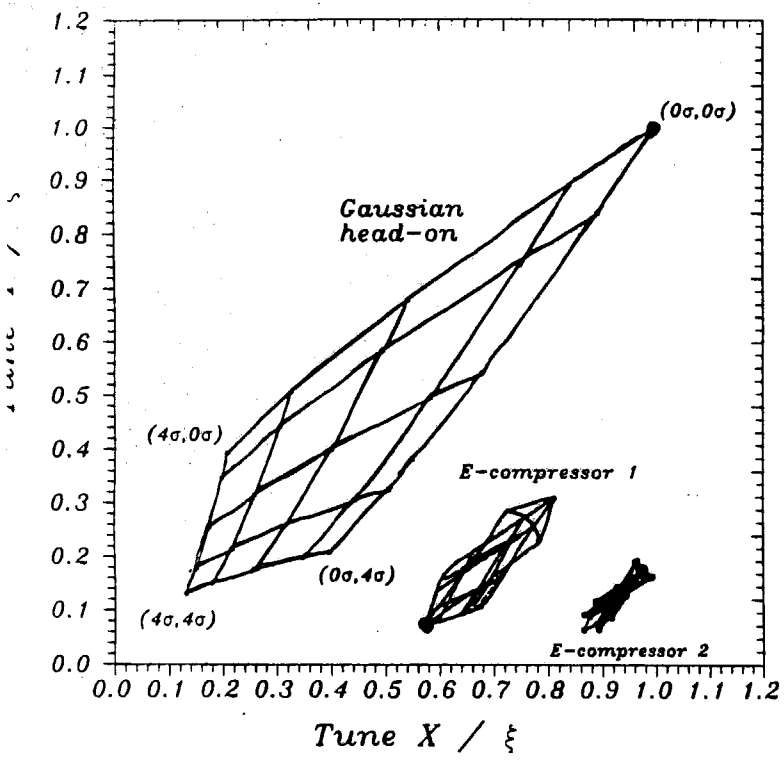

• STRENGTHES OF NON-LINEAR RESONANCES

"Electron Compressor" Device

basic configuration for "head-on" beam-beam tune spread compensation in Tevatron with 2 IPs

Beam length	**L = 3 m**
Beam radius	**a = 0.6-2 mm**
Beam current	**Je=1-2 A**
Maximum voltage	**Ue=10-40 kV**
Magnetic field	**B=1.5-4 T**

P. Bagley (Mar 97)

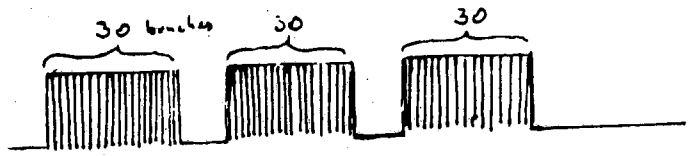

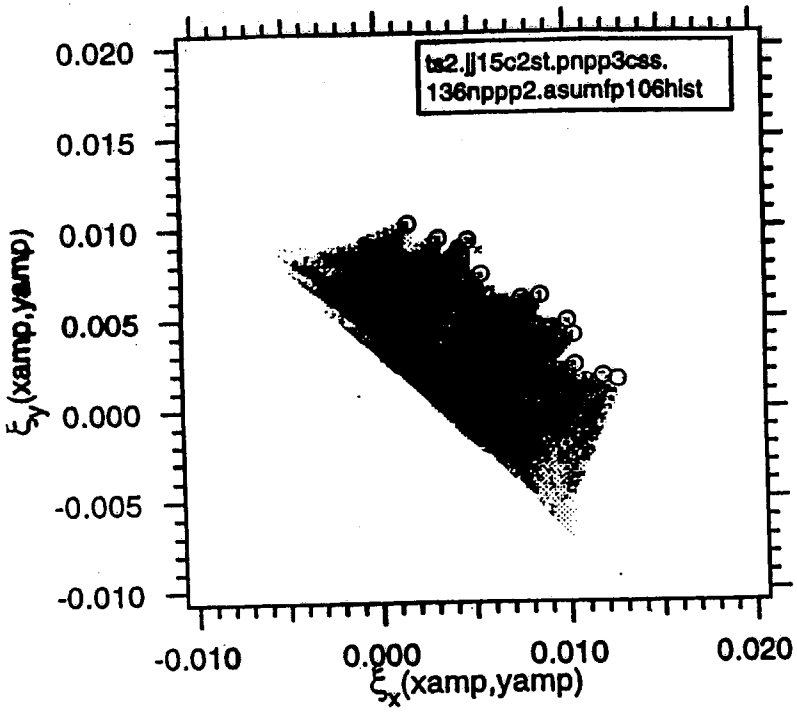

bunch-to-bunch SPREAD ALONG THE LINE $\Delta\nu_y = -\Delta\nu_x$ is ~2.5 times LARGER THAN along $\Delta\nu_y = \Delta\nu_x$ i.e. "head-on" COMPRESSOR is NOT EFFECTIVE

Tevatron Collider with Two "Electron Lenses"

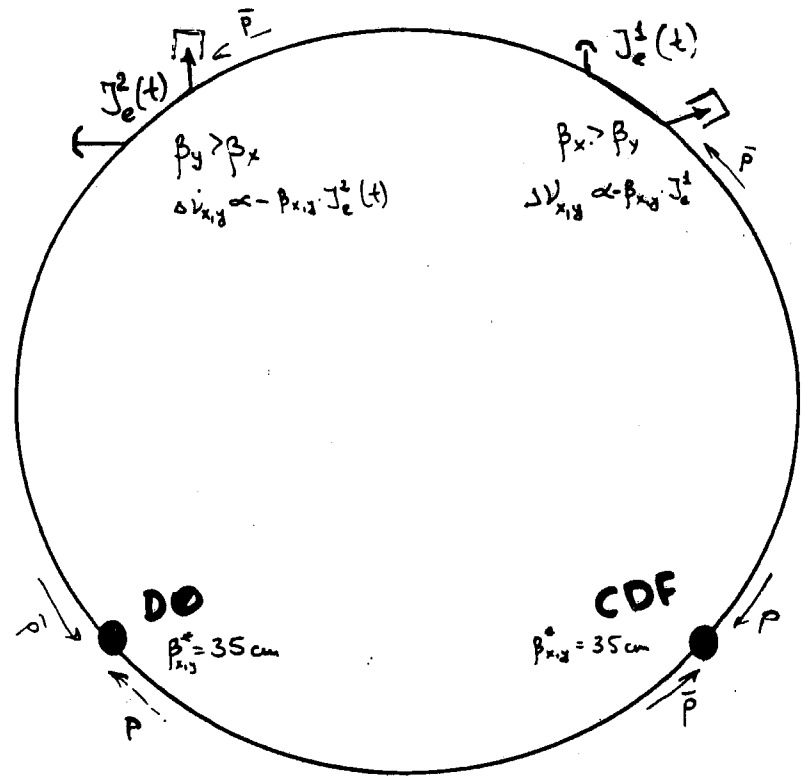

$\beta_x = 101.67$ m

$\beta_y = 30.89$ m

$D_x = 1.92$ m

$\sigma_x = 0.61$ mm

$\sigma_y = 0.31$ mm

(location 48)

$\varepsilon_n = 20\pi$ mm-mrad

($\varepsilon_n^{rms} = 3.3\pi$ mm-mrad)

$\beta_x = 59.0$ m

$\beta_y = 110.1$ m

$D_x = 1.69$ m

$\sigma_x = 0.47$ mm

$\sigma_y = 0.6$ mm

(up stream end of Cϕ)

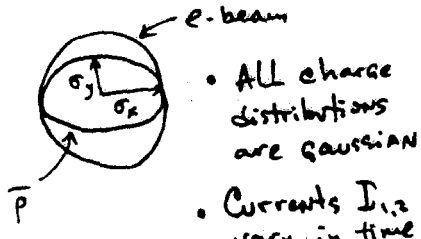

- All charge distributions are GAUSSIAN
- Currents $I_{1,2}$ vary in time

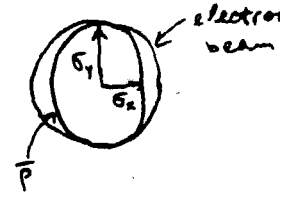

$$\begin{cases} \Delta\nu_x(t) = \beta_1^x \cdot I_1(t) \cdot C1 + \beta_2^x \cdot I_2(t) \cdot C2 = -\Delta\nu_x^{\bar{p}}(\text{bunch \#}) \\ \Delta\nu_y(t) = \beta_1^y \cdot I_1(t) \cdot C1 + \beta_2^y \cdot I_2(t) \cdot C2 = -\Delta\nu_y^{\bar{p}}(\text{bunch \#}) \end{cases}$$

$$C_{1,2} = \frac{4.4 \cdot 10^5}{a_e^2\,[\text{mm}]}, \quad a_e = \max(\sigma_x, \sigma_y)$$

(see solution)

Electron currents required in two electron lenses to compensate bunch-to bunch tune shift in 90x90 bunch scenario

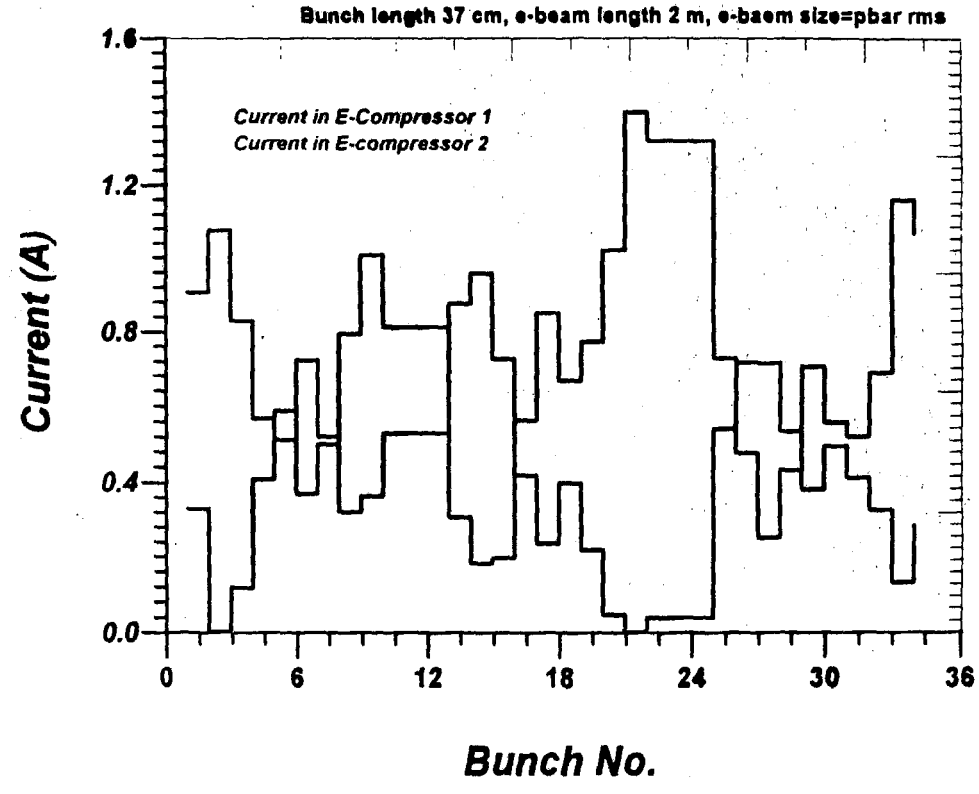

Bunch-to-bunch tune shifts in 90x90 scenario compensated by two e-lenses

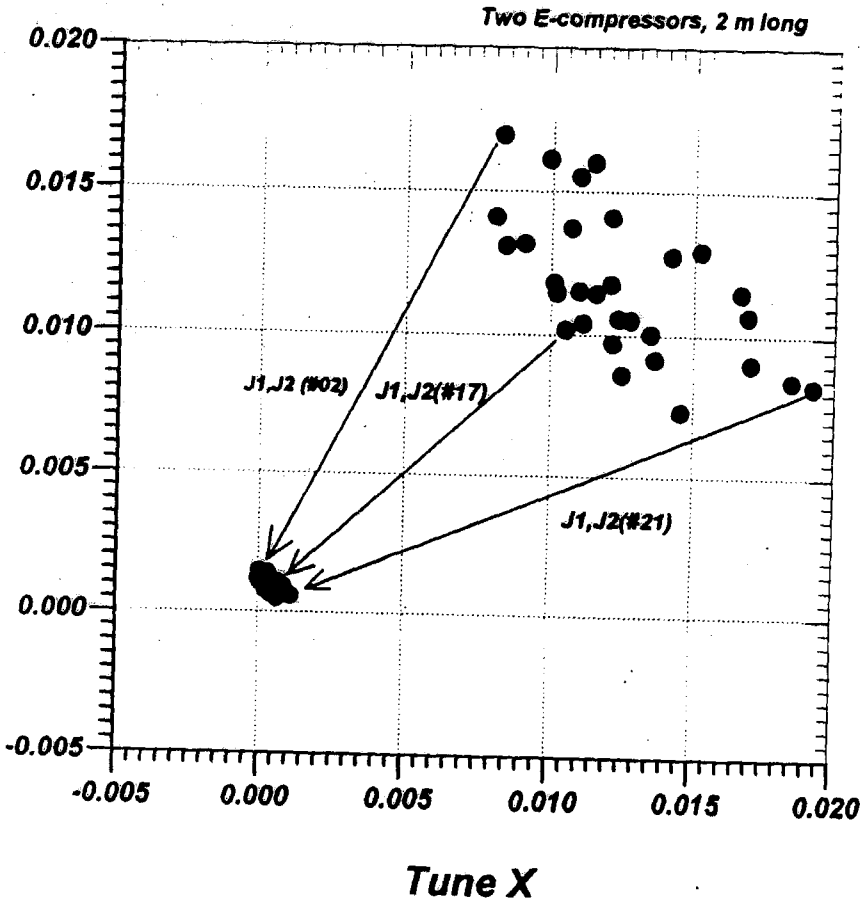

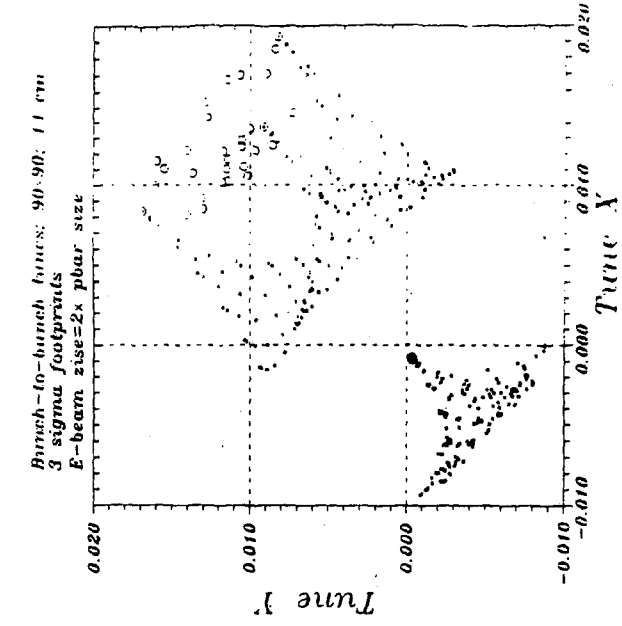

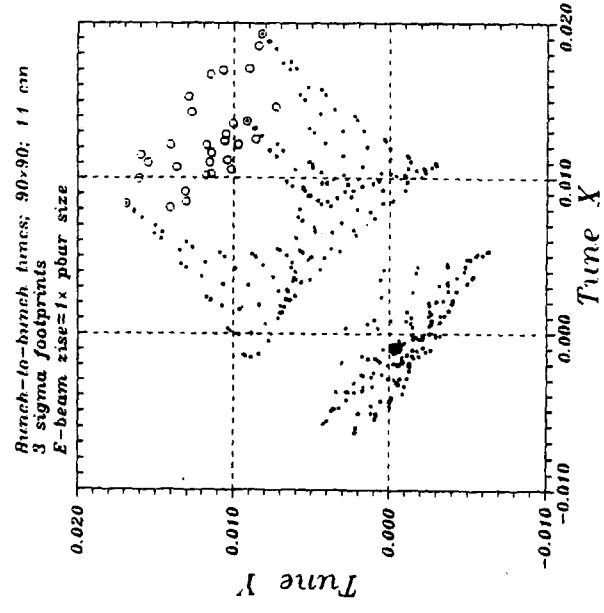

Electron currents required in two electron lenses to compensate bunch-to-bunch tune shift in 121 (pbar) x 140 (p) bunch scenario

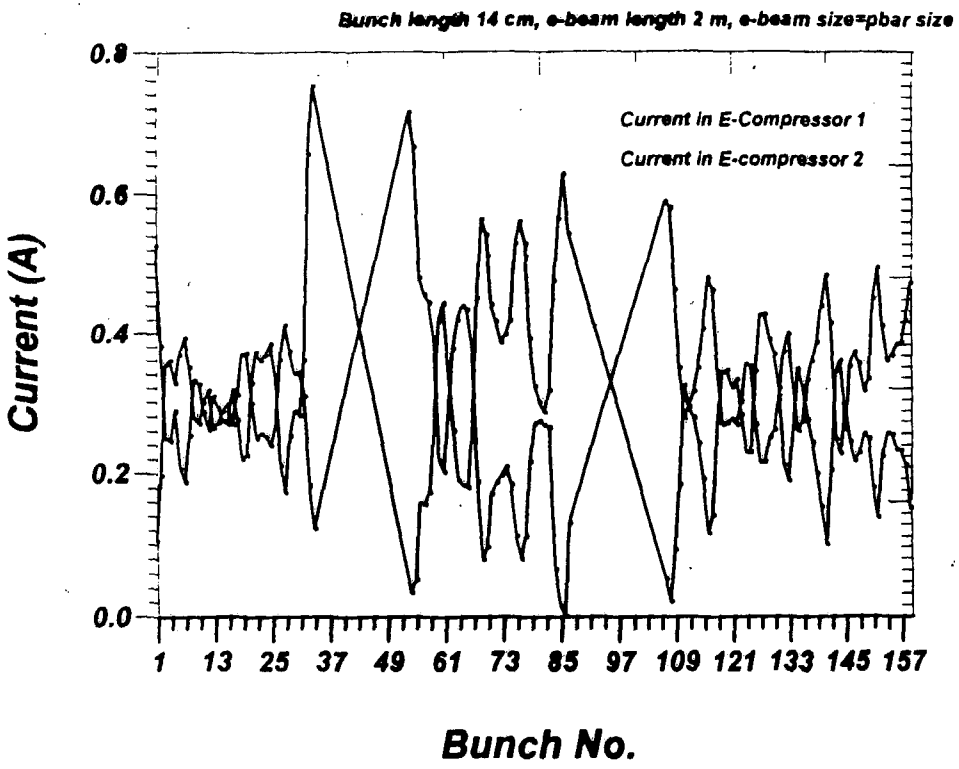

Bunch-to-bunch tune shifts in 121x140 scenario compensated by two e-lenses (with 10% error)

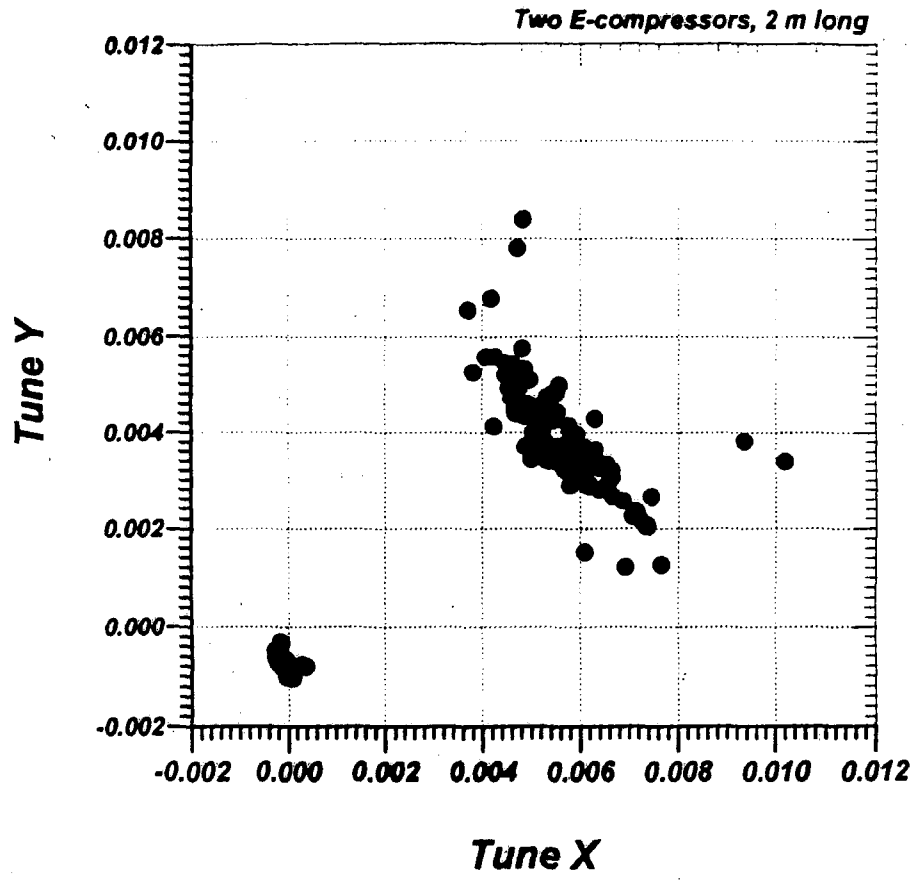

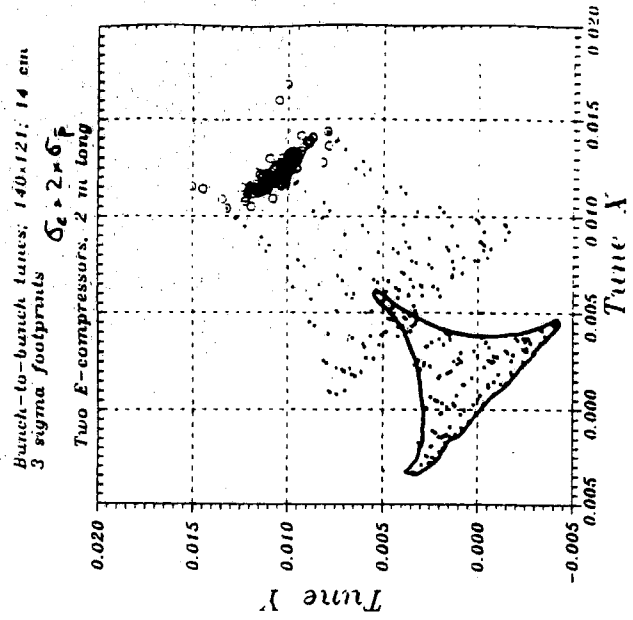

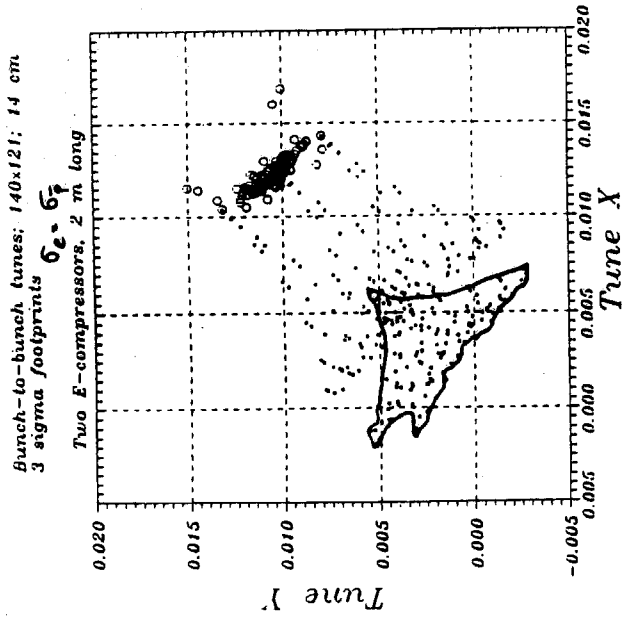

"Electron Lenses"

to eliminate bunch-to-bunch tune shift variation in Tevatron

Number of Set-Ups	2
Beam length	L = 2 m
Beam radius	a =1-2.4mm
Beam current	Je=0.5-5 A
Current modulation	dT=132 ns
Beam length	L = 2 m
Maximum voltage	Ue=10-40 kV
Magnetic field	B=1.5-4 T

causes synchro-betatron coupling ← bad
luminosity reduction ← bad

The Need for a Crossing Angle

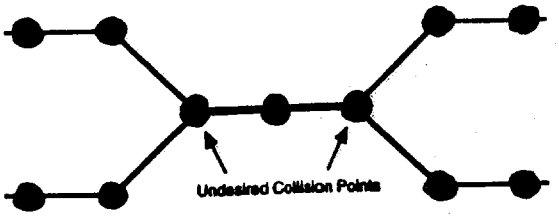

With a 7 rf bucket spacing a crossing angle is required

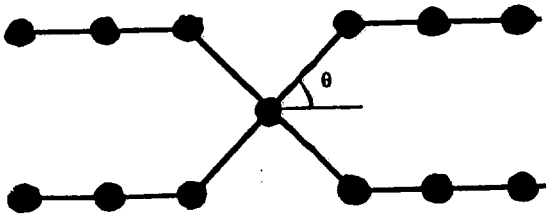

Luminosity vs Crossing Angle

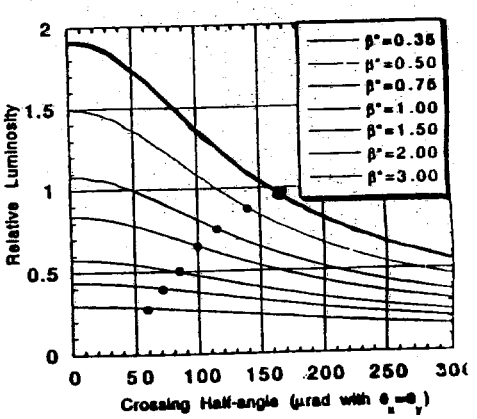

$\varepsilon_{Nx} = \varepsilon_{Ny} = \varepsilon_{Nq} = \varepsilon_{Nq} = 20\pi$ mm-mrad

$\sigma_{Lp} = \sigma_{Lq} = 35$ cm

Units are 10^{33} cm^{-2}sec^{-1} if

$N_p = N_{\bar{p}} = 270\times10^{9}$ and $n_b = 100$

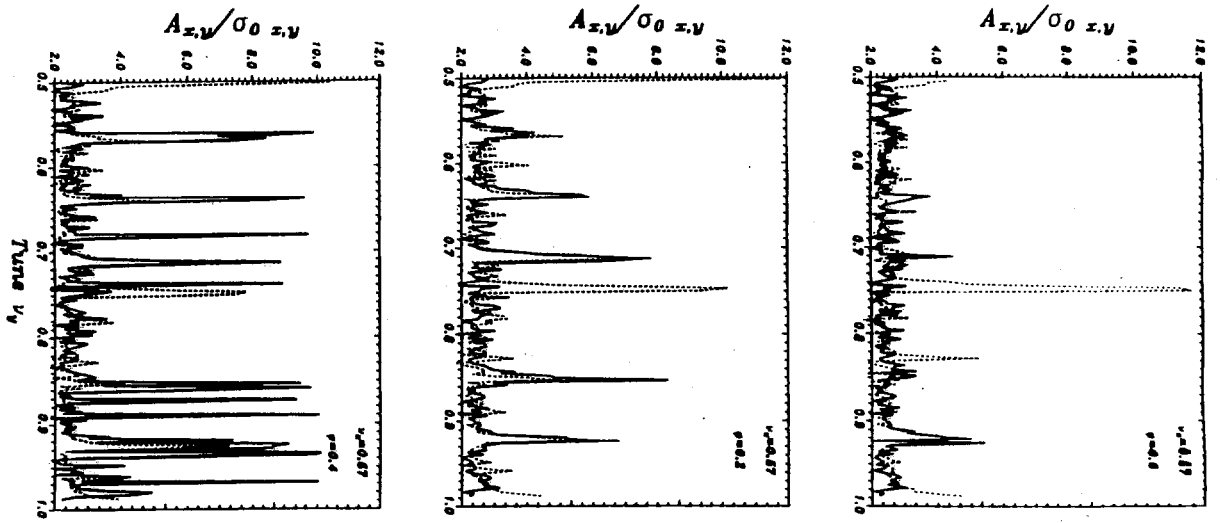

Figure 5: The ν_y dependence of maximum horizontal (A_x - solid) and vertical (A_y - dashed) amplitudes normalized on $\sigma^0_{x,y}$; $\nu_x = 0.57$, $\xi = 0.025$, $S = 0.6$. Crossing angle $\phi = 0$ mrad (upper plot), 0.2 mrad (center plot, $\Phi \simeq 1$), and 0.4 mrad (bottom

V Shiltsev, FUSL-FN-153 (1991)

I. Finchenko
Friday talk

"Electron Compressor" for Zero-Crossing Angle Scheme in Tevatron'33

Allows to have two(four) more head-on collision points around each interaction point as far as the "EC" compensates their effect too.

Near-IP collisions have minor luminosity as $L \propto 1/\beta$ and $\beta >> \beta^*$

Beam-beam effects are about the same as in main interaction point, i.e. $\xi \rightarrow (3\text{-}5)\xi_0$

Thus, the "electron compressor" current required $I \rightarrow (3\text{-}5)I_0$ = 4-7 A

The electron beam stability will require stronger magnetic field
$B \rightarrow B_0 * (3\text{-}5) = 4.5\text{-}8.5$ T

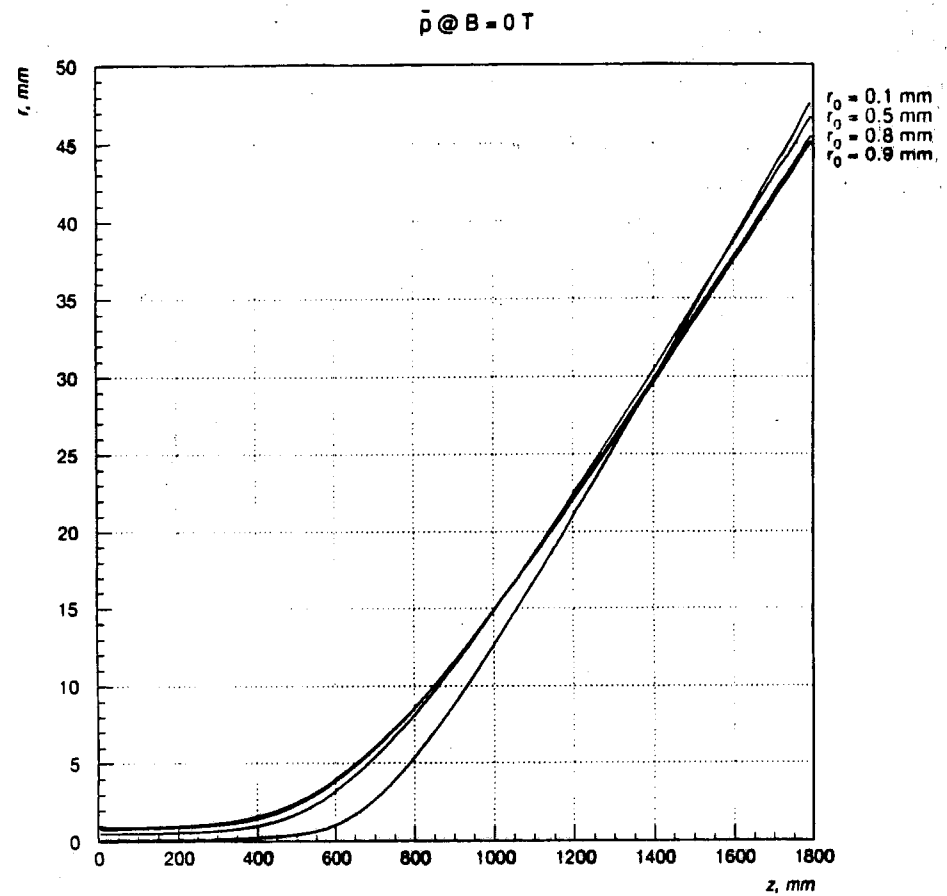

A Kirichenko

Friday talk

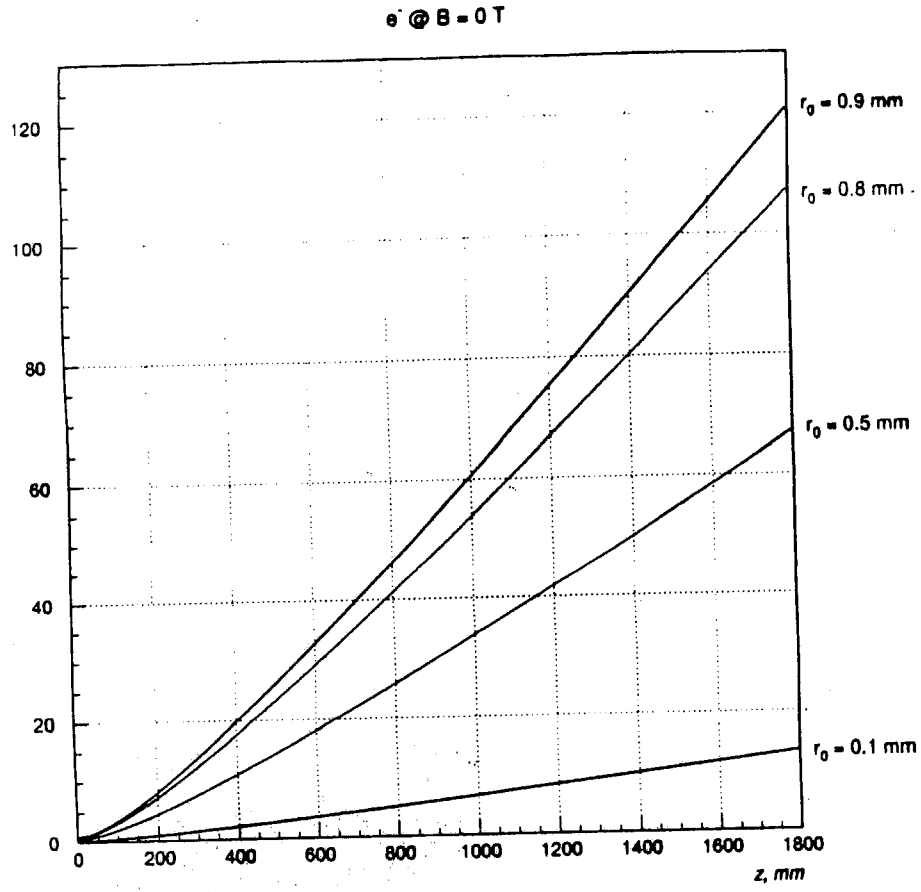

Transverse charge ditribution in e-beam before and after passage of the pbar bunch

$$\frac{\sigma_y}{\sigma_x} = 0.5$$

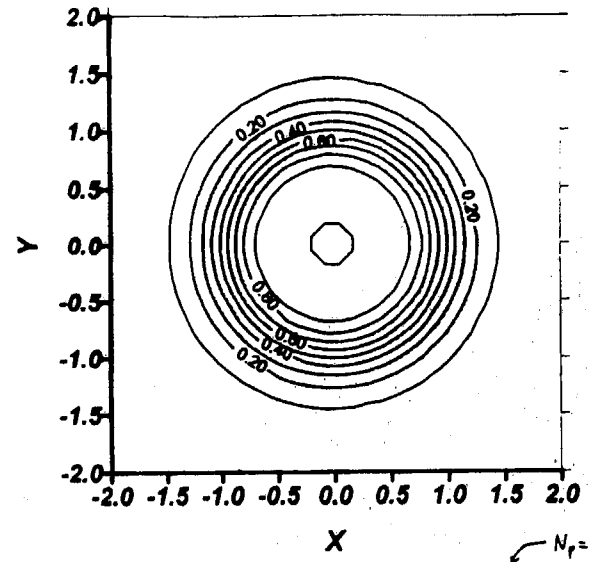

$N_p = 6 \cdot 10^9$ B = 4 kG

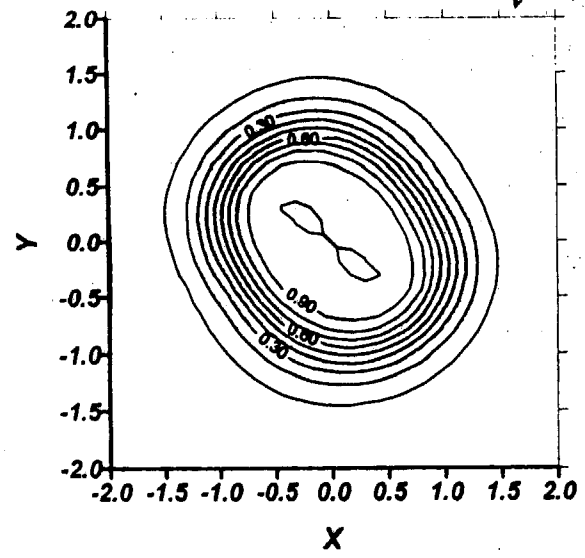

DISTORTION

$$\frac{\delta\rho}{\rho} \sim \frac{50\%}{B[kG]}$$

↳ B > 10 kG is needed for $\frac{\delta\rho}{\rho} < 5\%$

(see Friday talk of Smiltsev)

Motion of the electron beam excited by point charge displaced in X-direction Wake-field(s)=Const*[X(s),Y(s)]

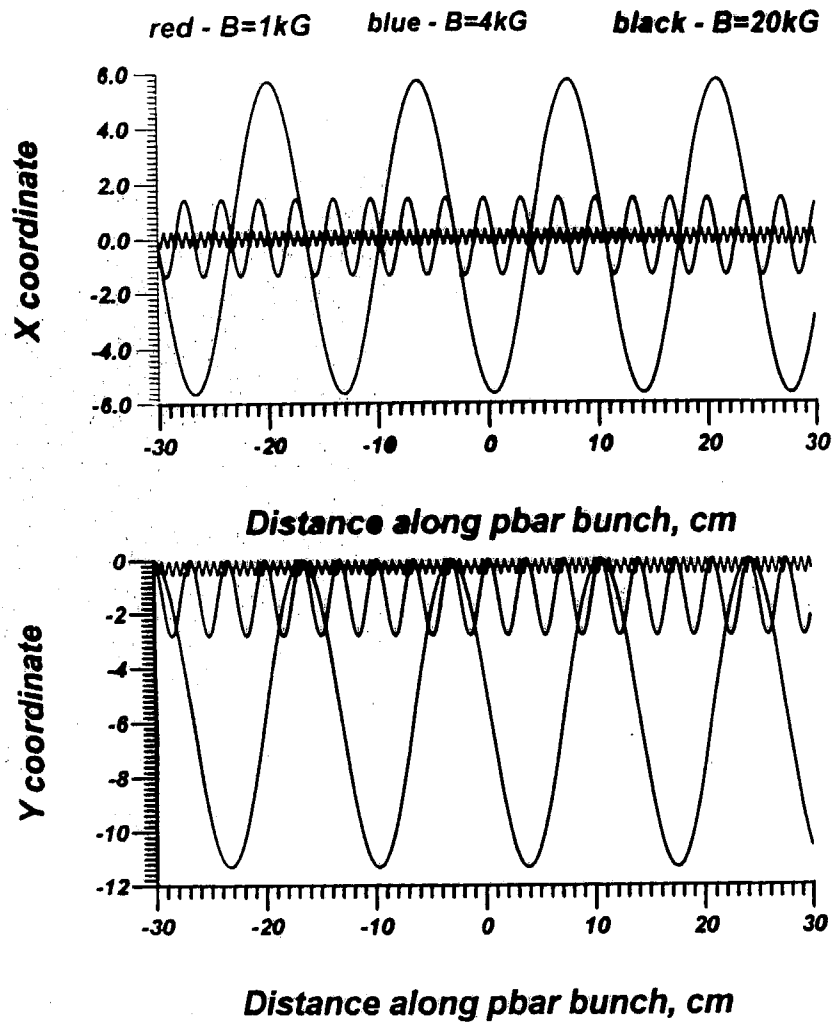

Minimum solenoid field B[kG] required to stabilize Pbar TMCI due to e-beam

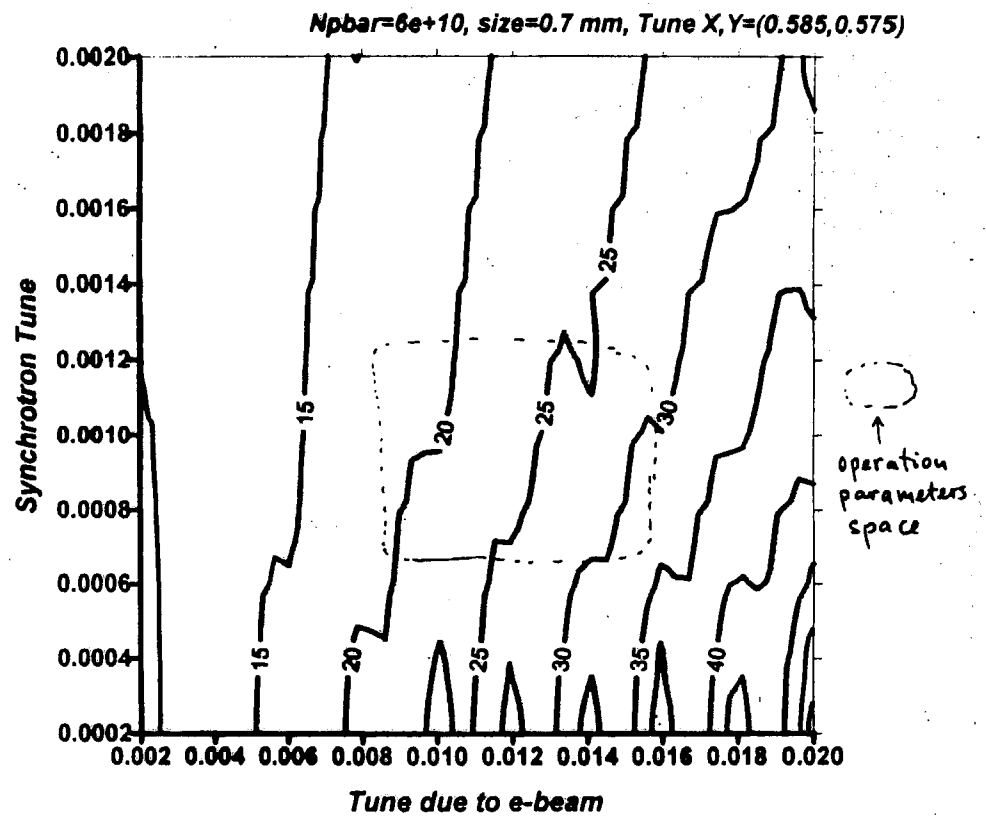

Choice of Solenoid Field:

IN LONGITUDINAL MAGNETIC FIELD $B(z)$; separate fast (Larmour) AND SLOW (distortion) MOTION:

$$x+iy = v(z)\cdot \exp\left\{-\frac{\int B(z)\,dz}{pc}\right\}$$

$$\frac{d^2 v}{dz^2} + v\cdot\left[\frac{1}{F_B^2} - \frac{1}{F_{\bar{p}}^2} - \frac{1}{F_e^2}\right] = 0$$

focusing $\quad F_B = \dfrac{6.6\,[mm]}{B\,[kG]} \quad @ \quad \beta_a = 0.2$

defocusing $\quad F_{\bar{p}} = \dfrac{1.2\ mm}{\sqrt{N_{\bar{p}}/6.10^{10}}} \quad @ \quad \beta_e = 0.2,\ \sigma_{\bar{p}} = 0.9\,mm,\ \sigma_s^{\bar{p}} = 35\,cm$

defocusing $\quad F_e = \dfrac{6.9\ mm}{\sqrt{J_e/1.4A}} \quad @ \quad \beta_e = 0.2,\ a_e = 0.9\ mm$

Pbar space charge	**B>0.5 kG**	. Fig
Electron space charge	**B>1 kG**	. Fig
5% elliptic distortion	**B>10 kG**	. Fig
TMCI due to electrons	**B>20-30kG**	. Fig

Adiabatic Magnetic Compression of Electron Beam

J=1.5A of electron current in about a=1mm radius corresponds to current density of :

$$j_e = \frac{J}{\pi a^2} \simeq 30\ A/cm^2$$

maximum from oxide cathode

$$j_{max} = 5-10\ A/cm^2$$

Solution: adiabatic compression in increasing magnetic field : $\quad \dfrac{\lambda_L}{B(z)}\dfrac{dB}{dz} \ll 1$

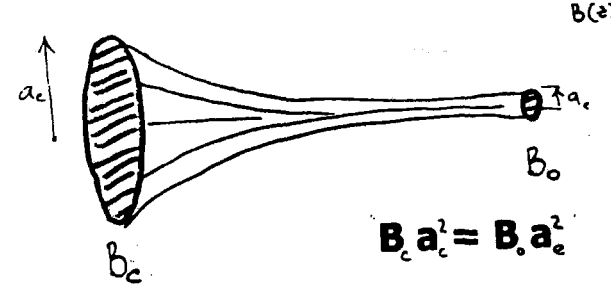

$$B_c a_c^2 = B_o a_e^2$$

E.g., B_c=200 G B_o=4 kG for bench test (no pbars)
a_c= 5 mm a_e= 1 mm
B_c=2 kG B_o=40 kG for Tevatron experiment

Choice of Electron Beam Energy

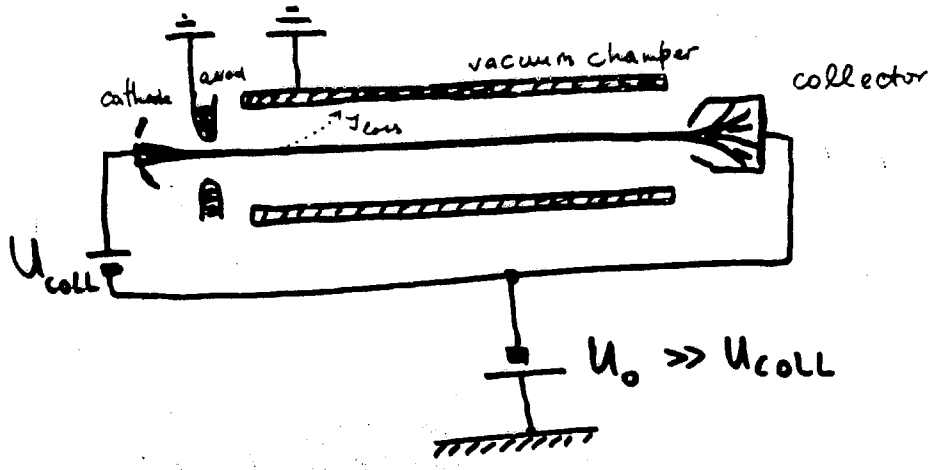

Required $N_e \simeq const(U_e) \rightarrow J_e = \frac{\beta_e e N_e c}{L} \propto \beta_e N_e$

$\beta_e = \sqrt{1 - \frac{2U_e}{mc^2}}$

Child's Law $J = P \cdot U^{3/2}$ $\quad$ P – GUN geometry dependent

$P \sim 0.2 - 5\ \mu P \equiv \mu A V^{-3/2}$

$\beta_e N_e \quad \beta_e^3$

$N_e \propto P \beta_e^2$ or $U_e \propto \frac{N_e}{P}$

Beam Power: $W_b = J_e U_e \propto U_e^{3/2} \propto N_e \left(\frac{N_e}{P}\right)^{3/2}$

e.g. $1A \times 10kV = 10kW$

$7A \times 20kV = 140kW$

Recuperation technique: $W_{recu} = J_{loss} \cdot U_e \simeq \alpha W_b$, $\alpha < 10^{-2}$

gives less power consumption + better vacuum near collector

High Perveance Electron Gun

Higher P: **less beam power**
lower voltage for modulation

Examples: LEAR GUN, $\mu P = 0.5$

$= 7.3 \mu P \cdot \left(\frac{a_c}{d}\right)^2$

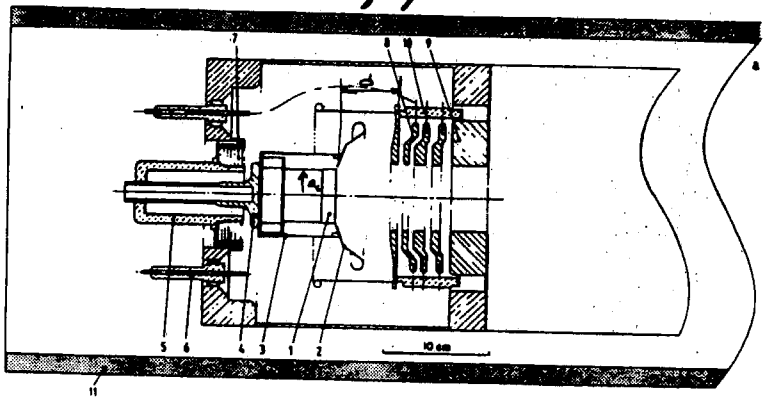

FNAL, F. Mills et al (1972)

$P \simeq 23$

$I = 28\ A$

$= 1\ A/cm^2$

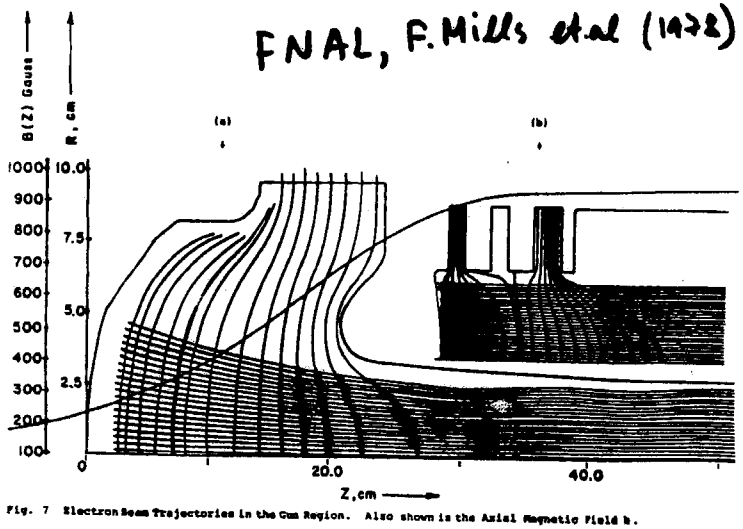

Fig. 7 Electron Beam Trajectories in the Gun Region. Also shown is the Axial Magnetic Field B.

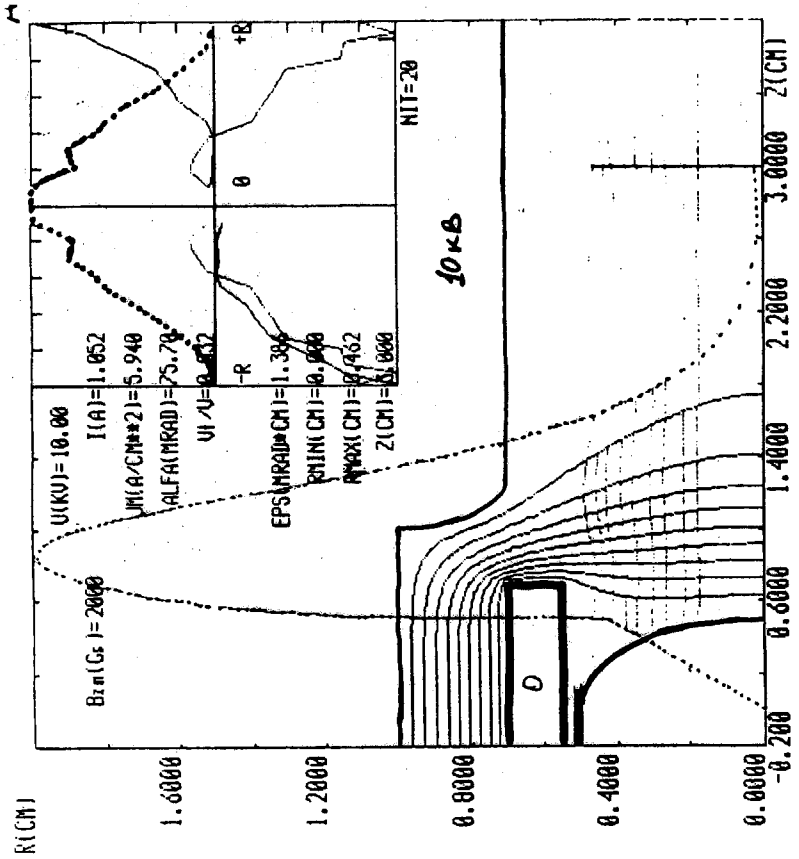

An 'IDEAL' GUN FOR E-COMPRESSOR

2A 7kV → μP=3.4

+ 132 ns modulation (low capacitance)

. current profile variation (by electrodes)

Other Important Issues

Turn-to-Turn Electron Current Stability

$$\frac{\delta J_e}{J} \lesssim 10^{-3} \text{ over } \Delta T = T_{TEV} = 21\,\mu s$$

OTHERWISE → EMITTANCE GROWTH

Talk Friday

Precise Solenoid Field

Deviation of magnetic field line $\delta x \sim 0.2\sigma_p \sim 0.2$ m

or field distortion $\frac{\Delta B_\perp}{B} \sim \frac{\delta x}{L} \sim 10^{-4}$

(especially important for nonlinear compensation)

Ion clearing of the electron beam

ion charge $\lesssim$ 1% × electron charge

OTHERWISE → DRIFT TWO BEAM INSTABILITY

Talk Friday

Impact on proton beam

Separation $\sim 10\sigma$

$$\Delta\nu_p \sim \frac{2\,\Delta\nu_F}{(d/\sigma)^2} \sim 2\cdot 10^{-4}$$

. but fields are only 10 times less...

Test of Beam-Beam Compensation with Electron Beam at the Tevatron
(R&D plan)

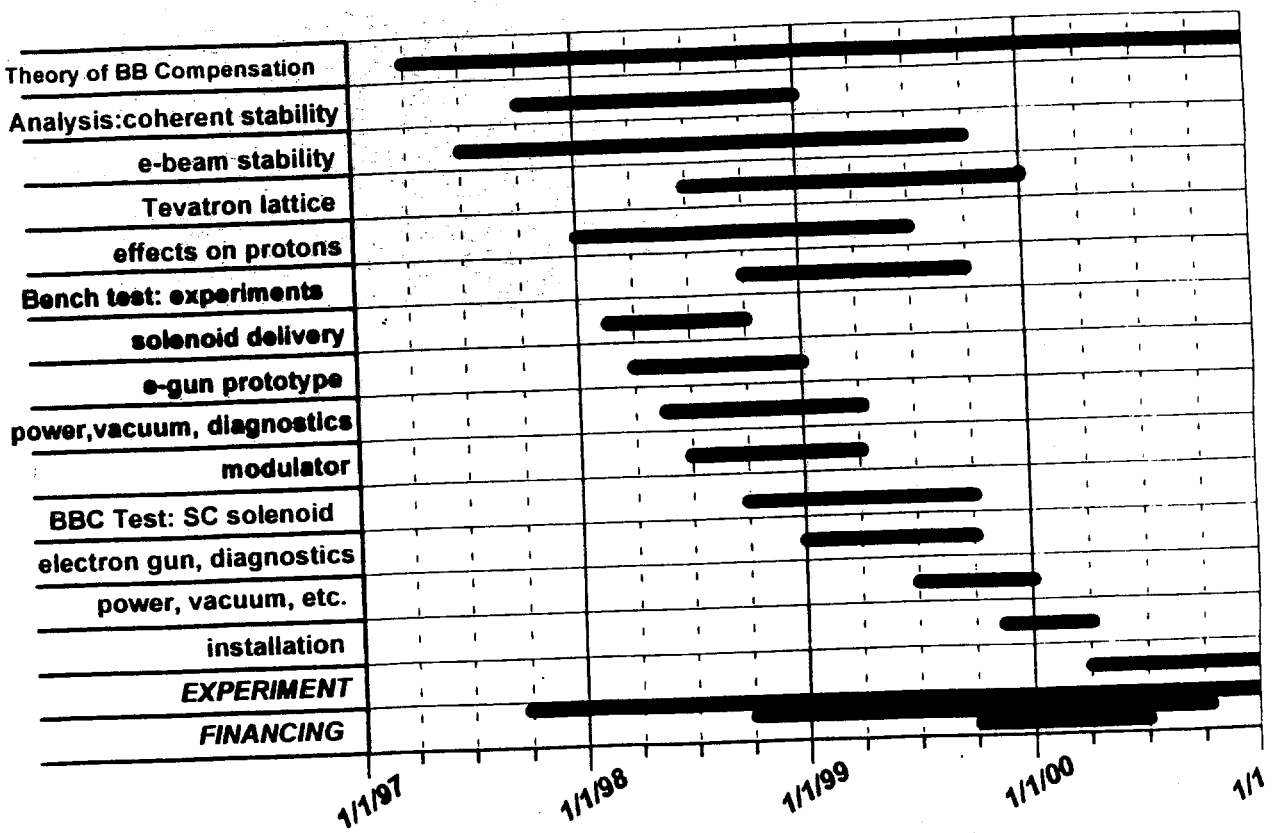

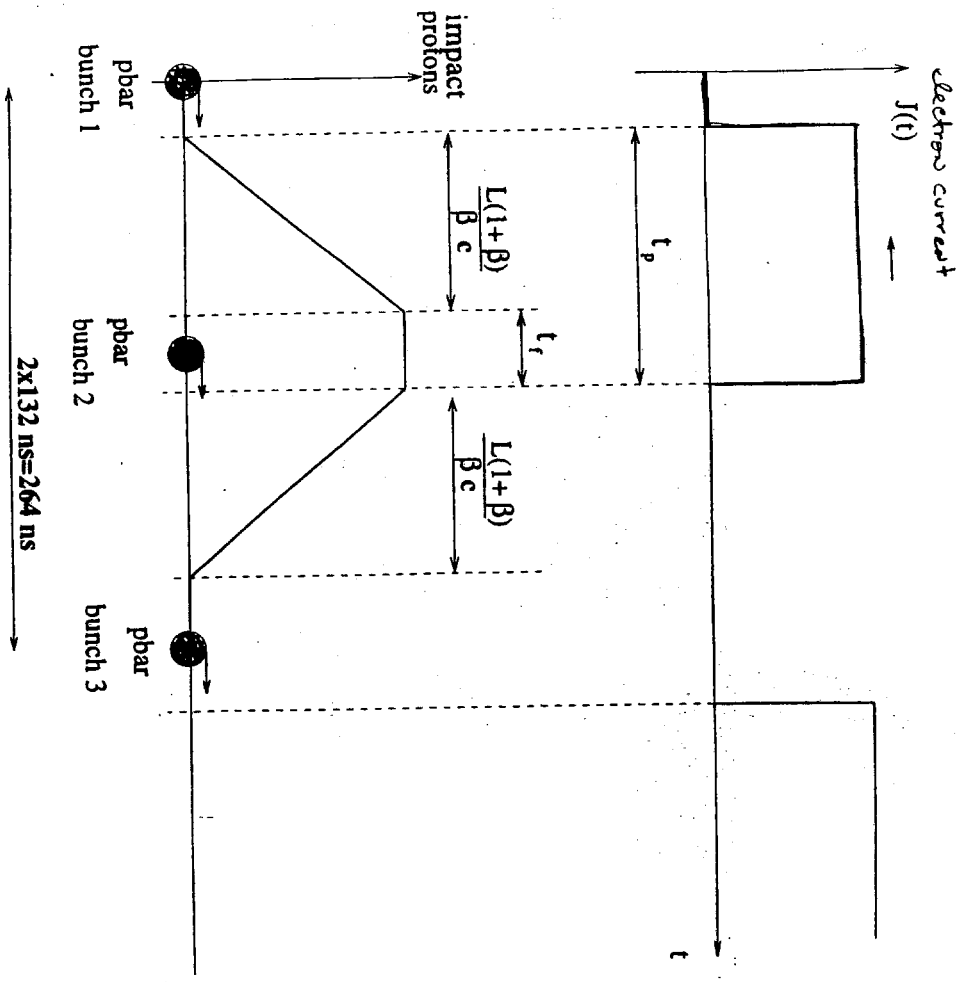

Choice of Electron Beam Energy (cont.)

Beam space-charge w.r.t. chamber walls

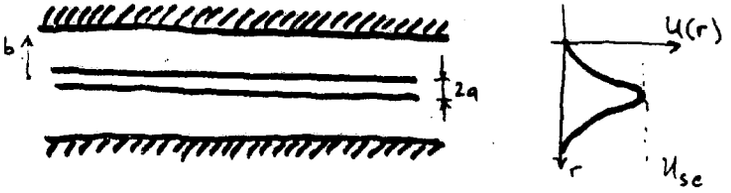

$$U_e > U_{sc} = \frac{2eN_e}{L}\cdot\left(\ln\frac{b}{a} + \frac{1}{2}\right) = 2.3\ \mathrm{kV}$$

$b = 60$ mm
$a = 1$ mm
$L = 3$ m

For fast current modulation, the electrons have to be fast enough • Fig.

$$\frac{L(1+\beta_e)}{c\beta_e} \le 132\ \mathrm{ns} \Rightarrow$$

$$\beta_e > 0.08 \quad \text{or} \quad U_e = \frac{\beta_e^2 mc^2}{2} > 1.6\ \mathrm{kV}$$

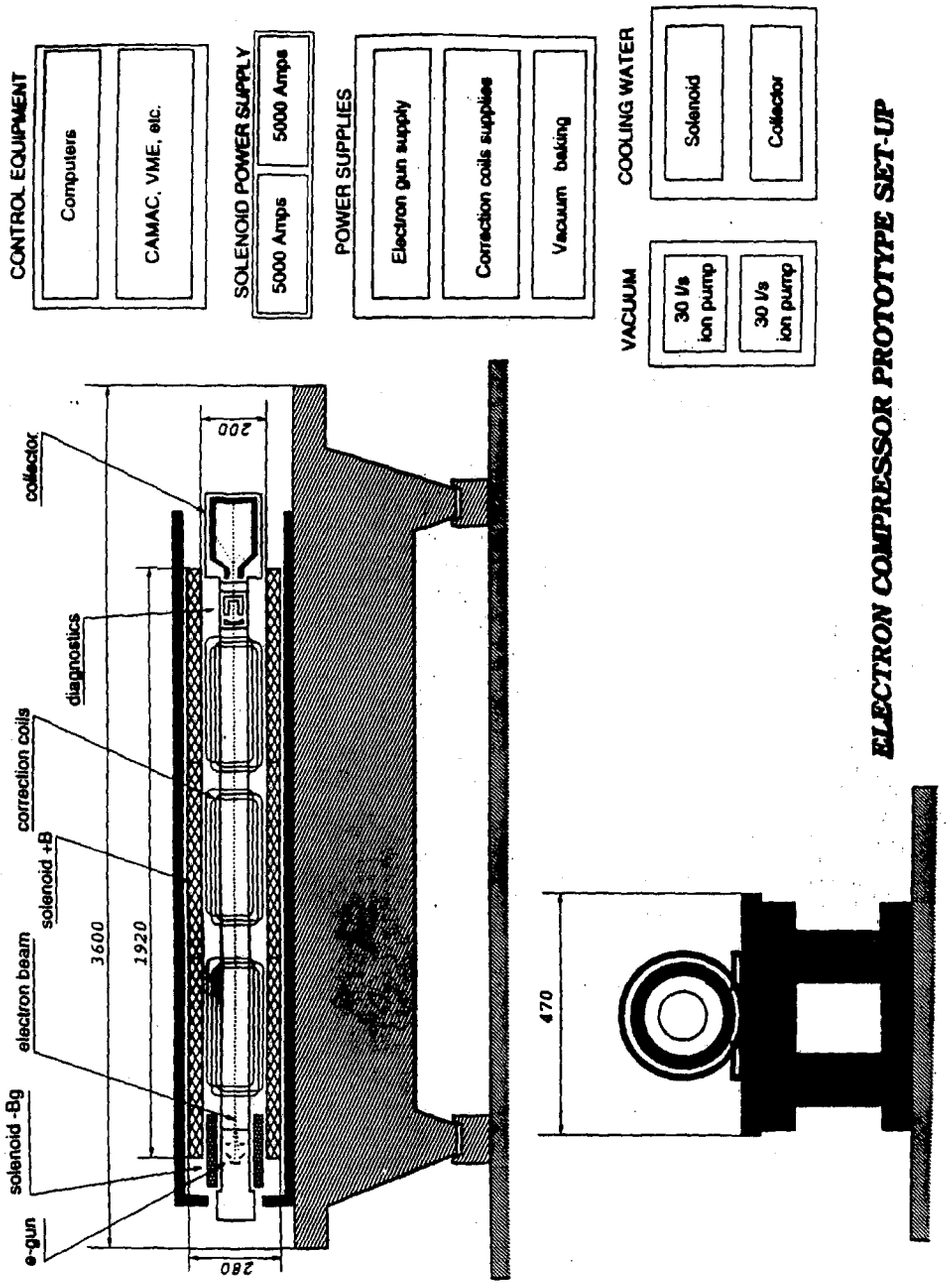

ELECTRON COMPRESSOR PROTOTYPE SET-UP

Where are we now?

Theory, analysis, simulations – this Workshop

Experimental test of electron beam For beam-beam compensation - see Fig.

Pressing Issues

= call for assistance, invitation to contribute

1. theory of beam-beam compensation with electron beam
2. modifications of the scheme
3. effect of the electron beam set-up on lattice functions
4. coherent stability
5. effects of ions, ion clearing
6. distortions of electron beam
7. high-perveance electron gun design
8. 5kV 132 ns modulator (continuous mode operation)
9. high-field solenoid
10. electron current fluctuation
11. electron beam diagnostics
12. pbar beam diagnostics

Q's:

Meshkov: You mentioned the TMCI as a major factor for choosing the magnetic field. I think, the e-beam distortion while pbars are coming through does play significant role.

Shiltsev: Both effects are comparable – see our Friday talks.

Nagaitsev: How are you going to measure (and, thus, control) the pbar bunch footprint?

Bagley: There is no reliable diagnostics for that in Tevatron now.

Shiltsev: One may rely on existing Tevatron models. Definitely, the e-beam distribution tuning will be done looking onto pbar or proton) beam loss rate and the beam size.

Slava DANILOV

Fermilab/Budker INP

Beam-Beam Effects in Presence of Electron Beam

#3

Beam-beam effects in presence of Electron Beam

V. Danilov

(FNAL/BINP)

1. Brief simulations of a weak-strong $\bar{p}$ behavior
2. Discussion of the problems.
3. New look at the problem: integrable systems with zero footprint
4. First results
5. Conclusions

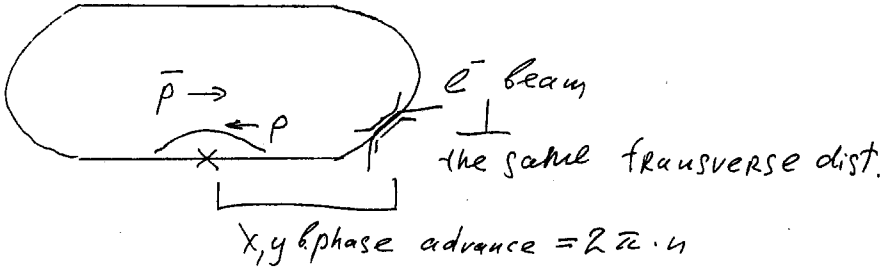

Parameters ~ (Tev 33)

$\beta_x = \beta_y = 35$ cm

$\ell_{\bar{p}} \approx 20\text{-}50$ cm

$\{\nu_x\} \approx .57$

$\{\nu_y\} \approx .58$

$\nu_s \approx 4.6 \times 10^{-3}$

Code — Kohji Hirata (KEK)

1) Symplectic map – includes Energy change due to opposite beam.
2.) Synchrotron osc. are taken into account
3) Statistics over 30.000 particles
4) $N_{turns} \sim 50.000$
5.) No nonlinearities of the ring.
6.) Noise on/off.

Maximal x-y amplitude vs. ξ_i.
$N_{turns} \sim 50.000$

Gaussian beam tails up to 2.8σ

Reminder $\Leftrightarrow$ $\xi_i \approx \frac{N r_0}{4\pi\gamma\varepsilon}$

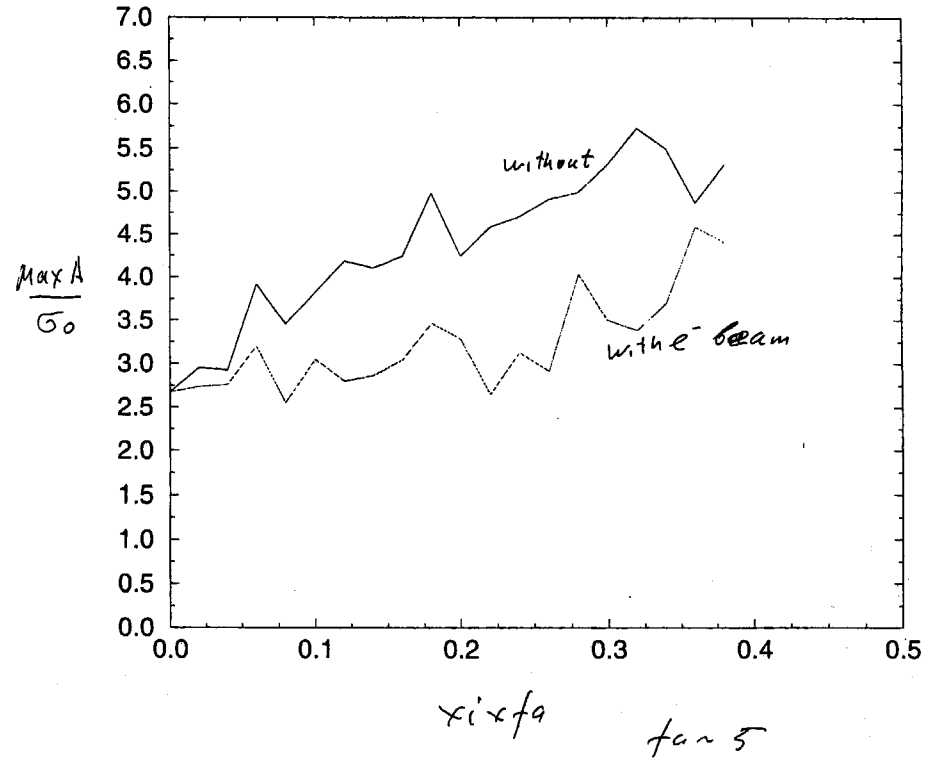

Transverse size vs. ξ_i.

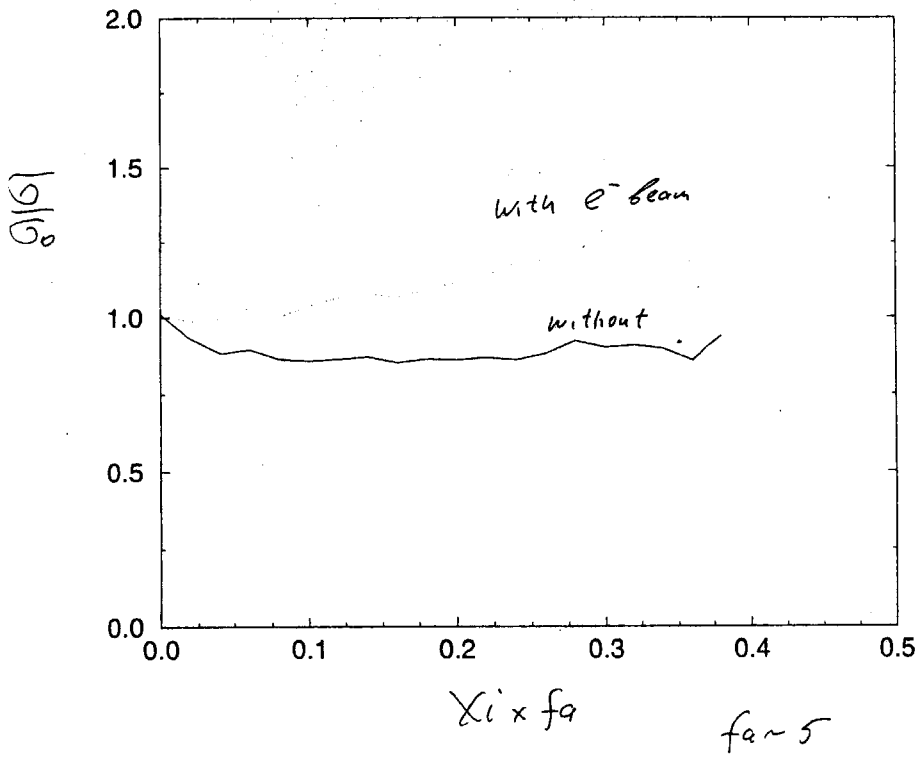

$\xi_i \sim .01$

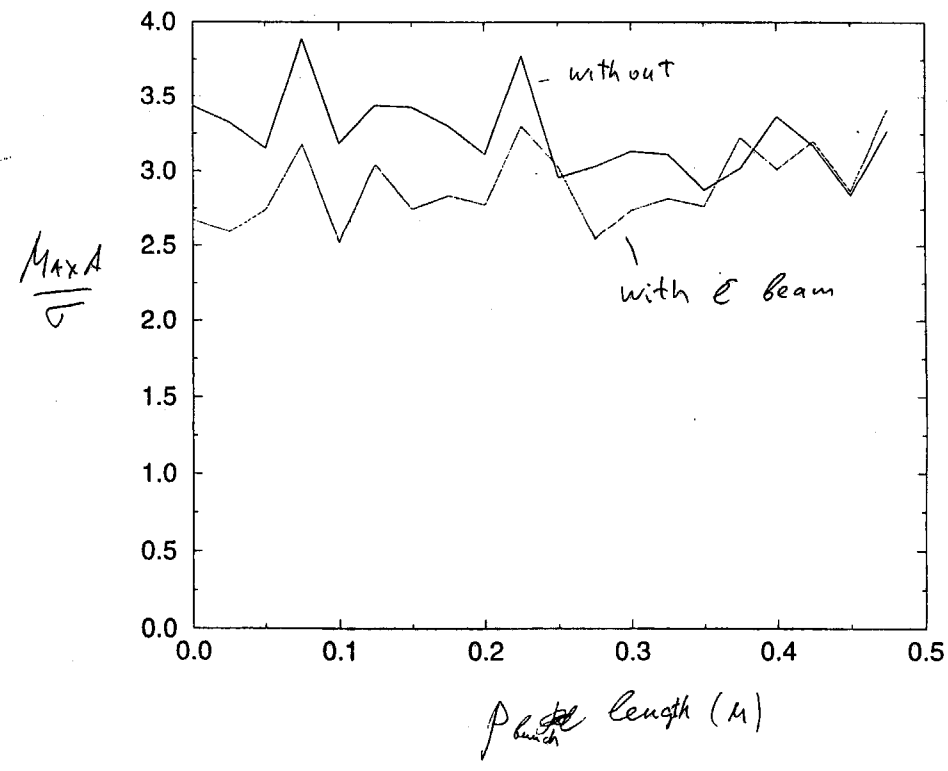

1 Beam-beam effects depend on bunch length.
(R Siemann, 1989)

b

Transverse size growth vs. longitudinal size

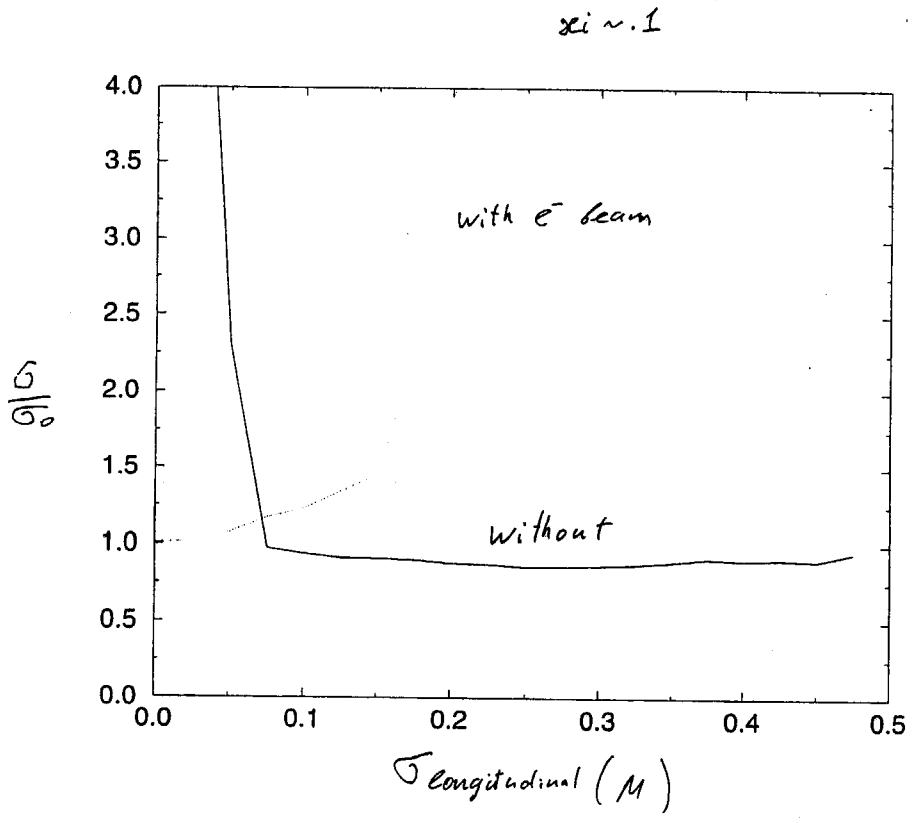

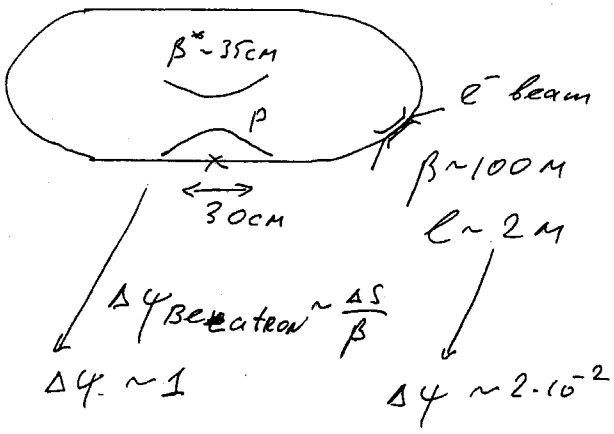

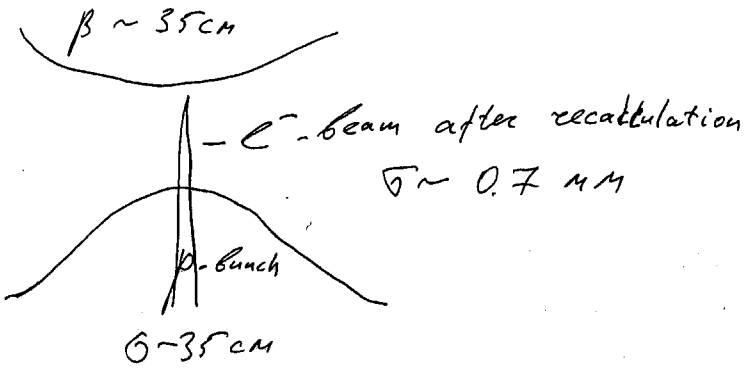

Limiting case

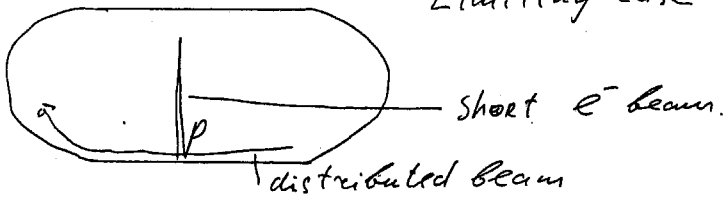

Preliminary conclusions

1 For $\xi i \leq 0.01$ e^- beam with the same tr. distribution can help

2 For $\xi i \gtrsim .01$ this scheme needs modification

3. In presence of strong nonlinearities of the ring it needs modification too

---

What is needed — elimination of resonances.

---

zero footprint zero strength of resonances

S. integrable systems

$\Downarrow$

Can be achieved by transformation of e^- beam distribution.

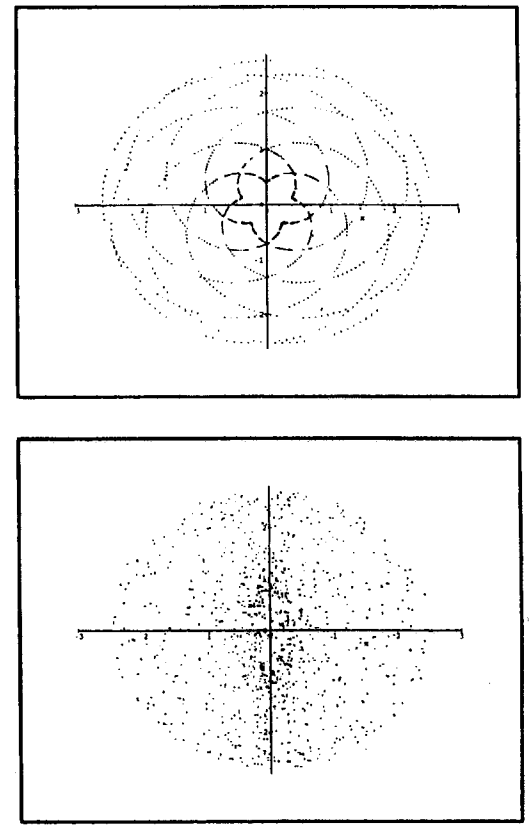

Figure 1: X-Y plane of the integrable map of example 1 (top) and the map without conservation of the angular momentum (bottom). The parameters of the kick are: $c = -2, a = 1, d = 1$. The initial conditions are: $x = 0, x' = 1, y = 1, y' = 0$.

a) Integrable systems

$\frac{1}{4}$ resonance force $\sim \frac{ax}{x^2+b}$

distribution $\sim \frac{1}{(x^2+b)^2}$

The motion is completely regular.

---

b) Integrable + zero footprint = 1 frequency

$$Map = \underbrace{U^{-1}}_{\text{inversed operator}} \underbrace{L_{in.}}_{\text{linear}} \underbrace{U(xp)}_{\text{operator of changing variables}}$$

For some variables the system is linear

Example

$$H = \frac{p^2}{2m} + \frac{m\omega_0^2 x^2}{2} + \frac{\varepsilon m x^3}{3} + \frac{m f(\varepsilon)}{4} x^4 \ldots$$

Iteration

$$f(\varepsilon) = +\frac{40\varepsilon^2}{3\omega_0^2}$$

$$\Delta\omega = \left(\frac{3 f(\varepsilon)}{8\omega_0} - \frac{5\varepsilon^2}{12\omega_0^3}\right) A^2$$

And so on

For time-independent Hamiltonian

Solution is shown in Landau, Lifshitz „Mechanics"

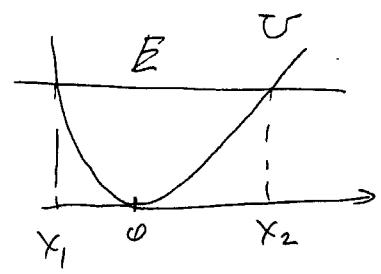

$$H = \frac{p^2}{2m} + U$$

$$x_2(U) - x_1(U) = \frac{1}{\pi\sqrt{2m}} \int_0^U \frac{T\,dE}{\sqrt{U-E}}$$

T - is period of oscillations

Numerical procedure

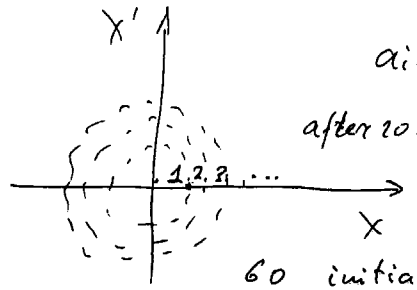

aim function for optimization

after 20 turns $= \sum_0^{60} \left((x-x_0)^2 + (x'-x'_0)^2\right)$

60 initial conditions up to 3σ (tr. size

distribution $= \sum_i^6 C_i e^{-\frac{i\varepsilon^2}{40\sigma^2}}$

Moderate xi -.05

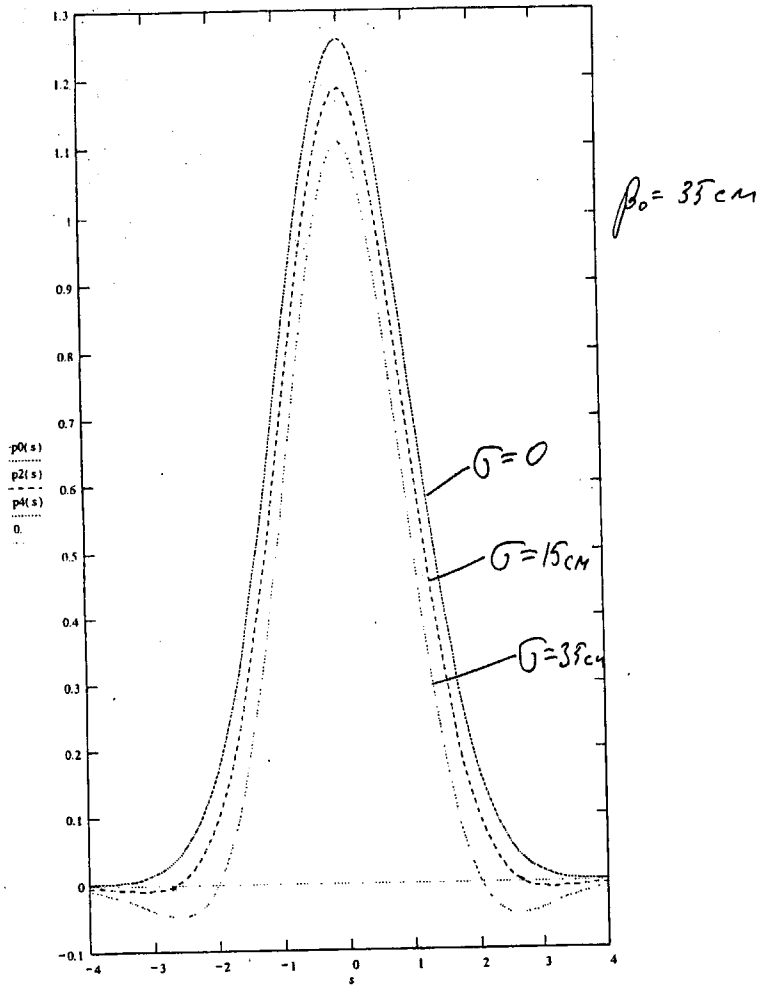

$\beta_0 = 35$ cm

$\sigma_{\parallel} = 35$ cm

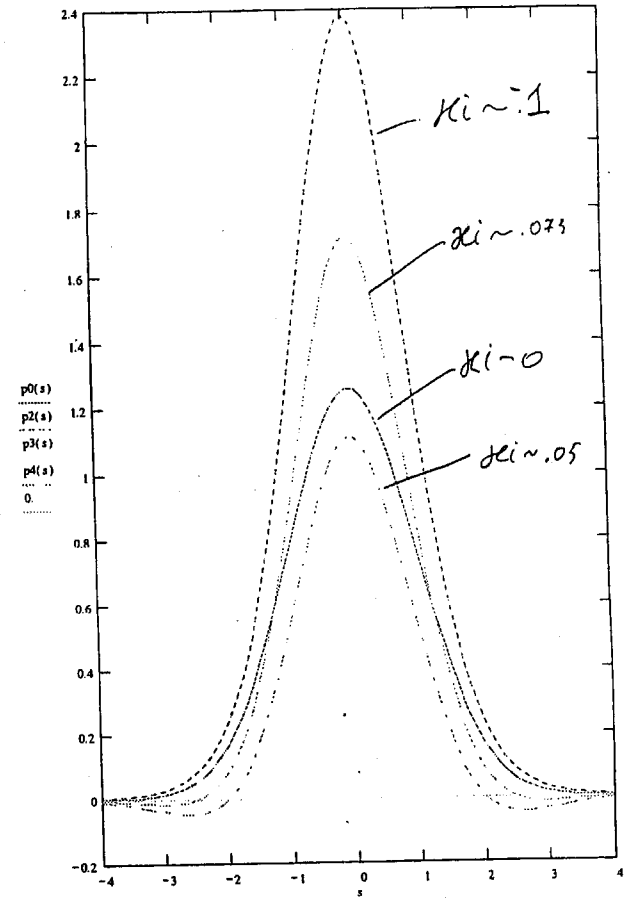

Problems

1 Nonlinearities of Tevatron – ?

2. Synchrotron motion

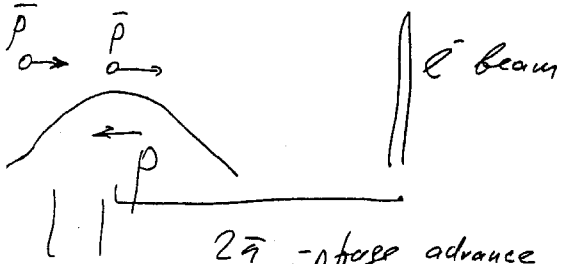

extra phase advance

System, which doesn't depend on it, must be found

3. The sensitivity of this system on parameters for non small ξ

Conclusion

1) By choosing appropriate e^- beam transverse distribution reducing of beam-beam effects and impact can be achieved in all the cases.

2.) Implication of integrable system with 0 footprint can be useful for e^+e^- fabrics.

It's convenient to use just round nonlinear lens (the solutions exist).

Q's:

Shiltsev: Is there an e-beam distribution which makes the resonance strengths equal to 0, while leaving non-zero footprint.

Danilov: Yes, and it can be found even easier than distribution for zero footprint and zero resonances strengths.

Stupakov: How the e-beam was represented in your simulations?

Danilov: As a very short nonlinear lens. It is effectively 0.7 mm long lens at IP.

Meshkov: One of issues is to eliminate the footprint dependence on synchrotron amplitude.

SLAC TRANS - 151

COLLECTIVE INSTABILITY OF COMPENSATED COLLIDING BEAMS

BY

YA.S. DERBENEV

Translated (January 1973) from the Russian *Kollektivnaya neustoichivost' kompensirovannykh vstrechnykh puchkov*. Preprint IYaF 70-72, Nuclear-Physics Institute, Siberian Division, Academy of Sciences of the USSR, Novosibirsk (1972), 9 pages. Presented at 3rd All-Union Conference on Accelerators, Moscow, 1972.

TRANSLATED FOR
STANFORD LINEAR ACCELERATOR CENTER

11th Int. Accl Conf. CERN, 1980

SPACE CHARGE COMPENSATION WITH DCI*)

J. Le Duff, M.P. Level, P.C. Marin, E.M. Sommer, H. Zyngier
Laboratoire de l'Accélérateur Linéaire, 91405 ORSAY CEDEX (France)

ABSTRACT

Extensive tests of space charge compensation, at the energy of .8 GeV, in similar conditions to those of the e^+e^- configuration are reported. Stability regions, smaller in size than those observed in that configuration, are found to decrease rapidly with current. Up to the limit, the beam cross-section stays constant. The value of ξ rather than the residual compensated value sets the limit. Comparison of the results is made to various predictions of the 4-beam instability : proximity of the integer and of non-linear resonances.

VOLUME 67, NUMBER 18 PHYSICAL REVIEW LETTERS 28 OCTOBER 1991

Coherent Beam-Beam Interactions in Electron-Positron Colliders

S. Krishnagopal
Lawrence Berkeley Laboratory, University of California, Berkeley, California 94720

R. Siemann
Stanford Linear Accelerator Center, Stanford University, Stanford, California 94309
(Received 15 August 1991)

Nuclear Instruments and Methods in Physics Research A313 (1992) 328–336
North-Holland

NUCLEAR INSTRUMENTS & METHODS IN PHYSICS RESEARCH Section A

Some aspects of the two beam performance of DCI

S. Krishnagopal
Lawrence Berkeley Laboratory, University of California, Berkeley, CA 94720, USA

R.Siemann
Stanford Linear Accelerator Center, Stanford University, Stanford, CA 94309, USA

Received 20 September 1991

PHYSICAL REVIEW E VOLUME 52, NUMBER 3 SEPTEMBER 1995

Coherent beam-beam interaction with four colliding beams

B. Podobedov and R. H. Siemann
Stanford Linear Accelerator Center, Stanford University, Stanford, California 94309
(Received 4 November 1994; revised manuscript received 12 April 1995)

The coherent beam-beam interaction in the absence of Landau damping is studied with a computer simulation of four space-charge-compensated colliding beams. Results are presented for the modes, phase space structures, widths, and growth rates of coherent beam-beam resonances. These results are compared with solutions of the Vlasov equation, and with measurements made at the Dispositif de Collisions dans l'Igloo (DCI) storage ring in Orsay, France, which operated with space-charge-compensated colliding beams.

PACS number(s): 29.27.Bd, 29.20.Dh

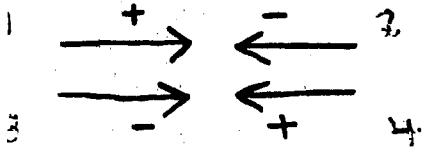

$Q_x = Q_y = Q_\beta$

BEAMS HAVE SAME CURRENTS, NOMINAL SIZES, SAME TUNES, β's, ...

THEORY EQUATION SOLUTION
Ya. S. DERBENEV – 4 BEAMS

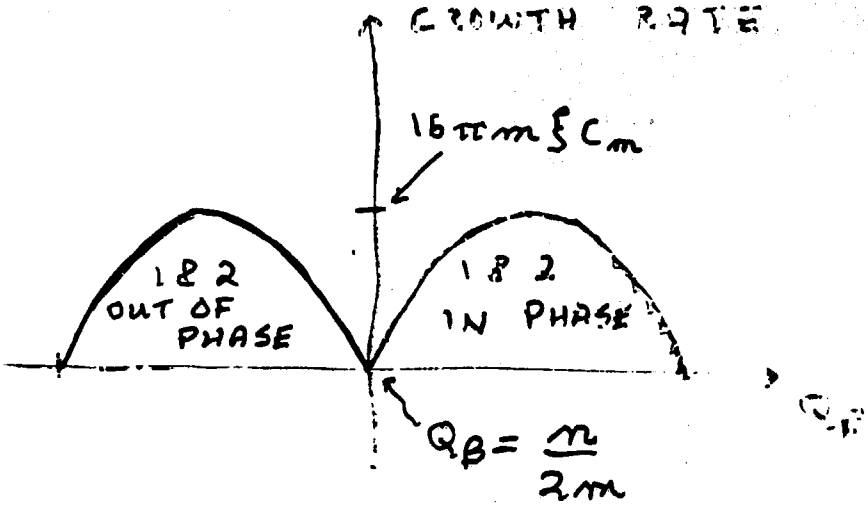

THERE ARE COHERENT INSTABILITIES WHEN

$$Q_\beta = \frac{n}{2m}$$

SINGLE BEAM B-B LINE SHIFT

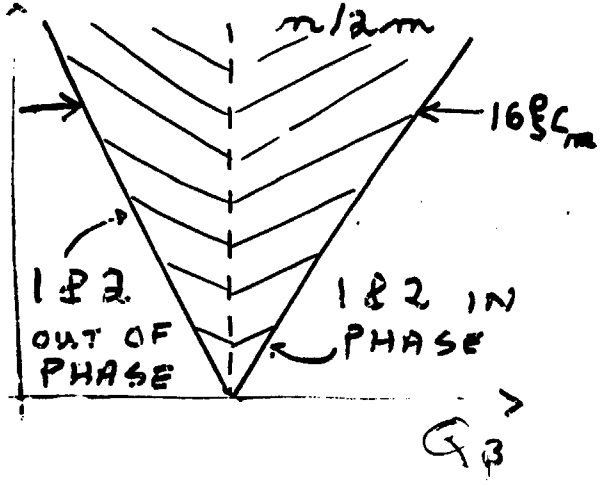

$$n = \frac{0.322}{m^{2.9}}$$

1 & 3, 2 & 4 ALWAYS OUT OF PHASE

SIMULATION

- P.I.C. CODE USING TECHNIQUES OF KRISHNAGOPAL & SIEMANN
- CIRCULAR MESH
  - 100 RADIAL BINS
  - 16 AZIMUTHAL BINS
- AREA WEIGHTING
- SPLINE SMOOTHING

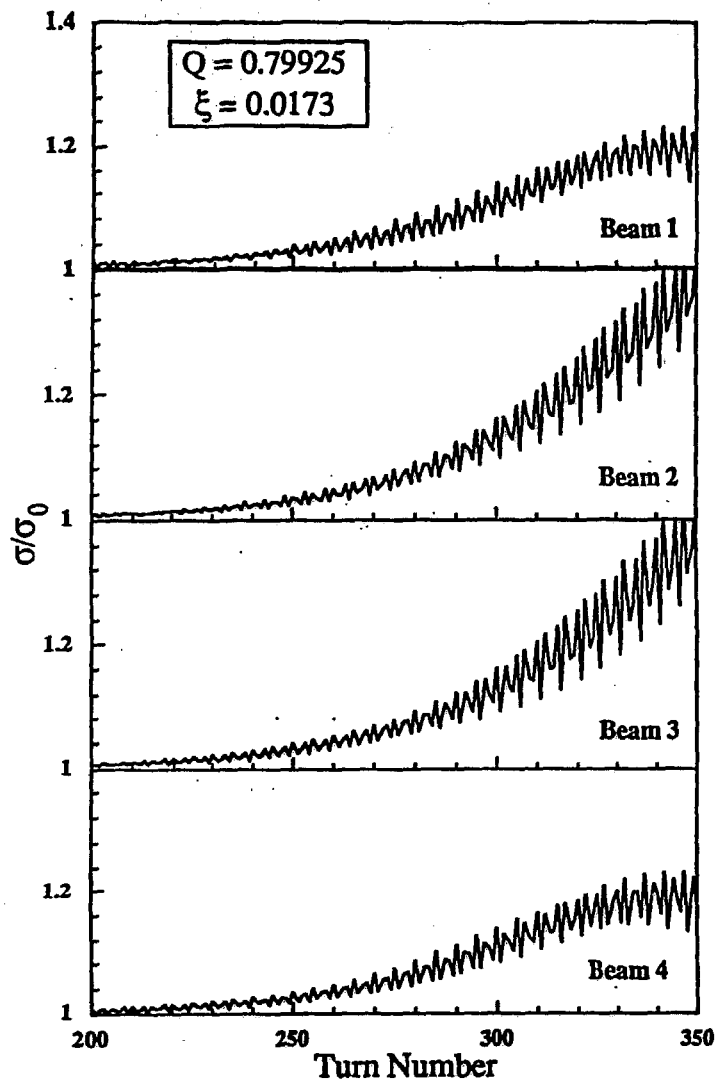

Figure 4: Horizontal beams sizes on the other side of the Q = 8/10 resonance.

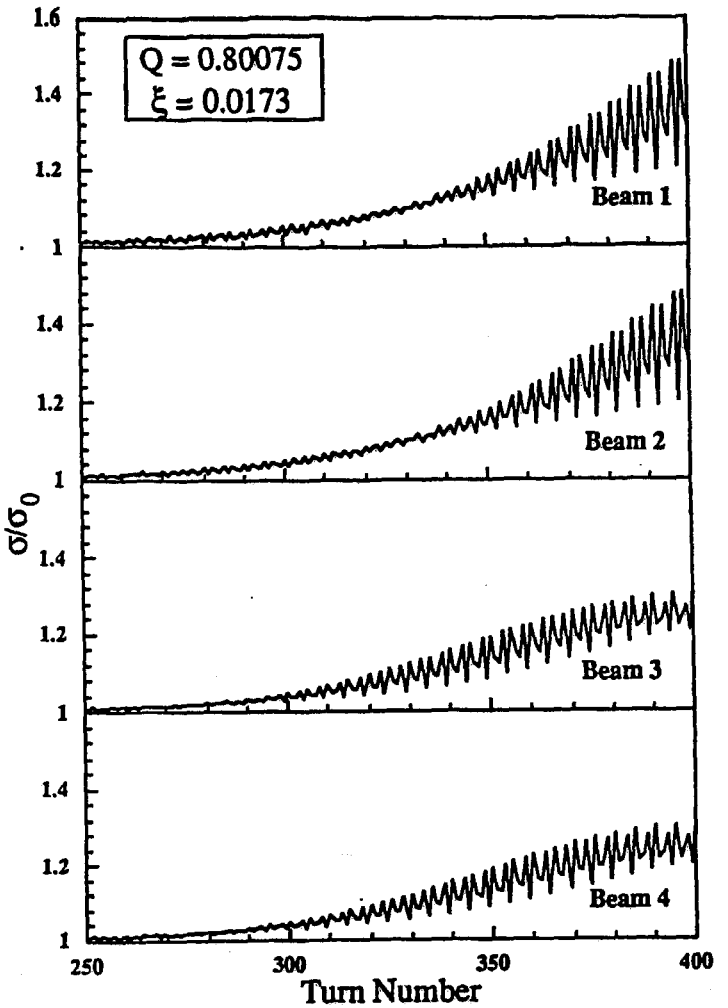

Figure 3: Horizontal beam sizes for turns 250 - 400 where the instability appears.

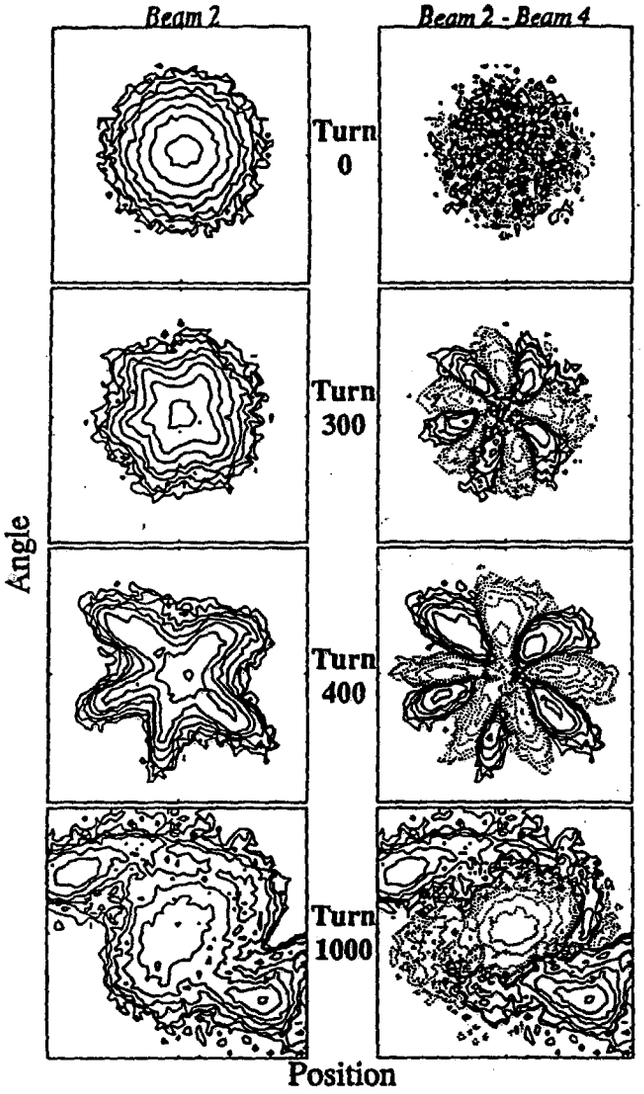

Figure 5: Horizontal phase space plots for Q = 0.80075 and ξ = 0.0173 for beam 2 (f_2) on the left and for (f_2 - f_4), the difference between beams 2 and 4, on the right. The plots cover ±5 times the nominal RMS sizes, and the dashed lines are contours of negative value.

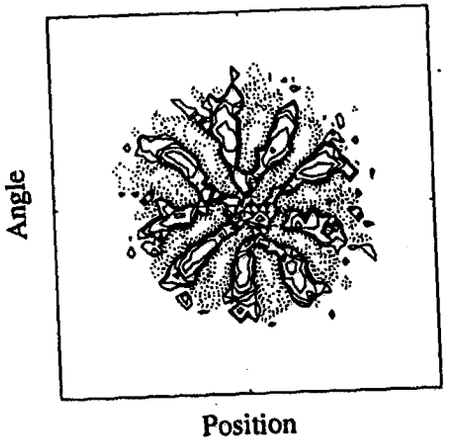

Figure 6: Horizontal phase space for Q = 0.777853 and ξ = 0.0173, a point within the Q = 14/18 resonance. The plots cover ±5 times the nominal RMS sizes, and the dashed lines are contours of negative value.

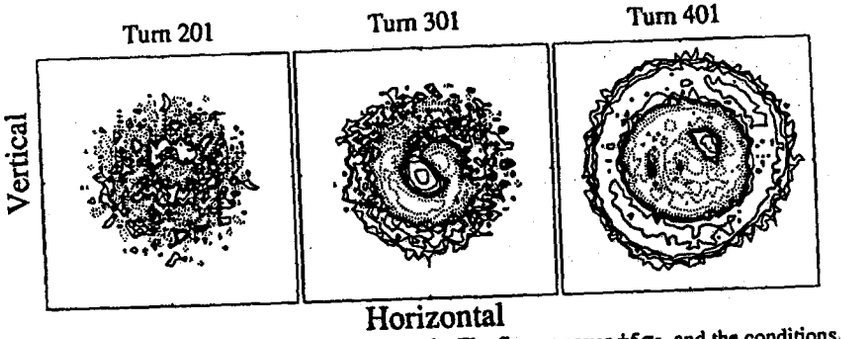

Figure 7: Contour plots in physical space for f_2 - f_4. The figures cover $\pm 5\sigma_0$, and the conditions are those of Figure 4: Q = 0.79925 and ξ = 0.0173.

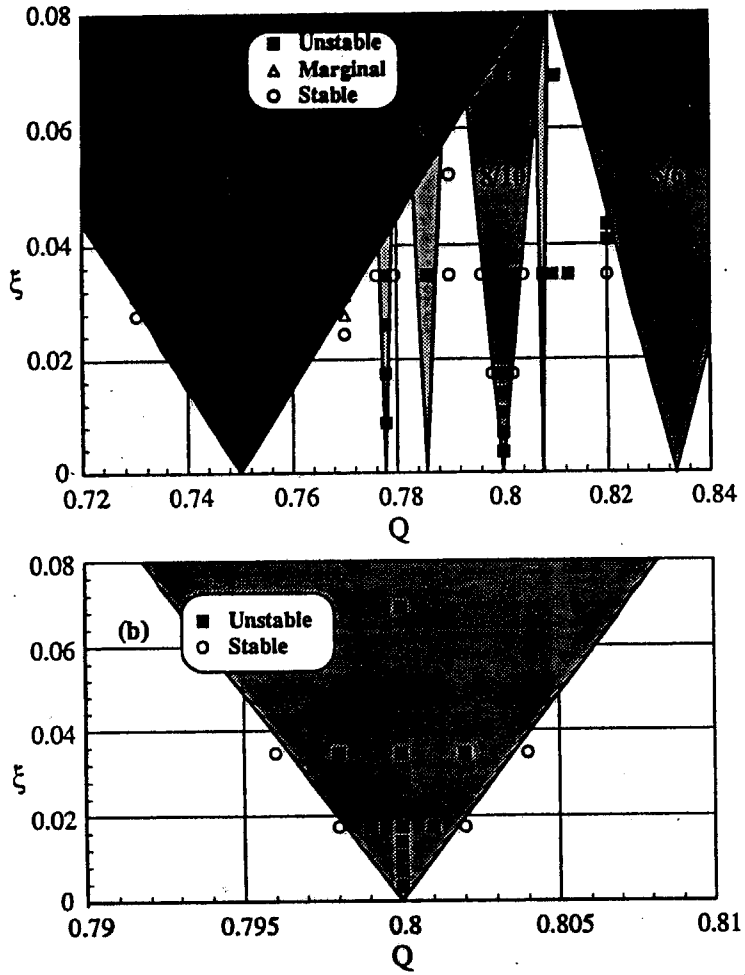

Figure 9: Stable and unstable regions after 20,000 turns compared with the resonance widths in eq. (21). In (a) the Q =3/4, 5/6, and 8/10 resonances are shaded and labeled, the Q = 11/14, 14/18, and 21/26 resonances are shaded, and there is an unstable point at Q = 0.8125 = 26/32. There is an expanded view of the Q = 8/10 resonance in (b).

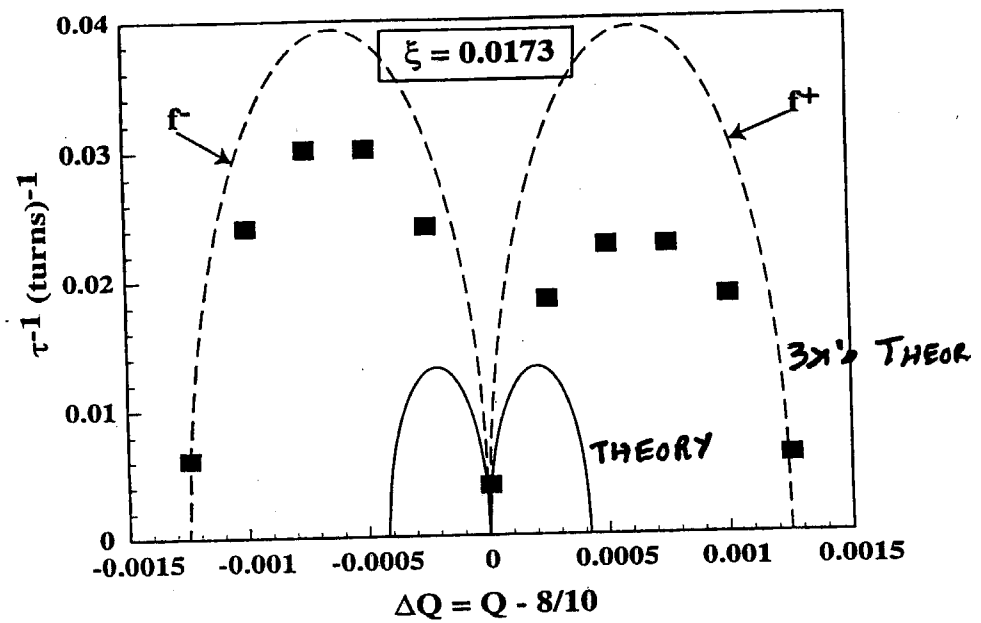

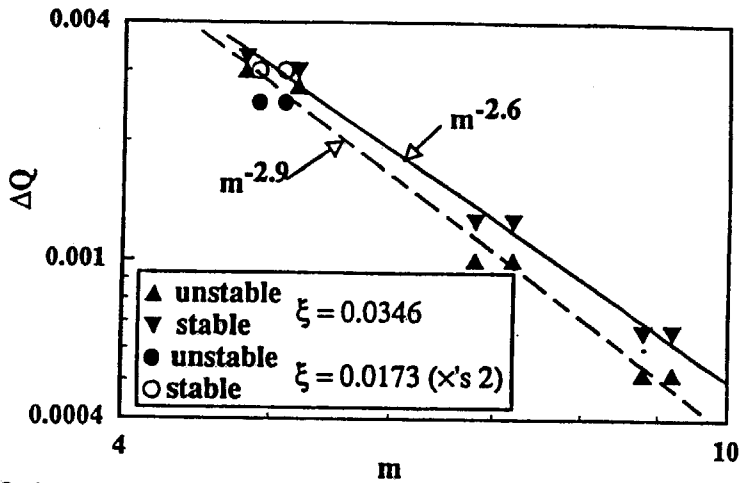

Figure 9: Resonance widths for different resonance orders. The first stable and last unstable points on each side of the resonance are indicated. The resonances are: 8/10 (m = 5), 11/14 (m = 7), and 14/18 (m=9). The resonance width for m = 5, ξ = 0.0173 was doubled for inclusion in the figure.

DCI PERFORMANCE

Four DCI operating points documented in LeDuff *et al*[8] were chosen for comparison between measurements and simulations. Two models of DCI, ONE and TWO, named after the number of interaction regions, were used. Reference [9] has details of these models. Parameters are given in Table 2.

Table 2: Parameters of DCI Models

Parameter		ONE	TWO
Interaction regions		1	2
Q		~0.88	~1.76
β* (m)	Horizontal	2.18	2.18
	Vertical	2.18	2.18
ε (μm)	Horizontal	0.282	0.282
	Vertical	0.015	0.015
Coupling Resonance Width[13]		0.001	0.002
Arc Errors [Horizontal, Vertical]		----	[.0005, -.002], [-.0005, .002]
Energy (γ)		1.57×10^3	1.57×10^3
Fractional Energy Loss per Turn		7.1×10^{-6}	14.2×10^{-6}
Feedback		No Feedback	No Feedback
Nominal Beam Sizes (μm)		569 (fully coupled)	569 (fully coupled)
Number of Test Particles/Beam, N_{TP}		10,000	10,000
Turns of Tracking		20,000	10,000

DCI = 2 CROSSINGS/TURN

La figure 24 montre que le paramètre de charge d'espace ξ dans le premier cas, croît linéairement jusqu'à .024, et dans le second cas sature pour la valeur .018.

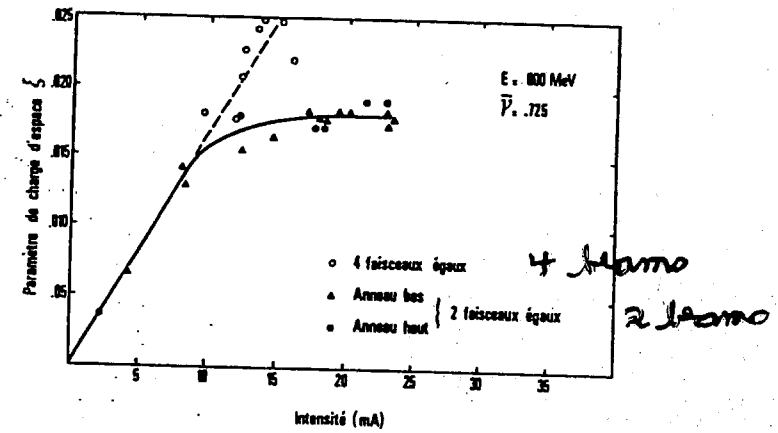

Fig. 24 : Comparaison des interactions à 2 et 4 faisceaux : ξ en fonction du courant à E = 800 MeV et $\bar{\nu}$ = .725

La luminosité totale maximum en e^+e^- obtenue avec 4 faisceaux compensés est de $1,2 \times 10^{29} cm^{-2}s^{-1}$, alors que la performance correspondante réalisée en e^+e^- avec chaque anneau séparément est de $6,7 \times 10^{28} cm^{-2}s^{-1}$ correspondant à des courants de 24 mA par faisceau (S^*/S^*_o = 2,5). Cette luminosité par anneau peut d'ailleurs être considérablement améliorée par un déplacement du point de fonctionnement (voir § 1), ce qui n'est pas le cas pour les 4 faisceaux compensés.

4.3 Influence du point de fonctionnement sur la stabilité à 4 faisceaux

4.3.1 Mise en évidence des résonances non-linéaires

L'influence du point de fonctionnement a d'abord été étudiée pour $3,6 < \nu_x < 3,9$ et $1,6 < \nu_z < 1,9$ avec deux points de croisement. On a utilisé les corrections quadrupôlaires en commande groupée, soit pour faire varier le nombre d'onde parallèlement ou perpendiculairement à la résonance de couplage, soit suivant ν_x et ν_z pour l'étude hors résonance.

Le long de la résonance de couplage, on observe des zones de stabilité discrètes comme en e^+e^- à un anneau (fig. 25), mais on constate qu'elles sont beaucoup plus petites pour des courants deux fois plus faibles et qu'elles sont situées à peu près à égale distance de deux résonances d'ordre relativement bas.

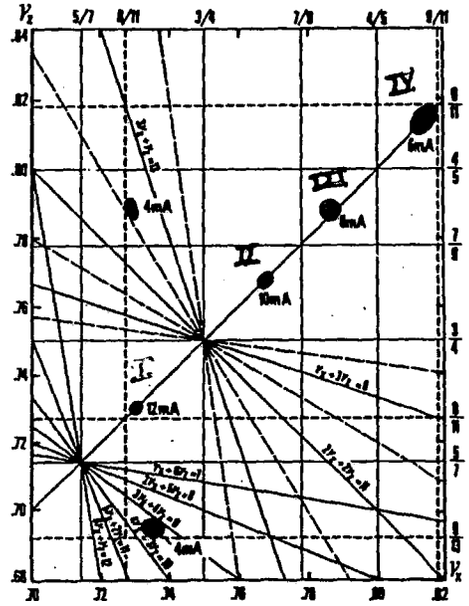

Fig. 25 : Diagramme de stabilité à 4 faisceaux compensés avec 2 points d'interaction à E = 800 MeV

Le tableau 5 montre que $\bar{\nu} + \xi$ et $\bar{\nu} - \xi$ ont une valeur limite proche d'une résonance non-linéaire. Le nombre d'onde $\bar{\nu}$ représente ici la valeur en bord de plage, et la quantité ξ calculée en supposant que la luminosité est la même en bord de plage qu'au centre, ce qui est vraisemblable puisqu'on n'observe pas d'augmentation de dimensions. On notera que les valeurs de ξ ne représentent pas des valeurs limites qui, elles, semblent être approximativement les mêmes pour les différentes zones : en particulier la zone IV faite à faible courant a sensiblement la même dimension que la zone I pour le même courant.

On notera par ailleurs que les résonances non-linéaires $\nu = .75$ et $\nu = .80$ sont respectivement d'ordre 8 et 10 pour deux points de croisement par tour.

	ξ	$\bar{\nu} + \xi$	p/q	$\bar{\nu} - \xi$	p/q	$\bar{\nu}$	$\Delta\nu$
Zone I	.022	.7540	.7500 (3/4)	.7060	.7140 (5/7)	.865	.003
Zone II	.018	.7880	.7780 (7/9)	.7470	.7500 (3/4)	.834	.002
Zone III	.014	.8030	.8000 (4/5)	.7710	.7780 (7/9)	.894	.002
Zone IV	.011	.8290	.8333 (5/6)	.7990	.8000 (4/5)	.907	.003

Tableau 5

PER LA STABLE REGION

Au vu des résultats précédents il semble que le paramètre important reste la valeur ξ, correspondant à l'interaction dans un seul anneau, et non le ξ_r résiduel de faisceaux partiellement compensés, ni même le glissement de fréquence cohérente $\pm 4\,\xi$ (mode dipôlaire).

En-dehors de la résonance de couplage, on observe également des zones de stabilité discrètes plus ou moins bien délimitées par des résonances non-linéaires couplées (fig. 25). Les courants limites obtenus à 4 faisceaux plats ne dépassent guère 4 mA. Un éventuel effet du ξ est ici plus difficile à introduire étant donné l'incertitude quant aux résonances qui jouent effectivement un rôle destructif.

On s'attendait à retrouver un effet des résonances non-linéaires dans l'interaction à 4 faisceaux en considérant, d'une part l'effet incohérent de la charge d'espace résiduelle due à une compensation imparfaite des faisceaux[11], et d'autre part les oscillations collectives de 4 faisceaux parfaitement compensés[12,13]. L'expérience montre que l'effet de ces résonances non-linéaires est beaucoup plus important que prévu.

Pour ce qui est de l'effet incohérent on estimait que les non-linéarités ne devenaient limitatives que pour des ξ_r résiduels du même ordre de grandeur que les ξ maxima que l'on réalise avec un seul anneau. Pour ce qui est de l'effet collectif, il n'était pas prévu, qu'il conduise, tout au moins pour un choix correct de point de fonctionnement, à un

Figure 10 shows the results for one point, Q = 0.865 and ξ = 0.022. There are strong, low order resonances, Q = 12/14 and Q = 7/8, on the two sides of this operating point leading to a region of width $\Delta Q \approx 0.011$ where the beam size has increased by less than 10% after tracking for 20,000 turns. This is to be compared with a measured stable operating region of $\Delta Q \approx 0.0020$ which was extracted from Figure 3 of reference [8] and reduced by a factor of two for comparison with the one interaction region model. The measured widths for stable operation at the four operating points are compared with the widths from simulation in Table 3. The simulation predicts stable regions 3 - 5 times wider than those measured.

The measurements themselves could be in error due to effects such as quadrupole power supply regulation narrowing the observed stable operating point, but this cannot be tested and must remain speculation at best. Synchrobetatron resonances could play a role, but the DCI bunch length was short compared to β^*, and the dispersion at the interaction region was small.[14] There are indications that phase advance errors between the interaction regions affected the DCI tune shift limit with two beams.[9] A simulation of DCI with two interaction regions and phase advance errors was performed to see if these errors affect the four-beam performance. These results are shown in Figure 10. Phase advance errors between interaction points do not change the width of the stable region in this case.

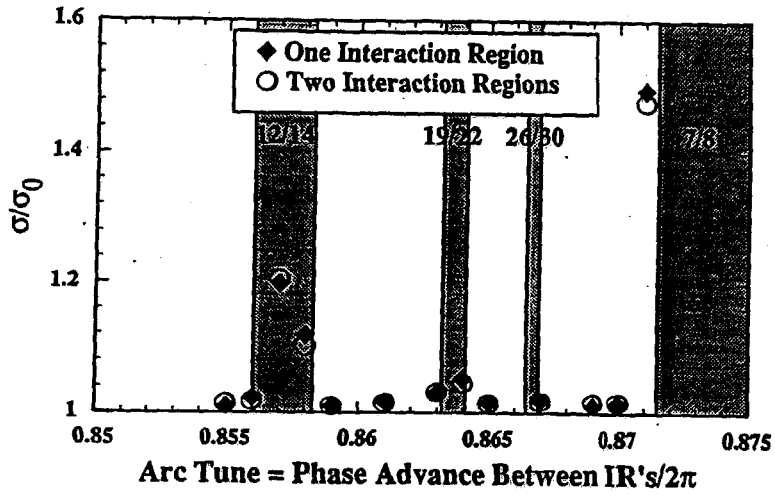

Figure 10: RMS beam size in DCI normalized to the nominal size for operating point 1: Q = 0.865, ξ = 0.0218. Even order resonances up to 30th order are plotted with widths from eq. (21).

Comparison of Measured and Simulated Widths of Stable Operating Regions

Region	I	II	III	IV
Q	0.865	0.884	0.894	0.907
ξ	0.022	0.018	0.014	0.011
Measured Width	0.0020	0.0027	0.0027	0.0034
Simulated Width	0.011	0.009	0.009	0.013
Bounding Resonances	12/14, 7/8	7/8, 16/18	16/18, 9/10	9/10, 11/12
Overlapped Resonances (up to 30th order)	19/22, 26/30	23/26	25/28	20/22

Measured widths are from LeDuff *et al.*[8] The table entries are the stable operating regions from Figure 3 of that reference divided by two for comparison with simulations of ONE.

SUMMARY AND CONCLUSIONS

- The simulation results are in excellent agreement with the qualitative features of Derbenev's theory:
  i) absence of odd order resonances for round beams
  ii) tune dependence of the stability of the f^+ and f^- modes
  iii) phase space structure of the unstable modes.
  iv) The widths and growth rates are comparable to those calculated, and the dependence on resonance order is in good agreement with that expected.

- The simulation agrees with the locations of stable operating points in DCI, but predicts operating regions three to five times wider than those measured. There are a number of possible explanations, but they are difficult to explore because DCI is no longer available for colliding beam experiments.

- High order coherent beam-beam instabilities (14th, 18th, 20th order) have been observed with modest beam-beam strength parameter, $\xi \sim 0.02 - 0.04$ The appearance of these high order resonances is in contrast to the two-beam situation where resonances higher than eighth order were never observed in simulation. The absence of Landau damping makes the coherent beam-beam interaction the important, limiting phenomena for space charge compensated colliding beams.

Q's:

Shiltsev: How precisely the four beams parameters were equalized? Is it about 5-10%?

Siemann: It is hard to say now, 20 years after experiment. At that time, people were rather limited with available beam diagnostics.

Danilov: May a feedback be used to cure those coherent effects?

Siemann: I doubt this, because of significant high order perturbations in the beams.

Shiltsev: What did happen while the working point was off the difference resonance?

Siemann: When the beams were not round, the coherent effects left even less freedom for operation and maximum stored current was much less.

Compensation Proposals for SSC and LHC

Alexandre Zinchenko
Joint Institute for Nuclear Research, Dubna, Russia

Mini-Workshop on Beam-Beam Compensation
Fermilab
February 12-13, 1998

---

1) The ideal compensation of the beam-beam effect would be an instantaneous collision of a "weak" bunch with a counterrotating beam of particles with a charge opposite to that of the "strong" bunch and the same transverse distribution. In this case the angular kick delivered to a primary proton by the space charge of the counterrotating proton bunch would be exactly canceled by the kick delivered by the space charge of the compensating beam.

2) In practice, the compensating collision point can placed in a more accessible location where the transverse beam distribution is the same as at the interaction point (but scaled). This could relax the requirement to form a beam of a very small size.

Deviation of the intensity of the individual proton bunches from the average value, if large, could be compensated by strobing the electron beam in time.

3) Stabilization of the electron beam:

- different electron energies,
- angular spread,
- magnetic field.

SSC parameters: $\sigma_x = \sigma_y = 100$ μm, $\sigma_z = 50$ mm, $E_{beam} = 20$ TeV, $N_{beam} = 10^{10}$.

LHC parameters: $\sigma_x = \sigma_y = 160$ μm, $\sigma_z = 77$ mm, $E_{beam} = 7$ TeV, $N_{beam} = 10^{11}$.

4) Design of a possible device for beam-beam effect compensation.

5) Conclusions:

"We believe that in this way it is possible to reduce the head-on beam-beam effect in practice...".

"The presented results show that for reasonable tolerances of the electron beam parameters it is possible to achieve a good beam-beam effect compensation with the resulting reduction of the beam tune spread by a factor of up to 100 and significantly improve the high-luminosity performance of future hadron colliders".

EF

SSCL -1 519

SSCL-Preprint-519

CERN LIBRARIES, GENEVA
P00018386

Compensation of the Beam-Beam Effect in Proton-Proton Colliders

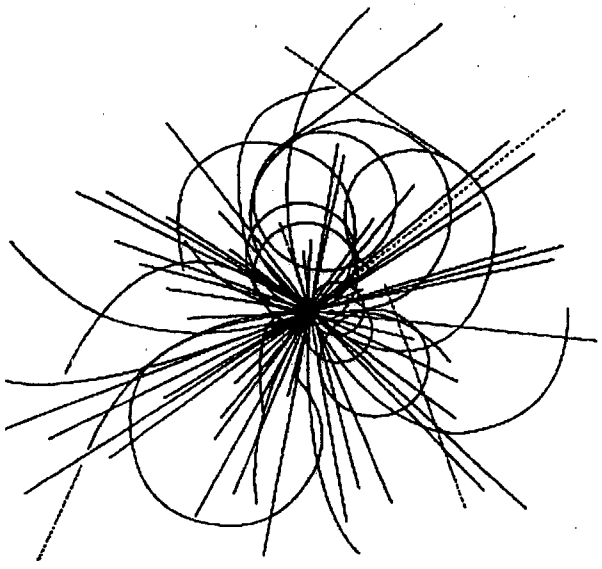

Superconducting Super Collider Laboratory

SSCL-Preprint-519
October 1993
Distribution Category: 414

E. Tsyganov
R. Meinke
W. Nexsen
A. Zinchenko

ОБЪЕДИНЕННЫЙ
ИНСТИТУТ
ЯДЕРНЫХ
ИССЛЕДОВАНИЙ

Дубна

E9-96-4

E.Tsyganov[1], A.Taratin[2], A.Zinchenko

COMPENSATION OF SPACE CHARGE EFFECT AT BEAM-BEAM INTERACTIONS IN PROTON-PROTON COLLIDERS

Submitted to «Physics Letters A»

[1]State University of New York, Albany, USA
[2]E-mail address: taratin@main1.jinr.dubna.su

1996

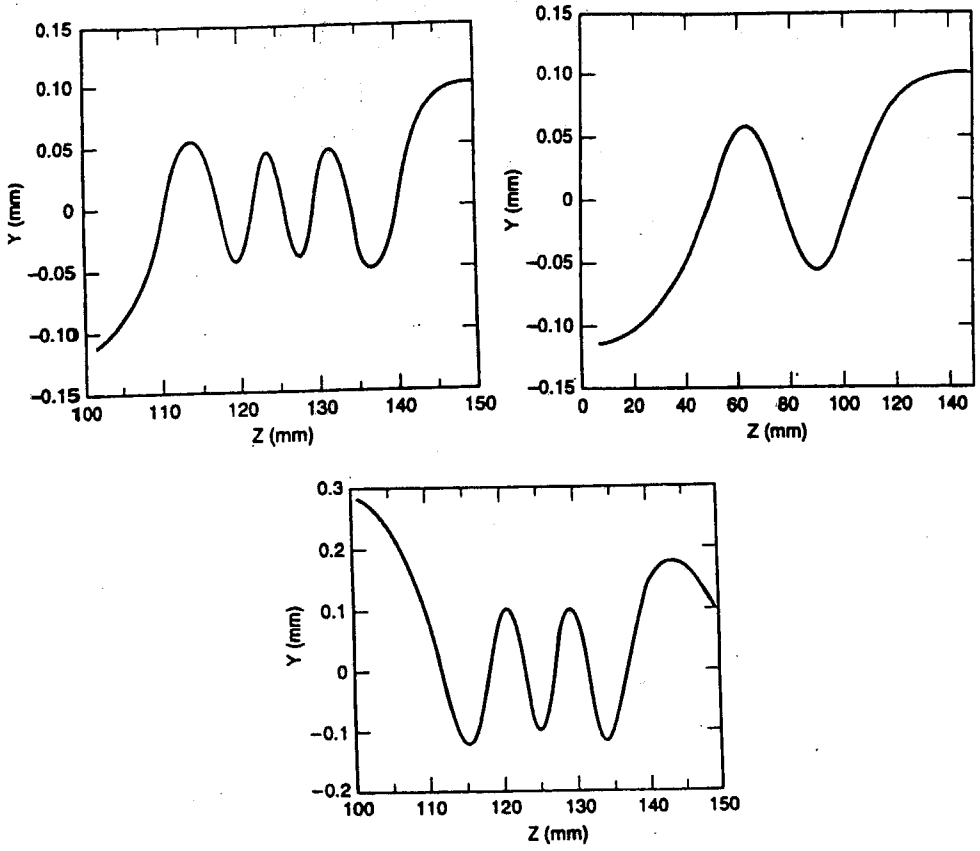

Trajectory of an electron with an impact parameter of 100 μm colliding with a proton bunch, Z-Y view. The proton bunch is moving to the right, and the electron is moving to the left. Plus/minus 3σ of the proton bunch charge distribution in Z-direction is treated by the tracing code. (top left) electron energy 10 keV; (top right) electron energy 1 MeV; (bottom) 10 keV electron with $\theta = 1°$.

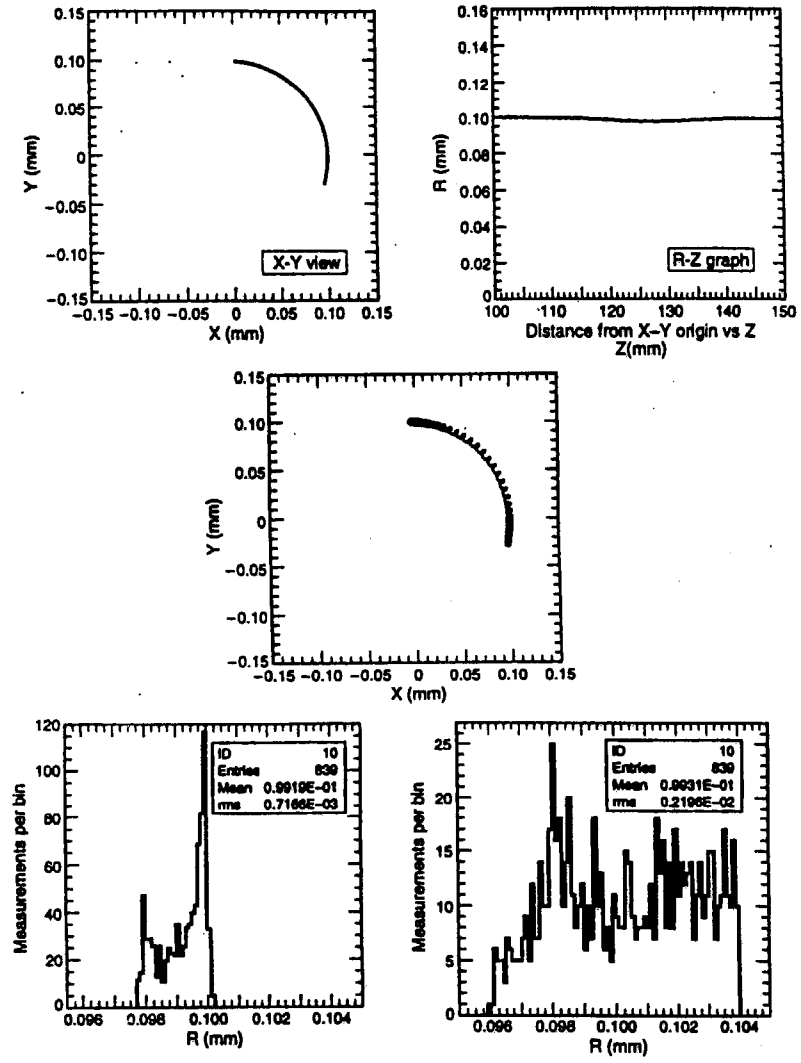

Motion of a 10 keV electron with an impact parameter of 100 μm colliding with a proton bunch when magnetic field is applied: (top row) $\theta = 0°$, (middle) $\theta = 1°$, (bottom row) distributions of the radial positions of the electron.

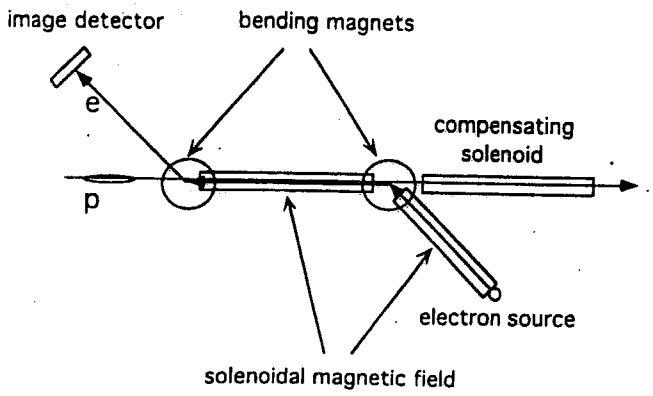

Schematics of a beam-beam compensating device. A low-energy electron beam collides with a bunch of protons. Electrons are kept stable in space by a solenoidal magnetic field. After collision with the proton bunch, an electron beam is deflected to the image detector, which is used to steer the electron beam relative to the proton bunch.

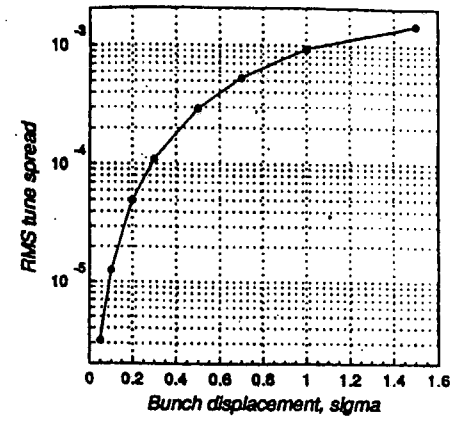

RMS tune spread of the proton beam particles versus the electron beam displacement. The rightmost point corresponds to the case without compensation. The curve is drawn to guide the eye.

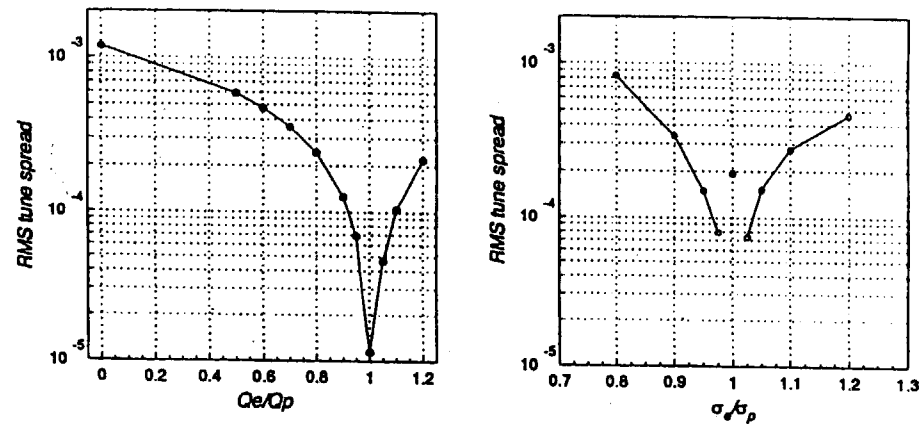

RMS tune spread of the beam particles: (left) versus the ratio of the electron to proton bunch charges. Displacement of the electron bunch is 0.1 σ. The leftmost point corresponds to the case without compensation. (right) the ratio of the rms size of the electron to proton bunch (white circles). Black circle presents the result for a cylindrical electron bunch (with radius r_e=1.3σ_p and Q_e=0.6Q_p).

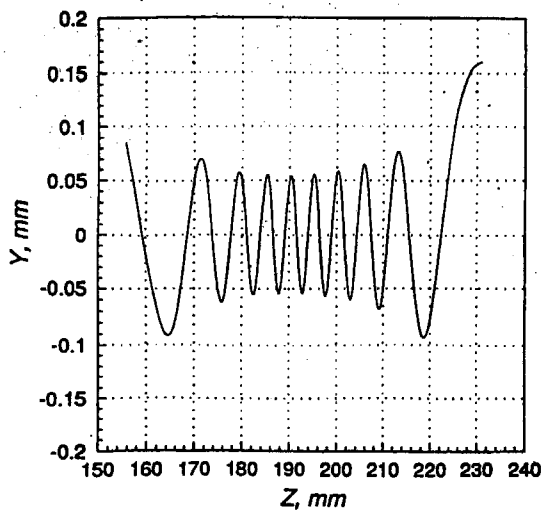

The trajectory of a 10 keV electron with an impact parameter of 160 μm colliding with a proton bunch, Z-Y view. The proton bunch is moving to the right, and the electron is moving to the left. Plus/minus 3σ of the proton bunch charge distribution in Z-direction is treated by the tracing code.

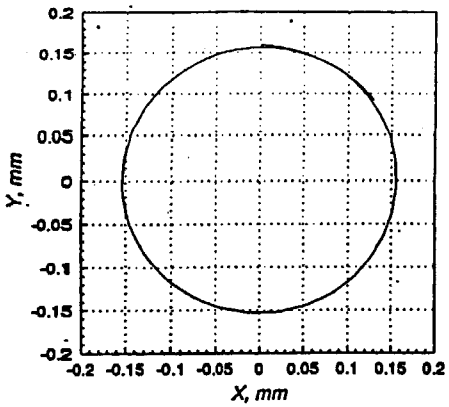

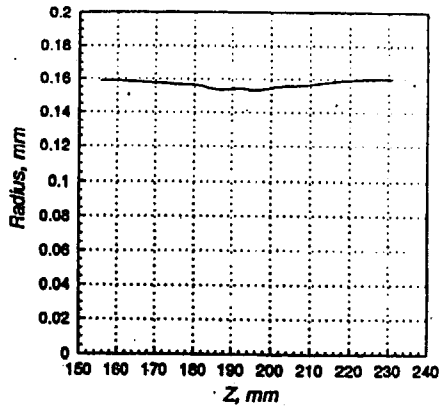

The trajectory of a 10 keV electron with an impact parameter of 160 μm inside a proton bunch when a solenoidal magnetic field of 2 T is applied: (left) X-Y view, (right) Z-R view (R is a distance of an electron from the center of a proton bunch).

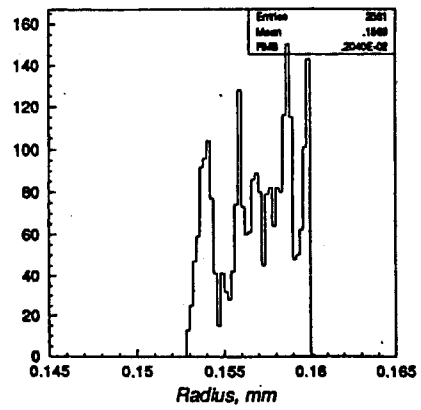

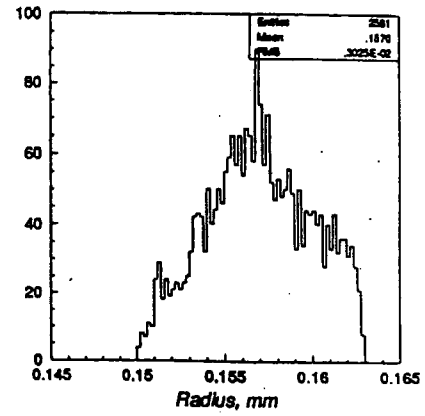

Distribution of the radial positions of the electron with incoming angle of 0° (left) and 1° (right).

Comment:

Shiltsev: The electron beam with reduced current can be used for p(bar) diagnostics too.

#6

WHAT COULD WE GAIN WITH BEAM NEUTRALIZATION IN LHC ?

Hans Riege

CERN LHC-Division, CH-1211 Geneva 23, Switzerland

Talk held at the Mini-Workshop on Beam-Beam Compensation,
Fermilab, February 12-13, 1998

Contents

1. **Background**
2. **Principle of LHC Bunch Space-Charge Neutralization**
3. **Practical and Design Considerations**
4. **Advantages for LHC Collider and Experiments**
5. **Conclusions**

1. Background

Only few practical attempts have been made to neutralize space-charge and current in high energy particle accelerators: for example

- **DCI/Orsay**, (not successful)
- **ATA/LLNL** (successfull)

However, there are well-known examples in the fields of:

- **Power generation** technology: **neutral beams** for MCF tokomaks,
- **Space technology**: **neutralized ion beam propulsion** systems for space-craft and satellites,
- **Integrated circuit techn.**: **space-charge compensated ion sources** for ion implantation.

Due to the rules of electricity the first two examples do not work at all without beam neutralization, the third case is an enhancement of emitted ion current compared with a Langmuir-Child limited source.

- Proposals for (heavy) ion **ICF drivers**:

  - HIGHBALL/ GSI
  - ICF - Driver proposed by C. Rubbia/CERN, GSI and European Community Study Group

do **ONLY** work, if the beams approaching the fusion target are **FULLY NEUTRALIZED.**

The question is:

why are **neutralization techniques**, which are **strongly supported by nature** and which are successfully applied in various fields of technology, so rarely considered in **accelerator technology?**

My own interest in this field is based on previous practical activities on similar topics, such as:

- neutralized, high-density electron beams from pseudospark plasma sources,
- current carrying plasma lenses,
- heavy ion source enhancement by neutralization with intense low-energy pulsed electron beams from ferroelectric cathodes.
- LHC beam space-charge reduction by screening or compensation (outside magnetic dipoles and quads) in order to minimize power losses via (photo-)electron clouds.
- In context with the latter problem I started to consider the potential advantages of neutralizing locally the space-charge of the LHC beams with low-energy electron beams near and at the **LHC interaction points (IP)**.

  Mostly **special technologies** are required when using the strong forces and materials of nature: ferromagnetics, ferroelectrics, super conductors, etc.

2. Principle of LHC Bunch Space-Charge Neutralization

The condition for complete space-charge neutralization of an ion beam of density n_i with electrons of density n_e is

$$n_e = Z\, n_i \tag{1}$$

If both types of charged particles are moving (beams) the condition holds

$$j_e = j_{LHC} \times v_e / c \tag{2}$$

Hence, it is **favourable to neutralize a relativistic ion beam with low-energy electrons** (e.g. the peak LHC bunch current of 60 A can be neutralized with 0.5 A electrons provided both currents occupy the same cross section).

The radial electric self-field

$$E_r(r) = \frac{j_{LHC} \cdot r}{2c\varepsilon_0} \tag{3}$$

and the azimuthal magnetic self-field

$$B_\varphi(r) = \frac{\mu_0 j_{LHC} \cdot r}{2}. \tag{4}$$

of the ion beam of radius σ and current density j_{LHC} cancel each other in the relativistic limit and for $r < \sigma$.

When E_r is neutralized, very strong forces are exerted on the beam by the remaining magnetic field of the ion beam (more than 0.5×10^5 T/m near the LHC IP's), as long as the electrons move slowly. The neutralization scheme proposed here aims to use these strong forces intelligently for improving the performance of the accelerator at the loction of the high energy physics experiments.

For a distance along x from IP greater than a few times the final focus radius σ_f at IP, the beam envelope can be approximated by the equation for the 'outer' trajectory

$$\sigma \cdot \frac{d^2\sigma}{dx^2} + \frac{e \cdot \mu_0 Z \cdot I_{LHC}}{2\pi\gamma m_i c} = 0 \tag{5}$$

Equation (5) leads to the tangent $\sigma' = d\sigma/dx$ of the **'beam envelope'**

$$\frac{d\sigma}{dx} = -\sqrt{B - 2A\ln\sigma} \tag{6}$$

and has the solution

$$x = \int_a^b \frac{d\sigma}{\sqrt{B - 2A \cdot \ln(\sigma)}} \tag{7}$$

with $A = \frac{e \cdot \mu_0 Z \cdot I_{LHC}}{2\pi\gamma m_i c}$, B = integration constant, Z = ion charge state, m_i = ion mass; I_{LHC} = peak LHC bunch current.

Figure 1a and 1b show schematically the focusing of the LHC beams near the IP without and with neutralization:

Figure 1a: the beam envelope is a **cone** converging almost **linearly** towards IP.

Figure 2a: no neutralization up to a distance L from the IP and full neutralization is assumed between x = 0 and x = L. The envelope is not anymore a linearly shrinking cone but shows **'progressive' focusing.** In order to maintain the previous luminosity and crossing at the original IP position the focusing effect of the neutralizing section must be **counter-acted by a different setting of the low beta insertion elements.**

In order to compensate the self-focusing in reality, a **lower focusing power and, hence, shorter β^* values** are adequately applicable in the low beta insertions.

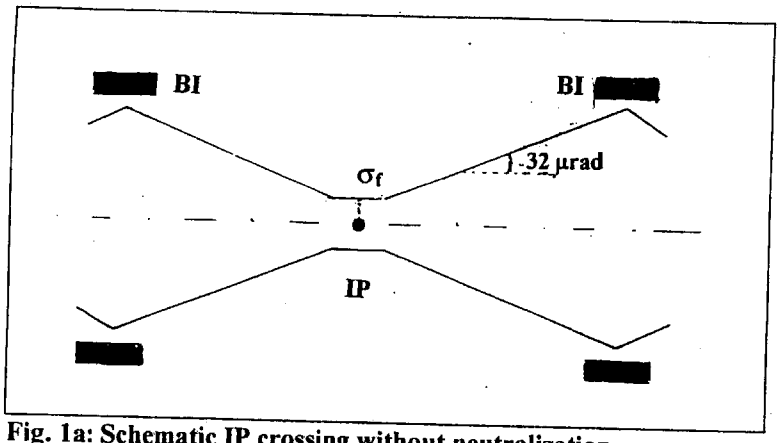

Fig. 1a: Schematic IP crossing without neutralization. BI = low beta insertion. Minimum σ_f = 16 μm at LHC.

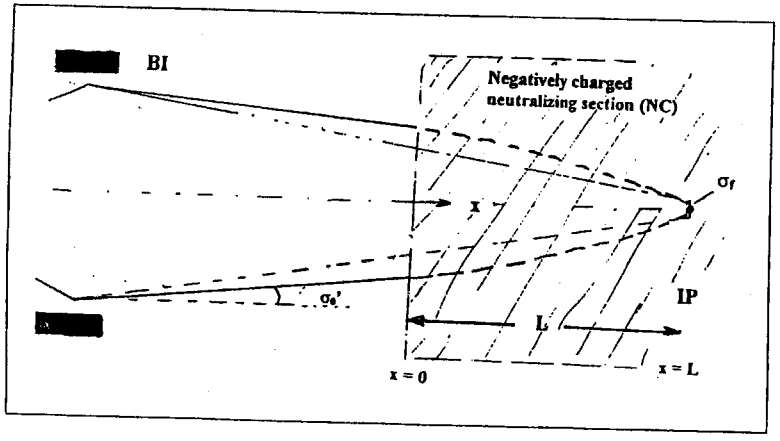

Fig. 1b: Schematic IP crossing with neutralization starting at L=3 m from IP and causing progressive focusing.

Figure 2a shows that the original **LHC beam radius at IP of σ_f = 16 μm is reached already after 2 m of neutralization, if full neutralization starts 3 m in front of IP.**

Since the **original angle** $(d\sigma/dx)_0 = \sigma_0'$ of the envelope is **increased from 32 μrad to 54 μrad, a smaller final radius σ_f = 8.5 μm and a larger final angle σ_f' = 59 μrad** can be reached after a neutralization length of **2.25 m** (Fig. 2b).

These values would correspond to an **increase of luminosity by a factor of about 3.5. This example** show the order of magnitude by which the standard focusing parameters can be changed.

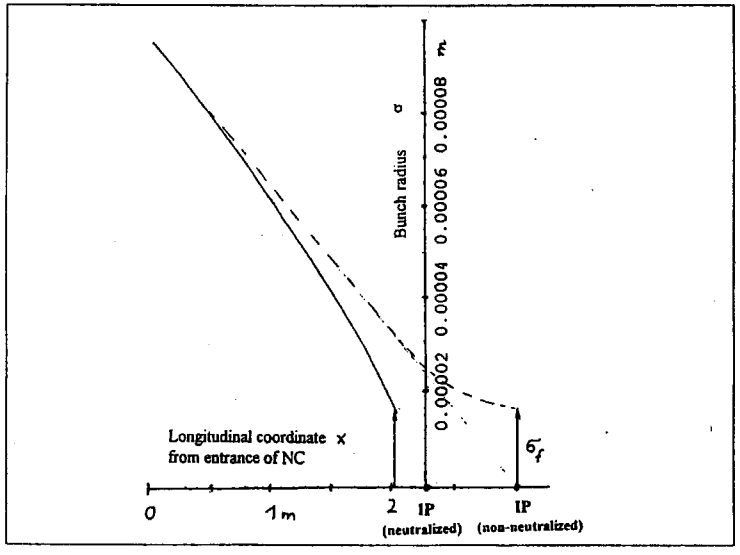

Fig 2a: Progressive focusing with full neutralization of LHC beam and BI with standard parameters down to 16 μm.

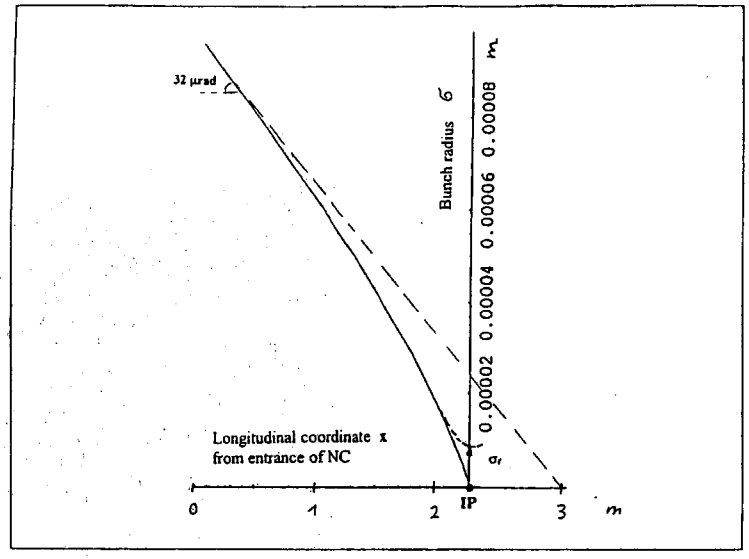

Fig. 2b: Beam envelope with neutralization. Focusing to minimum spot size of $\sigma_f = 8.5\ \mu m$.

4. Practical and Design Considerations (Fig. 3)

Annular electron guns EG1,2 are placed near to each side of the **central solenoid magnet S** belonging to the corresponding experiment. They generate two counter-moving **hollow D.C. electron beams** which are focused and channeled by the solenoidal end and main fields towards the axis and down to IP.

The slow parts of the two e^- beams are blowing up there due to their own space-charge and return on larger diameters to the solenoid ends. Another part of the electron beam is axially accelerated by the space-charge field of the non-neutralized LHC bunches entering the electron beam. The farther an LHC bunch proceeds the more e^- are 'collected' and its space-charge is more and more neutralized. The process is equivalent to the dynamics of the beam and plasma charges

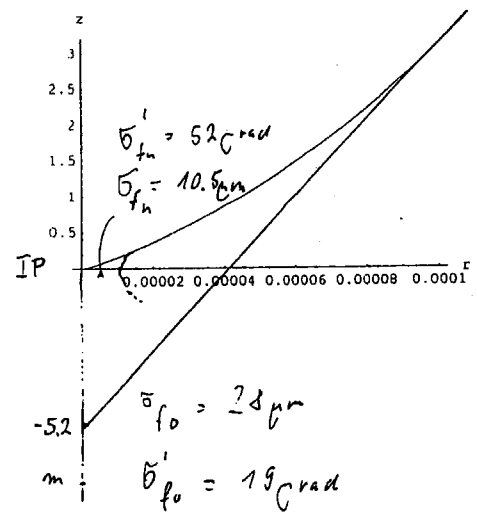

Input
$\sigma_0 = 100\ \mu m$
$\sigma_0' = 19\ \mu m$

$$\frac{L}{L_0} = 2.3$$

in a passive plasma lens. Therefore the system may be called an **Electron Beam Plasma Lens (EBPL).**

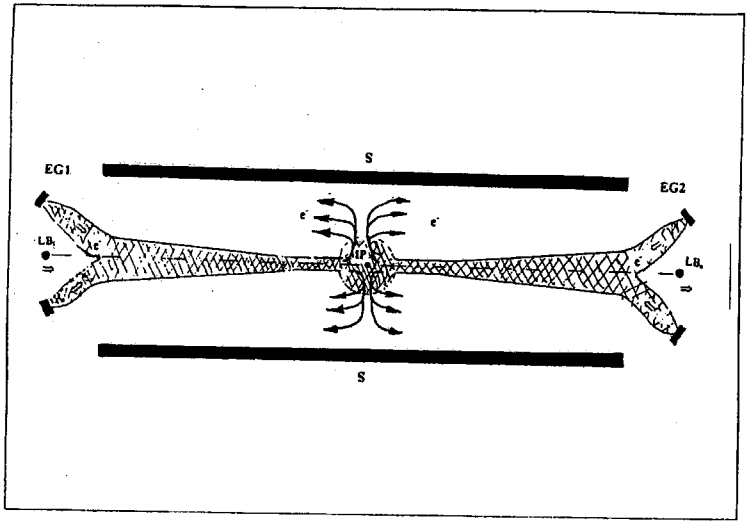

Fig. 3: Principle of EBPL neutralization system EG1,2 =electron guns; S=solenoid; $LB_{i,o}$=in- and outgoing LHC bunches

Not only the solenoidal field, also the average increase of electron velocity favours electron concentration near the LHC beam axis.

The LHC bunches, which have crossed with minimum beam-beam interaction at IP, are largely neutralized and do not exert sp-ch forces on the incoming electron beams.

The neutralizing electrons will be removed from the bunch either by dedicated deflectors or at last, when approaching the strong main dipole fields.

The strong focusing effect of the EBPL system must be **continuously compensated** by modifying the settings of the low beta insertions on either side of IP. Since **β* must be lowered**, the control of the low beta insertion elements becomes more practical.

Both arms **must** provide **equal focusing strength**.

A **tight feedback** between the momentary parameters of **EBPL and BI** is needed based on the **continuous measurement of luminosity as a criterion.**

Then **operation at a desired value of luminosity** can be envisaged.

* * * * * * * *

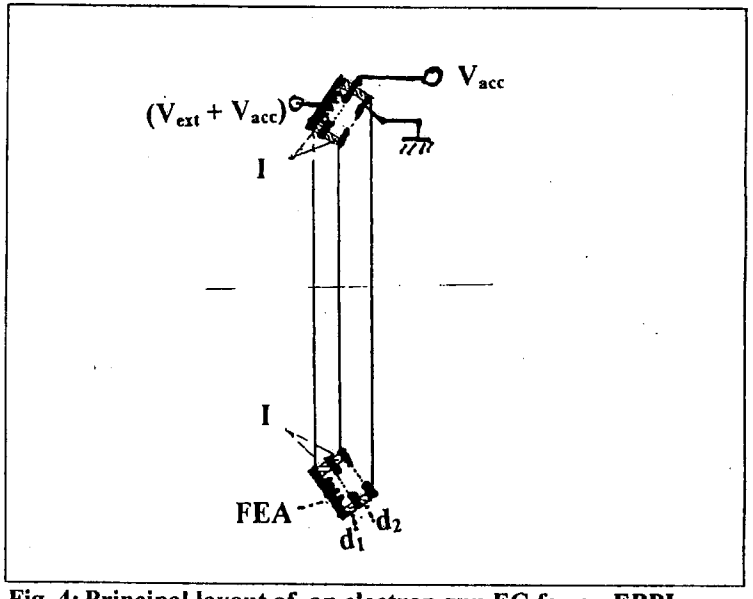

Fig. 4: Principal layout of an electron gun EG for an EBPL; FEA = field array emitter cathode; V_{ext} = extraction potential; $V_{acc} + V_{ext}$ = acceleration potential; I = insulator

Acknowledgements

Many thanks go to K. Eggert and B. Autin for discussing and helping me in some calculations and to A. Hofmann, who made valuable hints which allowed to produce this note. I am very grateful to P. Marin, who explained me the problems of the neutralization experiments at DCI, Orsay.

References

[1] O. Groebner, ISR neutr.....

[2] The Orsay Storage Ring Group, LAL/RT/79-01, PAC San Francisco 1979.

[3] J. Le Duff, M.P. Level, P.C. Marin, E.M. Sommer, H. Zygnier, LAL/RT/80-07, HEAC Geneva (1980).

[4] D.S. Prono et al., Survey of Initial Experiments on ATA Beam Dynamics, UCID-20264, LLNL (1984)

[5] D. Gabor, Nature 160m (1974) 89.

[6] D. Bloess et al., Nim 205 (1983) 173.

[7] HIBALL, Report KfK-3202 (1981).

[8] C. Rubbia, On Heavy Ion Accelerators for ICF, Paper presented at the IAEA Meeting on Drivers for ICF, Osaka, 1991 and Preprint CERN/PPE 91-117 (1991).

[9] H. Riege, U. Herleb, CERN/LHC 96-07 (DLO) (1996).

[10] U. Herleb, H. Riege, paper presented at the HIDIF Conference, Heidelberg, September 1997.

[11] H. Riege, Appl. Surf. Sci. 111(1997) 318.

[12] E. Tsyganov, A. Taratin, A. Zynchenko, CERN SL-Note 95-116 (AP) (1995).

[13] P. Chen, SLAC - Pub - 4049 (1986).

[14] V.D. Shiltsev, D.A. Finley, "Electron Compression of Beam-Beam Footprint in the Tevatron", Fermilab-TM-2008 1997).

[15] O.S. Brüning, LHC Project Report 158 (1997).

[16] LHC Design Study, CERN/AC/95-05 (LHC) (1995).

[17] H. Riege, 'Plasma Lenses for Focusing Particle Beams', Lecture held at the Workshop on New Developments in Particle Acceleration Techniques, Orsay 1987 and Preprint CERN/PS/87-49 (AA) (1987).

[18] H. Riege, LHC Note in preparation.

[19] K. Eggert, Private communication.

[20] K. Eggert, CERN AT/94-04 (DI) (1994).

[21] H.F. Gray, J.L. Shaw, Revue "Le Vide, les Couches Minces" - Suppl. au N° 271(1994) 29.

[22] J. Itoh, Appl. Surf. Sci. 111 (1997) 194.

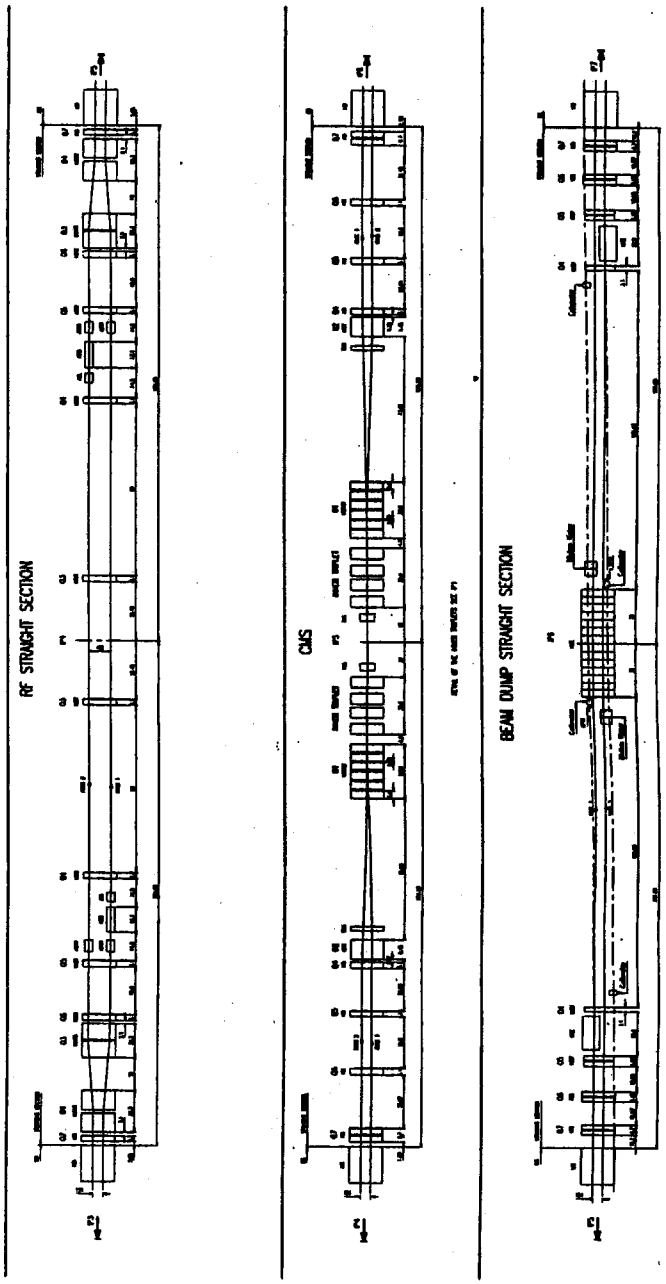

Q's:

Edwards:	You may get very nonlinear net field with this scheme which will affect the beams before collision point.
Riege:	There is no non-linearity if the beam profile is constant. If it is not – the electron distribution has to follow proton beam profile. May be it will do it automatically, like in a plasma lens.
Danilov:	But non-linear magnetic field remains in your scheme(?)
Meshkov:	How you are going to get so intensive electron current?
Riege:	Modern field effect emitter cathodes allow to get the gurrent we want.
Meshkov:	I am afraid there must be a bunch of coherent and incoherent effects in your scheme.

The production of **low-energy D.C. electron beams** of a few amperes and energies of at most a few keV are **in the reach of 'standard' technology.**

Electron guns with **cold cathodes** are proposed (Fig. 4).

Field Emitter Arrays (FEA) seem most suitable for EBPL's with the given specifications. They are **compact (only a small amount of matter) and reliable** for emitted current densities below 1 A/cm^2.

Electron beam generation (for example, with 100 V extraction voltage) **and acceleration** (e.g. 0.5 to several kV) **can be separated** (Fig. 4) rendering the control of electron beam current and energy rather simple.

The diameter of the annular electron gun can be adapted to the LHC experiment conditions valid at a given IP. If one is forced to approach closely the LHC beam axis, Roman-Pot type arrangements could be considered.

Power considerations:

Overall LHC beam power at 7 TeV:	**3.5 TW per beam**
Overall synchrotron radiation power:	**3.6 kW per beam**
e$^-$ beam generation for EBPL (2 arms):	**1 to 10 kW, but local**
e- beam power gain from LHC beam:	**40 to 80 kW, local**

This power gain results from the characteristics of the neutralization process:

- partially the LHC bunch is neutralized by quasi-stationary electrons and
- partially by electrons, which are attracted, accelerated and then carried along with the bunch. These electrons form a current of less than 0.5 A (= average LHC beam current). Assuming an average β of 0.6 (100 keV) a power gain of 65 kW per arm is obtained. The elimination of the energetic part of the electron beams has to be considered as the major problem of the EBPL system in the complex environment of detector and cryogenic equipment. Most probably the energetic electrons have to be magnetically deflected onto a cooled external dump, where the energy can be dissipated without risk.
- The ratio of slow / fast neutralizing electrons depends in a complex way on the parameters of the electron beam, and on the geometry and magnetic field of the central solenoid. The ratio has an influence on the focusing strength of the EBPL. If it is small, we also have current neutralization.

4. Advantages for LHC Collider and Experiments

The EBPL allows an experiment to take data during an LHC fill at **constant luminosity** (Fig. 5). Gradual beam losses are compensated by increasing focusing strength of the EBPL. The displacement of focus must be compensated by matching gradually the low beta insertion parameters.

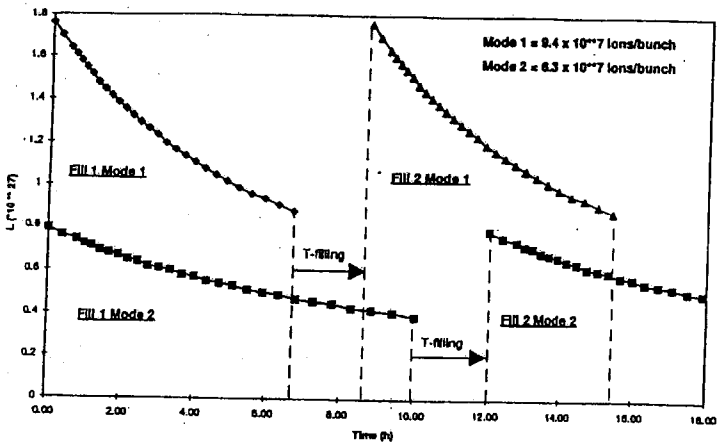

Fig. 5: Luminosity versus for 2 cases of half-life (6.7 and 10h)

If desired, a **higher luminosity** can be obtained (less than one order of magnitude). Then high-density **quasi-stationary** electrons are needed.

At very high LHC proton beam intensities the tune spread due to bunch crossing becomes an important limiting factor of the beam life-time. With charge (and current) neutralization the **increase of tune spread can be totally suppressed.** This goal can be better reached with a high portion of fast electrons obtained from low-density electron beams.

5. CONCLUSIONS

With **modest** low-energy electron currents **focusing** is achieved within short distances, which is much stronger than that of conventional or superconducting magnets and which **does not require bulky equipment** around the IP.

Contrary to the apparent difficulties for mankind to produce GeV and TeV charged particle beams, **nature helps greatly to neutralize** such beams. The neutralizing action on a high energy proton/ion beam is simple to describe and has been demonstrated in many experiments.

The neutralization process and its consequences resemble the phenomena and the action of passive **plasma lenses**. The complex details (say, the electron trajectories) of neutralization occuring in an **EBPL** have not been dealt with here. They should be studied for an EBPL application to a specific goal (e.g. operation of an LHC experiment at **constant luminosity**) in a real intersection region and with optimized electron gun characteristics.

The EBPL system is technically **feasible and not too expensive.** D.C. electron guns with the required performance are not at all beyond the state of the art. The most expensive parts of the EBPL system are the **electron beam dump equipment** for the elimination of the energetic part of the electron beam and the **continuous feedback system coupling EBPL and BI**, which enables to run the collider at a specific **(constant) luminosity.**

Nevertheless **pilot experiments** have to be carried through before the specific design of an EBPL for an LHC experiment can be started.

#7

Plasma Suppression of Beam-Beam Interaction in Circular Colliders

G. Stupakov and P. Chen

Stanford Linear Accelerator Center Stanford University, Stanford, CA 94309

Beam-Beam Compensation Mini-Workshop, February 12-13, 1998

Beam Plasma Interaction

If relativistic beam passes through plasma:

- $n_b \gg n_p$ – underdense regime. Electrons are expelled out of the plasma $\rightarrow$ focusing (plasma lens).

- $n_b \ll n_p$ – overdense regime. If electric field is canceled, the beam is focussed by its magnetic field. Full cancellation of the beam fields can also be achieved $\rightarrow$ plasma suppression of disruption and beamsstruhlung in linear colliders. *Suppression of beam-beam interaction.*

Adding plasma at the interaction point causes degradation of the lifetime.

BEAM FIELD NEUTRALIZATION IN PLASMA

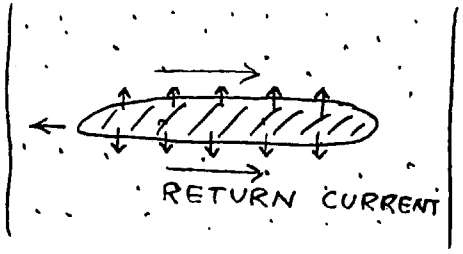

PLASMA

Original motivation for this work – suppression of beam-beam interaction in muon collider.

Beam-beam tune shift parameter
$\xi = N r_c / (4\pi\epsilon_n)$
N – number of particles in the bunch
r_c – classical radius of the particles
ϵ_n – the normalized emittance of the beam.

Electromagnetic Field of Beam in Plasma

$j(r,t)$ – beam current

$$B(r,t) = \frac{4\pi i}{c}\int \frac{k \times \tilde{j}(k,\omega)}{k^2 - \frac{\omega^2\varepsilon(\omega)}{c^2}} e^{-i\omega t + ikr} d^3k d\omega.$$

$$E(r,t) = 4\pi i \times$$

$$\int \left[\frac{\omega \tilde{j}_t(k,\omega)}{c^2k^2 - \omega^2\varepsilon(\omega)} - \frac{\tilde{j}_l(k,\omega)}{\omega\varepsilon(\omega)}\right] e^{-i\omega t + ikr} d^3k d\omega.$$

$\varepsilon(\omega) = 1 - \omega_p^2/\omega^2$ is the dielectric function of the cold plasma
ω_p is the plasma frequency, $\omega_p^2 = 4\pi n_p e^2/m_e$
n_p is the plasma density
m_e is the electron mass

$$\tilde{j}(k,\omega) = \frac{1}{(2\pi)^4}\int j(r,t)\, e^{i\omega t - ikr} d^3r dt.$$

Wavenumber k_p is associated with the plasma frequency

$$k_p = \omega_p / c = \sqrt{4\pi n_p r_e}$$

For a *round* beam moving along the z-axis, $j = (0, 0, j_z)$,

$$j_z(r,t) = Nec\lambda(z - ct)\,\rho(r),$$

N is the number of particles in the bunch
$\lambda(z)$ – longitudinal
$\rho(r)$ radial distribution function

We assume a long-thin bunch, $\sigma_z \gg \sigma_r$

$$\tilde{j}_z(\boldsymbol{k}, \omega) = Nec\tilde{\lambda}(k_z)\,\tilde{\rho}(k_\perp)\,\delta(\omega - k_z c),$$

where $\boldsymbol{k}_\perp = (k_x, k_y, 0)$ and $k_\perp = |\boldsymbol{k}_\perp|$,

$$\tilde{\rho}(k_\perp) = \frac{1}{(2\pi)^2}\int \rho(r)\, e^{-i\boldsymbol{k}_\perp \boldsymbol{r}} d^2 r,$$

$$\tilde{\lambda}(k_z) = \frac{1}{(2\pi)}\int \lambda(\xi)\, e^{-ik_z\xi} d\xi.$$

k_z is of the order of σ_z^{-1}, also $k_p\sigma_r \geq 1$. We have $k_p\sigma_z \gg 1$, and $\varepsilon(ck_z) = 1 - k_p^2/k_z^2 \approx -k_p^2/k_z^2$.

$$B_\varphi = -4\pi i N e\lambda(z - ct)\int \frac{k_\perp \tilde{\rho}(k_\perp)}{k_\perp^2 + k_p^2} e^{i\boldsymbol{k}_\perp \boldsymbol{r}} d^2 k.$$

For a Gaussian beam,

$$\tilde{\rho}(k_\perp) = (2\pi)^{-2}\exp\left(-k_\perp^2\sigma_r^2/4\right)$$

and

$$B_\varphi(r,z,t) = 2Ne\lambda(z - ct)\int \frac{k_\perp^2 dk_\perp}{k_\perp^2 + k_p^2} J_1(k_\perp r) \times \exp\left(-k_\perp^2\sigma_r^2/4\right).$$

Electric field,

$$\boldsymbol{E} = -4\pi i N e \int \frac{k_z \tilde{\rho}(k_\perp)\,\tilde{\lambda}(k_z)}{k_\perp^2 + k_p^2}\left(\hat{\boldsymbol{z}} + \frac{k_z \boldsymbol{k}}{k_p^2}\right) e^{i\boldsymbol{k}\boldsymbol{r}} d^3k,$$

By order of magnitude,

$$E_z \sim \frac{\sigma_r}{\sigma_z} B_\varphi, \qquad E_r \sim \left(\frac{\sigma_r}{\sigma_z}\right)^2 B_\varphi,$$

Electric field generated is always small compared to the magnetic one.

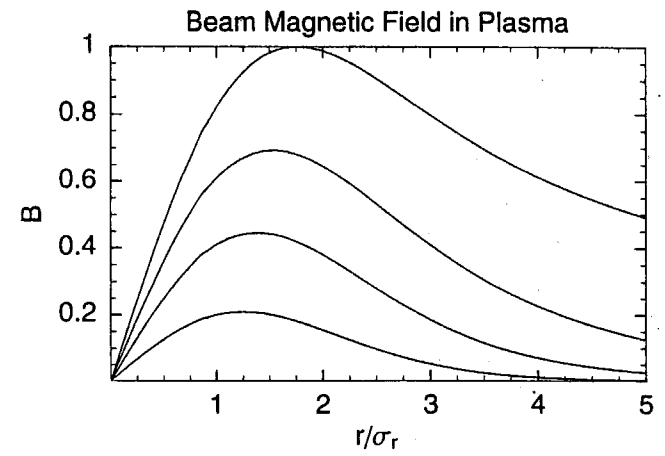

$k_p\,\sigma_r$ = 0, 0.5, 1, 2

The solution for two beams colliding in the plasma is a superposition of the single-bunch solution.

Beam-beam interaction parameter ξ

$$\xi \propto \int_{-\infty}^{\infty} \left[\partial B_\varphi(r,z,t)/\partial r\right]|_{r=0}\, dt$$

$$\xi = \frac{\xi_0}{2}\int_0^{\infty} \frac{\zeta^3 d\zeta}{\zeta^2 + k_p^2\sigma_r^2} \exp\left(-\zeta^2/4\right)$$

ξ_0 – the beam-beam interaction parameter in the vacuum.

We neglected the magnetic field on the plasma electrons: $N < \sigma_z/r_e$, where r_e is the classical electron radius.

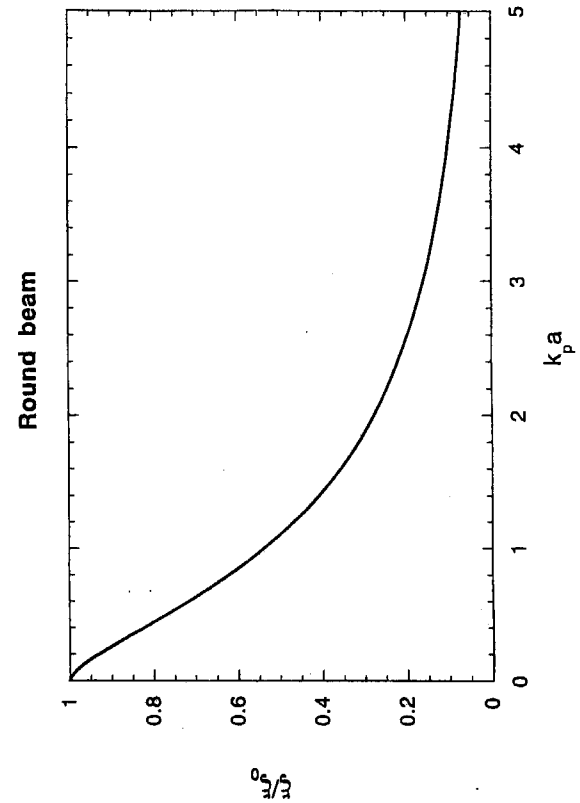

Deleterious effects of plasma

1. *Emittance growth of the beam due to small-angle elastic scattering on nuclei.*

$$\dot{\epsilon}_n = \frac{2\pi r_c^2 \sigma_r^2 Z^2 n_p l f}{\epsilon_n} \Lambda_1,$$

f – the revolution frequency
$\Lambda_1 = \ln(\lambda_D/\lambda_B)$ – a logarithmic factor
$\lambda_D = \left(kT/4\pi n_p e^2\right)^{1/2}$ – the Debye length (T is the plasma temperature)
$\lambda_B = 137 r_c/\gamma$ – the de Broglie wavelength for the beam particles.

Large angle collisions are relatively small.

2. *Bremsstrahlung on nuclei.*

Bremsstrahlung on nuclei of the plasma causes the energy losses of the beam particle due to radiation in collisions with the nuclei. If the relative energy loss $\delta E/E$ exceeds the RF acceptance, ε_{RF}, the particle gets lost.

$$\sigma_{brem} = \frac{16}{3}\frac{r_c^2 Z^2}{137}\Lambda_2 \left(\ln\frac{1}{\varepsilon_{RF}} - \frac{5}{8}\right),$$

$\Lambda_2 = \ln(2\lambda_D/\lambda_C)$ – a logarithmic factor
$\lambda_C = 137 r_c$ – the Compton wavelength for the beam particles.

3. *Elastic scattering on electrons.*

The incident particle collides with the plasma electrons and transfers to them part of its energy. The losses occur if the transfer is larger than ε_{RF}.

$$\sigma_{scat-e} = \frac{2\pi r_e r_c}{\gamma \varepsilon_{RF}}.$$

4. *Inelastic pp Scattering* .

At 1-20 TeV

$$\sigma_{inelastic-pp} \approx 30 \text{ mb}$$

Lifetimes for the beam associated with each loss channel, τ_{brem}, τ_{scat-e}, and $\tau_{inelastic-pp}$

$$\tau_i = (n_p \sigma_i l f)^{-1}$$

l – the length of the plasma layer
f – the repetition rate (revolution period).

For the emittance growth we define the emittance growth time

$$\tau_{scat-i} = \epsilon_n / \dot{\epsilon}_n$$

τ_0 – the design luminosity lifetime.

We assume $k_p \sigma_r = 4$; this gives about six-fold decrease in the parameter ξ. Hydrogen plasma – $Z = 1$. The length of the plasma $l = 2\sigma_z$. The plasma temperature is assumed 2 eV. For the RF exceptance, $\varepsilon_{RF} = 0.001$.

Beam-plasma parameters and lifetimes

Accelerator	μ-collider	LHC	Tevatron33
Beam			
Particle species	μ	p	p
E [TeV]	2	7	1
γ	1.9×10^4	7.5×10^3	1×10^3
σ_z [cm]	0.3	7.5	40
σ_r [μm]	2.7	15	30
f [Hz]	2.3×10^4	1.1×10^4	4.8×10^4
N	2×10^{12}	10^{11}	2.7×10^{11}
ϵ_n [m rad]	5×10^{-3}	3.75×10^{-6}	3×10^{-6}
ξ_0	0.05	0.003	0.012
Plasma			
$k_p\sigma_r$	4	4	4
ξ/ξ_0	1/6	1/6	1/6
n_p [cm^{-3}]	6.2×10^{19}	2×10^{18}	5×10^{17}
l [cm]	0.6	15	80
Lifetimes			
τ_0 [hour]	1×10^{-5}	10	3
τ_{scat-i} [hour]	4.1×10^6	13	0.4
τ_{brem} [hour]	50	8×10^3	1.3×10^3
τ_{scat-e} [hour]	2.5	23	0.6
$\tau_{inelastic-pp}$ [hour]		2×10^{-2}	5×10^{-3}

Conclusions

- Plasma suppression of beam-beam interaction looks promising for muon collider. Required plasma density is 6×10^{19} cm^{-3}.
- For proton machines, plasma causes strong deterioration of the beam lifetime.
- Suppression of the beam electric field only requires much smaller plasma density. Although this does not change ξ, the beam dynamics will be different (less destructive?).

Q's:

Meshkov: What kind of plasma is preferable for the compensation – under-dense or over-dense.

Stupakov: Overdense plasma allows both charge and current compesation, while underdense – only charge compensation.

Shiltsev: Is it dificult to obtain plasma density of 1e+18 or 1e+19 1/cm**3?

Stupakov: 1e+18 – is what people get with powerful laser pulsing into hidrogen gas.

Meshkov: Such a plasma must be unstable by itself.

Stupakov: Yes, but for plasma compensation, the plasma is necessary only for a short time when beams are colliding.

Meshkov: I believe, this is very undesirable solution when a source of an additional background is placed at a collision point (inside a detector!). Therefore the idea to use a dense plasma or slow electrons placed at the interaction area for neutralisation of beam-beam interaction will meet definitely a rejection from detector physicists.

Issues for Possible e-p Polarimetry in RHIC

Mike Syphers
BNL

- Polarized Protons in RHIC
- Possible Polarimeter Designs
- e-p Polarimeter Parameters/Issues

Polarized Proton Collisions at BNL

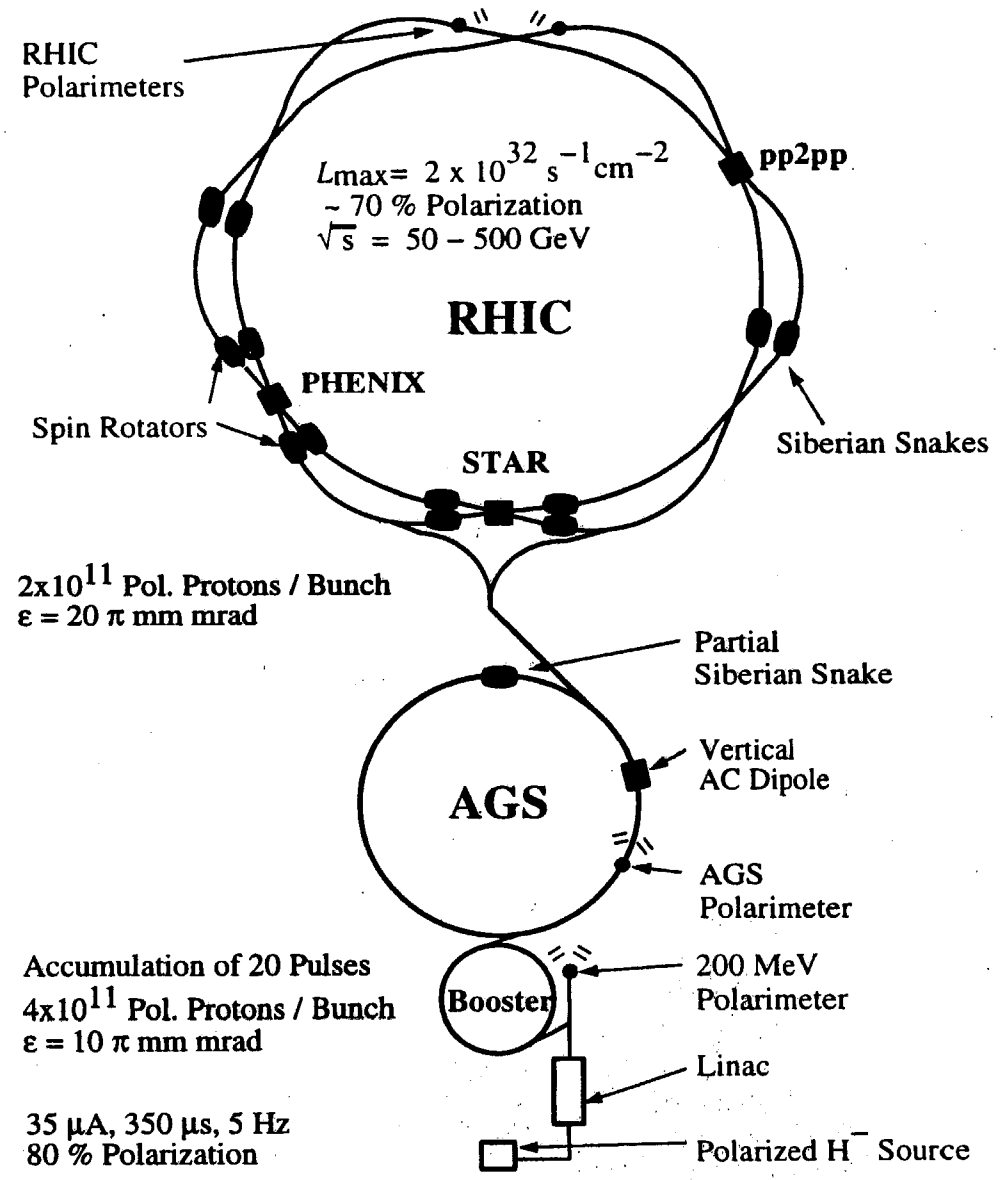

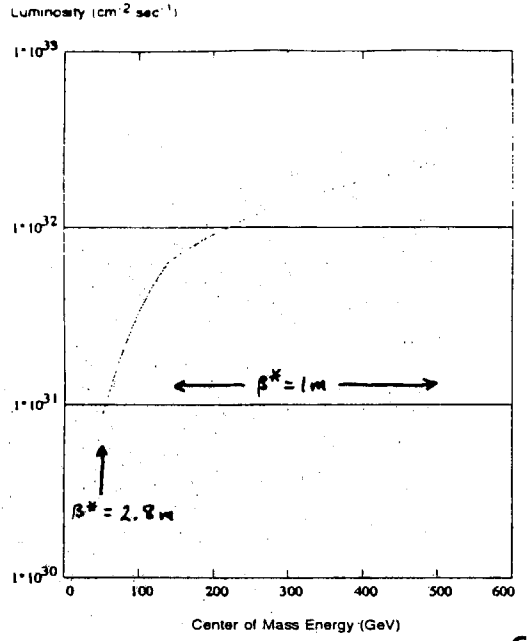

2×10^{11} $\vec{p}$ / bunch

$\epsilon_N (95\%) = 20\pi$ mm-mrad

120 bunches / ring

$\xi = 0.024$ (2 IR's)

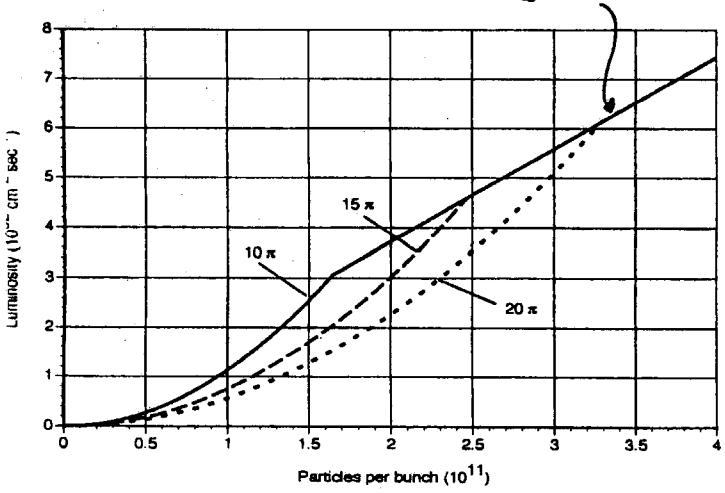

$\beta^* = 1$ m

$E_{beam} = 250$ GeV

120 bunches / ring

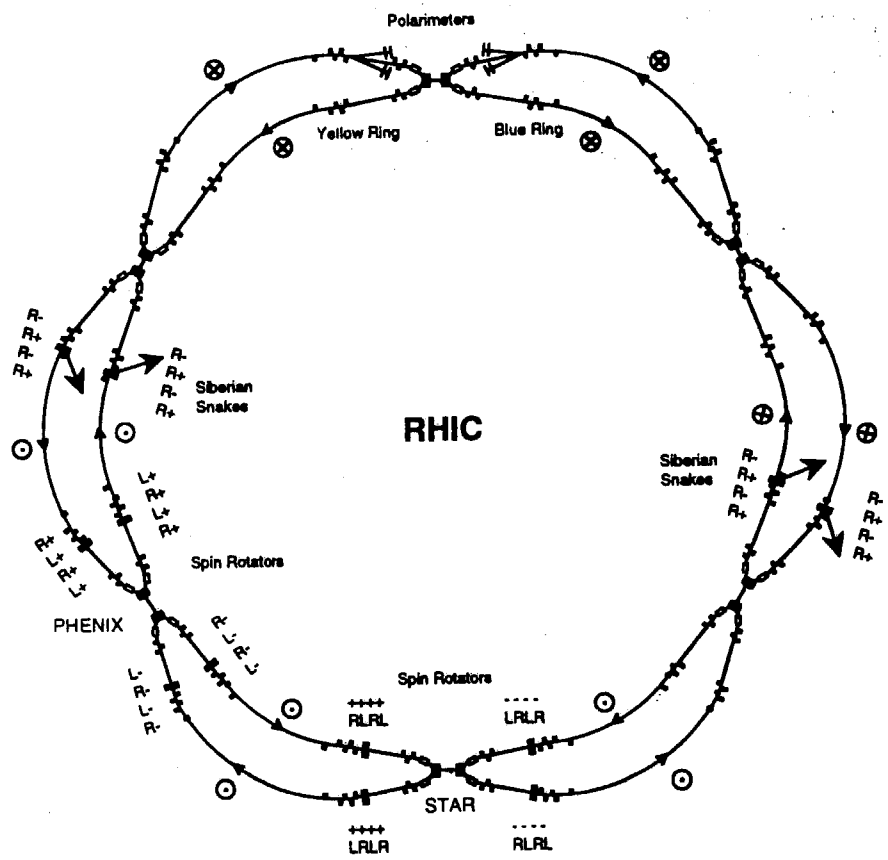

RHIC POLARIMETER

Polarimeter Issues:

- Pion polarimeter, toroid design, cost estimate: $1.5 M
  - Fast measurements -- seconds/minutes
  - 10% accuracy; 5% with some effort -- requires calibration
- Questions:
  - design is based upon results of E704 at FNAL -- p on p measurement at 200 GeV; RHIC polarimeter based upon p on C
  - can asymmetry be measured with p on C at RHIC energies?
- AGS experiment E925 set out to address -- data taken in November, 1997 at 25 GeV; being analyzed now. Looks encouraging.
- Meanwhile, other approaches being considered...
  - minimum pion polarimeter for commissioning RHIC, and for measurements at 100 GeV (first pol. Proton operation energy); could be single arm, two magnet, two target approach.
  - other possible "Day One" polarimeter options:
    pC CNI polarimeter; pp (jet) polarimeter
- A test at IUCF of pC CNI techniques (measuring recoil C atoms) will be performed early next year.

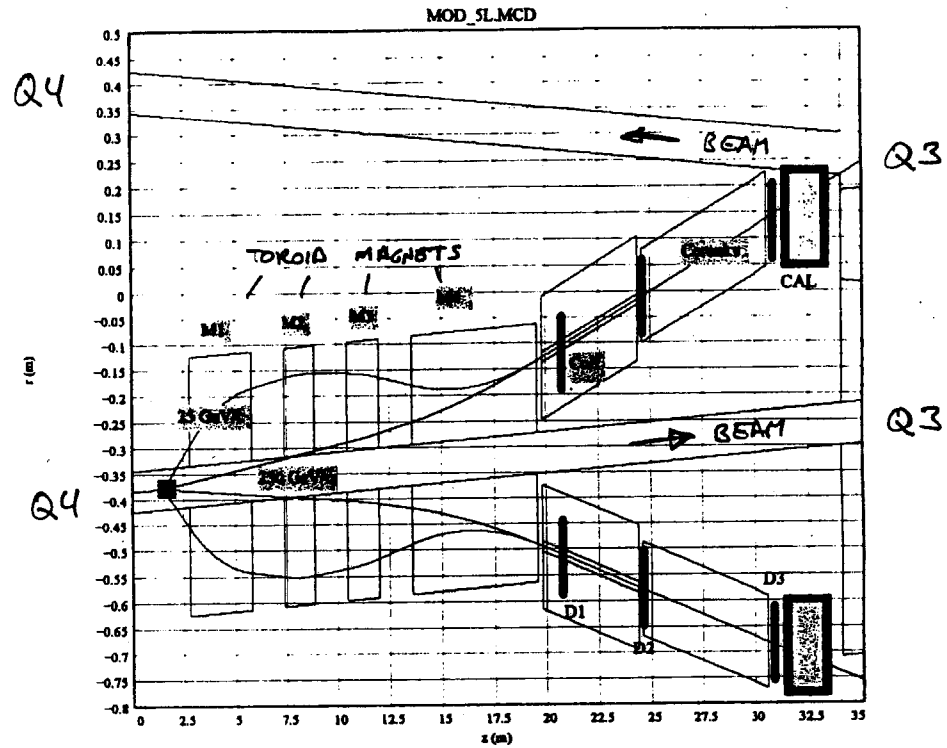

Polarimeter layout. The magnet positions and the final trajectory angles will be optimized. D1, D2 and D3 are tracking detectors. A possible calorimeter location is indicated

	TARGET	M1	M2	M3	M4	COLL	CRNK V
Length (M)	0	3	1.5	1.5	6	4.6	6
Position (m)	1.5	2.75	7.35	10.45	13.55	19.75	24.55
23 GeV/c		-1	-1	-0.85	+0.380		
25 GeV/c		-0.99	-0.65	-0.4471	+0.3321		
100 GeV/c		-0.2	-1	-0.9	+0.782		
200 GeV/c		0	0	-0.275	+0.94		
250 GeV/c		0	0	+0.9	+0.9		

Element positions and lengths and magnet settings, etc. Final trajectory θ=20.84 mrad

Measuring Polarization using e-p Elastic Scattering

Totally calculable problem, thus the polarization measurement is absolute, in principle

Analyzing power is large at

- small recoil angle
- proton energies around few 10 GeV

Requires high intensity electron target (POLARIZED)

Best if have electron beam moving in direction of proton beam, with velocity chosen to give highest available analyzing power

If optimum analyzing power for a stationary electron is given at a proton beam energy of E_{p0}, then the optimum electron beam momentum, P_e, for a given proton beam energy, E_p, is found by

$$m_p^2 P_e^2 - (2 m_e E_{p0} P_p) P_e + m_e^2 (E_p^2 - E_{p0}^2) = 0$$

For RHIC energies:

Proton energy	Electron energies (kinetic)	
25 GeV	13 keV	0.58 GeV
50 GeV	230 keV	1.2 GeV
100 GeV	0.818 MeV	2.3 GeV
150 GeV	1.44 MeV	3.5 GeV
200 GeV	2.07 MeV	4.6 GeV
250 GeV	2.7 MeV	5.8 GeV

Elastic pe-scattering as analyzer of high energy proton beams polarization (from RHIC to LHC)

I.V. Glavanakov[1], Yu.F. Krechetov[1], A.P. Potylitsin[1], G.M. Radutsky[1], A.N. Tabachenko [1] and S.B. Nurushev[2]

(1) Institute for Nuclear Physics, 634050 Tomsk, P.O.B. 25, Russia
(2) Institute for High Energy Physics, 142284 Protvino, Moscow Region, Russia

To find the proton beam polarization the measurement of two-spin polarization asymmetries for the elastic pe-scattering is proposed.

To determine the proton beam polarization we propose to measure the double spin polarization asymmetries for the elastic pe scattering. We calculated in the one-photon approximation which agrees fine with experiments within the considered range of the kinematic variables the spin correlation parameters and the elastic scattering differential cross section as functions of the proton energy in the range $5 < E_p < 8000$ GeV for several recoil electron angles. As far as even for the 8 TeV/c proton beam $|t|$ value is less than 0.25 (GeV/c)^2 in real experimental conditions, in our calculation we used the form factor scaling assumption, $\mu_p G_E = G_M$ (where μ_p is the proton total magnetic moment), which is true by definition in the limit of t=0, and has been found experimentally to be true to within about 5% for $|t|$ values up to 1 (GeV/c)^2 [1]. As a result the asymmetries are not influenced by the form factor dependence on t.

The main results of calculations are the following:

- A_{LL} is the most suitable for the polarization measurement at $P_p > 25$ GeV/c (see Fig.1);
- A_{NN} is large within the momentum range 10÷30 GeV/c at $\theta_e < 4$ mr (see Fig.2). $A_{SS} \simeq A_{NN}$ at small recoil angles of the electron (large $|t|$). With the increase of the angle A_{SS} is found to be very small;
- The A_{SL} spin correlation parameter has sufficiently large value in the proton momentum interval 10 ÷ 600 GeV/c for the same angular range and has the maximum at the recoil angles θ_e of about 2.5 mr (see Fig.3). A_{SL} is always much bigger than A_{LS}.

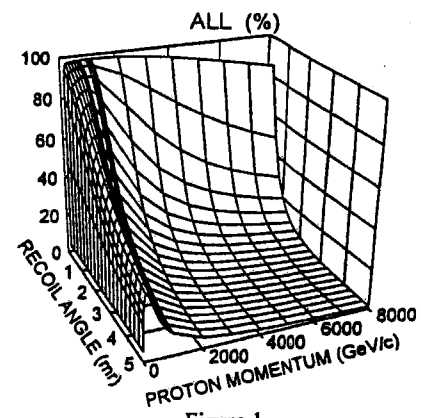

Figure 1

Though the cross-section diminishes with the decrease of θ_e (see Fig.4), the small angle region is more adequate for polarization measurement on the rest electrons, because of the figure of merit $A_{ij}^2 d\sigma/d\Omega_e$ is quite large there.

$$A = \frac{N_L - N_R}{N_L + N_R}$$

One can see that A_{LL}, A_{NN} and A_{SL} asymmetries are large to use for the proton beam polarization measurement in a wide range of energy. It is worth to mention that even for LHC (E_p =8 TeV) $\sqrt{s}$, the total energy in the c.m.s., is not large (about 3 GeV) so that the background contribution of the inelastic reactions is rather small and is absent at the proton energy less than 300 GeV.

The important problem is the measurement of the transverse proton polarization. One has seen that the A_{SL} or A_{NN} asymmetries have maxima at the proton momentum less than 100 GeV/c. With the increase of the proton energy the asymmetries decrease, that makes difficult the use of them to construct the polarimeter for the higher energy protons. This difficulty can be overcome, if we consider the case of "anticollider" scattering, when the target electrons move along the proton beam direction. The selection of the electron momentum P_e allows to measure polarization at $s = s_0$ at which the asymmetry has the maximum. There are two values of the momentum P_e that make $s = s_0$ at a fixed proton beam momentum P_p, as it can be seen from the expression

$$s = M^2 + m^2 + 2E_pE_e - 2P_pP_e.$$

As an example the dependence of A_{NN} from the initial energy and recoil angle of electron is shown for the proton beam momentum 800 GeV/c (see Fig.5). Two electron beam momenta regions, where asymmetry has the maxima, correspond to the initial electron velocity which is higher or less than the proton one.

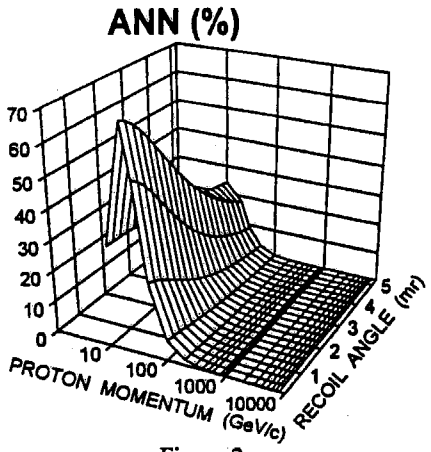

Figure 2

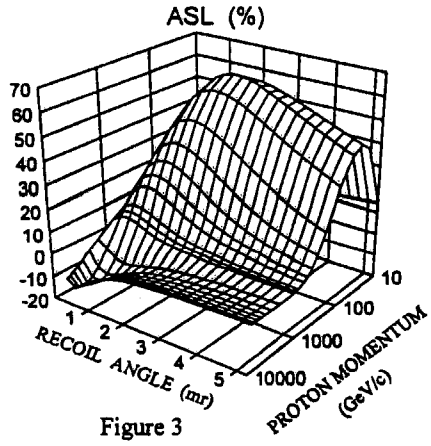

Figure 3

The value $s = s_0$ corresponds to the scattering of ~14 MeV/c electron on the rest proton. That is the essential advantage of the "anticollider" version of the pe - polarimeter. The lack of background processes (there is only background from the gas in the pipe of the collider) makes experimental setup more simple and inexpensive. To define the complete kinematic of event of the "anticollider" pe scattering it is enough to measure the electron recoil angle and energy. One of them may be measured with low accuracy which is enough to separate events corresponding to the two-valued solution of the kinematic equations. For the collider,

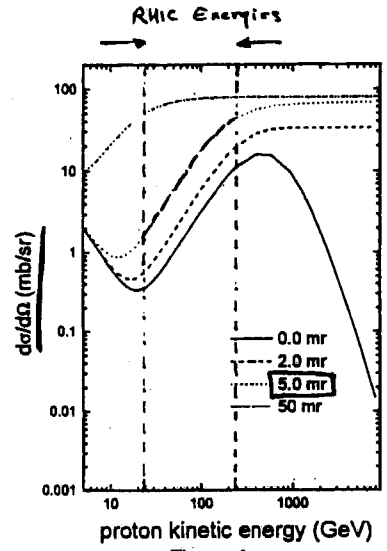

Figure 4

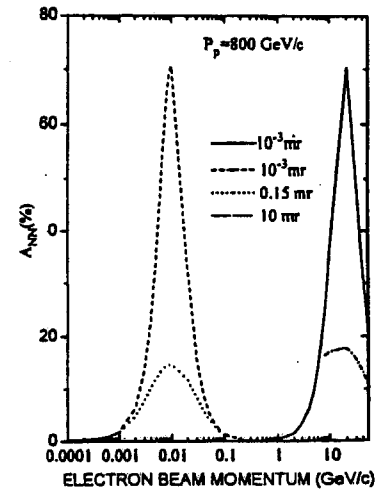

Figure 5

like HERA (in *ep*-version), the range of the second maximum is interesting since the asymmetry has the maximum in a wide interval of the recoil electron angles and the energy of the scattered proton is bigger than that of initial one. That can be useful for the polarimeter construction.

The same arguments are obviously applicable to the A_{SL}.

We conclude that the pe elastic scattering is a useful process to measure the proton beam polarization in the energy region from RHIC to LHC.

[1] T. Janssens et al., Phys. Rev. 142, 922 (1966); P.N. Kirk et al., Phys. Rev. D8 (1973) 63.

Notes on a Possible

RHIC e-p Elastic Scattering Polarimeter

The polarimeter would consist of a high intensity, low energy, polarized electron beam moving parallel to the RHIC polarized proton beam. To enhance the interaction rate, the electron beam is placed at a RHIC low-beta insertion tuned to $\beta^* = \beta_{ep}$. The electron beam is pulsed at the RHIC rf frequency and the electron pulse length is kept as small as reasonably possible. For this calculation, we assume the beam size of the low energy electron beam is matched to that of the proton beam.

Some RHIC (and other) parameters:

$c := 2.9979 \cdot 10^8 \cdot \frac{m}{sec}$

Revolution Frequency: $f_0 := 80 \cdot KHz$

Number of proton bunches: $B := 120$

Protons/bunch: $\boxed{N_p := 2 \cdot 10^{11}}$

Interaction Region β^*: $\beta_{ep} := 5 \cdot m$

Proton beam parameters:

$E_{0p} = 0.938 \cdot GeV$

$\varepsilon_n = 10 \cdot \pi \cdot mm \cdot mrad$

$E_p = 24 \cdot GeV$ $\quad \gamma_p := \frac{E_p}{E_{0p}}$ $\quad v_p := c \cdot \sqrt{1 - \frac{1}{\gamma_p^2}}$ $\quad v_p = 0.999 \cdot c$

Transverse beam size:

$\sigma_p := \sqrt{\frac{\varepsilon_n \cdot \beta_{ep}}{6 \cdot \pi \cdot \gamma_p}}$ $\quad \sigma_p = 0.571 \cdot mm$

Longitudinal bunch length: $\sigma_{pL} := 14 \cdot cm$

$\tau_p := \frac{2.35 \cdot \sigma_{pL}}{v_p}$ $\quad \tau_p = 1.098 \cdot ns$ (FWHM)

Electron beam parameters:

We assume the electron beam size is matched to that of the proton beam, and we use beam intensity parameters equivalent to or scaled from those of the SLAC polarized electron beam system, keeping the average beam current at or below 10 mA. We assume an electon beam energy of 10 keV.

$I_{ave} := 10 \cdot mA$ $\quad f_{rep} := f_0 \cdot B$ $\quad f_{rep} = 9.6 \cdot 10^6 \cdot Hz$

$E_e := 10 \cdot keV$ $\quad T_{rep} := \frac{1}{f_{rep}}$ $\quad T_{rep} = 104.167 \cdot ns$

$\gamma_e := \frac{E_e + 511 \cdot keV}{511 \cdot keV}$ $\quad \gamma_e = 1.02$ $\quad v_e := c \cdot \sqrt{1 - \frac{1}{\gamma_e^2}}$ $\quad v_e = 0.195 \cdot c$

Desired electron Bunch Length: $\tau_e := 1 \cdot ns$ (FWHM)

$\sigma_{eL} := \frac{v_e \cdot \tau_e}{2.35}$ $\quad I_{peak} := I_{ave} \cdot \frac{T_{rep}}{\tau_e}$ $\quad N_e := \frac{I_{ave} \cdot T_{rep}}{1.6 \cdot 10^{-19} \cdot coul}$

$\sigma_{eL} = 2.487 \cdot cm$ $\quad I_{peak} = 1.042 \cdot amp$ $\quad \boxed{N_e = 6.51 \cdot 10^9}$

To determine the longitudinal space required for the electron beam in RHIC, we estimate the effective interaction length L_{int}:

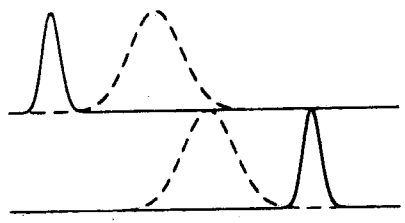

— p before
- - e before
— p after
- - e after

$$v_p \cdot \tau_{int} - v_e \cdot \tau_{int} := 6 \cdot \sigma_{eL} + 6 \cdot \sigma_{pL}$$

Interaction Time: $\tau_{int} := \dfrac{6 \cdot (\sigma_{eL} + \sigma_{pL})}{v_p - v_e}$ $\quad \boxed{\tau_{int} = 4.103 \cdot ns}$

Interaction Length: $L_{int} := v_e \cdot \tau_{int} + 6 \cdot \sigma_{eL}$ $\quad \boxed{L_{int} = 38.908 \cdot cm}$

Detector:

From Glavanakov, et al., SPIN96, pp. 794-796, $d\sigma/d\Omega$ for 5 mrad recoil angle is roughly 50 mb/srad at proton energies of 250 GeV. At 24 GeV, $d\sigma/d\Omega$ is about 2 mb/srad for this same recoil angle. Though $d\sigma/d\Omega$ is about 50 mb/srad at a recoil angle of 50 mrad for 24 GeV, the analyzing power is much stronger at small angles. Thus, we envision a system where a single recoil angle ($\theta_e := 5 \cdot mrad$) is analyzed. For 5mrad, the differential cross section is given approximately by:

$$d\Sigma_d\Omega(E_p) = 0.003 \cdot \left(\frac{E_p}{E_{0p}}\right)^{1.3} \cdot \frac{mb}{srad}$$

We assume a 2-gap toroid system similar to the pion polarimeter design, and compute the total acceptance $d\Omega$. The analyzing power for small recoil angles does not vary much over +/-1mrad, and so the acceptance can be estimated as:

$\phi_{gap} := 7 \cdot deg$ $\qquad d\Omega := 2 \cdot \phi_{gap} \cdot \theta_e \cdot (2 \cdot mrad)$ $\qquad d\Omega = 30.705 \cdot \mu srad$

The total cross section at energy $E_p = 24 \cdot GeV$ is then given by:

$d\Sigma_d\Omega(E_p) = 2.551 \cdot mb$ $\qquad \Sigma_{ep} := d\Sigma_d\Omega(E_p) \cdot d\Omega$ $\qquad \Sigma_{ep} = 6.234 \cdot nb$

The Luminosity from the proton bunch passing through the electron bunch is:

$$\boxed{L(E) := \frac{3 \cdot f_0 \cdot B \cdot N_p \cdot N_e}{2 \cdot \beta_{ep} \cdot \varepsilon_n} \cdot \left(\frac{E}{E_{0p}}\right)} \qquad L(E_p) = 3.054 \cdot 10^{29} \cdot cm^{-2} \cdot sec^{-1}$$

Thus, the interaction rate is:

$R := L(E_p) \cdot \Sigma_{ep}$ $\qquad R = 1.904 \cdot 10^{-3} \cdot Hz$

Assuming the analyzing power to be relatively constant for $\theta_e = 5 \cdot mrad$, with a value of about $A := 0.5$, then for a $\delta := 10 \cdot \%$ polarization measurement, the number of interactions required would be

$$N_{meas} := \frac{1}{(A \cdot \delta)^2}, \text{ or } N_{meas} = 400$$

This yields a measurement time of

$$T_{meas} := \frac{N_{meas}}{R}, \text{ or } T_{meas} = 3.502 \cdot 10^3 \cdot min$$

! @ injection

The measurement time can be plotted vs. energy:

$$T(E) := \frac{N_{meas}}{L(E) \cdot (d\Sigma_d\Omega(E) \cdot d\Omega)} \qquad E := 24 \cdot GeV, 25 \cdot GeV .. 250 \cdot GeV$$

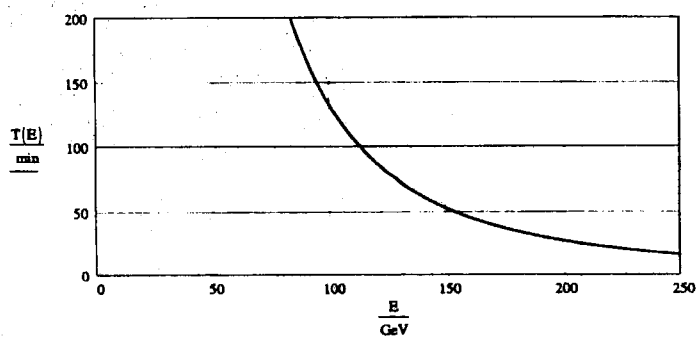

Future:

- electron beam optics
- recoil electron rigidity
- toroid magnet configuration and parameters

So, at injection energy (25 GeV), with

electron beam kinetic energy = 10 keV,
electron beam current = 10 mA (ave),
= 1 A peak, over 1 nsec duration
= 10^{10} per pulse

=====> measurement times of 10's of hours

Thus, need to improve

$\beta^* = 5$ m ---> 1 m
detector acceptance = 30 μsrad ---> 120 μsrad

=====> measurement times of 1.5 hours

Then, higher beam current

I_{beam} = 10 mA ---> 50 mA =====> 20 min. measurement times

NOTE: only need to do precise measurements like this once in a while; can use to calibrate other polarimeters, etc.

Q's:

Stupakov:	Non-polarized electron can also be used for polarimetry – and their sources are much more intensive.
Syphers:	Yes, but the resulting asymmetry is much smaller, and it may be a reason for polarized e-beam.
Danilov:	TMCI may occur in the ions beam. You will need several tesla solenoid field to keep it stable – compare to the Tevatron with electron compressor.
Shiltsev:	May be a scheme where spin interacts with Larmour circle magnetic moment will work? To increase the interaction time, the electrons and ions would better have same velocities. It may also require a gradient in electron density...

#9

Beam-Beam Interaction in Linear Colliders

Topics: *luminosity and beam-beam effects in linear colliders*
the SLC experience & NLC design
lessons and ideas for ring colliders (luminosity optimization, tuning, diagnostics, ...)

Fermilab, February 1998 Frank Zimmermann

Luminosity

$$\boxed{L = \frac{f_{rep}\, n_b N_b^2}{4\pi \sigma_x \sigma_y} H_D}$$

includes pinch & hourglass ($\lesssim 2$)

compared to ring collider:

f_{rep} ↓ $1/100$

$n_b N_b^2$ ↓ or ≈

need <u>much smaller</u> $(\sigma_x \sigma_y)$!

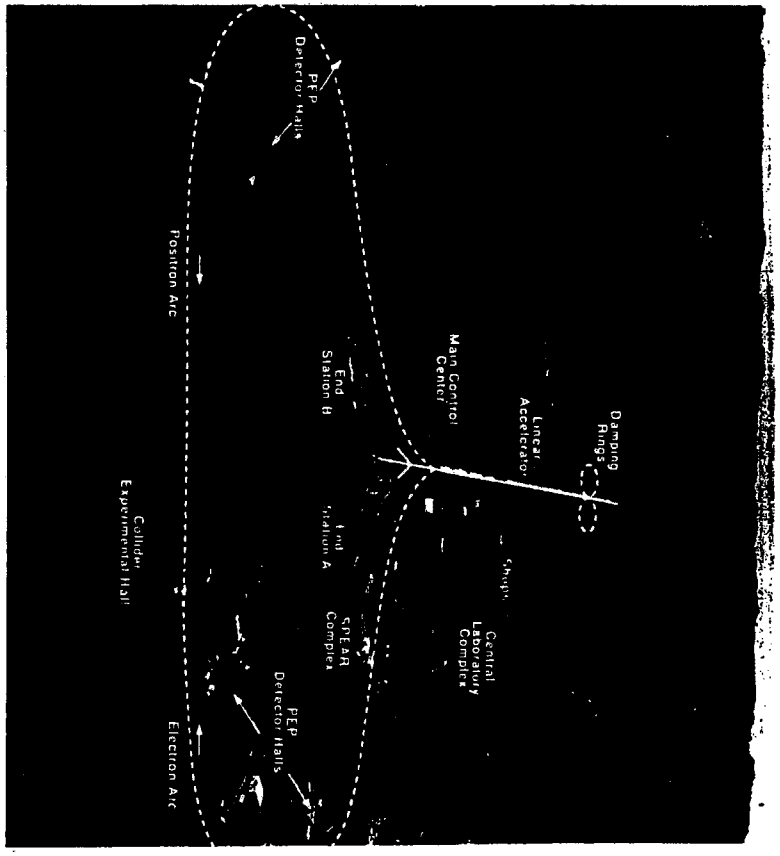

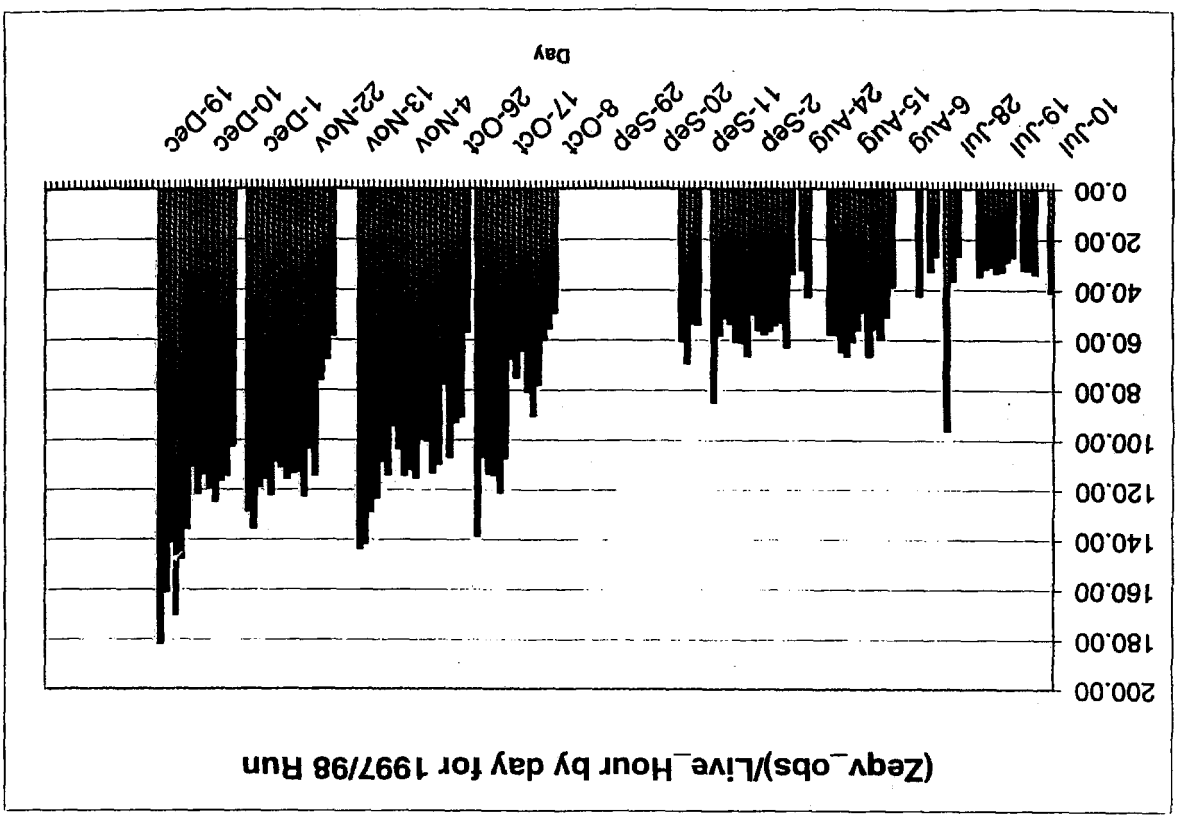

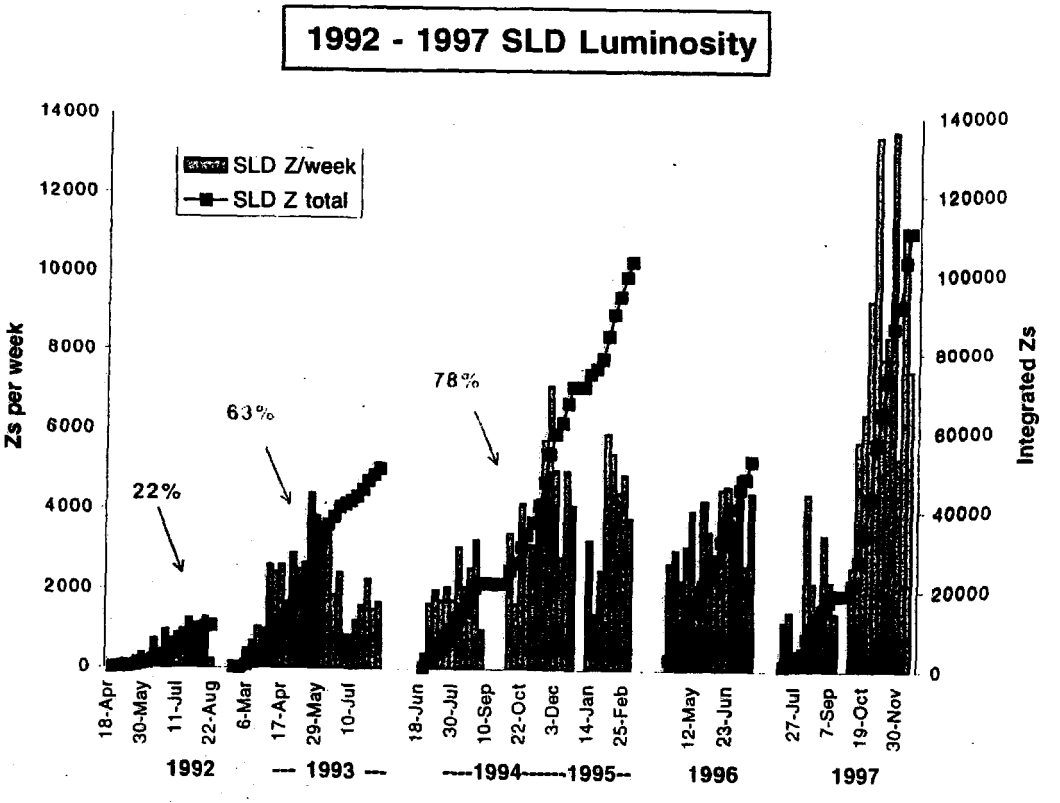

N. Phinney 1/20/98

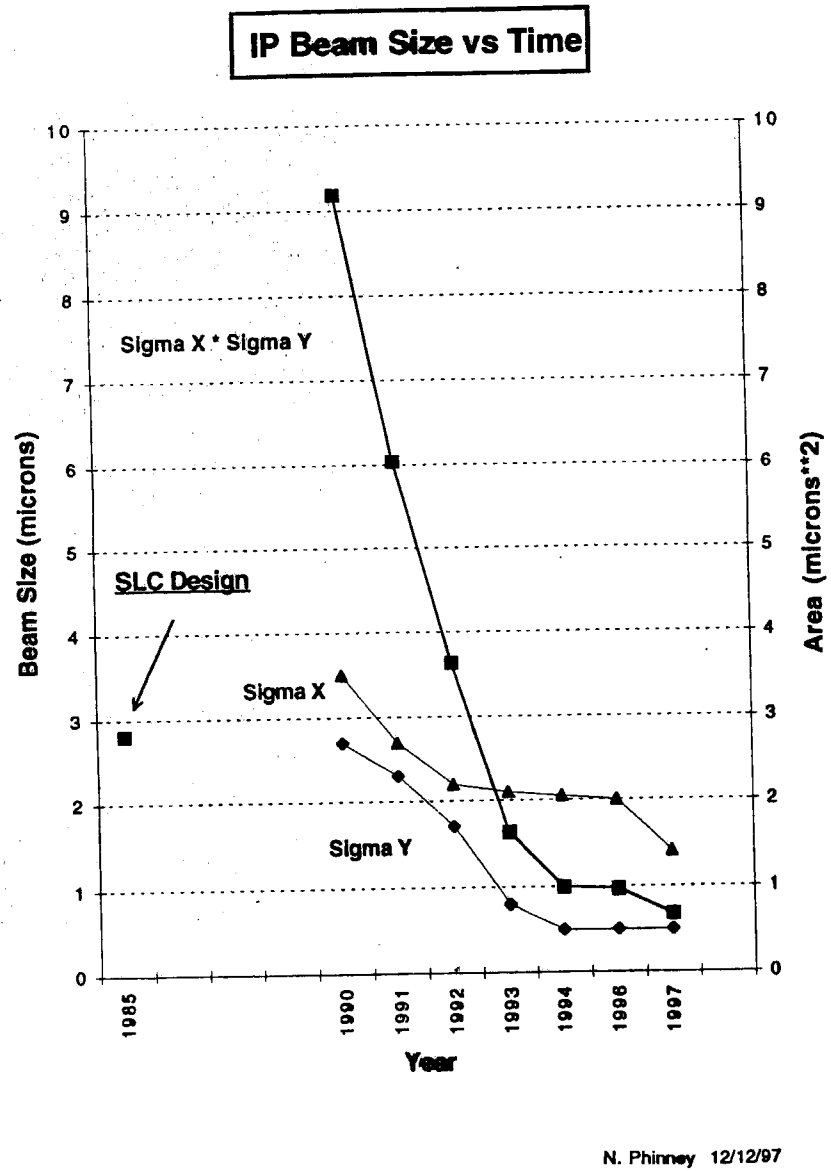

Collision strength

measured by "disruption parameter":

$$D_{x,y} \equiv \frac{\text{"}\sigma_z\text{"}}{f} = \frac{2 N r_e}{\gamma} \frac{\sigma_z}{\sigma_{x,y}(\sigma_x + \sigma_y)}$$

no. of oscillations during collision

$$\sim \sqrt{\sqrt{3} D} / 2\pi$$

SLC : $D_y \sim 1$

NLC : $D_y \sim 8$

NOTE

$$\xi_{x,y} = \frac{\beta^*_{x,y}}{\sigma_z} D_{x,y} \simeq D_{x,y}$$

beam-beam tune shift parameter

beamstrahlung

Synchrotron radiation in the field of the opposing bunch

critical energy:

$$\boxed{\Upsilon \equiv \frac{2}{3}\frac{\hbar\omega_c}{E} = \frac{5}{6}\frac{\gamma r_e^2 N}{\alpha \sigma_z(\sigma_x+\sigma_y)}}$$

$\Upsilon \approx 10^{-3}$ SLC

$\Upsilon \approx 0.3$ NLC

$\Upsilon \approx 0.3-0.5$ E144 at FFTB

want $\boxed{\Upsilon \lesssim 0.5}$ to limit coherent pair creation

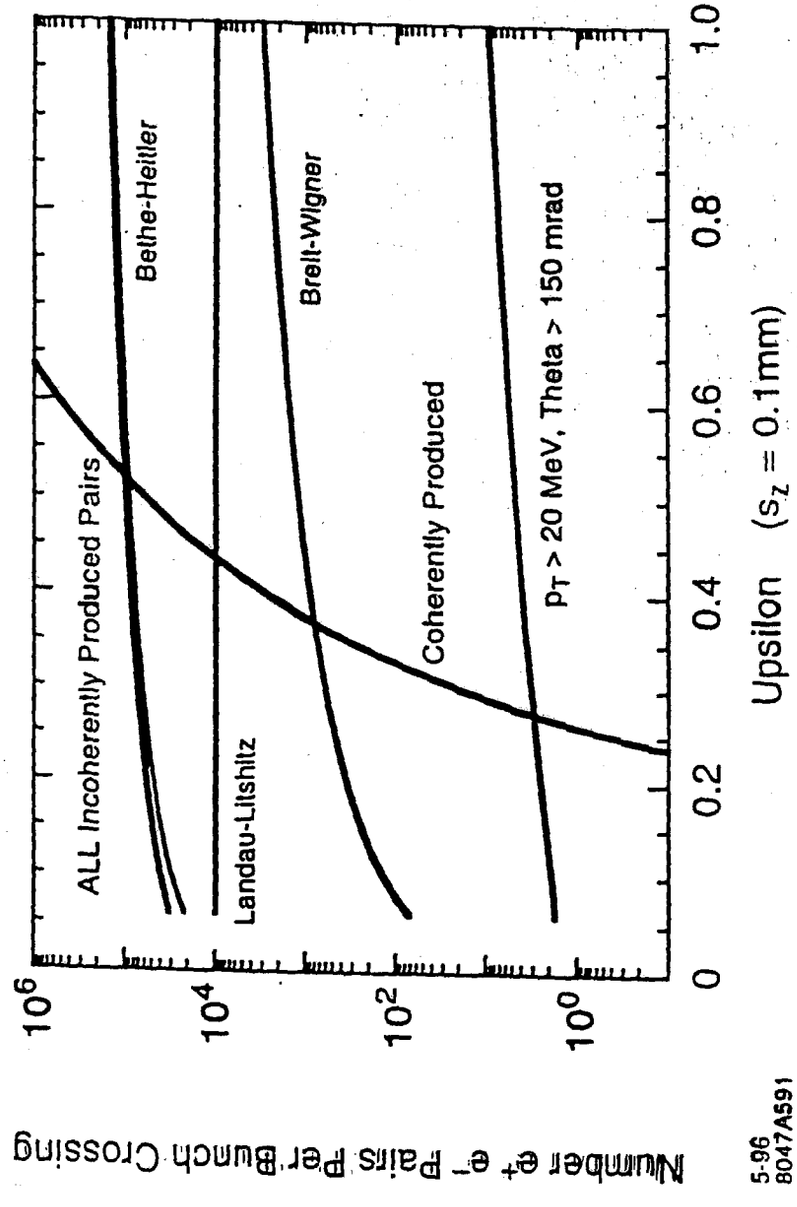

5-96
8047A591

number of beamstrahlung photons

- affects "purity" of luminosity spectrum

$$\boxed{\begin{aligned} N_\gamma &\approx \frac{5}{2}\,\frac{\alpha\,\sigma_z}{\gamma\,\mathcal{X}_c}\,\Upsilon\,\frac{1}{(1+\Upsilon^{2/3})^{1/2}} \\ &\approx 2\,\frac{\alpha\, r_e N}{\sigma_x+\sigma_y} \end{aligned}}$$

$$N_\gamma \approx \begin{cases} 0.7 & \text{SLC} \\ 1.0 & \text{NLC-I} \\ 1.7 & \text{NLC-II} \end{cases}$$

fraction of luminosity at E_{CM}

$$\boxed{\frac{\Delta L}{L} \approx \frac{1}{N_\gamma^2}\left(1-e^{-N_\gamma}\right)^2}$$

40% for $N_\gamma \simeq 1$

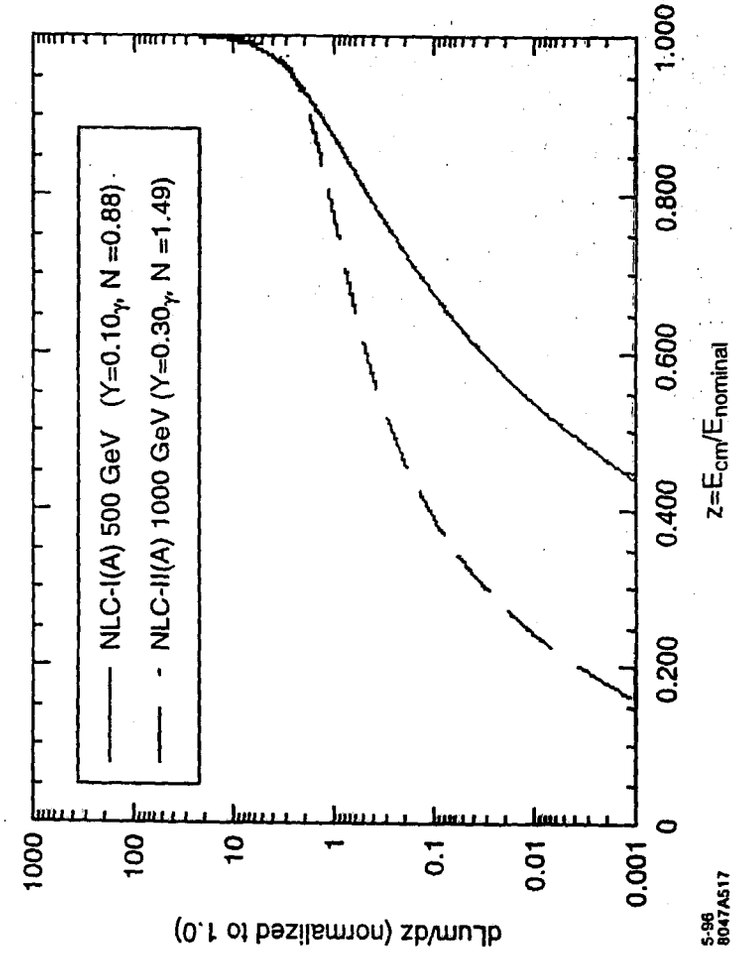

average energy loss :

$$\boxed{\delta_B \simeq \frac{1}{2} N_\gamma \Upsilon \simeq \frac{r_e^3 N^2 \gamma}{\sigma_z \sigma_x^2 \left(1+\frac{\sigma_y}{\sigma_x}\right)^2}}$$

$$\delta_B \simeq \begin{cases} 0.04\,\% & \text{SLC 1997} \\ 3\,\% & \text{NLC-I} \\ 10\,\% & \text{NLC-II} \end{cases}$$

Υ, N_γ, δ_B can be reduced by :

(1) flat beams ($\sigma_y \ll \sigma_x$)

(2) long bunches (diagnostic !)

(3) charge compensation

(4) plasma

LC luminosity rewritten as

$$\boxed{L \simeq \left(\frac{10}{r_e}\right) \frac{P_{wall}}{E_{beam}} N_\gamma \frac{1}{\eta \sigma_y}}$$

$\Rightarrow$ increase efficiency $\eta \equiv \frac{P_{beam}}{P_{wall}}$

reduce σ_y

$N_\gamma \sim 1$ and E_{beam} fixed

---

for comparison : ring-collider luminosity

$$\boxed{L \simeq \frac{I}{e}\left(\frac{1}{8\pi r_e}\right) \xi_y \left(1+\frac{\sigma_x}{\sigma_y}\right) \frac{1}{\beta_y^*}}$$

ξ_y fixed

hourglass effect

change of β around IP

$$\boxed{A_{x,y} = \frac{\sigma_z}{\beta^*_{x,y}}}$$

SLC: $A_y \approx 0.8$

NLC: $A_y \approx 1$

round beams:

$$\eta_A = \frac{\mathcal{L}_A}{\mathcal{L}_0} = \frac{2}{\sqrt{\pi}\,\sigma_z} \int_0^\infty \frac{e^{-z^2/\sigma_z^2}}{1 + z^2/\beta^{*2}}\, dz$$

$$\boxed{A = 1 \quad : \quad \eta_A = 0.76}$$

flat beams:

$$\eta_A = \frac{1}{\sqrt{\pi}\, A_y}\, e^{-1/2A_y^2}\, K_0\left(\frac{1}{2A_y^2}\right)$$

pinch effect

uniform cylinder beam with N particles

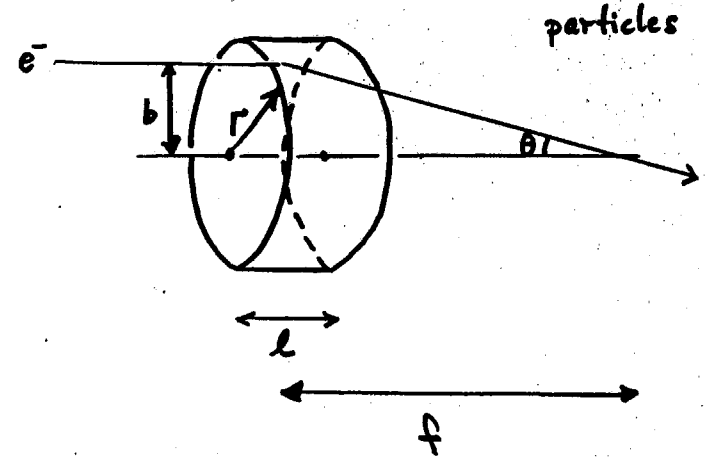

$$\boxed{\frac{1}{f} = \frac{2 N r_e}{\gamma r^2}} \qquad D \equiv \frac{\sigma_z}{f}$$

$D \geq 1 \;\hat{=}\;$ focal point within the bunch

$$\boxed{\text{Luminosity enhancement for large } \sigma_z \text{ ; enhancement factor } H_D \equiv \mathcal{L}/\mathcal{L}_0}$$

includes hourglass effect

P. Chen

round beams:

$$H_D^{round} = 1 + D^{1/4}\left(\frac{D^3}{1+D^3}\right)\left\{\ln(\sqrt{D}+1) + 2\ln\left(\frac{0.8}{A}\right)\right\}$$

empirical formula

P. Chen & K. Yokoya 1988

flat beams:

$$H_D^{flat} \simeq H_D^{round\ 1/3}$$

when $D_y, A_y = D, A$

$D_x, A_x \to 0$

round beams variable A

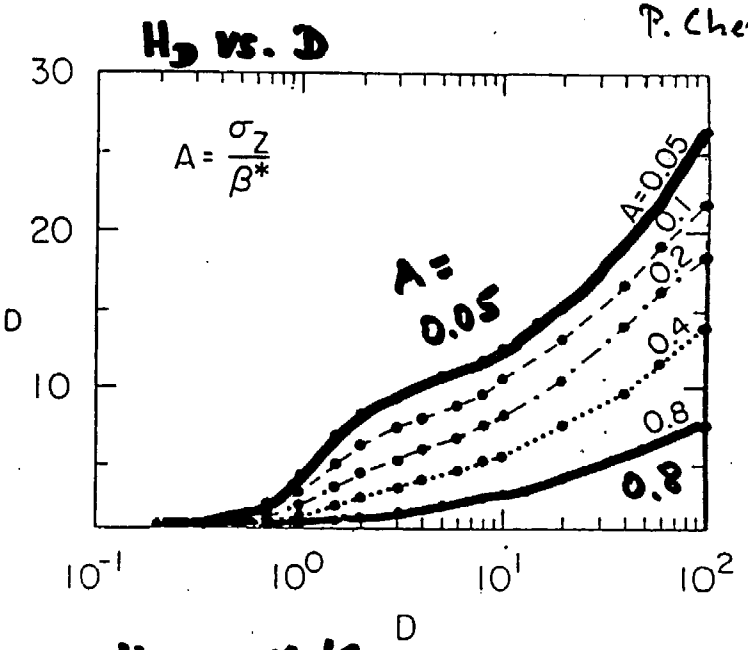

$A_{x,y} = 0.1$ variable D

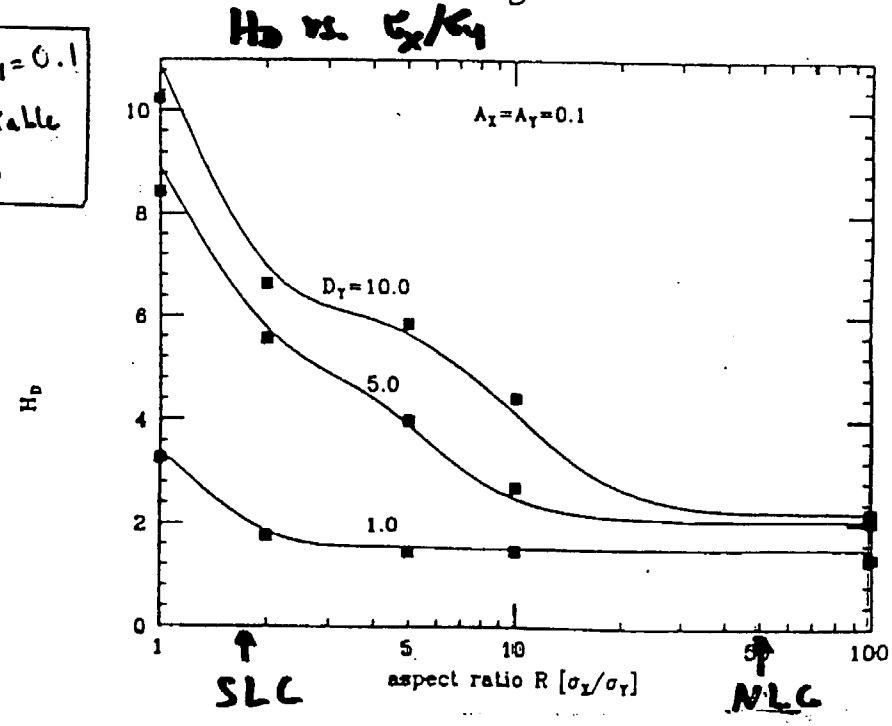

P. Chen

round beams:

$$H_D^{round} = 1 + D^{1/4}\left(\frac{D^3}{1+D^2}\right)\left\{\ln(\sqrt{D}+1) + 2\ln\left(0.8/A\right)\right\}$$

empirical formula

P. Chen & K. Yokoya 1988

flat beams:

$$H_D^{flat} \simeq H_D^{round\ 1/3}$$

when $D_y, A_y = D, A$

$D_x, A_x \to 0$

round beams variable A

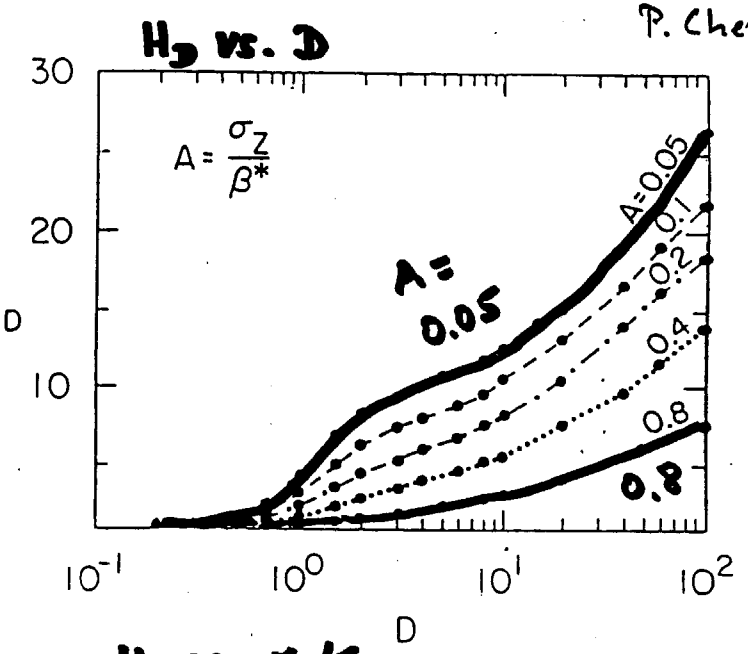

$A_{x,y} = 0.1$ variable D

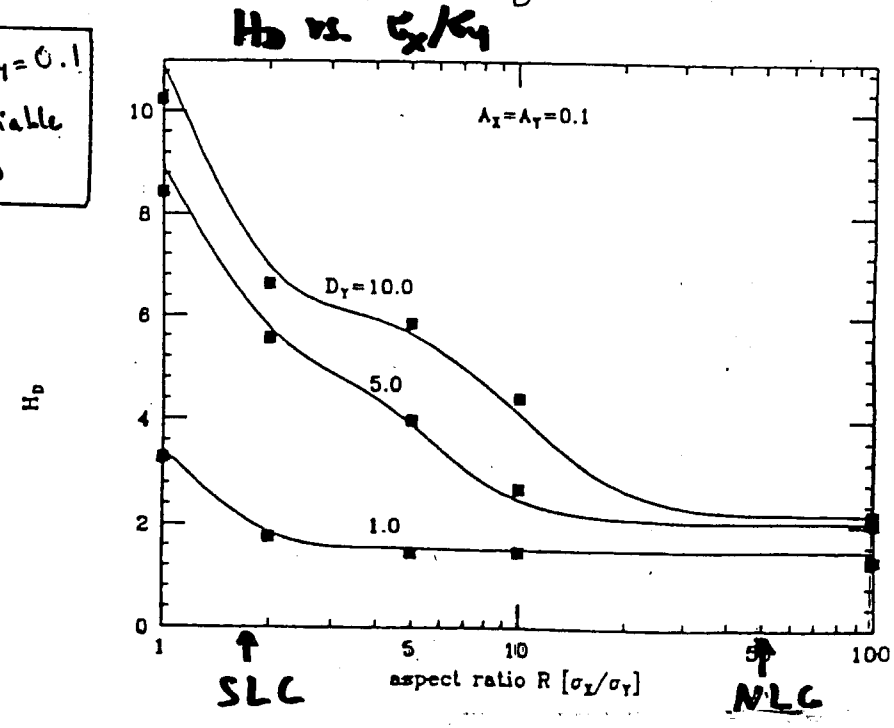

T. Markiewicz

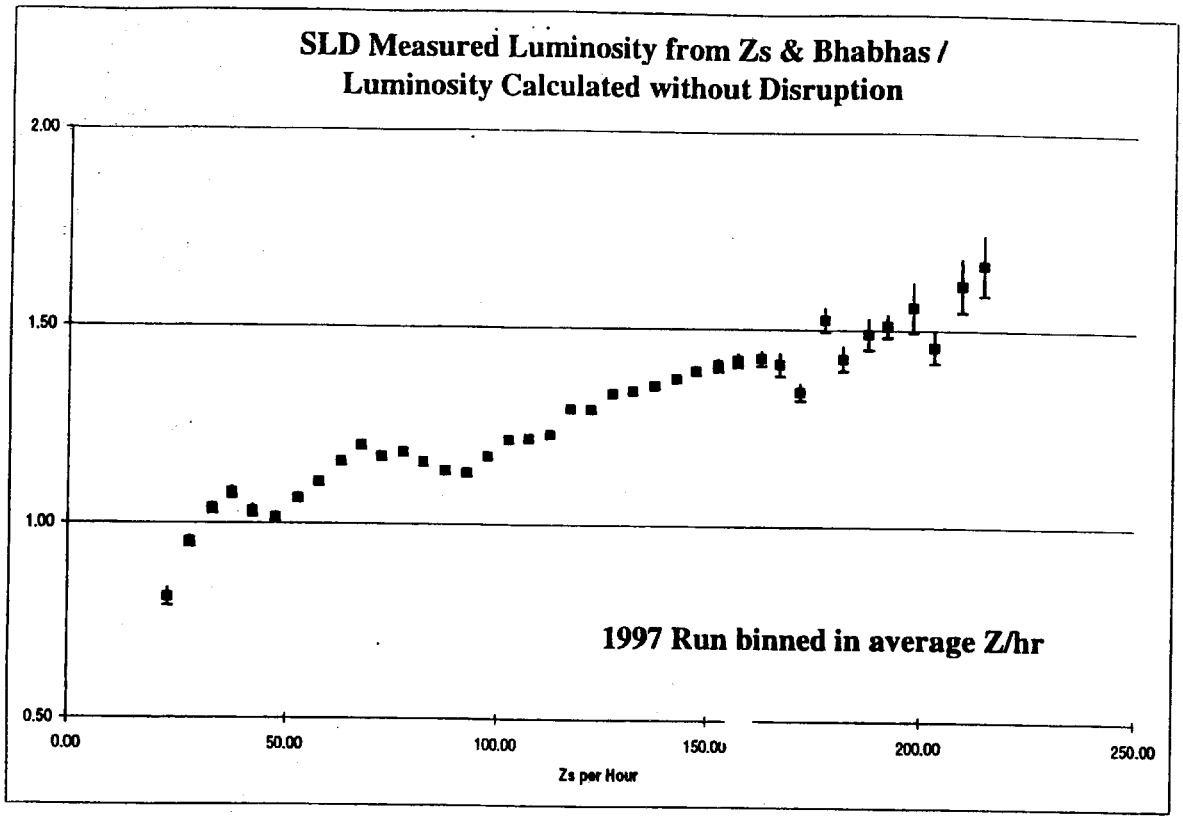

1/29/98

T. Markiewicz

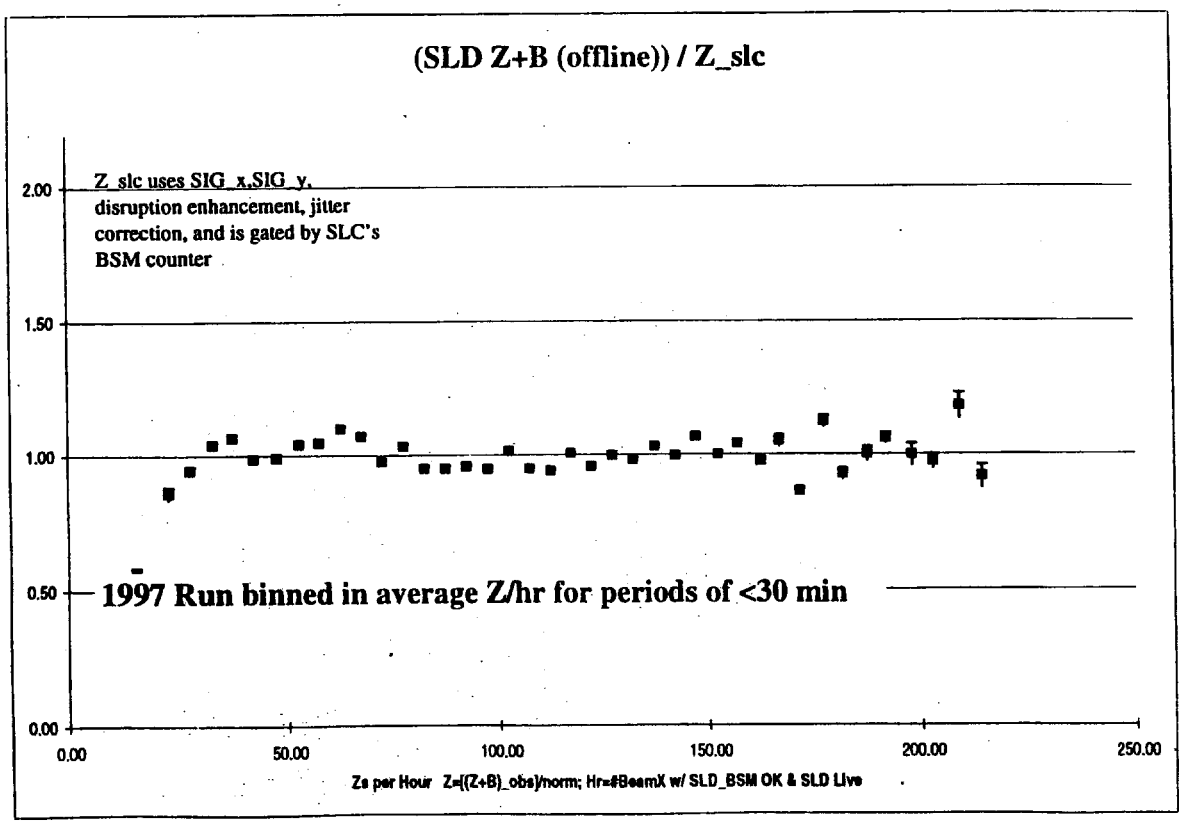

1/29/98

T. Markiewicz

Beam Sizes at Low Current ($\sim 5 \cdot 10^9$)

expected values achieved !

typical beam-beam deflection scans
at low current

applications of deflections

- fast $\boxed{\text{luminosity measurement}}$
- used by $\boxed{\text{IP collision feedback}}$
  (4 BPMs around IP
  → measure $\Theta_{x,y}$
  calculate correction
  $-\Delta x, -\Delta y$)
  robust
  fast convergence
- $\boxed{\text{spot-size optimization}}$

disruption angle

$$\boxed{\theta_0 \equiv \frac{2 N r_e}{\gamma(\sigma_x+\sigma_y)} = \frac{D_x \sigma_x}{\sigma_z} = \frac{D_y \sigma_y}{\sigma_z}}$$

$$\theta_0 \simeq \begin{cases} 1 \text{ mrad} & SLC \ (\simeq 4\,\theta_y^*) \\ 300\ \mu\text{rad} & NLC \ (\simeq 10\,\theta_y^*) \end{cases}$$

→ aperture of final quadrupoles

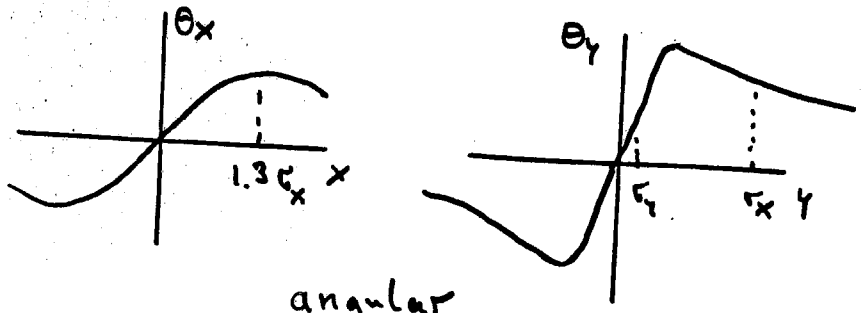

angular distribution

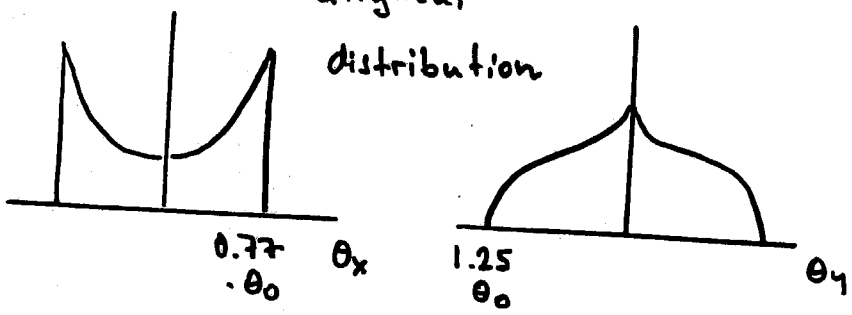

Center of mass deflection

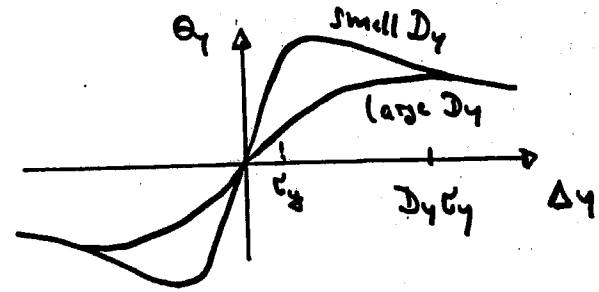

small D_y
small Δy
⇓
$\theta_y = \frac{1}{2}\theta_0 \frac{\Delta y}{\sigma_y}$

"beam-beam deflection scans"

$$\Rightarrow \boxed{\begin{aligned} \Sigma_x &= (\sigma_{xe^-}^2 + \sigma_{xe^+}^2)^{1/2} \\ \Sigma_y &= (\sigma_{ye^-}^2 + \sigma_{ye^+}^2)^{1/2} \end{aligned}}$$

Note: luminosity

$$\mathcal{L} = 2 f N_{e^-} N_{e^+} \int dx\,dy\,ds\,dt\; n_{e^-}(x,y,z_{e^-},t) \cdot n_{e^+}(x,y,z_{e^+},t)$$

(where $z_{e^-} = s-t$, $z_{e^+} = -s-t$)

$$= \frac{f N_{e^-} N_{e^+}}{2\pi \Sigma_x \Sigma_y} H_D$$

for Gaussian bunches

Kink instability

Luminosity with initial displacement Δy :

$$\boxed{\mathcal{L} \propto e^{-\Delta y^2 / 4\sigma_y^2} \quad \text{for } D_y = 0}$$

for large enough D_y, kink instability can bring beams into collision if

$$\boxed{\Delta y \lesssim \frac{\pi}{4} \sigma_y D_y}$$

→ reduces sensitivity to displacements

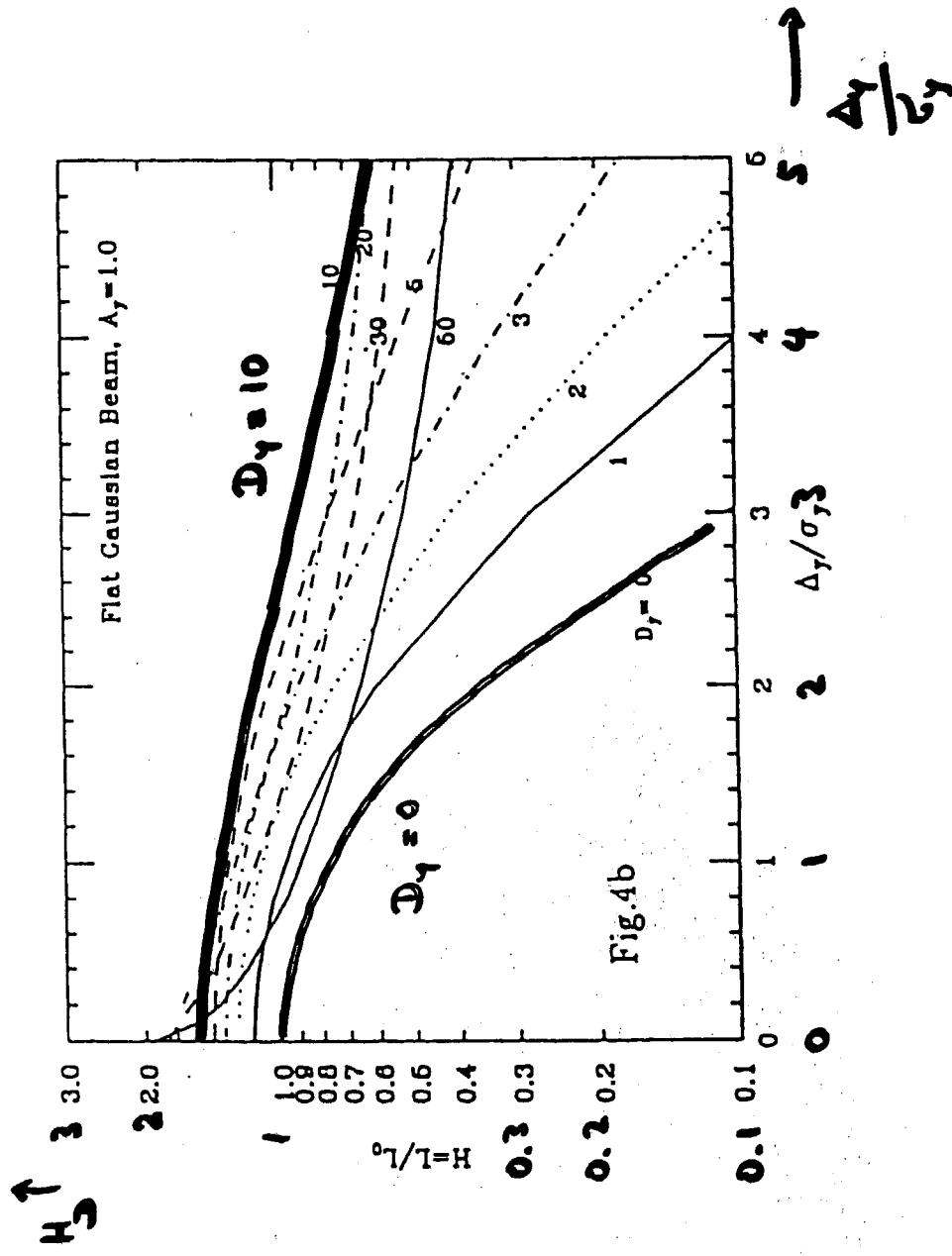

Fig.4b

depolarization

(1) spin-flip radiation

$$\boxed{\Delta P = 2 N_\gamma u_{f0} \qquad (u_{f0} \lesssim 0.02)}$$

$N_\gamma = 1 \rightarrow \Delta P \lesssim 4\,\%$

(2) precession in the magnetic field

$$\boxed{\Delta P \approx 0.006 \left(N_\gamma / u_0\right)^2 \quad \text{with } u_0 \approx 1 \text{ for small } \Psi}$$

$\lesssim$ a few percent

multibunch crossing instability

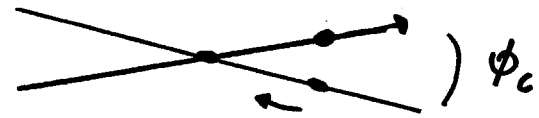

amplification of vertical displacements serious if

$$\boxed{C\,(m_b - 1) \gtrsim 1}$$

Chen & Yokoya

or $\gtrsim \sqrt{\frac{1}{2} + \frac{3\gamma}{3}}$

with m_b : # primary + peripheral collisions

$$C = D_x D_y \left[\frac{\sigma_x/\sigma_y}{\phi_c}\right]^2$$

Activity Report

Date/Time	10-16-00;11:42
Local ID	16308406654
Local Name	INFORMATION RESOURCE
Company Logo	

** Send **

No.	Doc	Remote Station	Start Time	Duration	Pages	Mode	Comments	Results
1			8-25-00;15:28					PI
2	025	95620190	8-28-00;14:56	52"	3/ 3	EC		CP 14400
3	064	6770	8-29-00;17:25	3'15"	6/ 6	EC		CP 14400
4			8-30-00;17:08					PI
5	002	918472291200	17:10	0"	-/ 4			TM
6	004	918474650985	17:12	4'13"	4/ 4	G3		CP 14400
7			8-31-00; 8:16					PI
8			9- 5-00; 8:27					PI
9	047	919082319890	18:02	48"	1/ 1	G3		CP 9600
10	063	99804242	9- 6-00;15:11	1'39"	3/ 3	EC		CP 9600
11	074	95771989	9- 7-00;12:46	0"	-/ 2			0569
12			16:13					PI
13			9- 8-00; 7:56					PI
14			9-11-00; 8:15					PI
15			9-13-00;10:00					PI
16			10:45					PI
17			11:52					PI
18	076	918474463523	9-15-00;12:28	46"	2/ 2	EC		CP 14400
19			9-18-00;14:09					PI
20	029	918474650985	16:36	3'07"	3/ 3	G3		CP 14400
21	031	94430795	16:47	1'15"	3/ 3	EC		CP 14400
22			9-22-00;15:38					PI
23	107	912062772763	9-28-00;10:13	1'28"	1/ 1	G3		CP 9600
24	109	912062772763	10:15	56"	1/ 1	G3		CP 9600
25	114	2062772763	10:18	0"	-/ 2			TM
26	116	912062772763	10:21	0"	-/ 2			056D
27	145	916305728267	10- 2-00;13:36	43"	1/ 1	EC		CP 14400
28	147	916305728267	13:39	43"	1/ 1	EC		CP 14400
29			10-16-00; 9:12					PI
30			11:21					PI
31			11:40					PI

Total 29

** Receive **

No.	Doc	Remote Station	Start Time	Duration	Pages	Mode	Comments	Results
1	038	630 562 0190	8-28-00;18:16	36"	2	EC		CP 14400
2	141	2176325533	9- 1-00;12:26	1'06"	2	EC		CP 9600
3	007	EC	9- 5-00;10:07	52"	2	EC		CP 14400
4	029	EC	14:37	1'21"	3	EC		CP 14400
5	031	EC	14:39	29"	1	EC		CP 14400
6	033	EC	14:39	36"	1	EC		CP 14400
7	058	630 980 4242	9- 6-00;12:06	1'17"	3	EC		CP 9600
8	061	IL DEPT OF REVENUE	14:56	1'28"	3	EC		CP 14400
9	065	EC	15:24	45"	2	EC		CP 14400
10	070	630 761 1065	9- 7-00;10:27	56"	3	EC		CP 12000
11	072	630 761 1065	10:29	54"	3	EC		CP 12000
12	094	630 761 1065	16:10	1'20"	5	EC		CP 12000
13	045	EC	9- 8-00;17:05	36"	2	EC		CP 14400
14	113	2176325533	9-18-00;11:36	1'08"	2	EC		CP 9600
15	117	EC	12:32	1'01"	3	EC		CP 14400
16	054	6313444745	9-21-00; 8:48	2'38"	11	EC		CP 14400
17	056	631 344 3238	8:52	2'55"	11	EC		CP 14400
18	143	630 572 8267	10- 2-00;13:24	1'31"	2	EC		CP 7200
19	153	EC	10- 3-00;12:22	55"	3	EC		CP 14400

Total 64

** Notes **

EC: Error Correct
BC: Broadcast Send
CP: Completed
LS: Local Scan
RE: Resend
MP: Multi-Poll
RM: Receive to Memory
LP: Local Print
PD: Polled by Remote
PG: Polling a Remote
DR: Document Removed
FO: Forced Output
MB: Receive to Mailbox
PI: Power Interruption
TM: Terminated by user
WT: Waiting Transfer

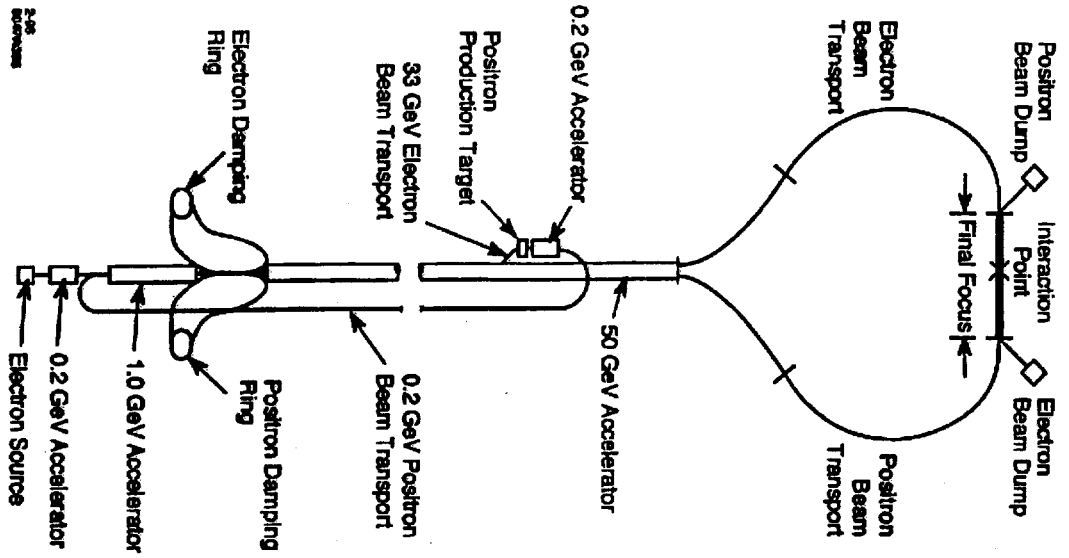

simulation study of longitudinal bunch shape & disruption for 1997 SLC

Bane, Thompson, Zimm.

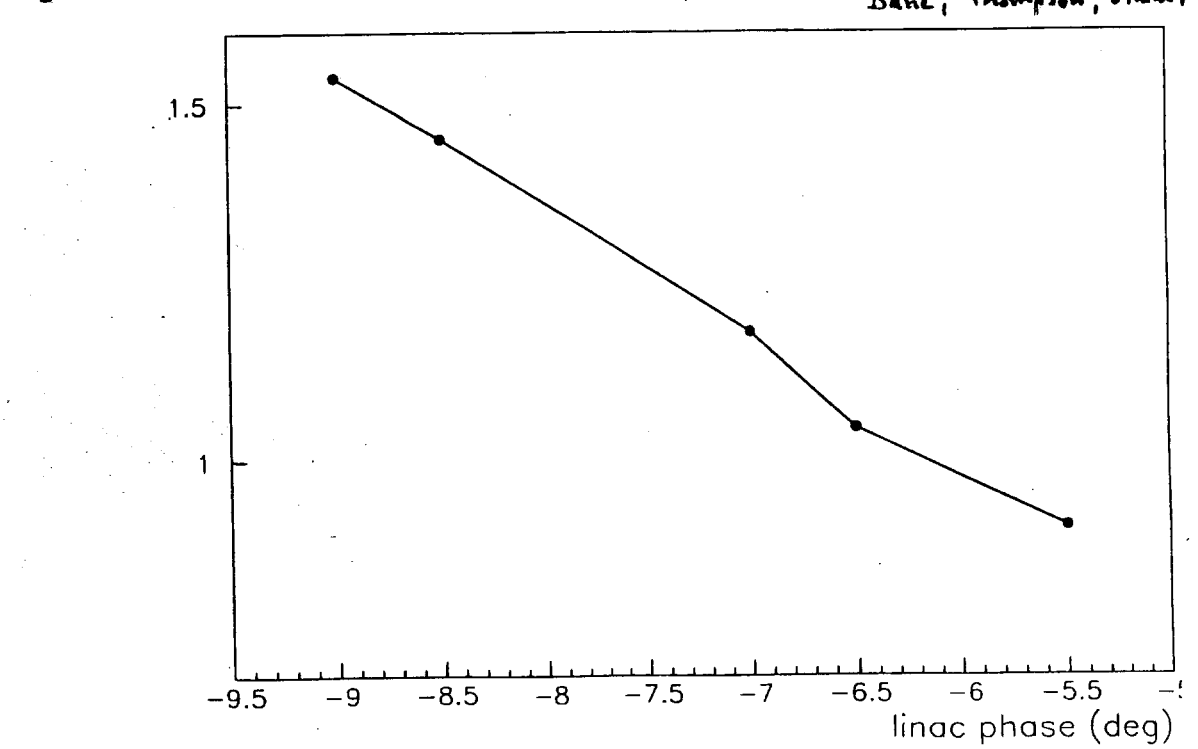

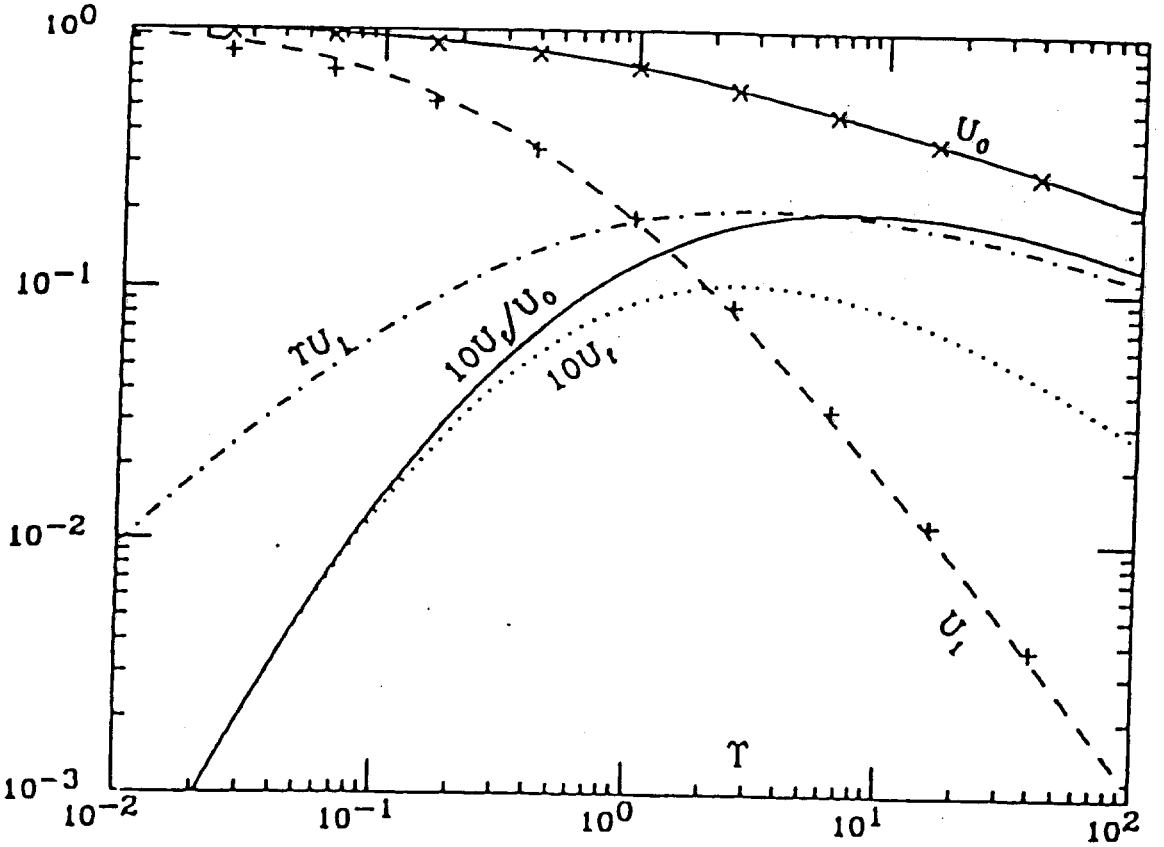

slow variation ...

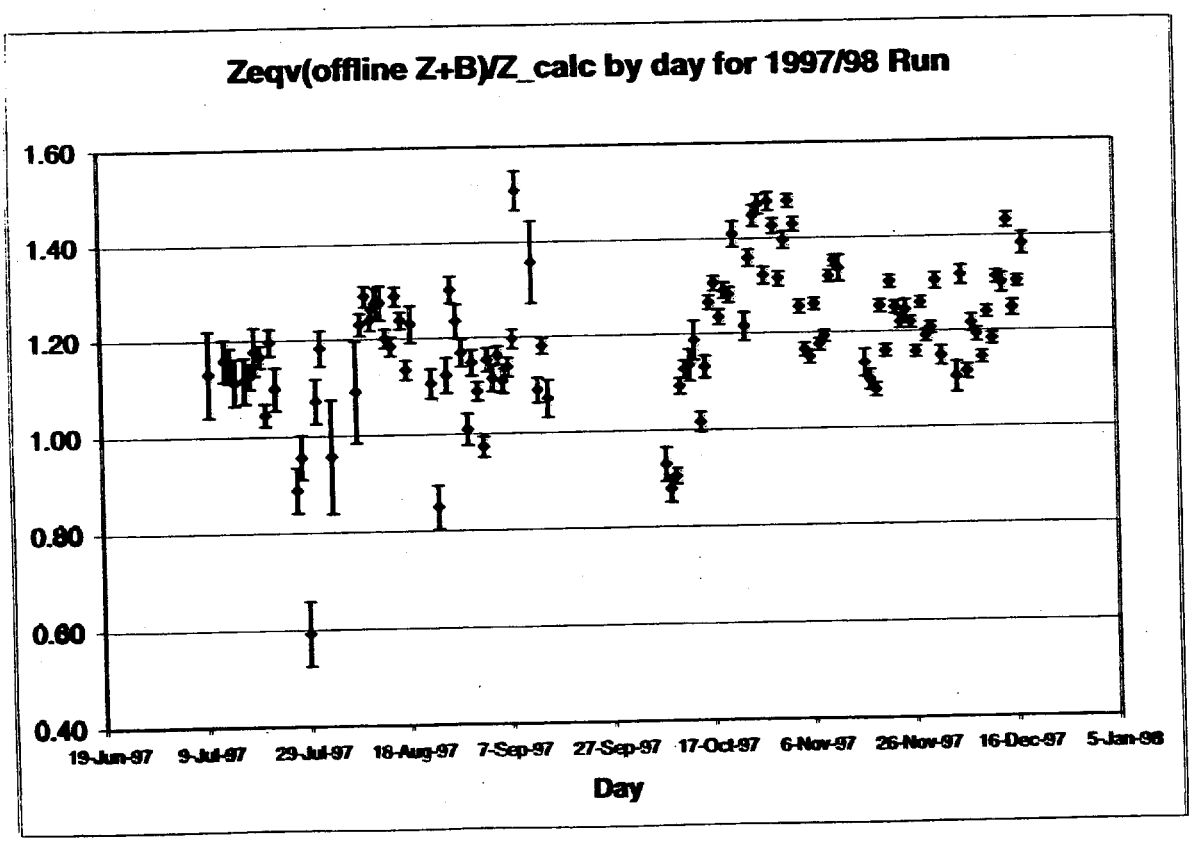

$\left(\frac{\Delta E}{E}\right)_{FWHM}$ in %

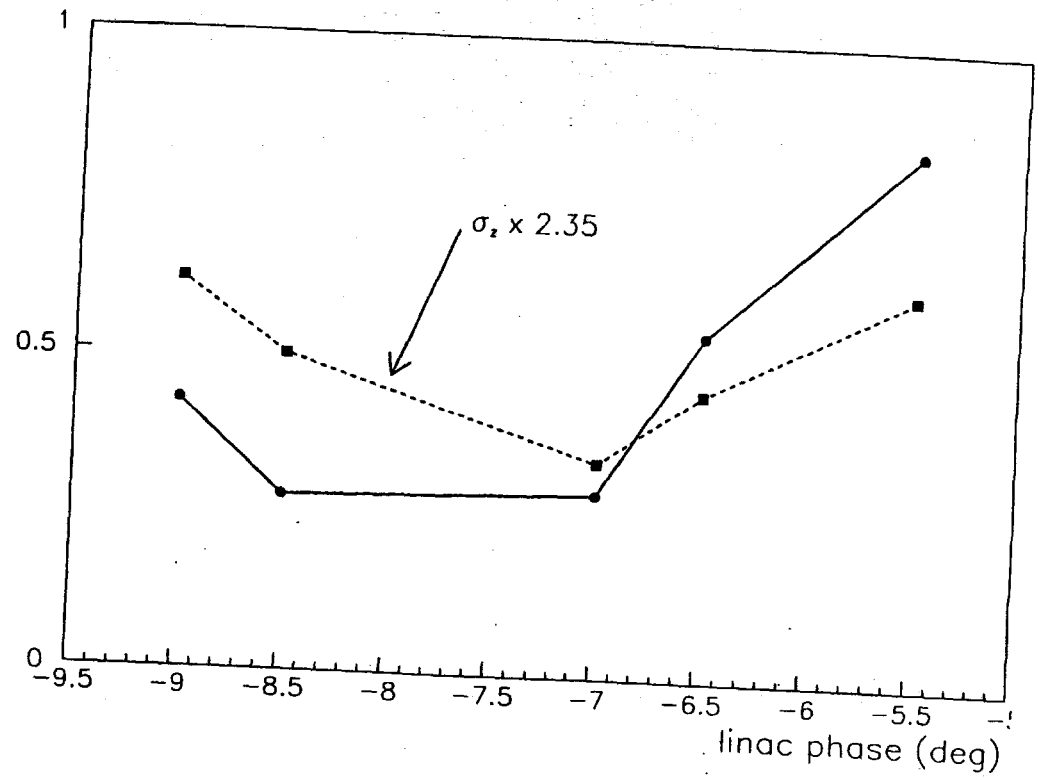

Variation of linac phase

deflection angle

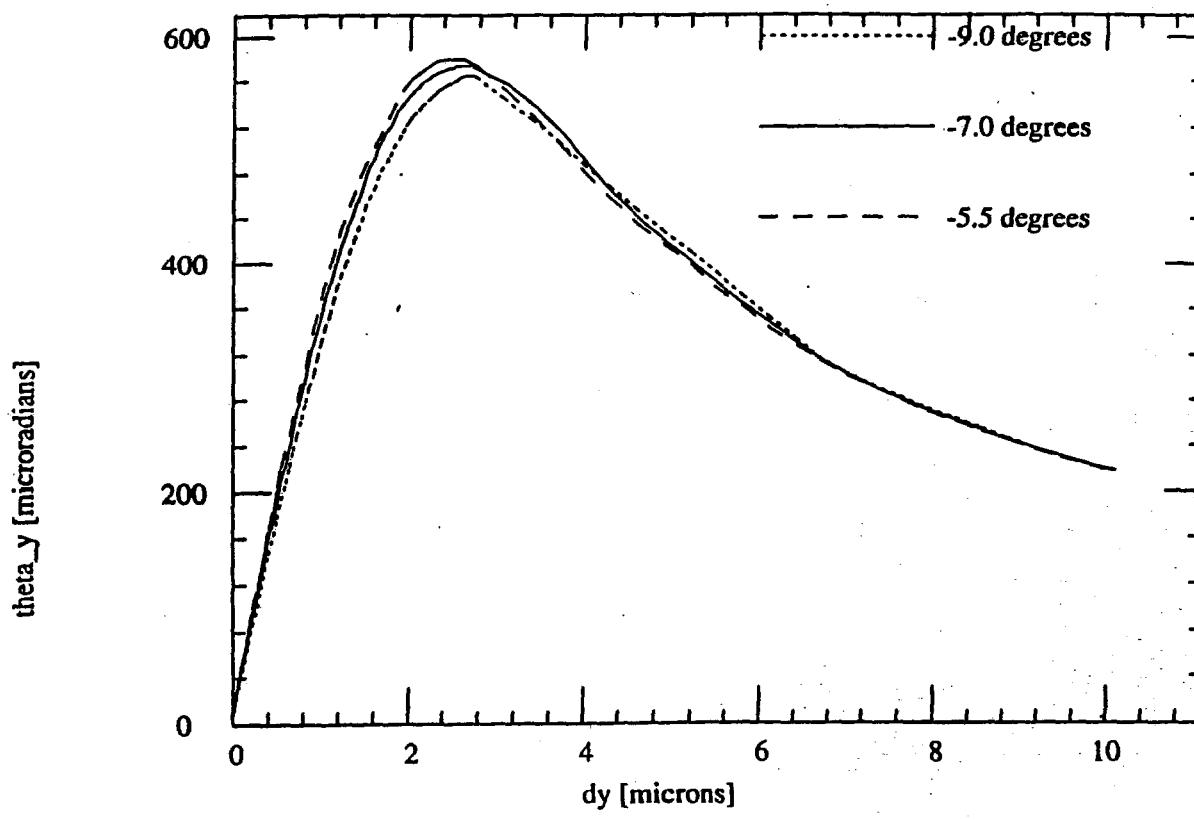

Variation of linac phase H_D

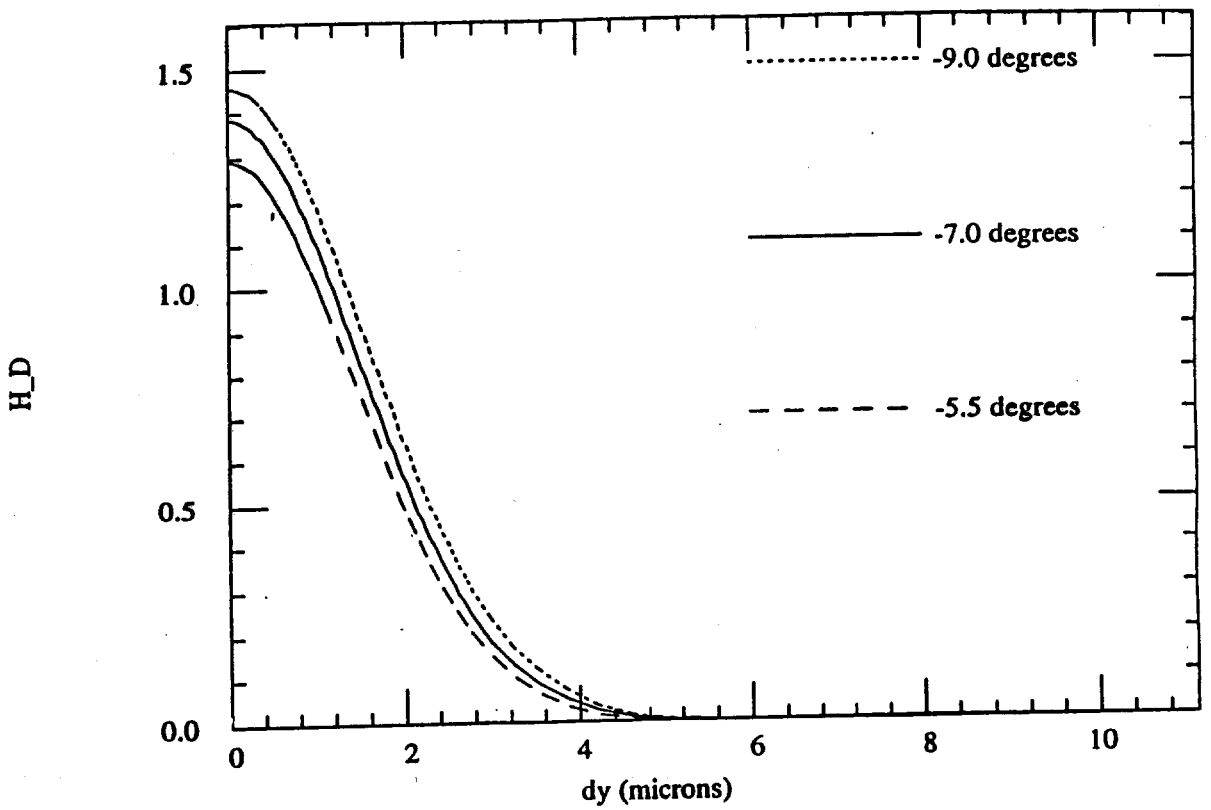

Variation of linac phase energy loss

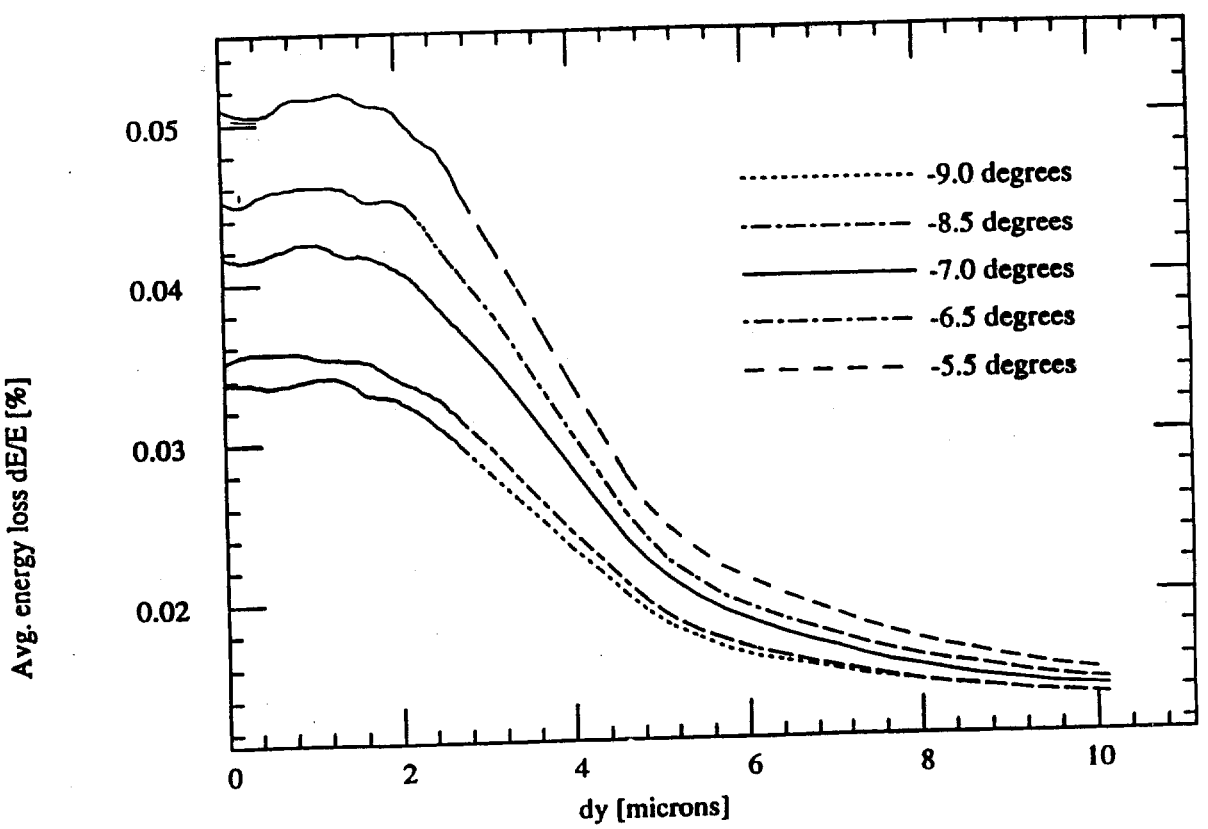

e^+/e^- timing monitor

D. Whittum

Apparatus

Previous reports describe the SLC south final focus bunch length monitor (BLM) assembly and BLM signal analysis.[1] The setup for beam timing monitor (BTM) is illustrated in Fig. 1.

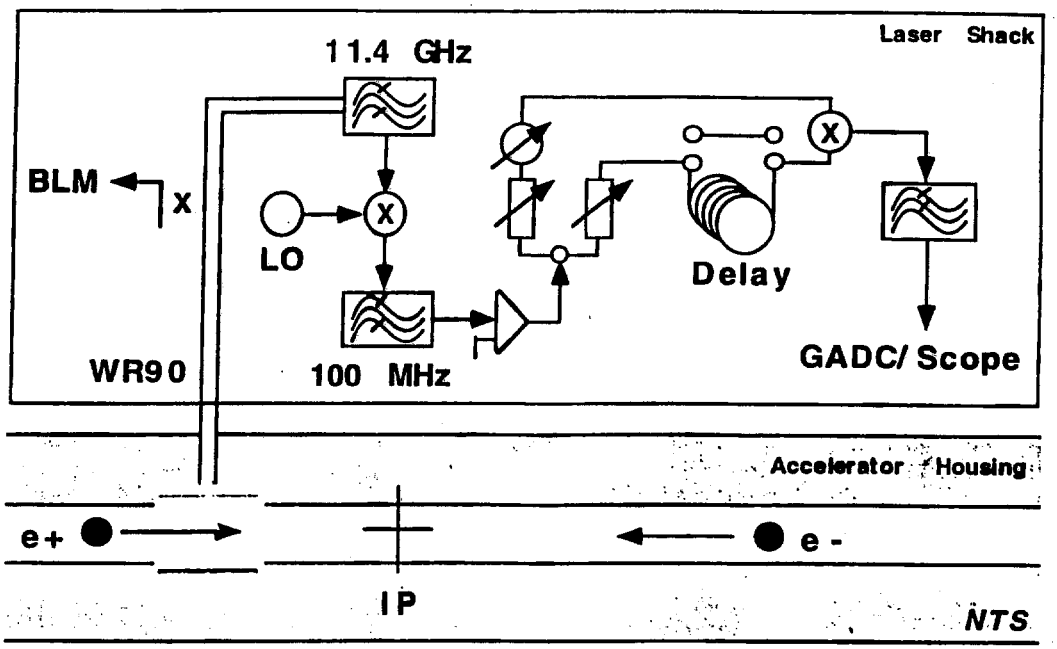

FIGURE 1. Schematic for BTM signal processing.

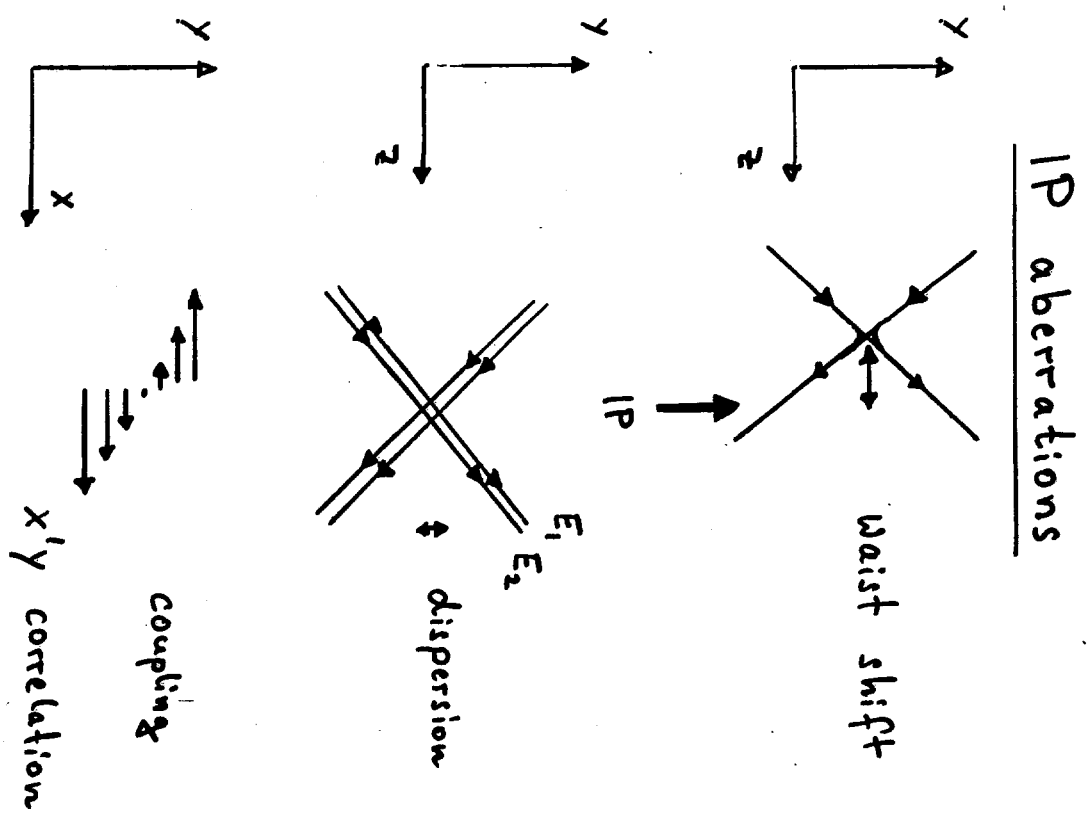

σ_z deduced from energy loss due to beamstrahlung

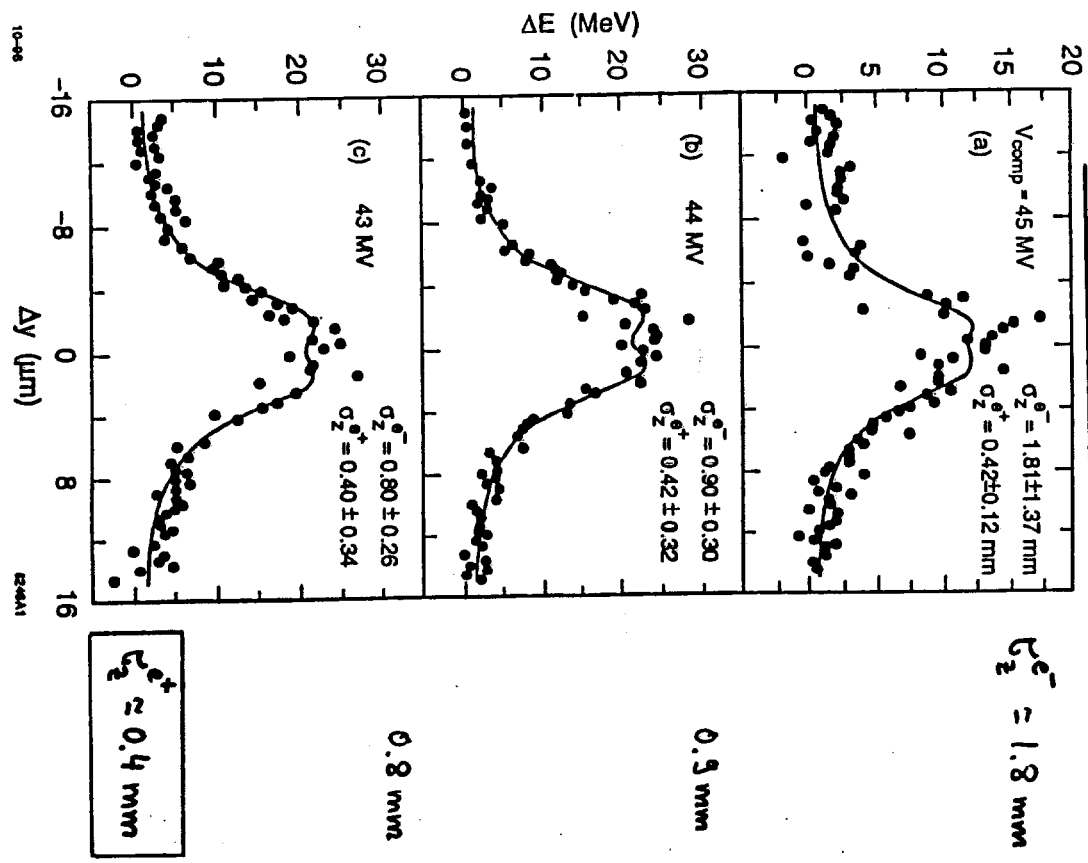

$\sigma_z^{e^-} \approx 1.8$ mm

0.9 mm

0.8 mm

$\sigma_z^{e^+} \approx 0.4$ mm

Raimondi

D. Whittum

G. Yocky, D. McCormick

M. Seidel, F. Zimmermann

DRAFT - 9/28/96

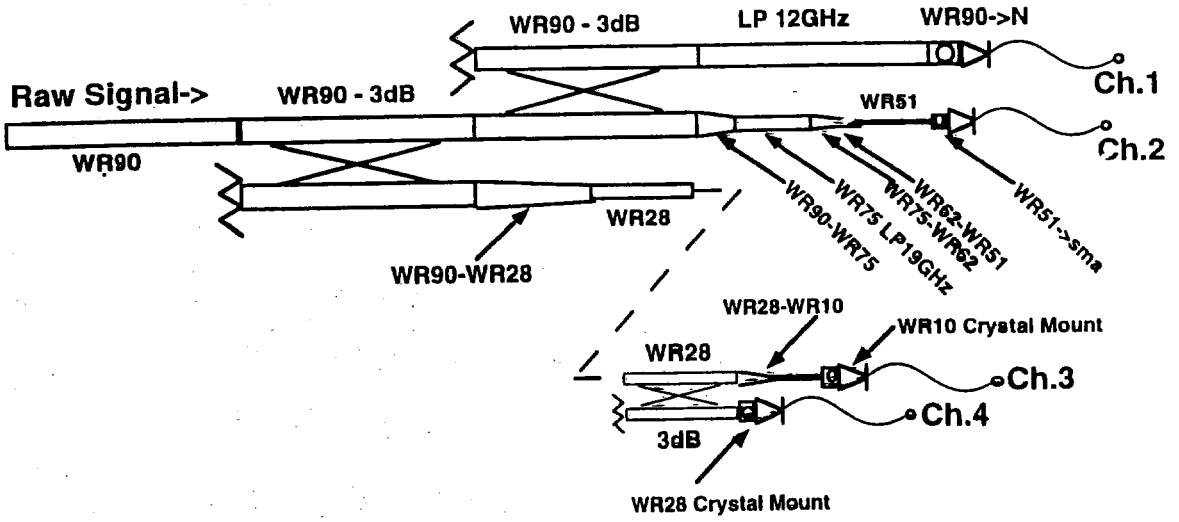

Comments

(1)Use symmetric splitters/tees where possible, for 3dB couplers.

(2)1 N-crystal, 1 sma crystal, 1 ea for WR28, WR10 mount

DRAFT - 9/28/96

Signal Processing for SFF-BLM

IP aberration tuning

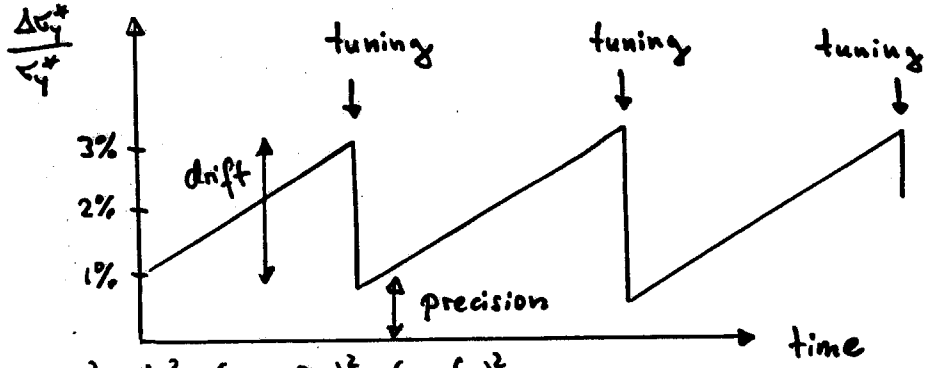

$$\sigma_y^2 = \sigma_{y_0}^2 + (\Delta w \cdot \theta_y)^2 + (\eta_y \cdot \delta_E)^2 \cdots\cdots$$

tuning of 5 aberrations :

x/y dispersion

x/y waist

skew coupling

routine procedure performed by operators ~ 1 / shift

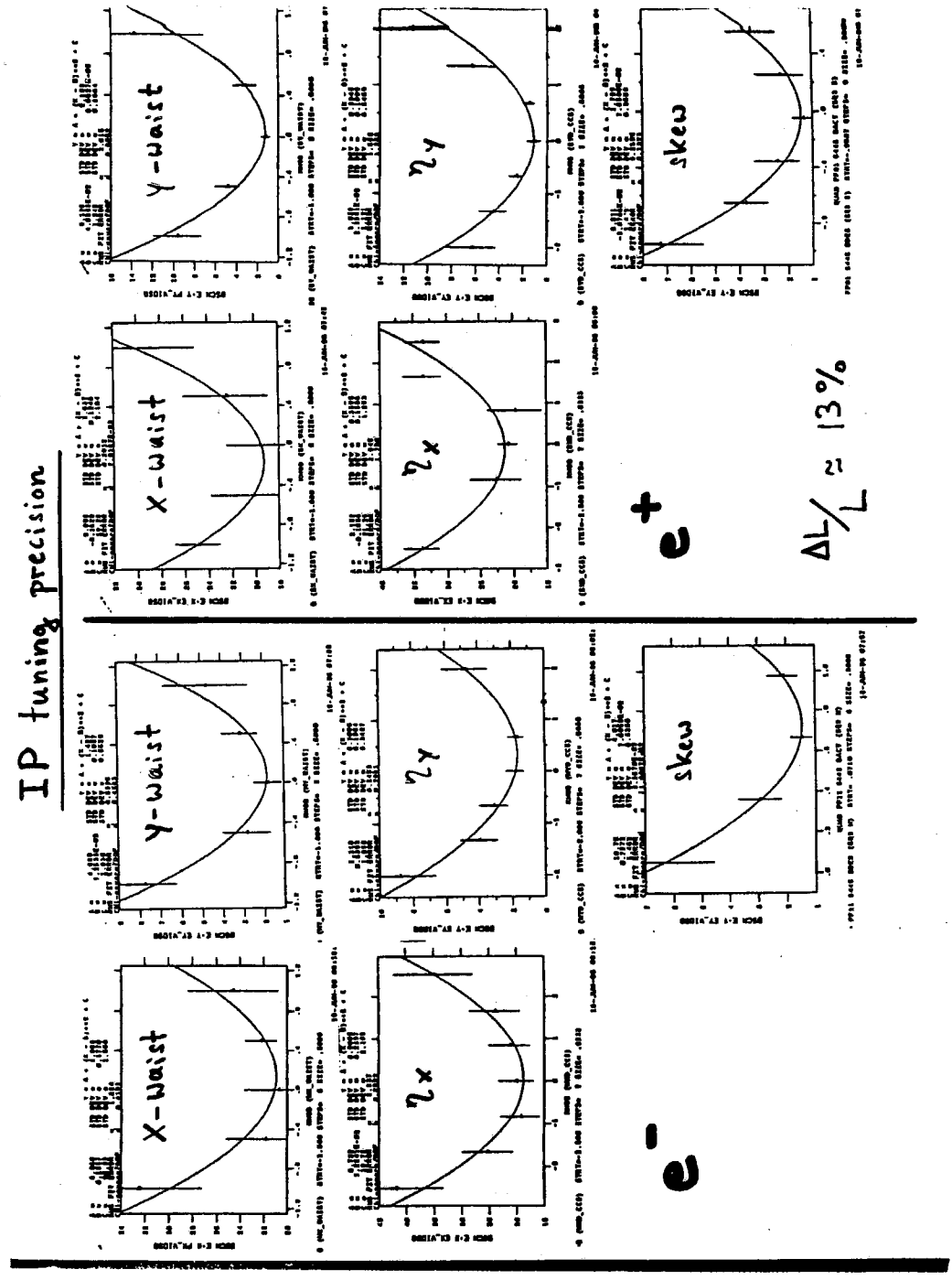

IP aberration tuning, May-July 96

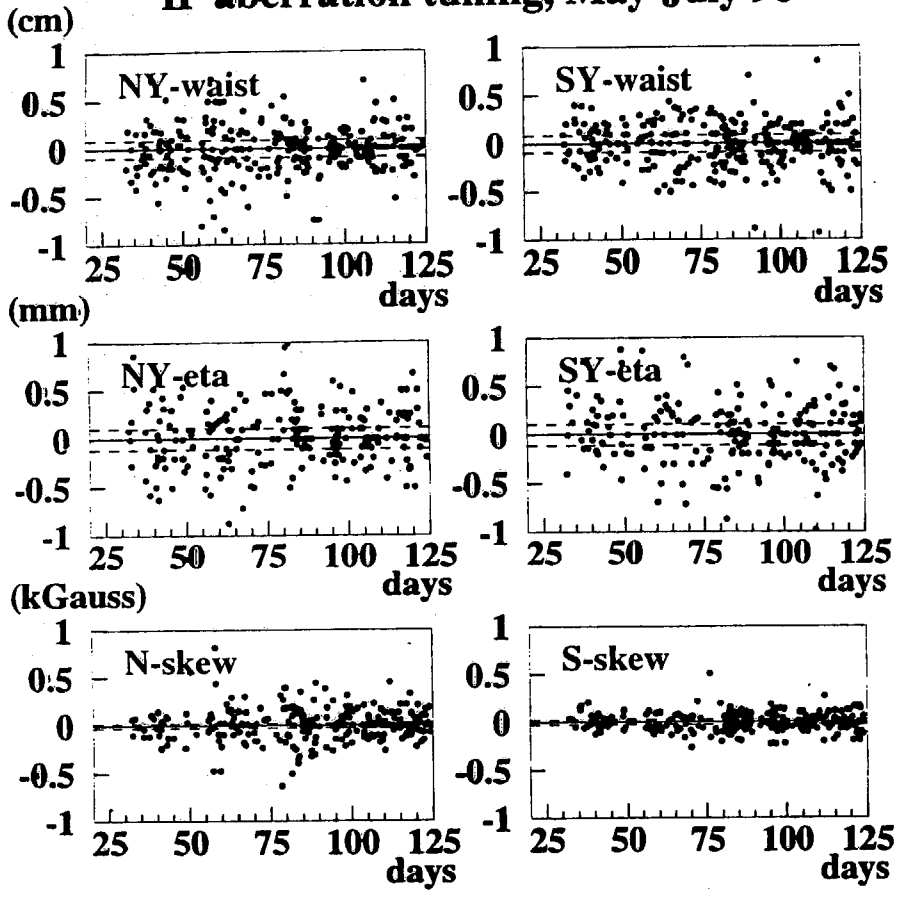

drifts: $\frac{\Delta L}{L} \simeq 20-40\%$

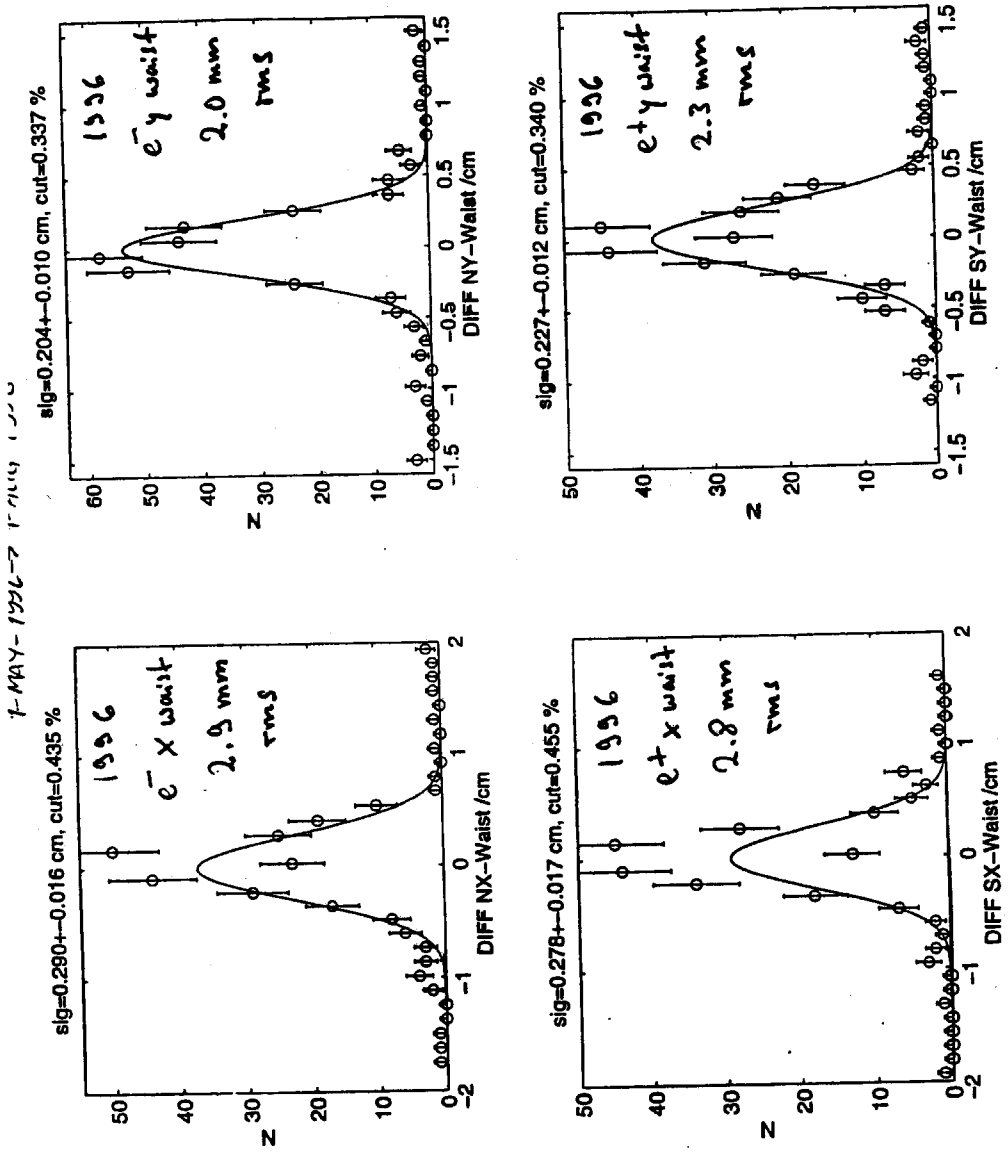

27-OCT-1997 → 15 NOV 1997

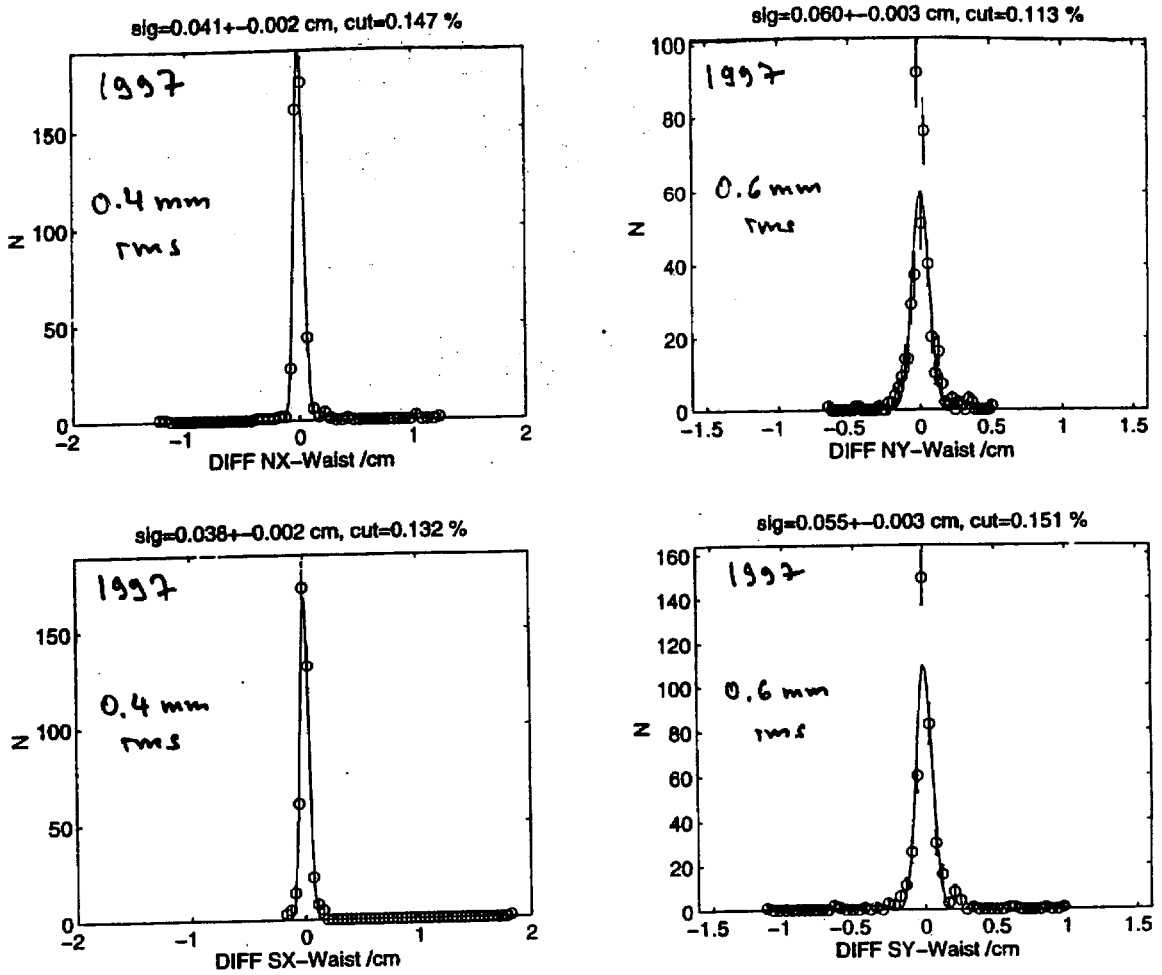

Spot-Size Tuning

in 1997 abandoned beam-beam deflections

new IP optimization feedback:

- scans waists, dispersions, coupling on beamstrahlung monitor;
- automatic and scheduled;
- much improved resolution

-> small spot size!

feedback maintains optimal conditions;

rapid recovery from interruptions

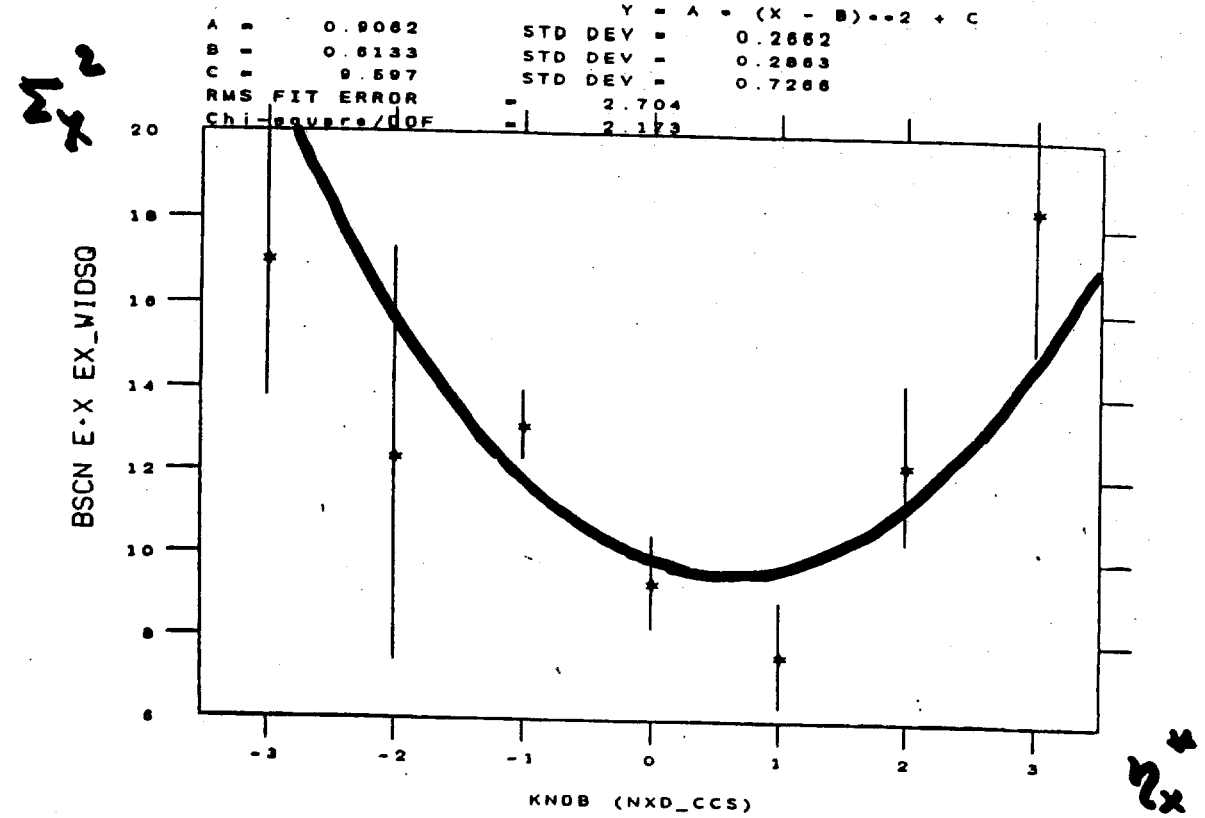
Y = A * (X - B)**2 + C
A = 0.9062
B = 0.6133
C = 9.597
STD DEV = 0.2662
STD DEV = 0.2863
STD DEV = 0.7266
RMS FIT ERROR = 2.704
Chi-square/DOF = 2.173
BSCN E·X EX_WIDSQ
KNOB (NXD_CCS)
KNOB (NXD_CCS) STRT=-3 000 STEPS= 7 SIZE= 1.000
21-OCT-97 10:14:35

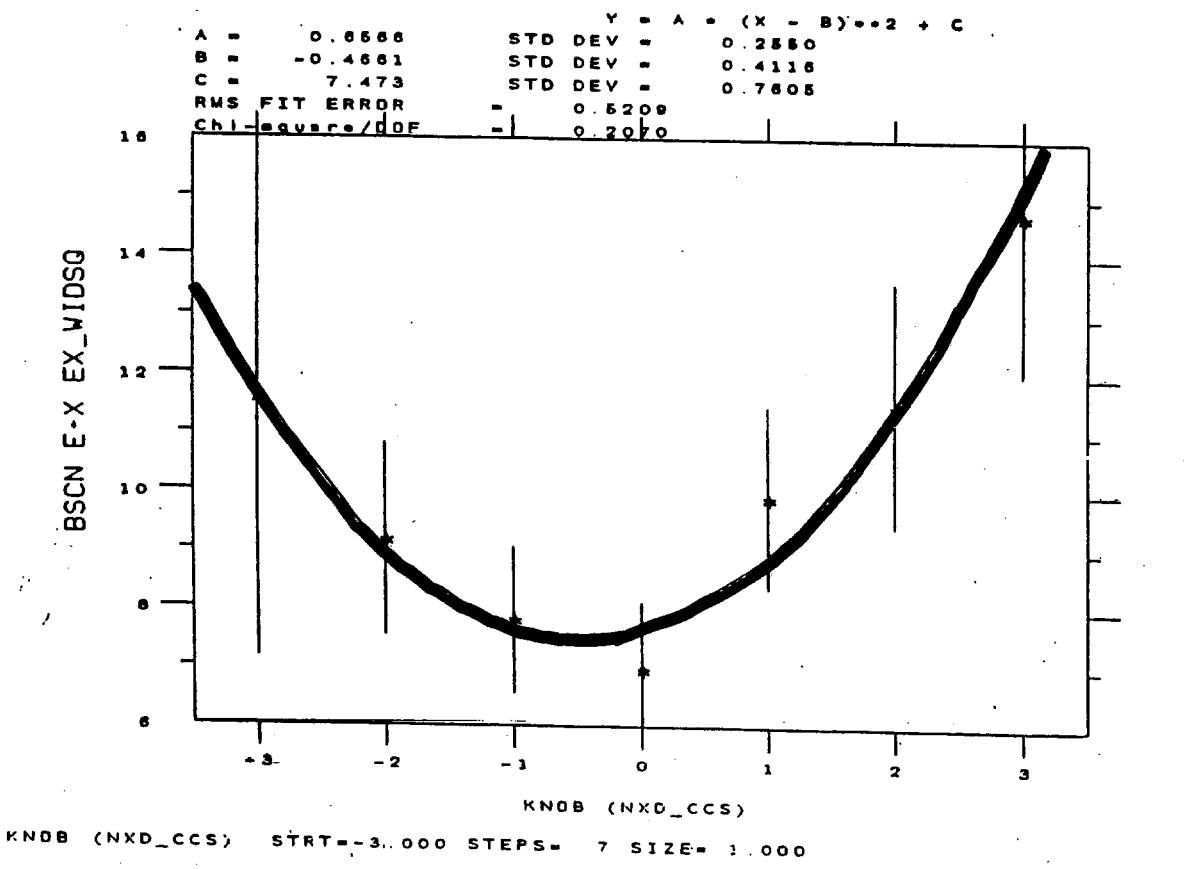
Y = A * (X - B)**2 + C
A = 0.6566
B = -0.4661
C = 7.473
STD DEV = 0.2550
STD DEV = 0.4116
STD DEV = 0.7605
RMS FIT ERROR = 0.5209
Chi-square/DOF = 0.2070
BSCN E·X EX_WIDSQ
KNOB (NXD_CCS)
KNOB (NXD_CCS) STRT=-3.000 STEPS= 7 SIZE= 1.000
21-OCT-97 10.20.19

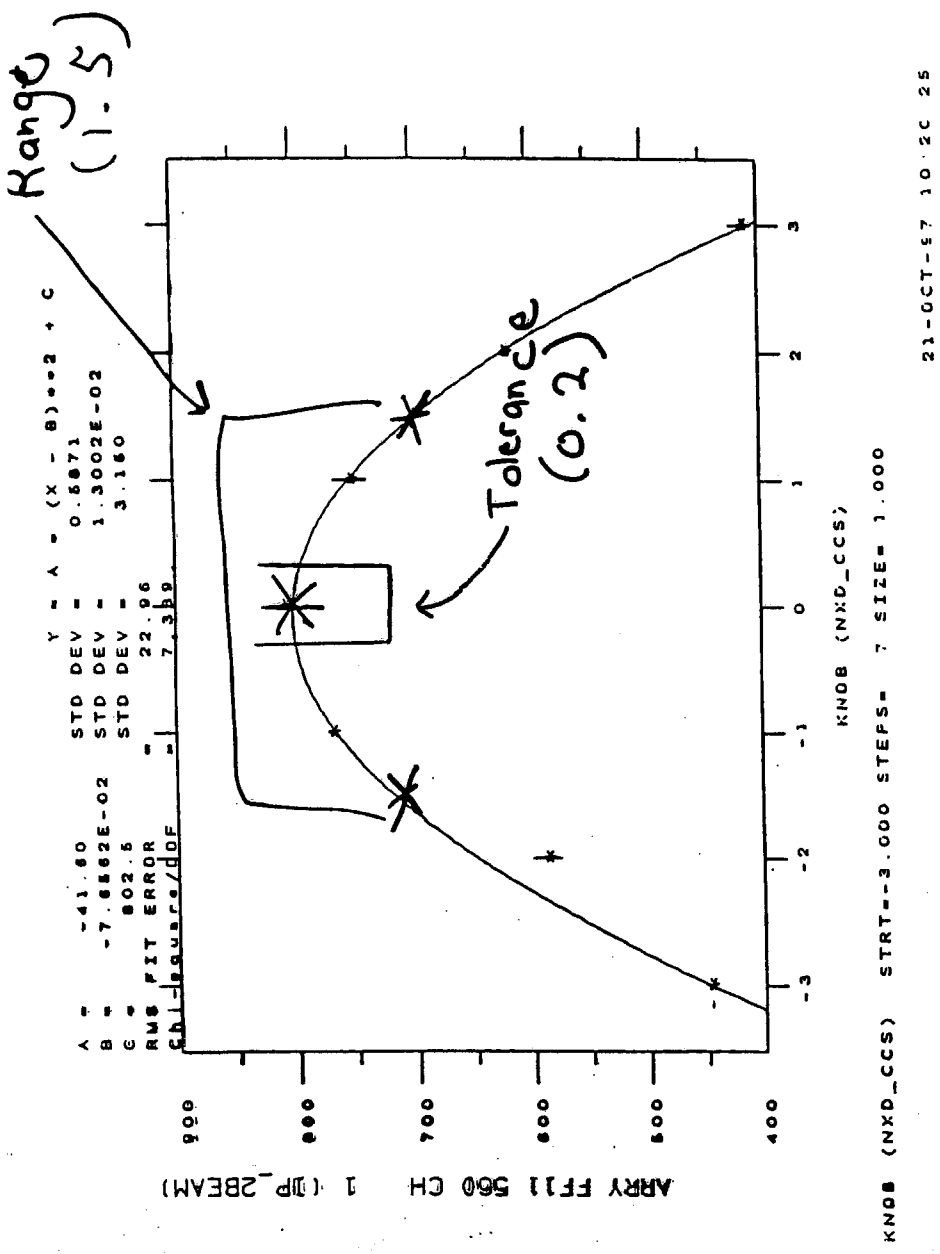

LUMINOSITY OPTIMIZATION SYSTEM DESIGN

Fast Feedback: create 10 feedback loops that don't know about each other.

Scheduling process: turns the individual feedback loops on and off.

Fast feedback:

- Fully database-driven to allow future expansion.
- Acquire digitized luminosity monitor readout at 120 Hz.
- Perform dithering (nominal, up, down). Control linear combination of devices.
- Calculate parabolic offsets (every 38 seconds) and apply corrections.

Scheduling Process:

- Turn on and off fast loops; only one is on at a time.
- User configurable scheduling for each parameter.
- Check convergence of feedback; turn off when converged or if timeout is exceeded.

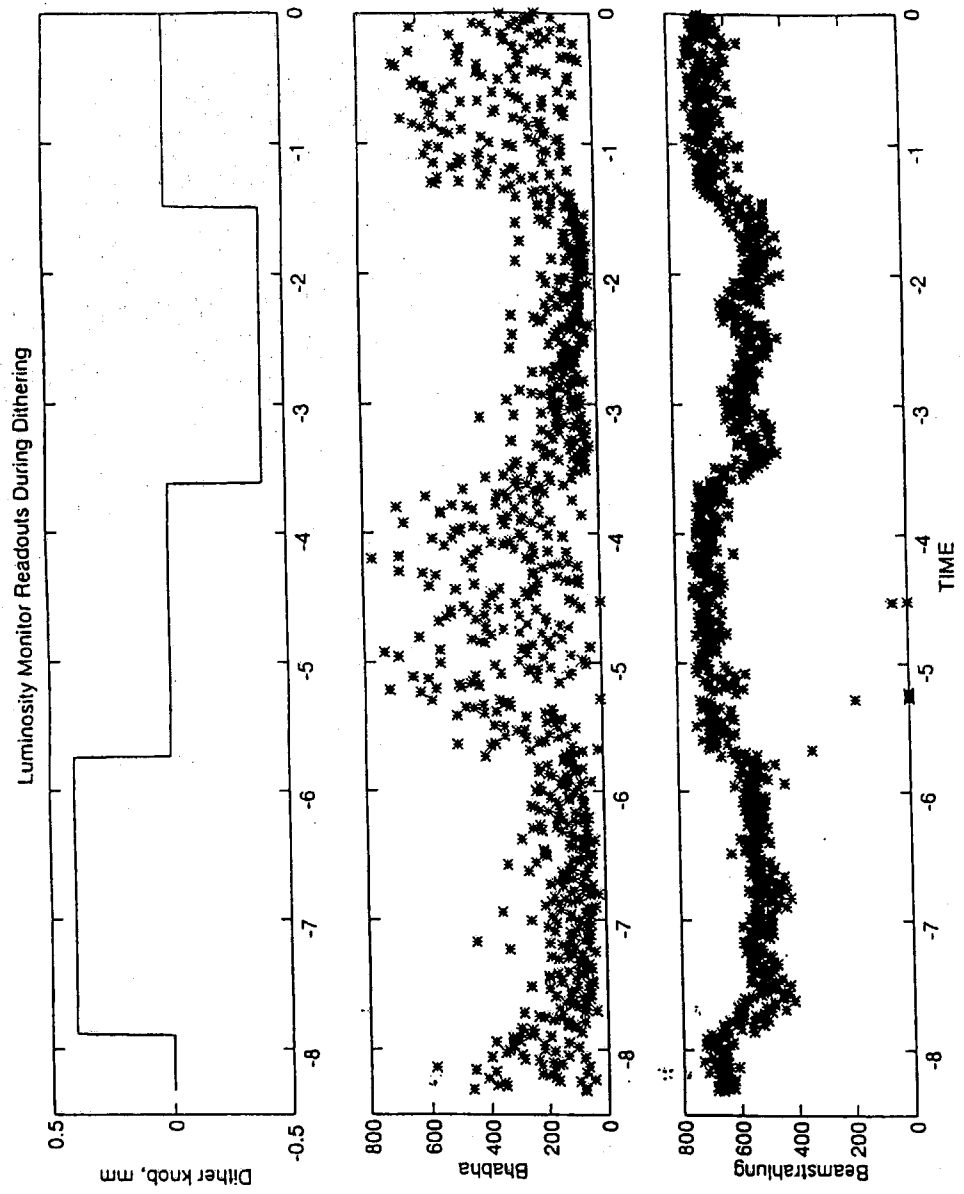

LUMINOSITY OPTIMIZATION FEEDBACK:

Dithering and luminosity losses.
(LJH 27Oct97)

- 40 minute timer
  17.5 minutes average for 1 iteration (10 loops)
  They are running 44% of the time.

  Average 3200 good pulses.

- How much of data is used?

  Average 38 seconds for a calculation.

  This is 4560 pulses, but only 3200 good pulses are used.

  For each dither step, settle for 30 pulses before collecting 200 good pulses.
  The rest is filtered.

  → 70% of the pulses are used
  11% is for settle time
  19% is filtered/rejected

- How much luminosity is lost?

  Average dither is 16% luminosity loss
  Dither is at center half the time.
  Optimization is on 44% of the time.

  → **3.4% luminosity loss due to dithering.**

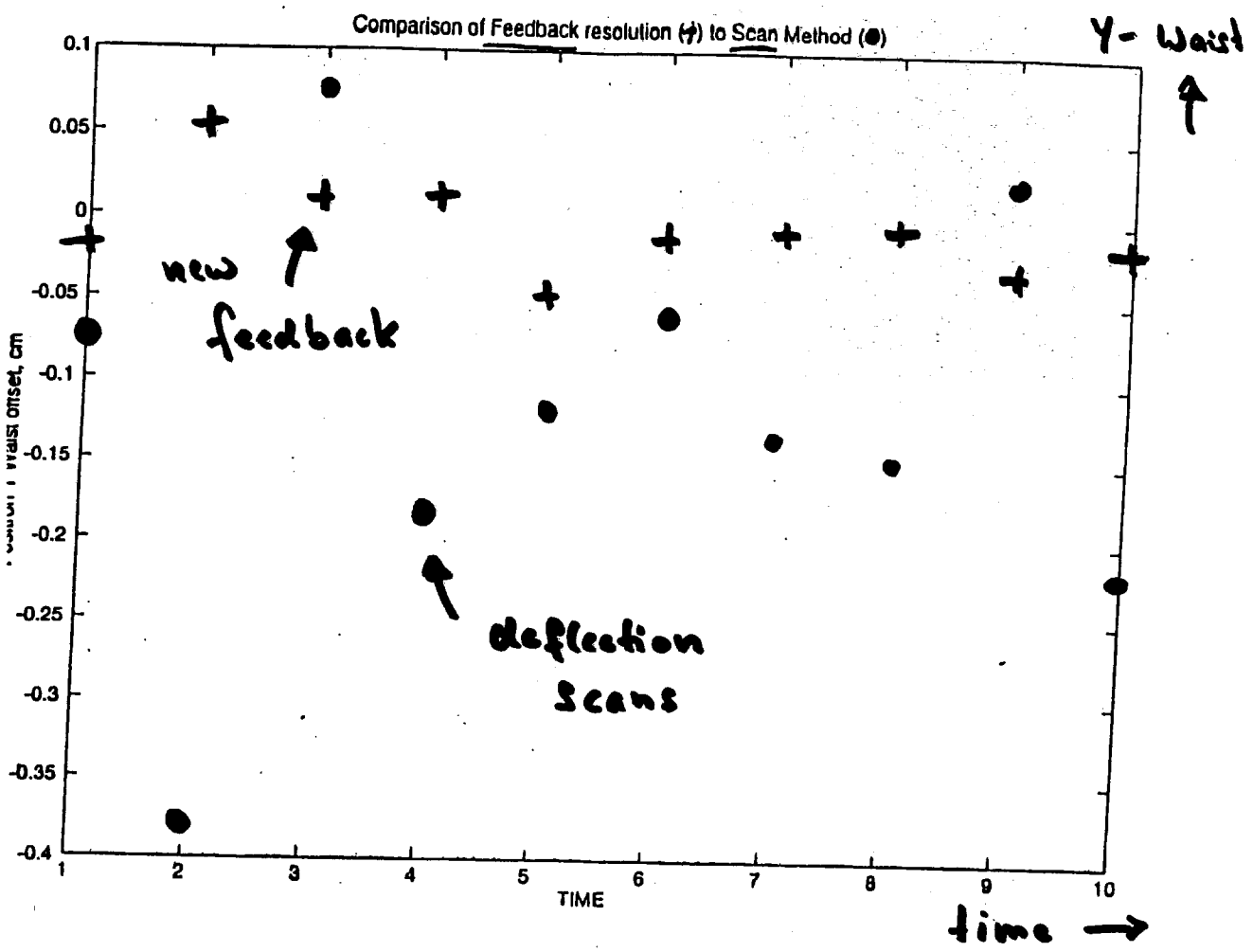

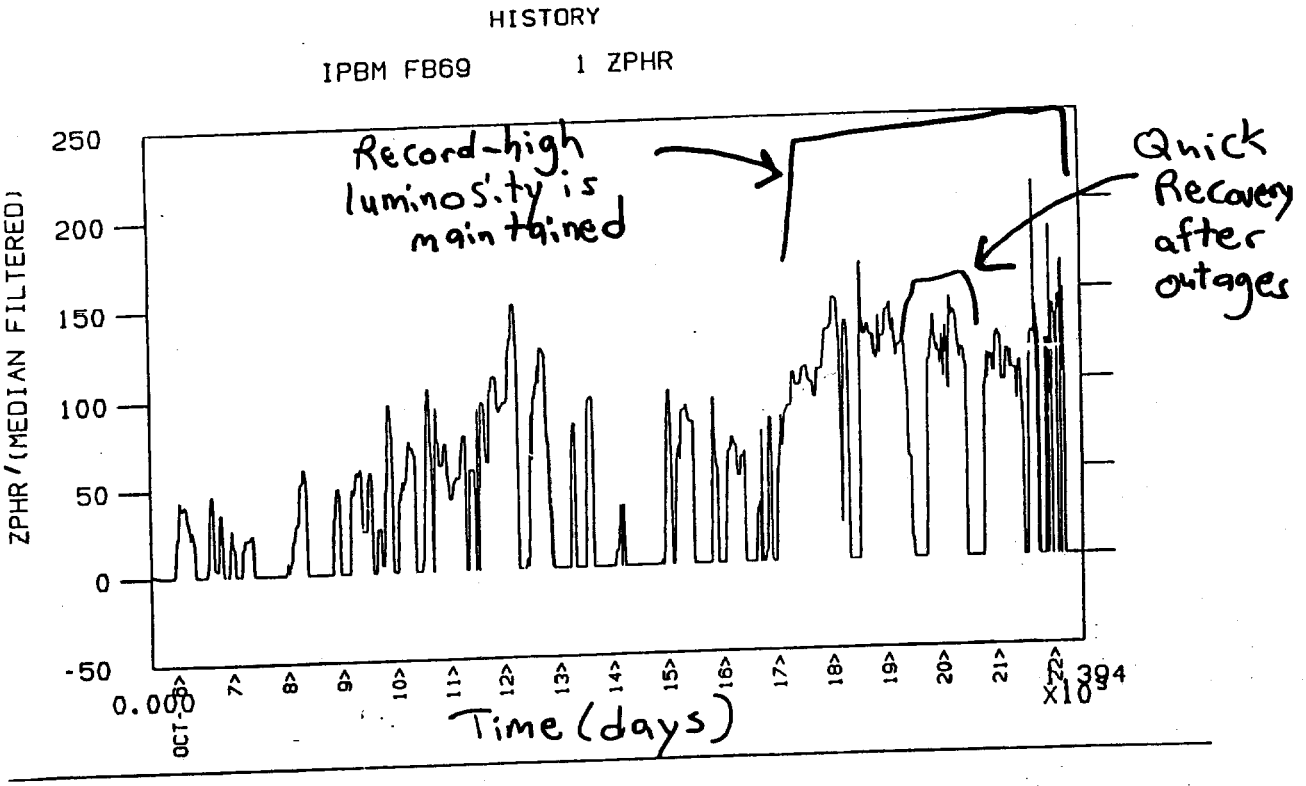

NTERVAL: 120 MEAN: 55.287 MIN: 0.0000
SIGMA: 58.204 MAX: 209.62
AST DATA POINT: 22-OCT-1997 12:29:56 MAX-MIN: 209.62
29-OCT-97 12:32:59

FFBK Hist Panel	HELP	RETURN FBCKMG NT	INDEX

F11 Luminosity FBCK

pecial Parameters

User-entered optimization configuration

Q3 Loop -> (BDES) ->	DITHER AMOUNT .20000	DITHER SETTLE PULSES 30.000	N AVERGE PULSES 3200.0	DITHER STEP PULSES 200.00	PRINT Graph Disply MCCIMGN
					SQ3 Knob VALU
					SQ3 Knob CMND
ETA Loop -> (mm) ->	DITHER AMOUNT 1.5000	DITHER SETTLE PULSES 30.000	N AVERGE PULSES 3200.0	DITHER STEP PULSES 200.00	ETA Knob VALU
ETA Loop -> (mm) ->	DITHER AMOUNT .75000	DITHER SETTLE PULSES 30.000	N AVERGE PULSES 3200.0	DITHER STEP PULSES 200.00	ETA Knob CMND
WAIST Loop-> (cm) ->	DITHER AMOUNT .40000	DITHER SETTLE PULSES 30.000	N AVERGE PULSES 3200.0	DITHER STEP PULSES 200.00	Waist Knob VALU
WAIST Loop-> (cm) ->	DITHER AMOUNT .40000	DITHER SETTLE PULSES 30.000	N AVERGE PULSES 3200.0	DITHER STEP PULSES 200.00	Waist Knob CMND

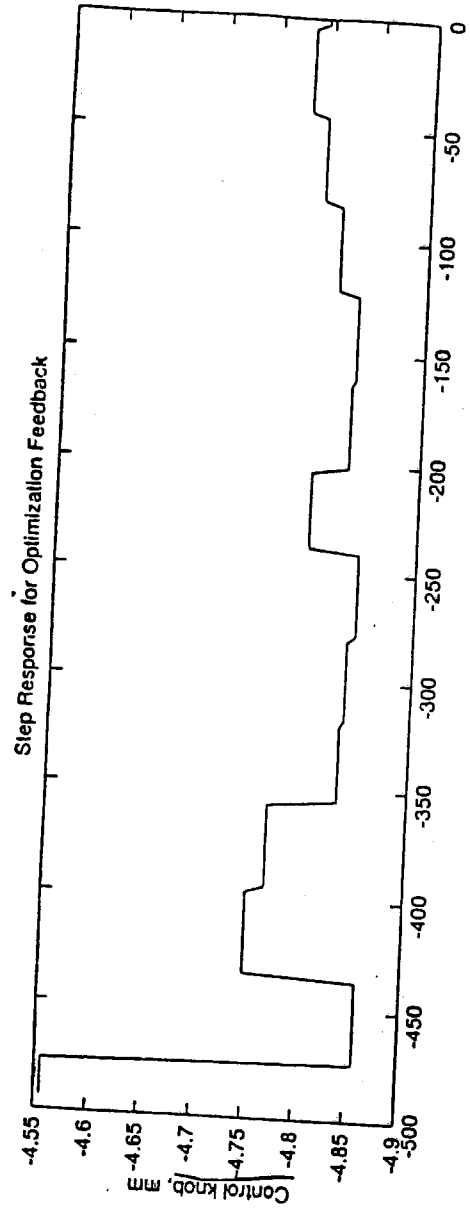

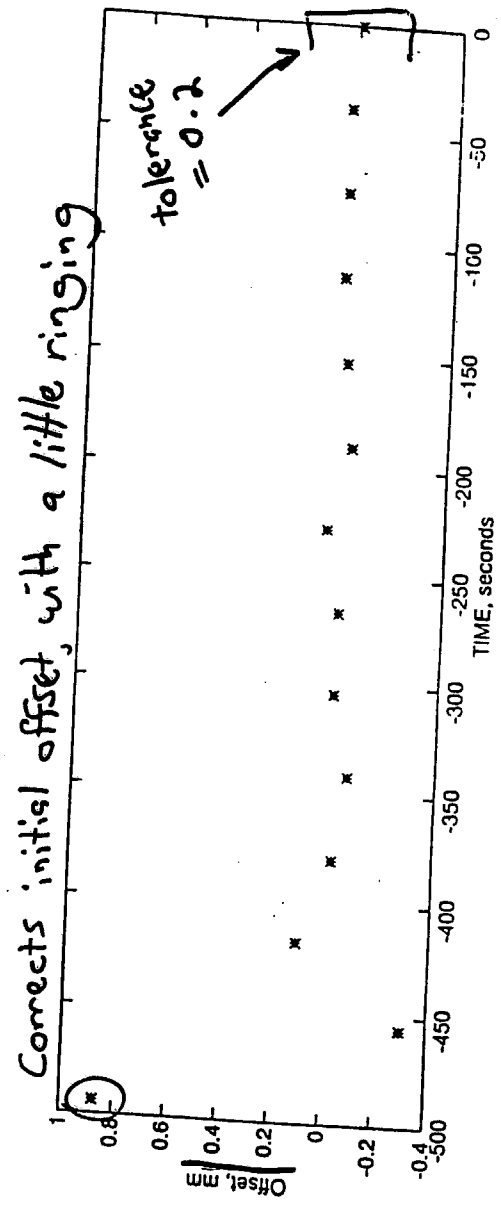

IP and beam-beam parameters

parameter	SLC 1997 (SLC)	NLC-I (0.5 TeV) (NLC-I)	NLC-II (1 TeV) (NLC-II)	comments
L [10^{30} cm^{-2} s^{-1}]	2	5800	10200	luminosity w pinch
N_b [10^{10}]	4	0.65	0.95	# particles per bunch
n_b	1	90	90	# bunches per train
f	120	180	120	# bunch trains per s
σ_x [nm]	1600	264	231	hor. spot size
σ_y [nm]	850	5.07	4.35	vert. spot size
β_x^* [mm]	2.4	8	10	hor. IP beta function
β_y^* [mm]	1.5	0.125	0.125	vert. IP beta function
$\gamma\epsilon_x$[10^{-8} m rad]	4800	400	400	norm. hor. emittance
$\gamma\epsilon_y$[10^{-8} m rad]	900	7	9	norm. vert. emittance
$\sigma_{x'}$ [μrad]	470	32	20	hor. IP divergence
$\sigma_{y'}$ [μrad]	250	34	27	vert. IP divergence
σ_z [mm]	1	0.1	0.125	bunch length
θ_c [mrad]	0	20	20	crossing angle
H_D	1.5	1.41	1.33	enhancement factor
$D_{x,y}$	0.6, 1.2	0.09, 5.7	0.132, 8.3	disruption parameter
Υ	0.001	0.1	0.3	field-strength parameter
N_γ	0.7	0.98	1.67	no. of beamstrahlung photons per electron
δ_B [%]	0.04	3	10	average relative energy loss

LC beam-beam interaction

minus:
- -> luminosity constraints
- -> background, -> instabilities
- -> complicates beam extraction
- -> depolarization

plus:
- -> aid in maintaining collisions
- -> pinch enhancement
- -> use as a diagnostic tool

linear-collider techniques which are (may be) of interest to ring colliders:

- IP collision feedback using deflections
- automatic IP spot-size control based on luminosity signal, coherent bremsstrahlung, or deflections
- crossing angle + crab crossing
- control of longitudinal distribution & timing
- traveling focus, use of rf quadrupoles?
- neutral-beam collisions
- plasma lens for focusing or charge compensation

VOLUME 68, NUMBER 6 PHYSICAL REVIEW LETTERS 10 FEBRUARY 19

Coherent Bremsstrahlung at pp or $\bar{p}p$ Colliders

I. F. Ginzburg,[1] G. L. Kotkin,[2] S. I. Polityko,[3] and V. G. Serbo[2]
[1]*Institute of Mathematics, 630090 Novosibirsk, U.S.S.R.*
[2]*Novosibirsk State University, 630090 Novosibirsk, U.S.S.R.*
[3]*Irkutsk State University, 664003 Irkutsk, U.S.S.R.*
(Received 20 May 1991)

We consider radiation caused by the collective electromagnetic field of one beam deflecting particles of the other. We find the number of photons for a single collision is $dN_\gamma \approx N_0 dE_\gamma/E_\gamma$ in the energy range $E_\gamma < E_c = 4\hbar c\gamma^2/l$, where l is the length of the bunch. At the Superconducting Super Collider, for example, $N_0 = 50$ and $E_c = 6$ keV. Specific features of this radiation can be used for a fast control over collisions and for measuring beam parameters. A background due to synchrotron radiation in the magnetic field of a collider is estimated.

PACS numbers: 41.70.+t, 41.80.Gg

TABLE I. Calculation parameters for various colliders.

Parameter	SSC	LHC	$S\bar{p}pS$	Tev
E_p (TeV)	20	8	0.45	1
$\sigma_\perp$ (μm)	4.8	10	70	43
l (cm)	6	7.5	20	5
E_c (eV)	6000	770	0.9	1.5
N_0	50	2×10^4	770	1.7
$\dot{N}_0$ (10^9 s^{-1})	2.6	10^3	0.2	0.0

"Properties and possible use of beam-beam synchrotron radiation"

M. Bassetti,
J. Bosser,
M. Gygi-Hanney,
A. Hofmann,
E. Keil, and
R. Coisson

IEEE Tr. N.S.
NS-30, 4
1983

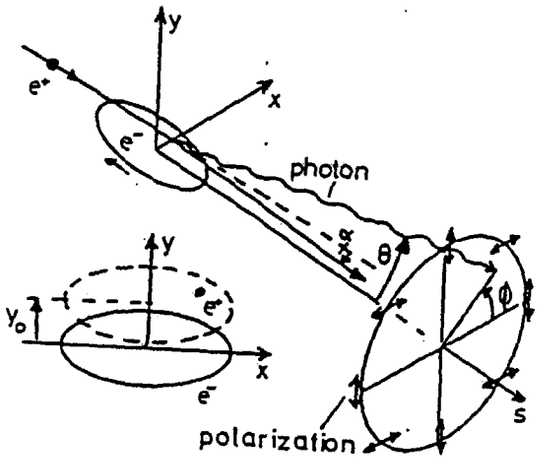

Fig. 1 Geometry of the beam-beam synchrotron radiation

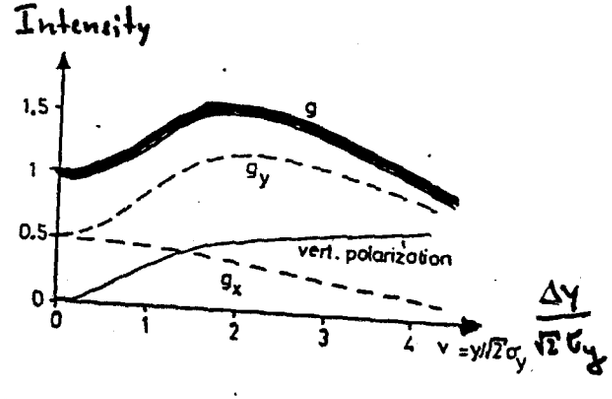

Fig. 2 Relative intensities g_x, g_y, g due to horizontal, vertical and total bending and polarization vs. vertical separation y_0 for beams with $\sigma_y/\sigma_x = 1/16$.

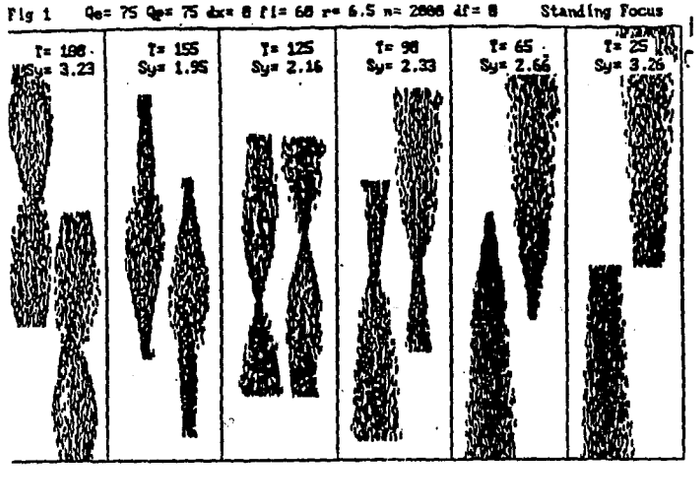

V. Balakin

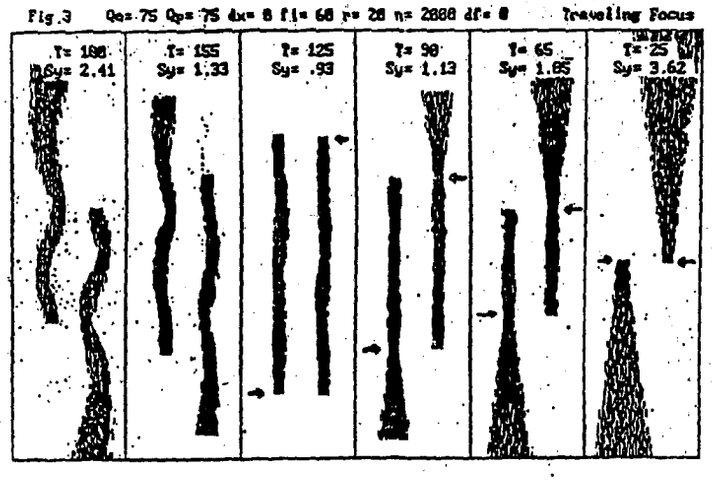

V. Balakin

"This year SLC is breaking new territory and nearing design luminosity.
Lessons learnt from the SLC operation are invaluable for understanding the issues and techniques required for a future linear collider"

Nan Phinney

References & Acknowledgements

[illegible] Hendrick[illegible]
[illegible] Pa[illegible]
[illegible] Chen [illegible]
[illegible] Daniel Schulte, Olivier Napo[illegible]
Kathy Thompson, Karl Bane

Q's:

Tollestrup: Why the SLC luminosity is still below design value while the beam sizes you just shown are well below design ones?

Zimmerman: Design luminosity relied on higher repetition rate and higher bunch intensities then what is achieved to now.

Shiltsev: How different will be beam-beam effects in e-e- linear collider?

Zimmerman: There is no more attraction between the two beams and , therefore, no luminosity enhancement – in opposite, only decrease. The effect is especially significant in round beams, while not so important for flat beams collisions. The major benefit in e-e- scheme is that one needs no complicated injection complex for positrons (target, collection, damping ring, bunch compressor) – electrons can be taken directly from RF gun injector.

Meshkov: What is the source of long-term variation of the SLC correction?

David Whittum

SLAC

Beam-Beam Compensation in Linear Colliders

LINEAR COLLIDER BEAM-BEAM COMPENSATION

WHY IS THIS INTERESTING?

I. WHY & HOW HIGH GRADIENT ARE INTERESTING

II. CURRENT RESEARCH ON PROBLEMS OF HIGH-GRADIENT

III. COLLIDER CONCEPT

IV. BEAM-BEAM NEUTRALIZATION (HOW DOES IT WORK?)

Whittum

Gradients Today

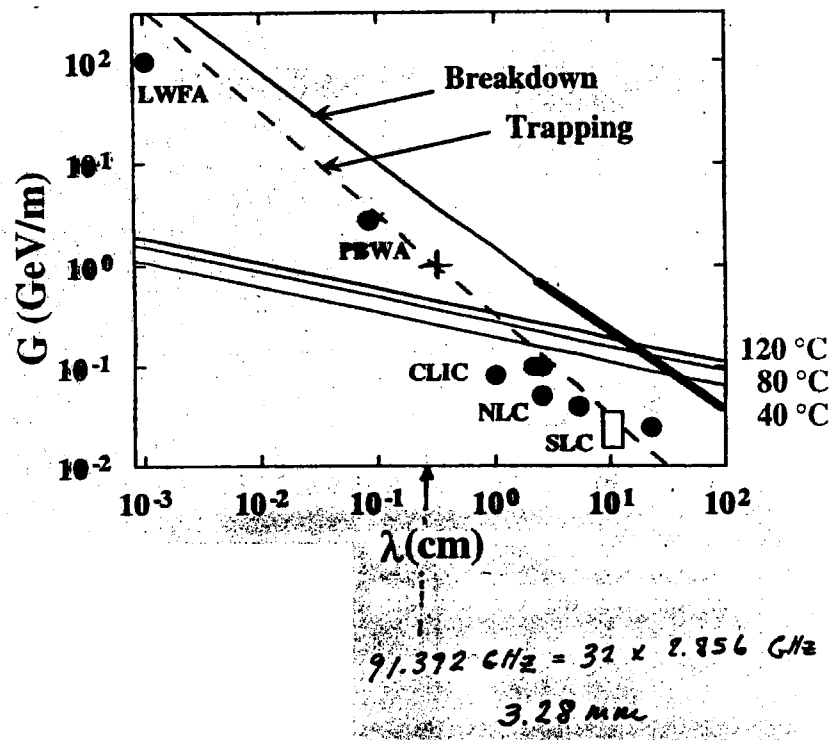

CONVENTIONAL

COLLIDER PROBLEMS @ 1 GeV/m

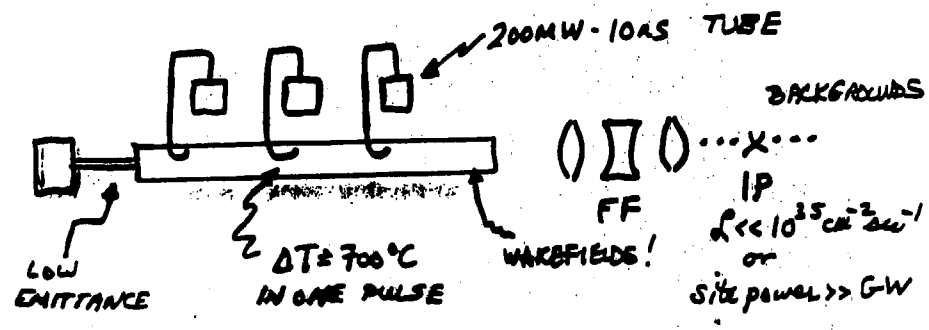

TUBE DOESN'T EXIST

LINAC MELTS IN ONE SHOT

EMITTANCE BLOWS UP

BEAMS DESTROY THEMSELVES IN COLLISION

MACHINE REQUIRES A DEDICATED POWER PLANT

A DIFFERENT KIND OF TUBE → PLANAR VELOCITY + PULSE COMPRESSION

A DIFFERENT KIND OF LINAC

A DIFFERENT KIND OF FINAL FOCUS

MULTI-BUNCH TEST

SHORT EXPOSURE TIME FOR CAMERA

$$\mathcal{L} = \frac{N_b^2 N_p^2 f}{4\pi \sigma_x \sigma_y}$$

CONVENTIONAL COLLIDER PICTURE FAILS AT < 1 GeV/m

(Zimmermann et al)

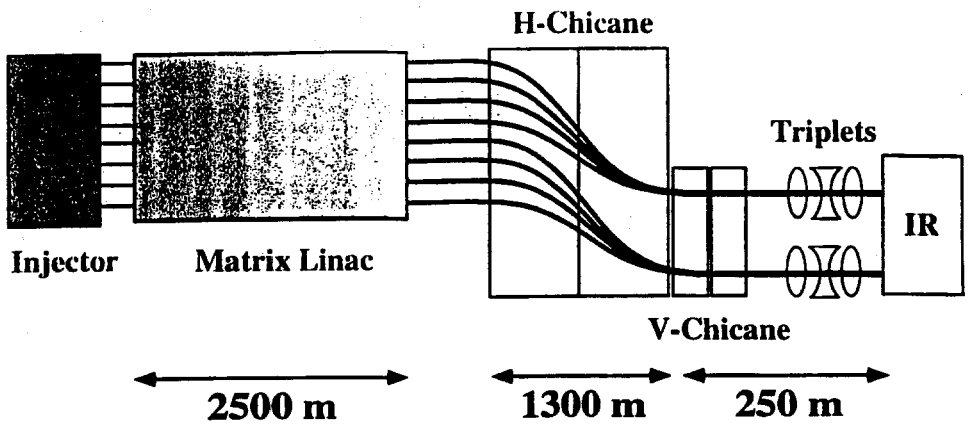

$$\mathcal{L} \propto N_p^2 N_b^2$$

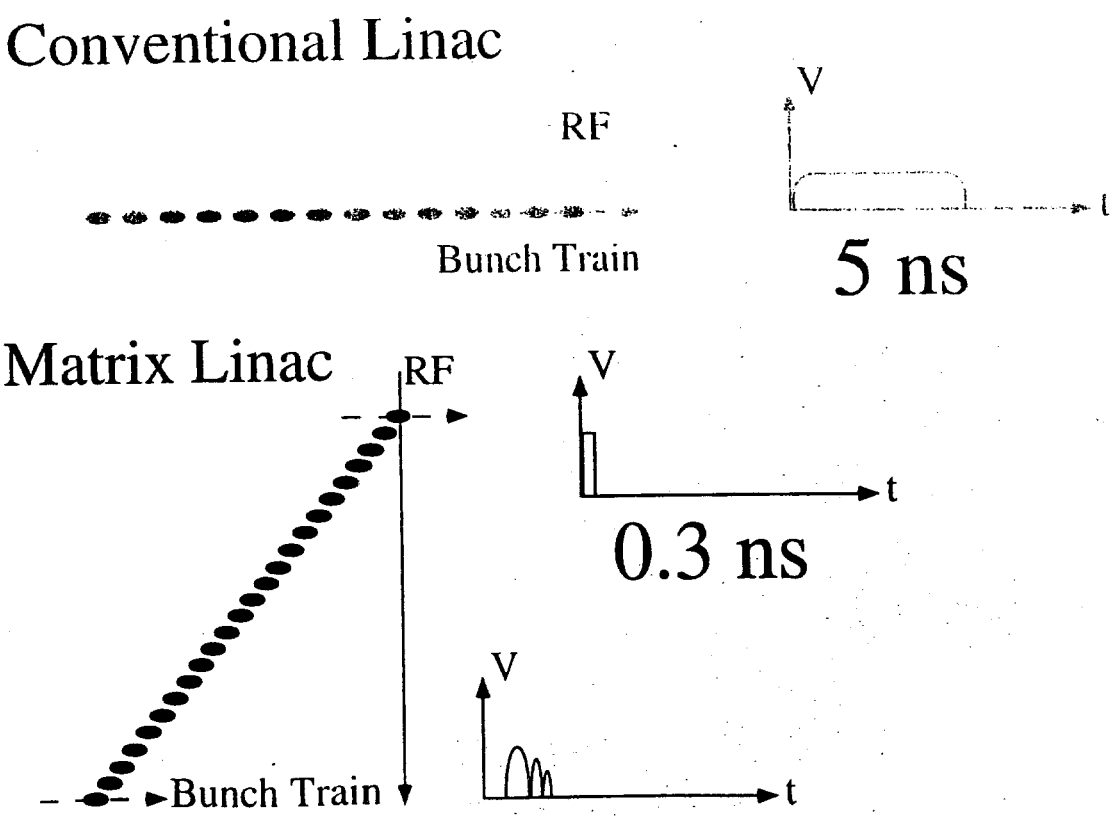

(Zimmerman)

Scaling for Final Focus Length

$$\delta_{rad}^2 \propto \gamma^5 \frac{\theta_B^3}{\ell^2}$$

$$\xi_y \delta_{rad} \ll 1$$

$$\xi_y \propto \frac{1}{\beta_y^*} \propto \gamma \qquad (@\ \varepsilon_{n x,y}$$

$$\eta_{sy} \propto \theta_{BL} \quad \& \quad 2\,\eta_{sy}(k_{sy}\,l_{sy})\,\beta_{sy,y}$$

$$(k_{sy}\,l_{sy})\,\beta_{sy,y} \leq \frac{1}{\Delta}$$

$$\ell \propto \gamma^2$$

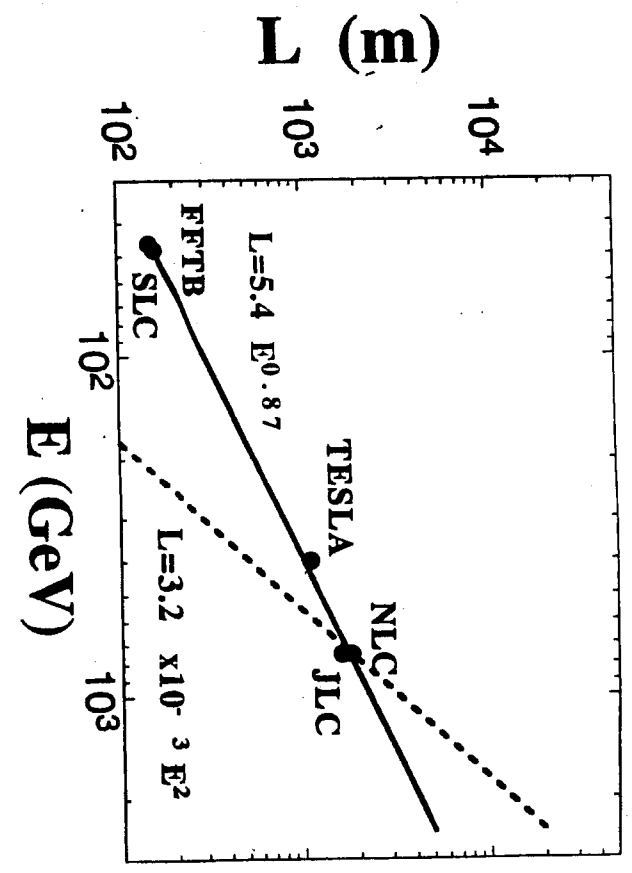

(Zimmermann)

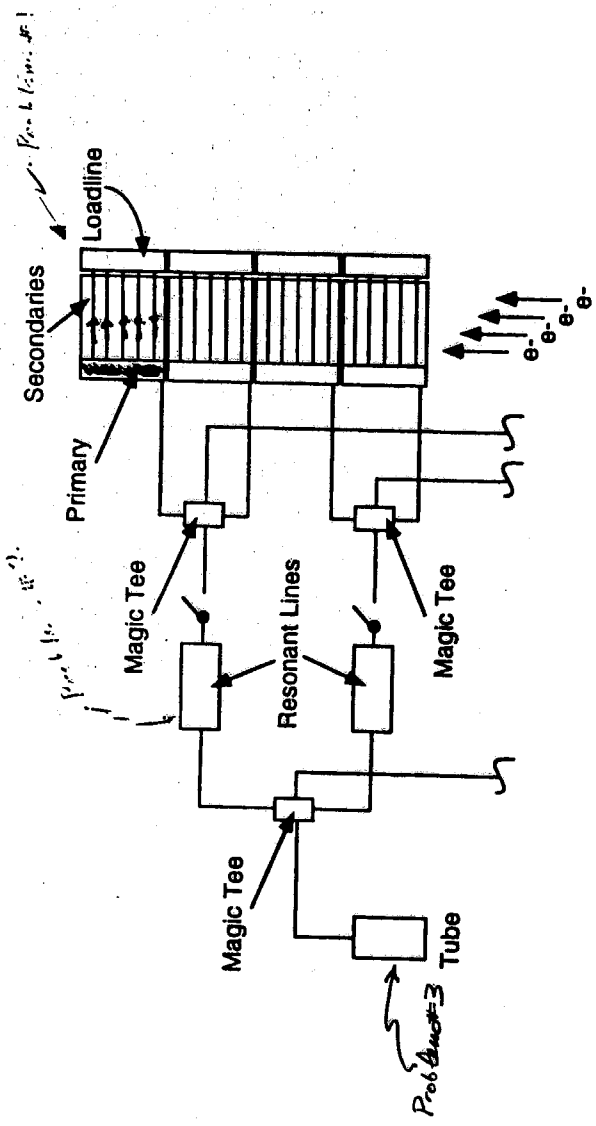

SHORT-TERM AIM: One 5MW × 1μs Tube Feeding One GeV/m structure

LONGER-TERM: One 20MW × 1μs Tube Feeding Four GeV/m structures

WITH < EIGHT TUBES FOR 1 GeV

KEEP AT < 200°C

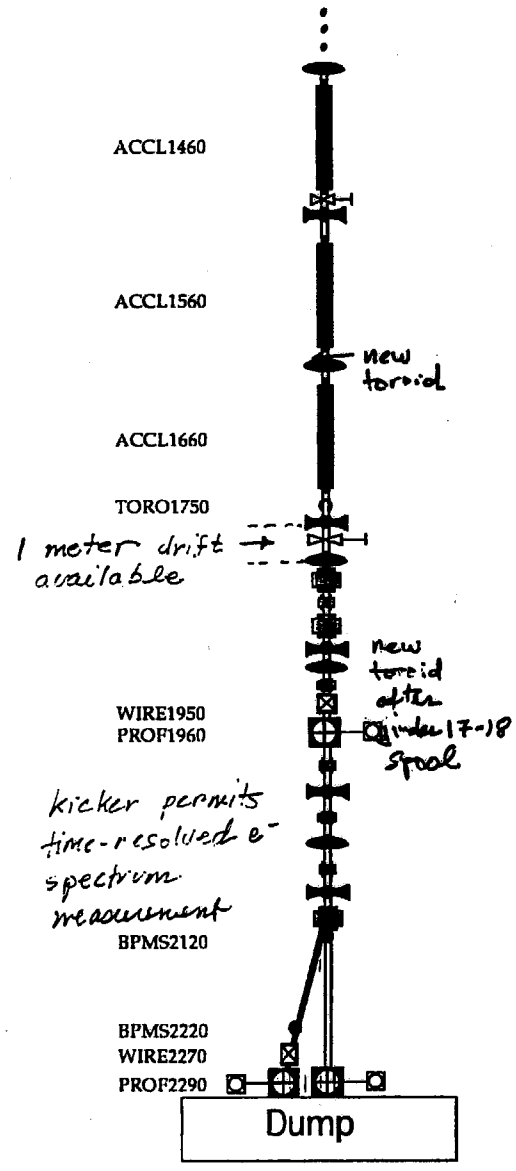

NOT TO SCALE

MEDIUM POWER W-BAND TEST at girder #17

Next Linear Collider Test Accelerator

0.5 Amp 300 MeV [illegible] bunched at 11.424 GHz

5° rms beam width.

TEST #0 aperture test

TEST #1 MAY '98 [illegible]

25 cell structure

~30-40 kW

includes component testing for

TEST #2 FALL '98

50/25 cell structure in resonant ring configuration

~1 MW

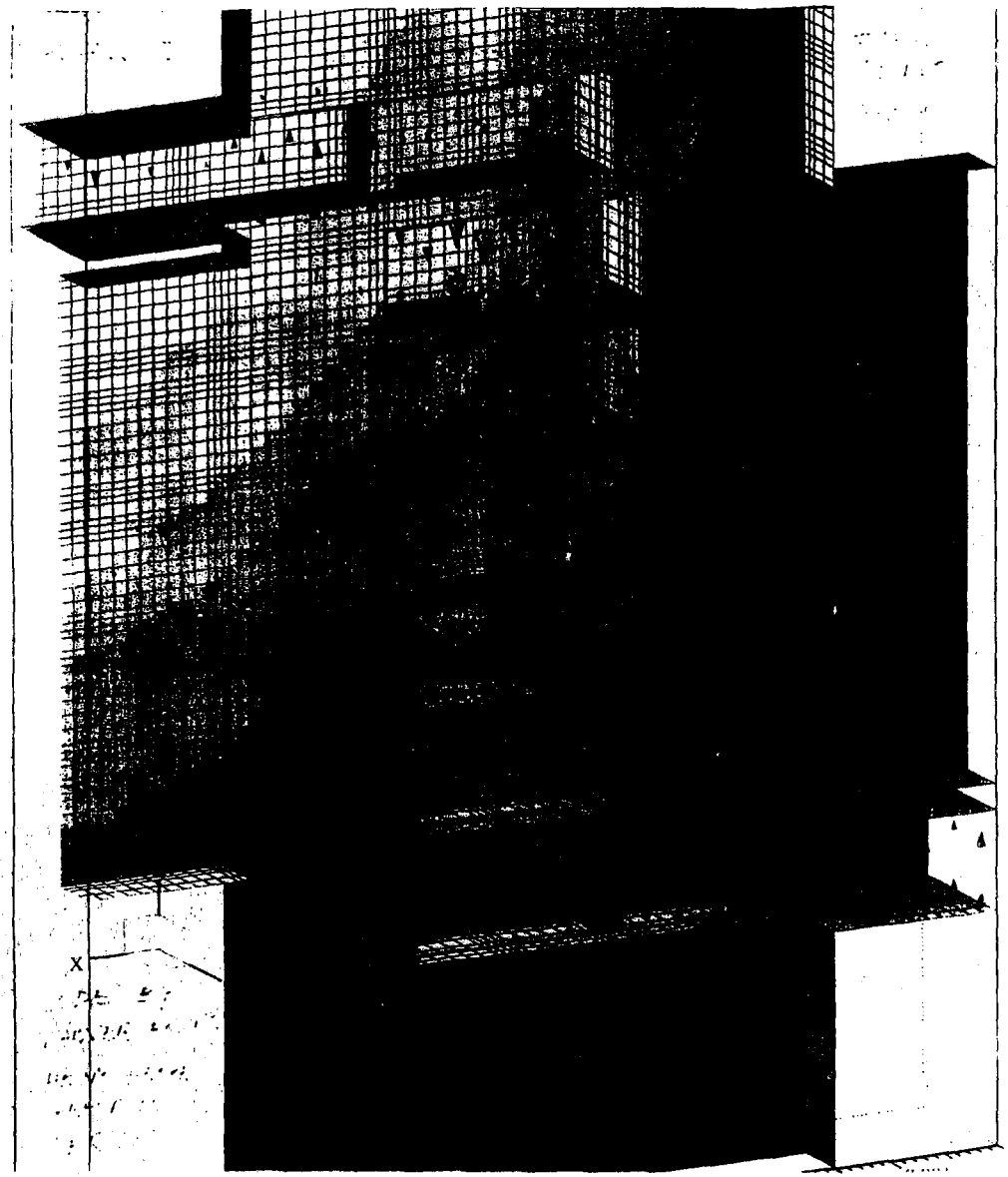

ВЛЭПП. ЭФФЕКТЫ ВСТРЕЧИ

В.Е. Балакин, Н.А. Солях
Институт ядерной физики СО АН СССР,
Новосибирск, 630090

лучение высокой светимости во ВЛЭППе при ней частоте столкновений связано с использова- плотных сгустков, сфокусированных в месте чи в пятно порядка одного квадратного микрона. ом случае действующие между встречными ками силы становятся настолько большими, что главным образом определяют поперечную дина- движения частиц, а значит, и многие важнейшие ктеристики ускорителя, такие как светимость, нохроматичность, конечный фазовый объем пучка а.

столкновениях противоположно заряженных сгус- их электрические поля компенсируются, а маг- ые складываются, поэтому сила носит характер ияния и частицы будут осциллировать в попе- ом направлении. Силу каждого сгустка будем ха- теризовать безразмерным параметром, численно ным среднему количеству колебаний, которые со- шает встречная пробная частица противоположно- заряда за время пролета внутри сгустка. Значение го параметра для каждого из поперечных направ- ий x, y равно:

$$n_x = \frac{k}{2\pi}\left(\frac{r_e N \sigma_z}{\gamma \sigma_x^2}\,\frac{R}{R+1}\right)^{1/2}; \quad n_y = \frac{k}{2\pi}\left(\frac{r_e N \sigma_z}{\gamma \sigma_x \sigma_y}\,\frac{R}{R+1}\right)^{1/2}. \qquad (1)$$

: $r_e = e^2/mc^2$; N—число частиц в сгустке, σ_x, σ_y— перечные, σ_z—продольный размеры сгустков; $=\sigma_x/\sigma_y \geq 1$, γ—релятивистский фактор; k—число рядка единицы, зависящее от формы распределения ряда внутри сгустка. Часто вместо параметра n одят параметр «разрушения» D, который равен $_x = (2\pi n_x)^2$; $D_y = (2\pi n_y)^2$.

Синхротронное излучение частиц, движущихся в льных полях встречного сгустка, приводит к появле- ю дополнительной немонохроматичности в пучке, а кже создает фон γ-квантов, спектральное и угловое спределение которых определяется траекториями стиц. Параметр немонохроматичности, вычисленный приближении слабовзаимодействующих пучков, авен

$$\Delta = \frac{\Delta\omega}{\omega_0} = \frac{\zeta R^2 \gamma}{\sigma_x(\sigma_x+\sigma_y)}. \qquad (2)$$

Для ВЛЭППа требуется, чтобы параметр L по совокупности всех эффектов, влияющих на него, не превышал величины $\sim 1\%$. Это требование накладывает определенные ограничения на возможные размеры пучков в месте встречи. Другое условие на размеры связано с получением необходимой светимости:

$$L_0 = f\frac{N^2}{4\pi\sigma_x\sigma_y} \simeq 10^{33}\ \text{см}^{-2}\text{с}^{-1}, \qquad (3)$$

где f—частота повторений. Взаимодействие сгустков приводит к тому, что получаемая светимость L может существенно отличаться от геометрической L_0, вычисленной по (3).

Авторами эффекты встречи изучались для цилиндрических и плоских сгустков[1,2,3,4]. Анализ показал, что использование цилиндрических сгустков приводит к большим потерям на излучение и немонохроматичности, близкой к 100%. Уменьшение немонохроматичности до уровня $\sim 1\%$ ведет к необходимости использования плоских сгустков.

Самосогласованная задача движения частиц в месте встречи решалась численно методом «крупных» частиц (1600—3000 частиц в каждом сгустке). Мы ограничились случаем плоских сгустков ($\sigma_x \gg \sigma_y$), где существенно движение частиц лишь вдоль направления y. Рассчитываются такие характеристики, как светимость, немонохроматичность, спектр γ-квантов и конечный фазовый объем для лобового и нелобового столкновений сгустков.

Результаты расчета светимости для лобового столкновения противоположно заряженных сгустков с гауссовым распределением плотности представлены на рис. 1 (сплошной линией). Из графика видно, что в

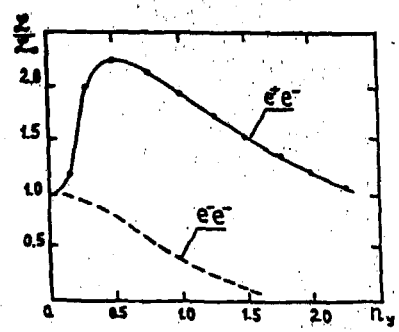

Рис. 1. Лобовое столкновение (штрихом для одинаково заряженных сгустков).

диапазоне изменения параметра $n_y \leq 1.5$ наблюдается увеличение светимости по сравнению с геометрической L_0 в результате пинч-эффекта. Максимальное увеличение светимости $L/L_0 \simeq 2.2$, что ниже, чем для цилиндрических сгустков[3], поскольку, сгустки сжимаются только в одном направлении, вдоль оси y. При дальнейшем увеличении параметра $n_y \gtrsim 2$ развивается неустойчивость, разрушающая пучки; светимость при этом падает.

Результаты вычислений для случая нелобового столкновения приведены на рис. 2, где представлена зависимость относительной светимости L/L_0 от прицельного параметра $x_y = \Delta y_0/2\sigma_y$ (где Δy—начальное смещение центров встречных пучков) при различных значениях параметра n_y. С ростом поперечного смещения сгустка светимость падает, однако благодаря их притяжению при $n_y = 0.5 \div 1$ это падение медленнее, чем для слабовзаимодействующих пучков ($n_y \simeq 0$). Светимость не исчезает даже при полном разведении сгустков $x_y > 1$ и обращается в нуль лишь при

$x_{мин} = \pi^2 n_y^2$, что для $n_y \simeq 1$ составляет ≈ 10 размеров сгустка. Притяжение сгустков облегчает их настройку и нацеливание; так, при смещениях порядка $x_{мин}$ пучок как целое приобретает угол в направлении к противоположному пучку $\theta_y = r_e N/(\gamma\sigma_z) \sim 10^{-4}$ при энергии $\varepsilon = 500$ ГэВ. Это на базе 10 м вызовет смещение пучка ~ 1 мм, что легко измерить и скорректировать положение сгустков в следующем импульсе.

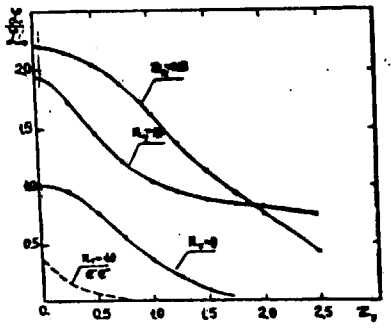

Рис. 2. Нелобовое столкновение (штрихом для одинаково заряженных сгустков).

Для нелобового столкновения при $n_y \gtrsim 2$ развивается дипольная мода колебаний сгустков друг относительно друга, что приводит к их разрушению. Другой характерной чертой этого случая является увеличение потерь на излучение с ростом n_y, так как в среднем сгусток движется в более сильных полях.

Результаты встречи одинаково заряженных сгустков представлены штрихом на рис. 1, 2. Видно, что светимость быстро падает с ростом n_y даже для лобового столкновения и для параметров ВЛЭППа ($n_y = 0.6 \div 1.0$) будет в 4—5 раз ниже, чем для сгустков противоположного заряда. Неточное нацеливание ухудшит это соотношение; таким образом, ожидаемая светимость ВЛЭППа при работе с одинаково заряженными сгустками будет на порядок ниже, чем для сгустков противоположного заряда.

Была рассмотрена встреча компенсированных сгустков (рис. 3). В этом случае при лобовом столкновении силы полностью скомпенсированы и частицы не совершают поперечных движений. Однако, как показали расчеты, такая система оказывается неустойчивой и неполная компенсация либо незначительное начальное смещение сгустков друг относительно друга приводит к разделению заряда в пучках и их разру-

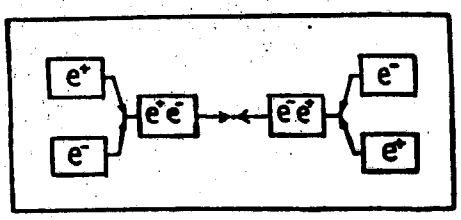

Рис. 3. Компенсированные сгустки.

неполной зарядовой компенсации в одном из встречных сгустков на светимость при различных значениях параметра n_y демонстрирует рис. 4.

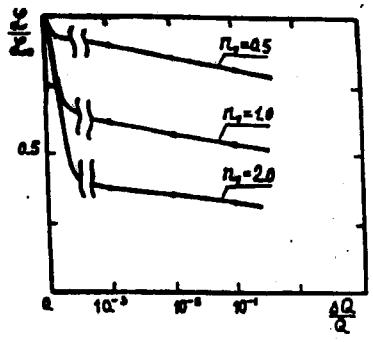

Рис. 4. Влияние неполной зарядовой компенсации на светимость в компенсированных сгустках.

Из графиков видно, что даже малое нарушение зарядовой компенсации сгустков ($\Delta Q/Q_0 \lesssim 10^{-3}$) приводит к резкому уменьшению светимости, которая затем слабо падает с ростом $\Delta Q/Q$. Аналогичный эффект наблюдается и в том случае, когда заряд в сгустках полностью скомпенсирован, но один из 4 сгустков смещен относительно трех других. Для двух значений прицельного параметра x_y этого сгустка на рис. 5 приведена зависимость относительной светимости L/L_0 от параметра n_y.

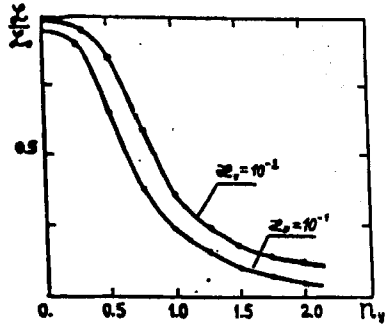

Рис. 5. Компенсированные пучки. Влияние смещения одного из сгустков на светимость.

Несмотря на изменение прицельного параметра на порядок, светимость изменяется незначительно. Из приведенных результатов можно сделать вывод, что любые малые возмущения в системе компенсированных сгустков служат затравкой, которая приводит к пространственному разделению зарядов в них. Это происходит тем быстрей, чем интенсивней сгусток, т. е. чем больше значение параметра n_y. После этого сгустки перестают быть компенсированными и для них справедливы результаты, полученные для встречи заряженных сгустков. Таким образом, применение компенсированных сгустков не позволяет значительно проникнуть в область больших светимостей.

эффектов встречи плоских сгустков позволяет вывод о том, что в диапазоне энергий для электрон-позитронных пучков требуемая 10^{32} см$^{-2}$с$^{-1}$ может быть достигнута при точности $\Delta \simeq 1\%$. Необходимые размеры параметры n_x, n_y, а также конечный угловой $\Delta\theta_y$ представлены в таблице. При этом 10^{12} частиц, $2\sigma_z = 0.8$ см, $f = 10$ Гц.

Энергия (ГэВ)	2×150	2×500
$2\sigma_x$, мкм	107.0	3010
$2\sigma_y$, мкм	0.2	0.11
$R = \sigma_x/\sigma_y$	94	270
n_x	0.15	0.04
n_y	1.06	0.56
θ_x, мрад	0.98	0.46
θ_y, мрад	0.17	0.06

Литература

1. Балакин В.Е., Буднер Г.И., Сиринский А.Н. Труды VI Всесоюз. совещания по ускорителям заряженных частиц.–Дубна, 1978, т.I, с.27. Препринт ИЯФ 78-101.–Новосибирск, 1978.
2. Balakin V.E., Skrinsky A.N. A Superhigh Energy Colliding Electron-Positron Beam Facility (VLEPP). Proc. of Second ICFA Workshop, 1979.
3. Балакин В.Е., Соляк Н.А. Эффекты встречи на ВЛЭППе.–Труды VII Всесоюз. Совещания по ускорителям заряженных частиц.–Дубна, 1983, т.II, с.263. Препринт ИЯФ 82-123.–Новосибирск, 1982.
4. Balakin V.E., Solyak N.A. VLEPP Beam Effects. Proc. of XII Intern. Conf. on High Energy Accelerator, USA, Batavia, 1983, p.134.
5. Hollebeek R. Nucl. Instr. Meth. 184 (1981) 333.

References

V. E. Balakin & N. A. Solyak
Proc. XIII Internat'l Conf. on
High Energy Accelerators
(Novosibirsk USSR 1986)

J. B. Rosenzweig, B. Autin and P. Chen
Proc 1989 Advanced Accelerator Workshop

PAC '97

INSTABILITY OF NEUTRALIZED BEAMS

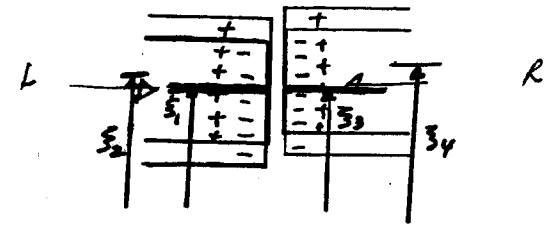

Momentum Conservation:

$$\frac{d^2}{dt^2}(\vec{\xi}_3+\vec{\xi}_4) = \frac{d^2}{dt^2}(\vec{\xi}_1+\vec{\xi}_2) = 0$$

$$\vec{\xi}_A = \vec{\xi}_4 - \vec{\xi}_3 \qquad \vec{\xi}_c = \vec{\xi}_2 - \vec{\xi}_1$$

$$\frac{d^2\vec{\xi}_A}{dt^2} = -\frac{2e}{m\gamma}\langle\vec{\nabla}\psi_+\rangle$$

$$\frac{d^2\vec{\xi}_c}{dt^2} = \frac{2e}{m\gamma}\langle\vec{\nabla}\psi_-\rangle$$

Maxwell's Equations:

$$\nabla^2\psi_+ = 8\pi e(n_1-n_2)$$

$$\nabla^2\psi_- = -8\pi e(n_3-n_4)$$

$$\frac{d^2 \xi_R}{d\tau^2} = \Omega_R^2 \, \xi_L \qquad \Omega_R^2 = 2 k_L^2 \left(\frac{1}{\gamma_{R+}} + \frac{1}{\gamma_{R-}} \right)$$

$$\frac{d^2 \xi_L}{d\tau^2} = \Omega_L^2 \, \xi_R \qquad \Omega_L^2 = 2 k_R^2 \left(\frac{1}{\gamma_{L+}} + \frac{1}{\gamma_{L-}} \right)$$

$$\left(\frac{d}{d\tau}\right)_R = \frac{\partial}{\partial \tau} - \frac{\partial}{\partial z} \equiv \frac{\partial}{\partial \tau_R} \qquad k_{R,L}^2 = 4\pi r_e n_{R,L+} = 4\pi r_e n_{R,L-}$$

$$\left(\frac{d}{d\tau}\right)_L = \frac{\partial}{\partial \tau} + \frac{\partial}{\partial z} \equiv \frac{\partial}{\partial \tau_L}$$

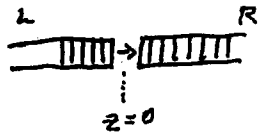

$$\tau_R = \frac{\tau - z}{2} \qquad \tau_L = \frac{\tau + z}{2}$$

$$x_L(\tau_L = 0, \tau_R) = 2\Delta \qquad \frac{\partial x_L}{\partial \tau_L}(\tau_L \doteq 0, \tau_R) = 0$$

$$x_R(\tau_L, \tau_R \doteq 0) = 0 \qquad \frac{\partial x_R}{\partial \tau_R}(\tau_L, \tau_R \doteq 0) = 0$$

$$\max \; x_L \approx \frac{\Delta}{\sqrt{2\pi}} \frac{e^A}{A^{1/2}} \qquad A = \sqrt{\Omega_1 \Omega_2}\, \tau$$

at $z = 0$, max $\tau \iff \tau_L = \tau_R = \frac{c T}{2}$

$$A \sim \sqrt{\frac{4D}{\pi}}$$

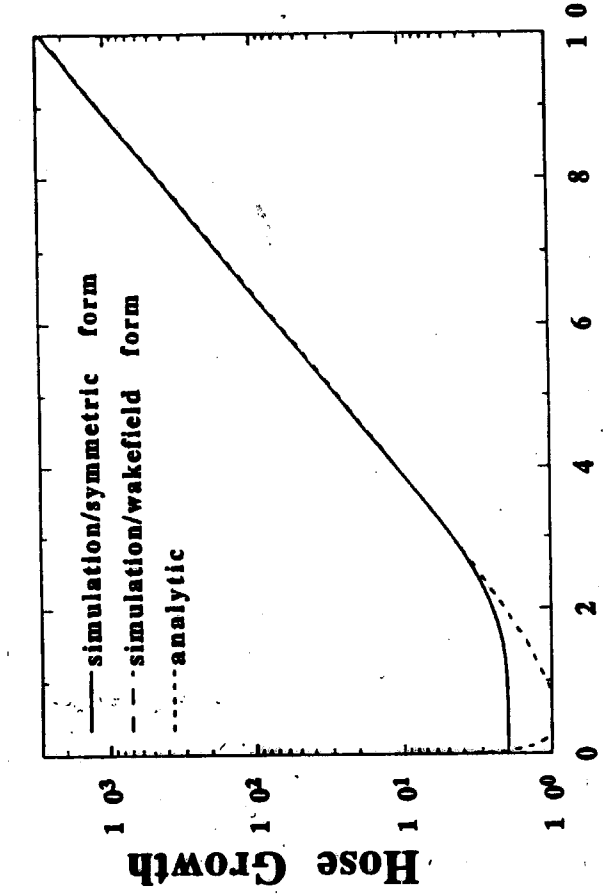

Fig. 2

$$\tilde{\xi}_r(L_\ell, p) = \frac{2}{p}\Delta\cdot\cosh\left(\frac{2DL_\ell}{L^2 p}\right).$$

which can be inverse transformed after expanding the cosh in a Taylor series to give

$$\frac{1}{2\Delta}R_r(L_\ell, L_r) = 1 + \sum_{n=1}^{\infty}\left(\frac{1}{(2n)!}\right)^2\left(2D\frac{L_\ell}{L}\frac{L_r}{L}\right)^{2n}.$$

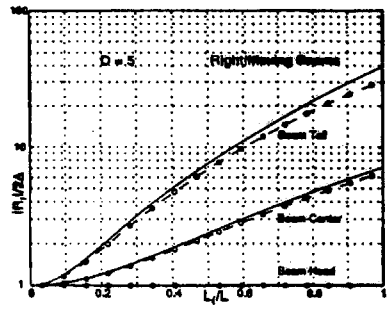

Figure 2: Centroid separation normalized to the initial offset for the right moving beams that were initially offset. The circles are from the simulation, and the solid curve is the analytical result.

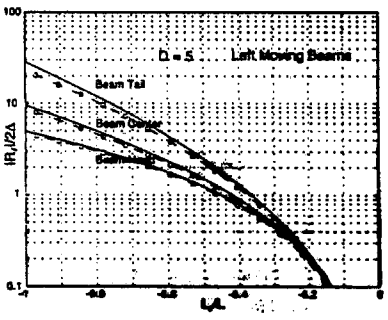

Figure 3: Centroid separation normalized to the initial offset for the left moving beams that were not offset initially. The circles are from the simulation, and the solid curve is the analytical result.

The separation of the left moving beams for this case is

$$\frac{1}{2\Delta}R_\ell(L_\ell, L_r) = \frac{1}{2D}\left(\frac{L}{L_\ell}\right)^2\sum_{n=0}^{\infty}\frac{1}{(2n)!}\frac{1}{(2n-2)!}\left(2D\frac{L_\ell}{L}\frac{L_r}{L}\right)^{2n}.$$

Note that the last two equations are exact solutions.

These two equations can be compared with simulation results. Figures 2 and 3 show the results for the case of for $D = 5$ and $2\Delta/\sigma_r = 0.05$. The simulation and calculation are in good agreement. We consider this to indicate that the simulation is correct and can be used to study tolerances for realistic situations including Gaussian profiles and unequal charges.

4 CONCLUSIONS

Collision of neutral beams permits operation in a region of IP parameter space that, for simple e+e- collisions would correspond to Y, $\delta >> 1$. With neutral beams much larger emittances, higher bunch charges, and shorter wavelength linacs may be contemplated. Control of 2.5 TeV neutral beams in collision are likely to require an uncompensated disruption parameter $D < 10$, and a correspondingly short bunch length.

We have developed and tested a simulation that can be used to make quantitative estimates of tolerances in neutral beam collisions.

REFERENCES

[1] Robert N. Cahn and Gerson Goldhaber, **The Experimental Foundations of Particle Physics** (Cambridge University Press, Cambridge, 1989)

[2] *Proceedings of the 1996 DPB/DPFWorkshop on New Directions for High Energy Physics* (AIP, New York, *to be published*).

[3] R. Hollebeek, Nucl. Instrum. Meth. **184** (1981) 33; G. Bonvicini, *et al.*, *Phys. Rev. Lett.* 62 (1989) 2381.

[4] P. Chen and V. Telnov, *Phys. Rev. Lett.* 63 (1989) 1796.

[5] K. Brown, *Conceptual Design of Final Focus Systems for Linear Colliders*, in **Fontiers of Particle Beams**, M. Month and S. Turner (eds.), Lecture Notes in Physics (Springer-Verlag, New York, 1988) pp. 481-494.

[6] D. Whittum, H. Henke and P. J. Chou (*these proceedings*).

[7] K. Oide, *Phys. Rev. Lett.* 61 (1988) 1713.

[8] V. E. Balakin and N. A. Solyak, *Proc XIII International Conference on High Energy Accelerators*, Novosibirsk, USSR, 1986.

[9] J. B. Rosenzweig, B. Autin and P. Chen, *Proc 1989 Lake Arrowhead Workshop on Advanced Accelerator Concepts.*

[10] S. Krishnagopal and R. Siemann, *Phys Rev Lett* 67, 2461 (1991).

[11] B. Podobedov and R. H. Siemann, *Phys Rev E* 52, 3066 (1995).

I. INTRODUCTION

HIGH ENERGY PHYSICS REQUIRES A NEW MACHINE

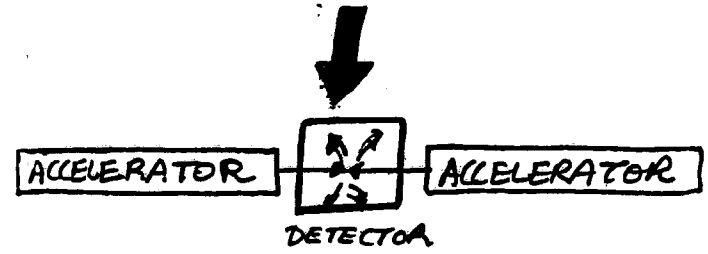

LINEAR COLLIDER

- AT 1 TeV TECHNOLOGY IS ADEQUAT
- AT 5 TeV AND BEYOND NO TECHNOLOGY IS ADEQUATE

$$\text{LENGTH} \simeq \frac{\text{ENERGY}}{\text{GRADIENT}}$$

HIGH GRADIENT

Slava DANILOV

Fermilab/Budker INP

Collective Instability of p-bar Bunch Due to Interaction with Electron Beam

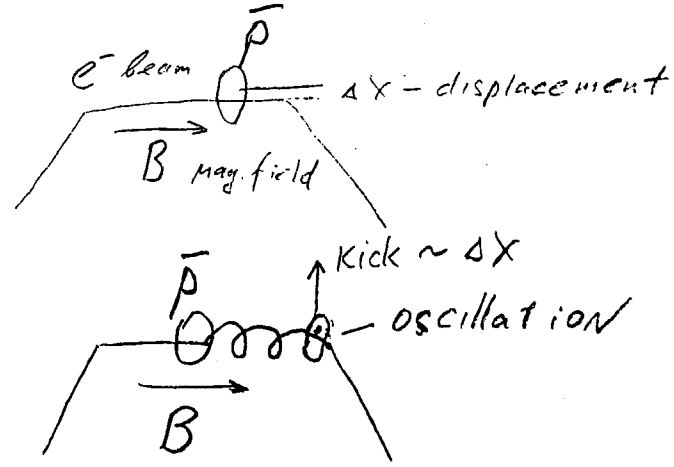

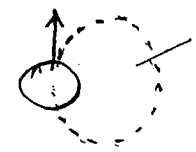

rotation in magnetic field

$$\frac{V_e}{c} = \beta_e \ll \beta_{\bar{p}}$$

$$\Delta z' = 2e^2 W_{Normal} = Z\, f_a \xi \frac{2\pi r_e N_{\bar{p}}}{\sigma^2 K_z \beta \cdot \beta_e} \cdot \sin(2K_z z \beta_e)$$

$$\Delta x' = 2e^2 W_{skew} = \mathrm{sign}(B)(\text{the same})\,(1 - \cos(2K_z z \beta_e))$$

f_a ~ 2 – numerical factor

ξ – tune shift $\bar{p}$ due to electrons

r_e – cl. radius of e^-

β – beta-function

σ – el. beam size

$\beta_e = \frac{V_e}{c}$ $\qquad K_\perp = \frac{B(kG)}{\gamma_e \beta_e \cdot 3.3[cm]}$ – rot. length

$Z_\perp \sim 3\text{-}10\ M\Omega/m$

$Z_{\perp\ el.\ comm} \sim 20\ M\Omega/m$

Usual head-tail $\to 0$

$\xi \to 0$

Strong head-tail (TMCI)

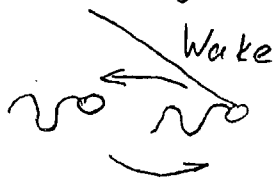

Threshold for $\Delta\nu_c \sim \nu_s$

Factors

1 Betatron tune spread
2. Synchrotron motion nonlinearities
3. ...

Further the worst prediction for threshold will be made.

$\beta \sim 100\ m$

$\sigma \sim 50\ cm$

$\nu_s = 0.001$

$\nu_x \approx .57$

$\nu_y \approx .58$

$B \approx 1T$

$N_{\bar{p}} \approx 6 \cdot 10^{10}$

$\beta_\varepsilon \sim 0.3$

Hollow beam

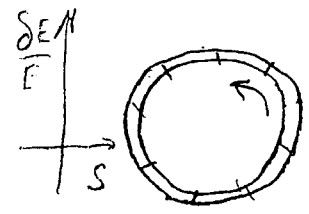

7 parts

- Synchrotron Rotation
  Betatron Oscillations
  +
  Kick

$\nu_x = \nu_y = .55$

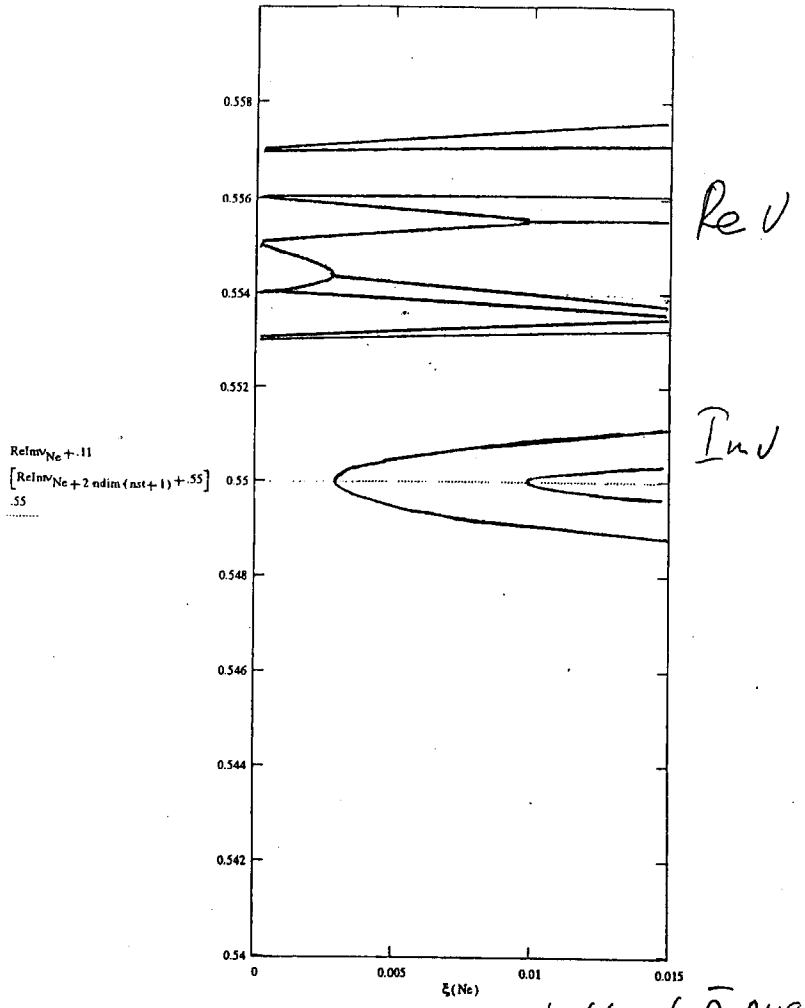

ξ – Tuneshift of $\bar{p}$ due to e^- beam

4

5.

1 d case

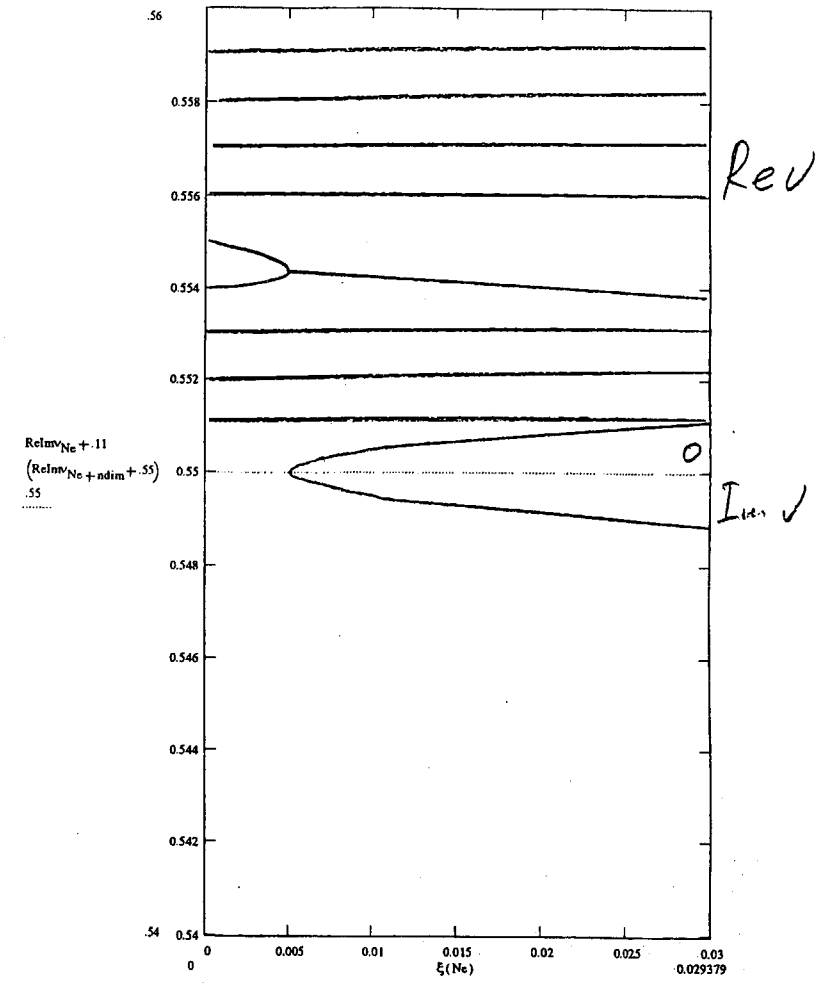

$\xi_{th} \sim .007$

3

6.

$\nu_y - \nu_x = 5.5\ \nu_s$

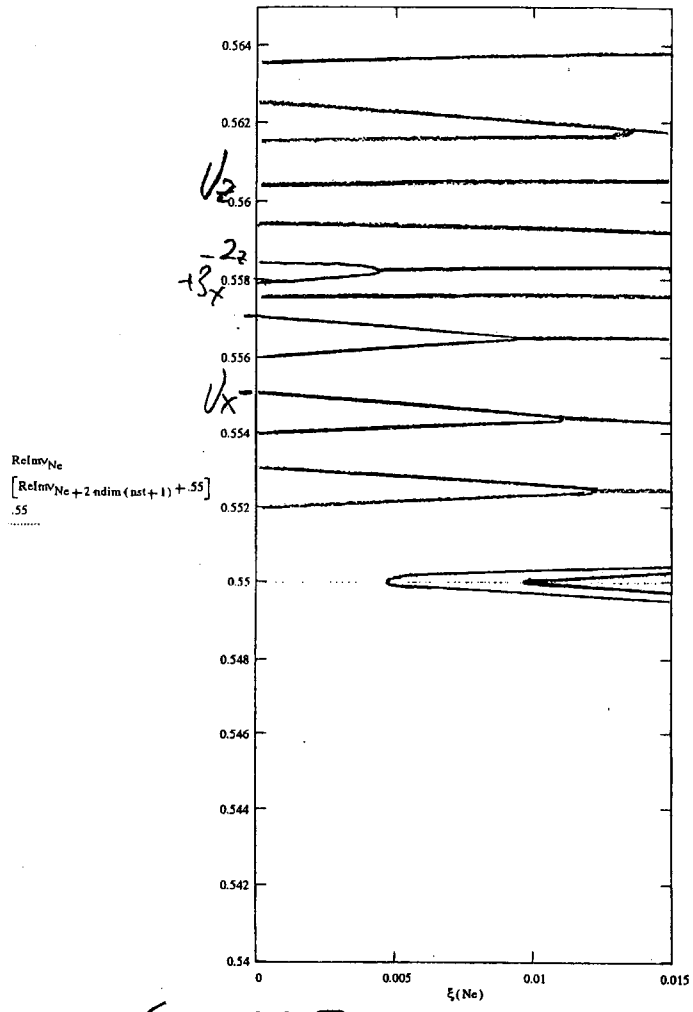

$\xi \sim .005$

7.

$\nu_x - \nu_s = 3\ \nu_s$

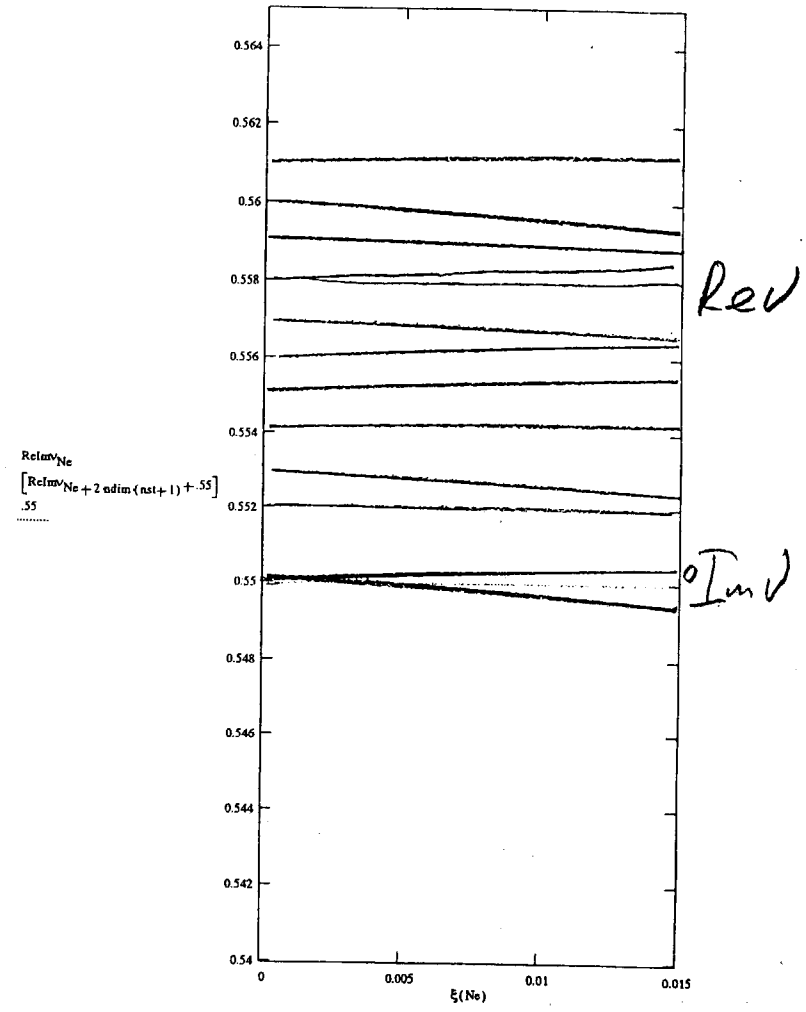

$\xi_{ch} = 0.$

8.

SBR

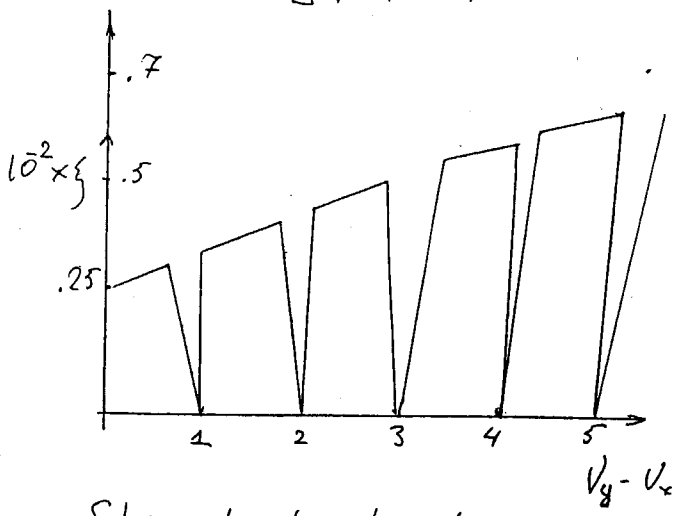

Schematical dependence of ξ_{th} vs. $\nu_y - \nu_x$

Conclusion

1) For $\xi \sim .01$ $B \sim 2T$ is needed

2) Skew-Wake can be eliminated by using 2 e^- beams with opposite $B_{\parallel}$

3.) For larger ξ additional tools for coping TMCI are needed

Q's:

Bagley:	The oscillating fields you are talking about – are they due to the whole bunch?
Danilov:	No, it is only response of e-beam to δ-function perturbation. Real motion is a convolution of such responses over the whole pbar bunch.
Meshkov:	The effect you are considering looks similar to Derbenev recent idea of collective electron cooling.

A.Burov (Budker INP/Fermilab)

Transverse Instabilities Driven by Compensating Electron Beam

Transverse instabilities driven by the compensating e-beam.

A. Burov

1. Wake Functions.

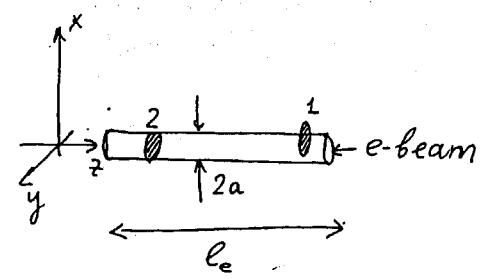

Head particle - 1
Tail particle - 2

head → e-beam → tail

$$\Delta v_{xe} = \frac{2 r_e X_1}{a^2(1+\beta)} c \quad ; \quad \beta = v/c$$

$$\Delta x_e(t) = \frac{\Delta v_{xe}}{\omega_L} \sin \omega_L t \quad ; \quad \Delta y_e = \frac{\Delta v_{xe}}{\omega_L}(1 - \cos \omega_L t)$$

$$\omega_L = \frac{eB}{mc} \rightarrow \text{Larmour frequency}$$

From here:

Direct wake

$$W_d(s) = W \sin(ks)$$

Sqew wake:

$$W_s(s) = W(1 - \cos ks)$$

$$W = \frac{4\pi n_e \ell_e}{(1+\beta)^2(\beta/e)a^2}$$

$$k = \frac{\omega_L}{(1+\beta)c}$$

For $B = 1\,T$, $\beta = 0.3$, $\sigma = 30\,cm$

$\underline{k\sigma = 140}$ (!)

2. Sqew Instability. (or 2D)

Air-bag model:

$$\begin{cases} \left(\frac{\partial}{\partial t} + \Omega \frac{\partial}{\partial \psi}\right)^2 y + \omega_y^2 y = \frac{\mathcal{F}}{2\pi} \int_{-|\psi|}^{|\psi|} d\psi'\, x(\psi') \\ \left(\frac{\partial}{\partial t} + \Omega \frac{\partial}{\partial \psi}\right)^2 x + \omega_x^2 x = -\frac{\mathcal{F}}{2\pi} \int_{-|\psi|}^{|\psi|} d\psi'\, y(\psi') \end{cases}$$

$$\mathcal{F} = \frac{W r_p N_{\bar{p}} c^2}{\gamma \Pi}$$

Ω - synchrotron freq.
$\Omega \equiv \nu_s \omega_0$

Two-mode approximation:

$$\mathcal{F}_{th} = 3\omega_x \sqrt{\Omega |\omega_y - \omega_x|} \Rightarrow B_{th} = 1.3 \frac{e \xi N_{\bar{p}}}{a^2 \sqrt{\nu_s \Delta\nu}}$$

$$|\omega_y - \omega_x| \equiv \Delta\nu \cdot \omega_0$$

Betatron tune spread $\delta\nu$:

Does not influence, when $\delta\nu < \nu_s$

Otherwise: $\underline{\nu_s \rightsquigarrow \delta\nu}$ in threthold formulae.

For $\xi = 0.01$, $N_{\bar{p}} = 6\,10^{10}$, $a = 1\,mm$, $\nu_s = 10^{-3}$, $\Delta\nu = 10^{-2}$ $B_{th} = 1\,T$

3. 1D - Instability

Driven by the direct wake $\sim \sin(ks)$, $k\sigma \gg 1$.

Applying microwave approximation, one finds:

$$\mathcal{F}_{th} \simeq 2\omega_x \Omega (k\sigma) f \qquad f \simeq 1 \leftarrow \text{number}$$

$$\frac{(\mathcal{F}_{th})_{1D}}{(\mathcal{F}_{th})_{2D}} \simeq k\sigma \cdot \sqrt{\frac{\nu_s}{\Delta\nu}} \gtrsim 30$$

4. Sgew Instability Suppression

Two places with e-beams:

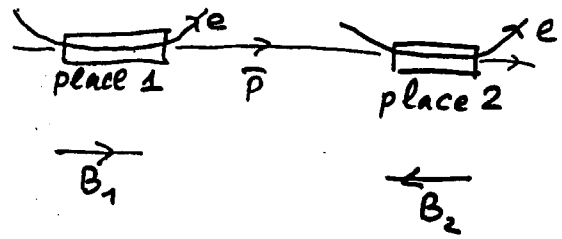

Coupling x-y is suppressed, when

$$\frac{\beta_1}{B_1} = \frac{\beta_2}{B_2} \Rightarrow \boxed{\frac{\beta_{1x}}{\beta_{2x}} = \frac{\beta_{1y}}{\beta_{2y}}}$$

Q's:

Stupakov:	In fact, nonlinear modes can play role too, therefore, solution of Vlasov equation is more appropriate.
Burov:	This is right. There is no small parameter like beam size to vacuum chamber radius as in usual wake-problem, and higher modes (quadrupole, etc.) may play role as well as dipole one.

Beam-Beam Compensation Workshop
Fermilab, Feb. 12-13, 1998

Vladimir SHILTSEV

Computer Simulations of Antiproton Beam Transverse Stability in Tevatron with "Electron Compressor"

Content:

1. Physical Model
2. Code
3. Mode Coupling
4. Threshold vs. electron current
   synchrotron tune
   "direct" wake only
   Pbar intensity
   working point
   tune spread
5. Comments

I. Physical Model

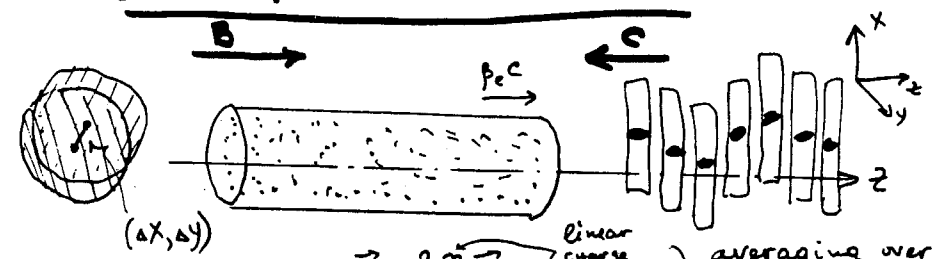

~ rectang. e-beam field $\vec{E} = \frac{2\varkappa}{a_e^2}\vec{r}$ linear charge density

~ Gaus. $\bar{p}$-beam field $\vec{E} = \frac{2\varkappa}{r^2}\left(1-e^{-\frac{r^2}{2\sigma^2}}\right)\vec{r} \approx \frac{\varkappa \vec{r}}{\sigma_p^2}$

averaging over charge distrib. $\vec{r} \to (\Delta X, \Delta Y)$ centroid

Number of $\bar{p}$ in one slice $\Delta N_p = \frac{N_{\bar{p}}}{M}$ ← number of macroparticles = slice

$M = 128 \div 2048$

After passing of each slice of $\bar{p}$s, electrons get kick

$$\Delta\vec{\theta}_e = \frac{\Delta\vec{P}_\perp}{\gamma_e m c \beta_e} = -\frac{\Delta N_{\bar{p}}}{\gamma_e \beta_e}\frac{r_0}{\sigma_p^2}\left(\vec{r}_p - \vec{r}_e\right), \quad r_0 = 2.8\cdot 10^{-15}\,m$$

or $\Delta\vec{v}_e^{\,i} = v_\parallel \Delta\vec{\theta}$ due to slice i amplitude $\frac{\Delta v}{\omega_H}$

Then, the e-beam starts to oscillations in solenoid field B and the next slice sees e-beam centroid displaced by

$$x_e^{i+1} = A\cdot\left[(x_e^i - x_p^i)\cdot\sin\omega_H t^i - (y_e^i - y_p^i)\cdot(1-\cos(\omega_H t^i))\right]$$

$$y_e^{i+1} = A\cdot\left[(y_e^i - y_p^i)\cdot\sin\omega_H t^i + (x_e^i - x_p^i)(1-\cos\omega_H t^i)\right] \qquad \omega_H = \frac{eB}{\gamma_e m c}$$

Coefficient $A = \frac{c}{\omega_H}\frac{\Delta N_p}{\gamma_e}\frac{r_e}{\sigma_p^2} \approx \frac{0.48\ \Delta N_p/10^{10}}{B[kG]\ \sigma_p^2[mm]}$

$\omega_H t^i$ is phase advance of Larmour oscillation between two slices

e.g. if distance $S_{i+1} - S_i = \Delta S$ $\quad \omega_H t^i = \frac{\Delta S}{1+\beta}\,0.587[cm^{-1}]\cdot\frac{B[kG]}{\gamma_e}$

Total displacement of e-beam is sum of excitations from previous slices:

$$\begin{Bmatrix} x_e^i \\ y_e^i \end{Bmatrix} = \sum_{i=\text{slices before}} \begin{Bmatrix} x_e^i \\ y_e^i \end{Bmatrix}$$

The kick experienced by macroparticle is:

$$\beta_{x,y}\,\theta^i_{x,y} = -4\pi\,\Delta\nu_e \cdot \left\{ \begin{matrix} x_e^i - x_p^i \\ y_e^i - y_p^i \end{matrix} \right\}$$

linear tune shift due to electron beam

at location of macroparticle

$$\Delta\nu_e = C \cdot I_e \,, \quad C = \frac{\beta[m] \cdot L[m]}{a_e^2\,[mm]} \cdot 2.2 \cdot 10^{-5}\ [1/A]$$

e.g. $\Delta\nu_e = 0.01$ $\quad \beta = 100\,m$ $\quad L = 2\,m$ $\quad I_e = 1.5\,A$ $\quad a_e = 0.8\,mm$

The rest of accelerator is presented by linear lattice

e.g.
$$\begin{pmatrix} x \\ \beta_x\theta_x \end{pmatrix}_{New} = \begin{pmatrix} \cos 2\pi\nu_x & \sin 2\pi\nu_x \\ -\sin 2\pi\nu_x & \cos 2\pi\nu_x \end{pmatrix} \begin{pmatrix} x \\ \beta_x\theta_x \end{pmatrix}_{old}$$

If e-beam is rigid (electrons do not move in x,y), then only tune shift occurs:

$$\Delta\nu_x \approx -\Delta\nu_e - \mathrm{ctg}(2\pi\nu_x)\cdot\pi\cdot\Delta\nu_e^2$$

Otherwise, there is "head-tail" interaction

Motion of the electron beam excited by point charge displaced in X-direction

red - B=1kG blue - B=4kG black - B=20kG

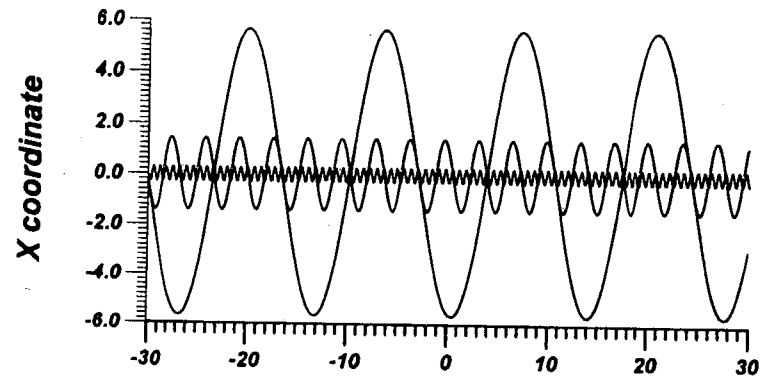

Distance along pbar bunch, cm

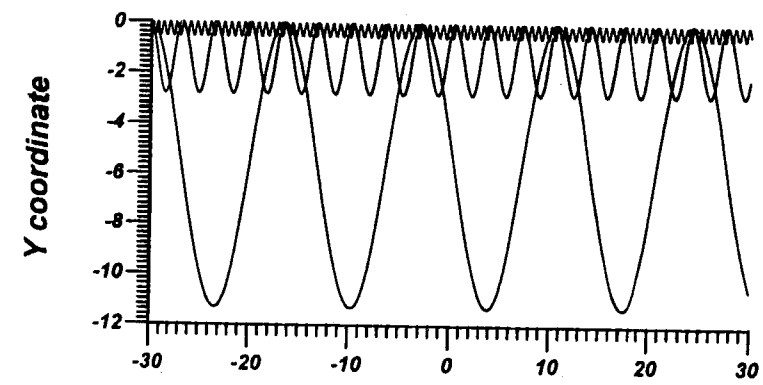

Distance along pbar bunch, cm

Motion of the electron beam excited by point charge displaced in X-direction

red - B=1kG blue - B=4kG black - B=20kG

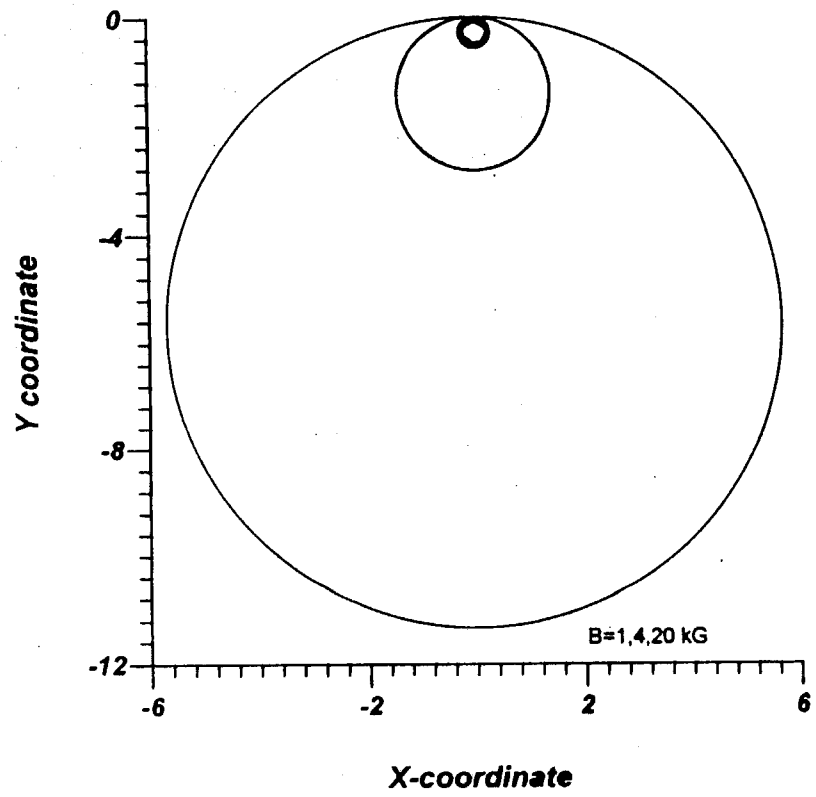

Electron beam center motion while oncoming displaced pbar beam passing through; solenoid field B=1, 10 and 40 kilogauss

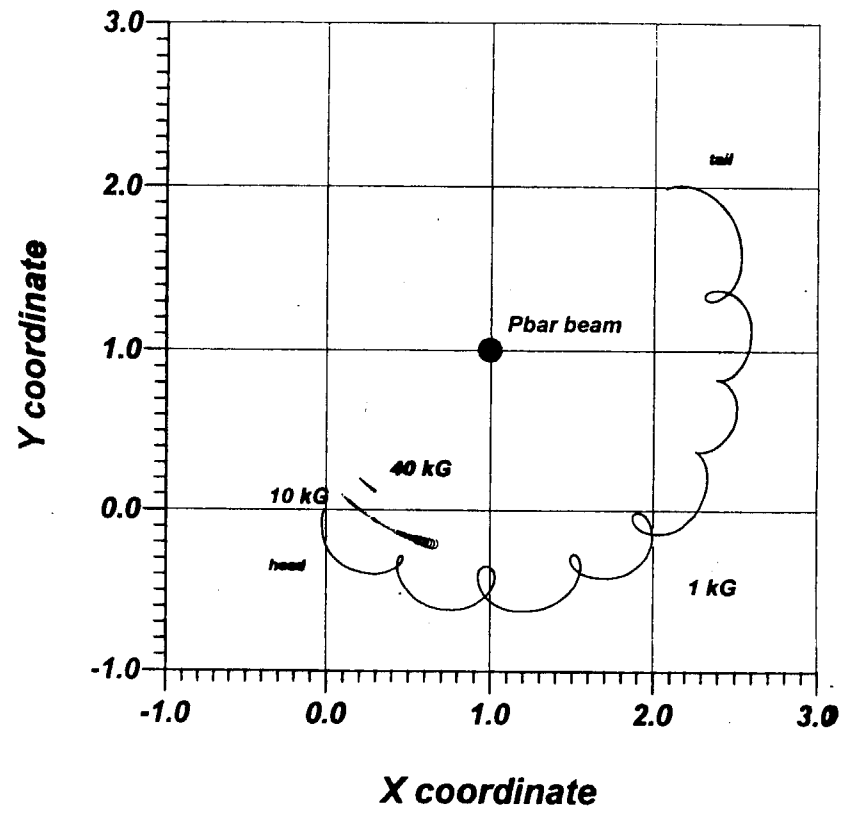

I. Code

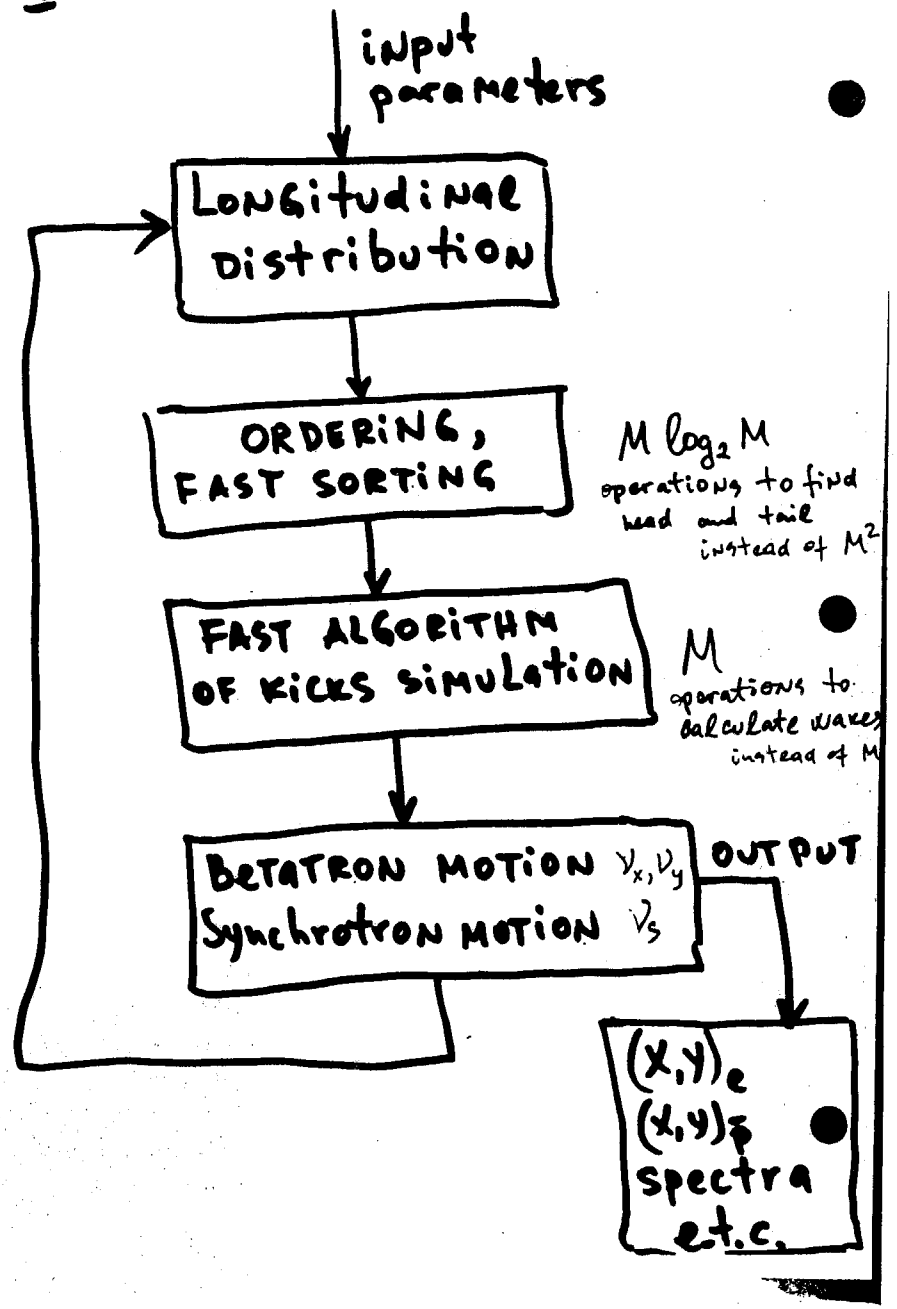

Longitudinal coordinates of macroparticles:

τ_k — RF phase

$v_k = \frac{d\tau_k}{\nu_s d\theta}$ — Energy deviation

are derived via (T_k, V_k) ← uniformly random in [-1, 1] circ

$$(\tau_k, v_k) = L\,(T_k, V_k) \cdot \frac{\left[1-(1-R_k^2)^{\frac{1}{1+\mu}}\right]}{R_k}$$

$$R_k^2 = T_k^2 + V_k^2 \le 1 \quad , \; L \text{ - length}$$

Smoothed density $\sim (L^2 - \tau^2 - v^2)^{\mu}$

line density $\sim (L^2 - \tau^2)^{\mu + 1/2}$ → see Figs

Longitudinal variables are updated once per turn using a rotation with angle

$$2\pi \nu_s$$

Distribution of macroparticles in synchrotron plane with μ=-0.5

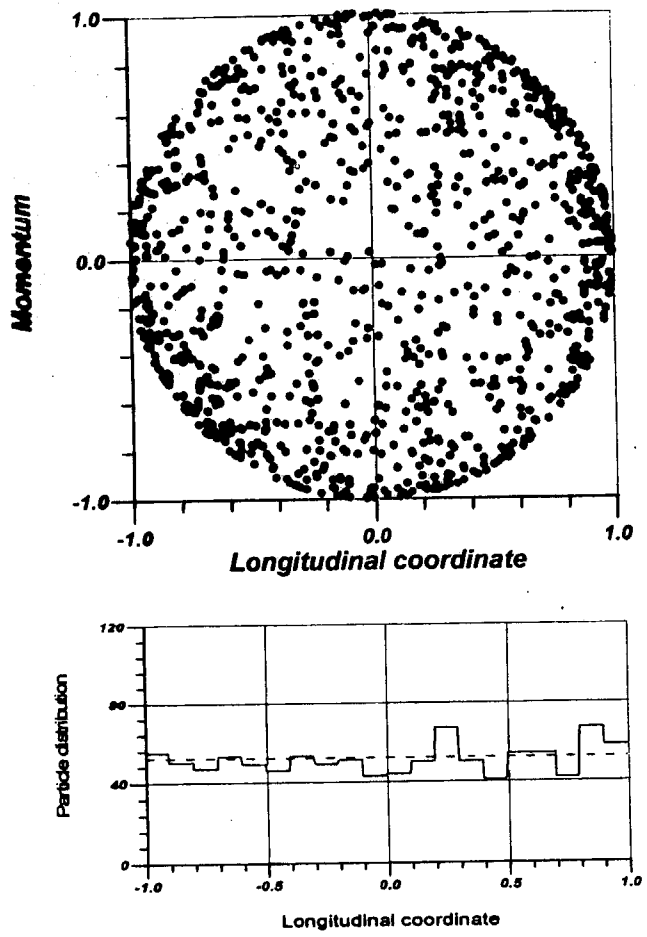

Distribution of macroparticles in synchrotron plane with μ=1.5

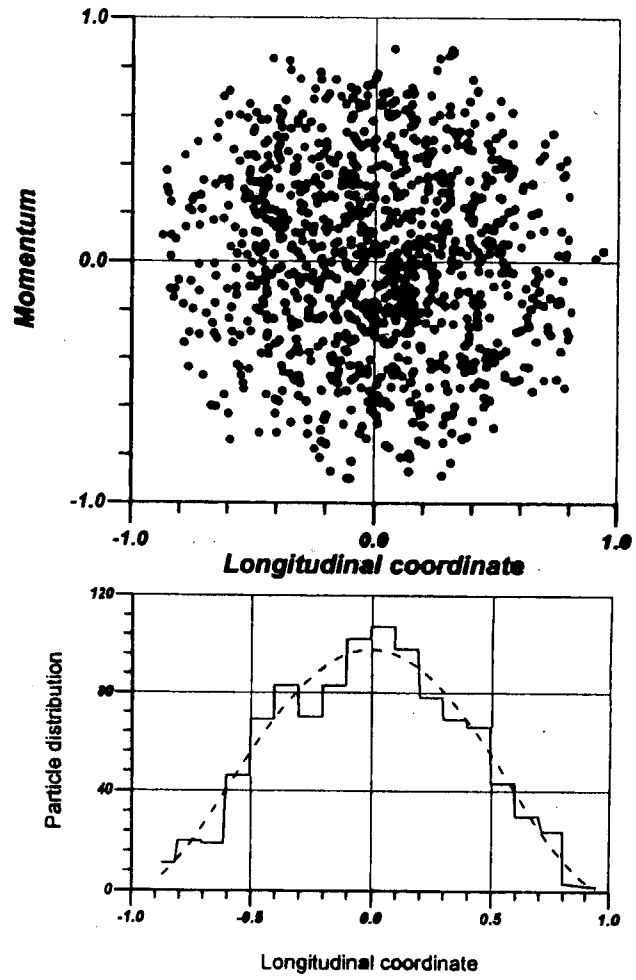

The code was tested with a constant wake $W(s) = \Theta(s) \cdot W_0$ ← Heaviside

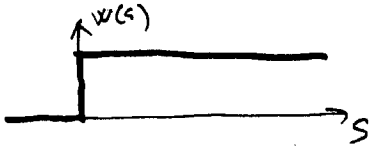

- TMCI occured in numerical agreement with theory
- threshold does not depend on bunch length

$$W_0^{th} = 0.14 \frac{\nu_s}{0.01}$$

if kick $\beta \Delta\theta^i_{x,y} = W_0 \left(\sum_{j<i} x_j\right)/M$

Our 2-D problem:

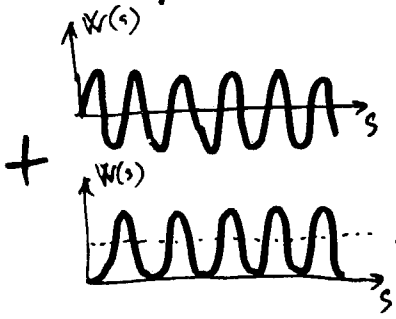

"Direct" wake $F_{x,y} \sim (x,y)$

"skew" wake $F_{x,y} \sim (y,-x)$

Spectra of horizontal beam centroid motion

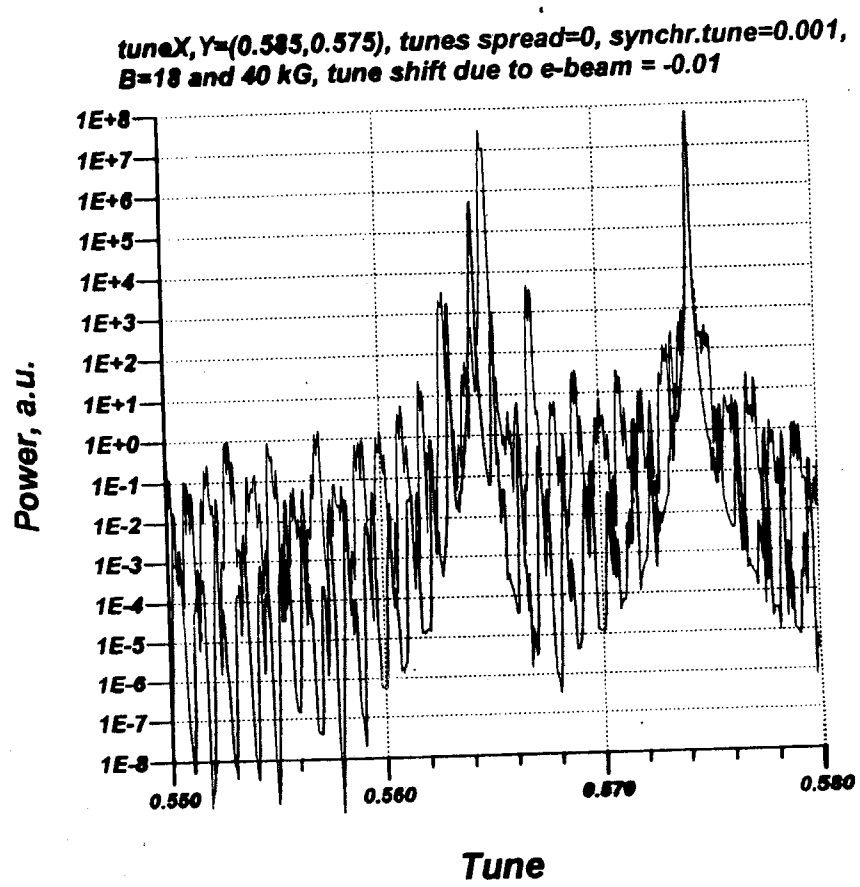

Spectra of horizontal beam centroid motion

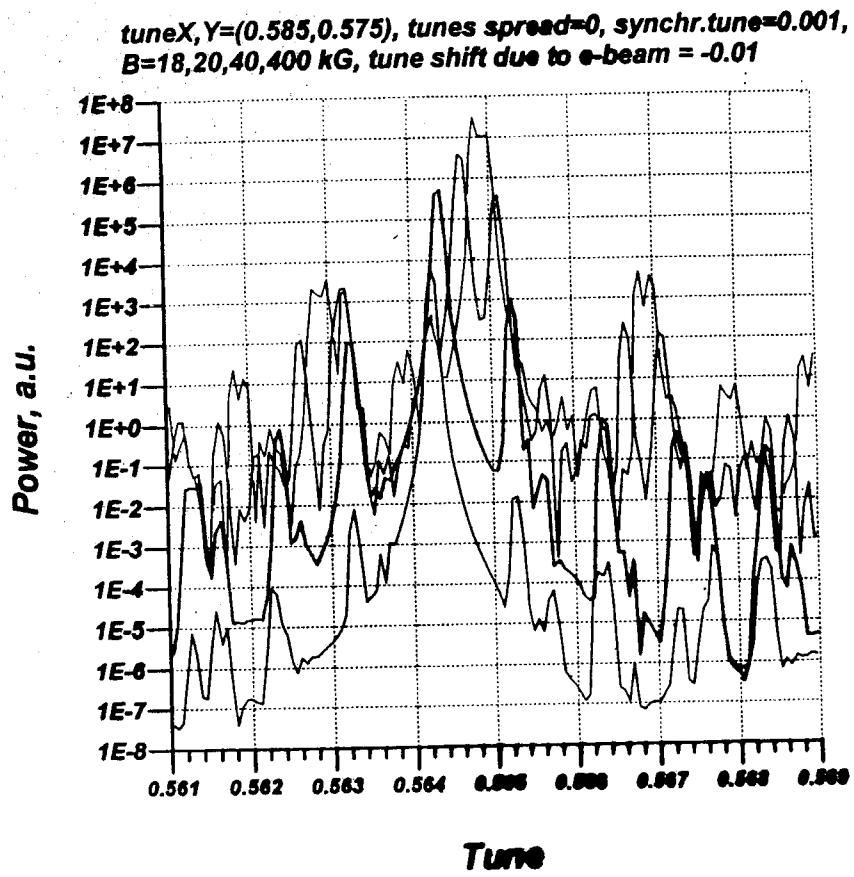

Coupling of horizontal modes of pbar beam near vertical tune in presence of magnetized electron beam

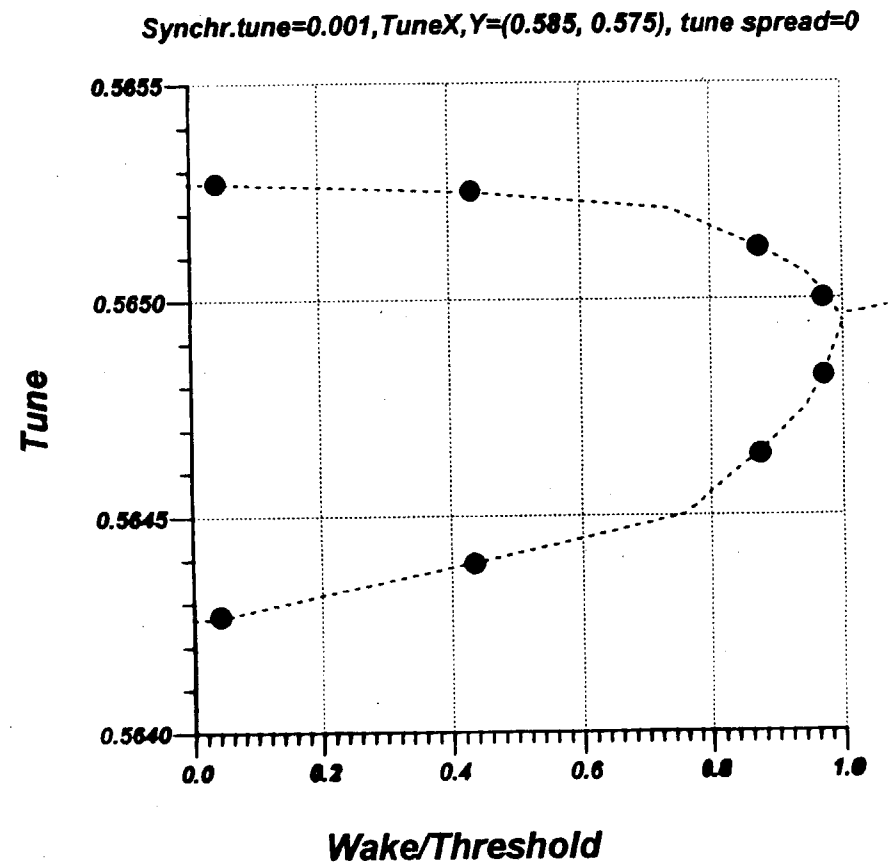

Minimum solenoid field B[kG] required for stability of pbar beam vs tune shift due to e-beam (intensity)

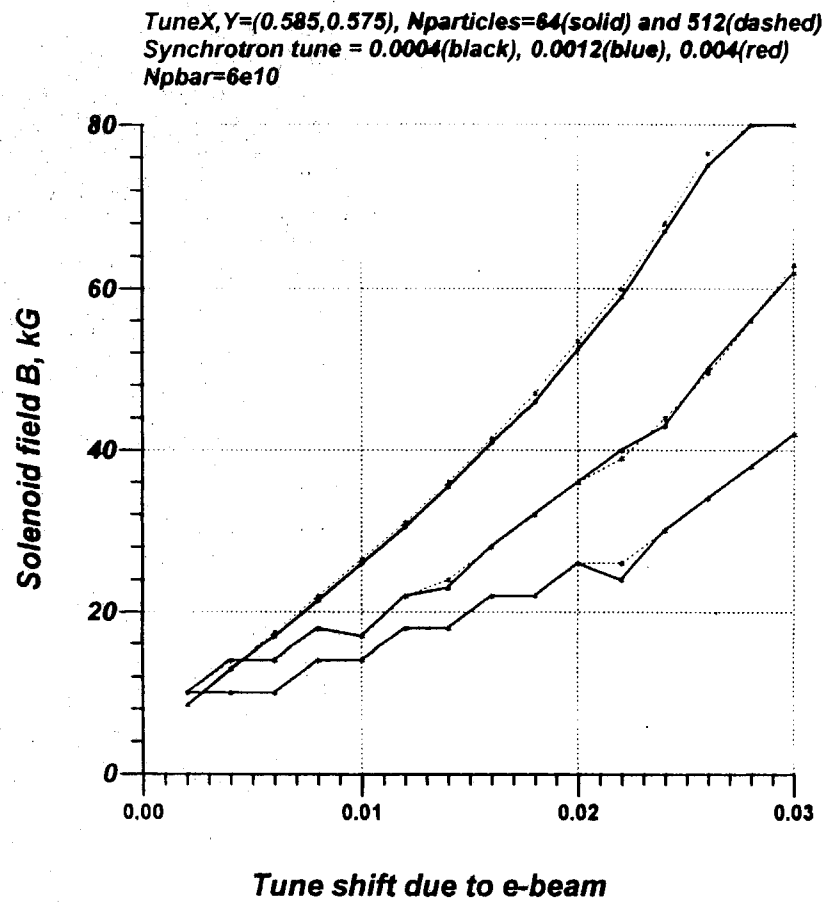

Contour plot of minimum solenoid field B[kG] required for stability of pbars with e-beam

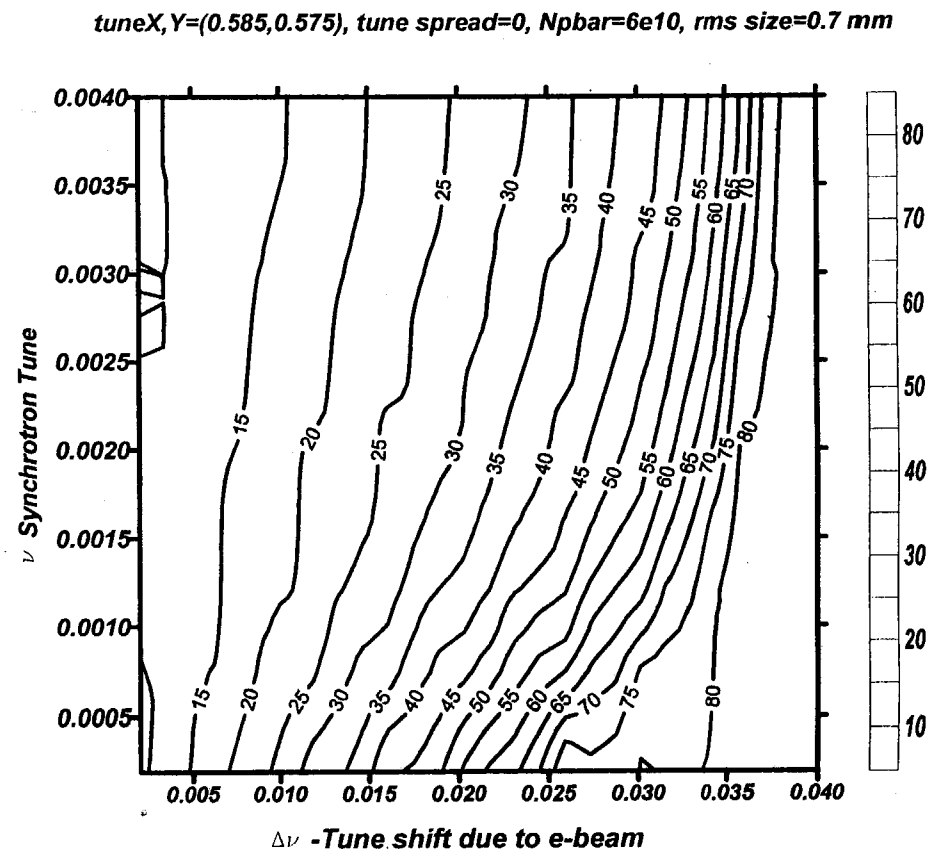

Minimum solenoid field B[kG] for pbars stability without non-diagonal DC component of the e-beam wake

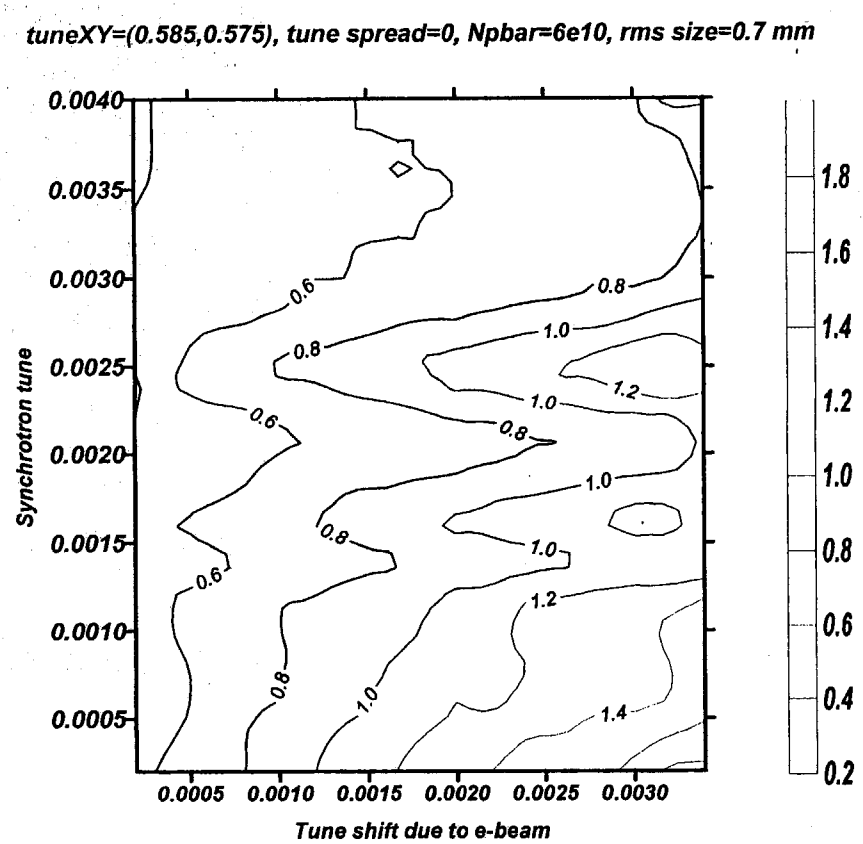

Minimum solenoid field B[kG] required for stability of pbar beam vs tune shift due to e-beam

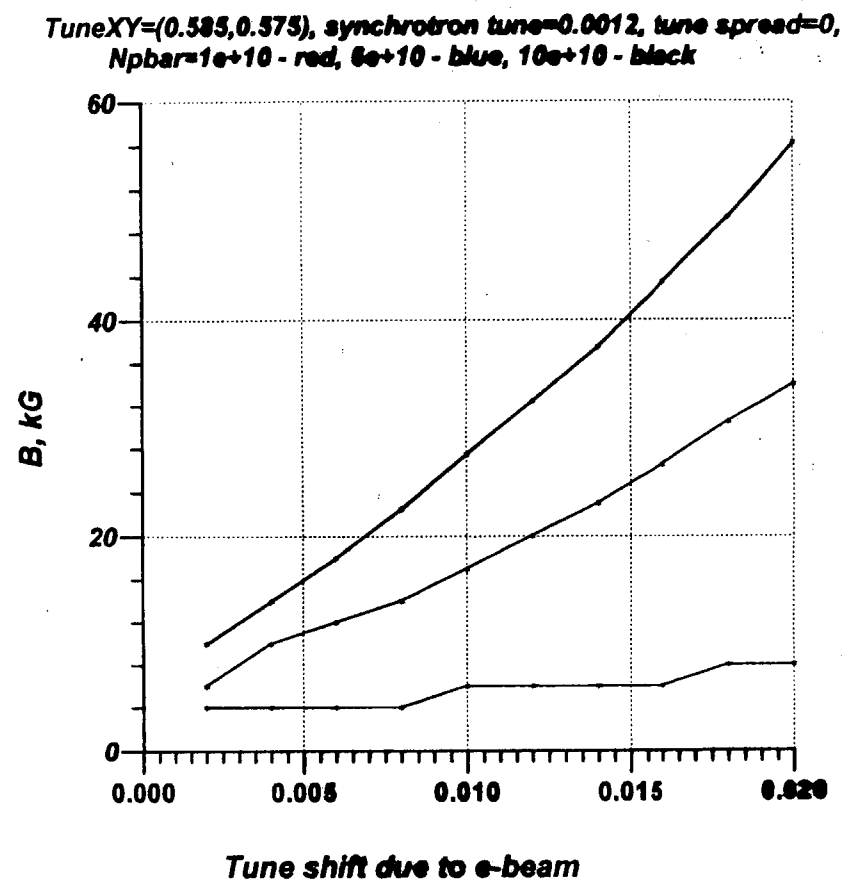

Minimum solenoid field B[kG] required for stability of pbar beam vs tune shift due to e-beam

Npart=64, synchrotron tune=0.0012, Npbar=6e10,
TuneX,Y=(0.585, 0.575) - black,(0.595,0.575) - blue, (0.615,0.575) - red

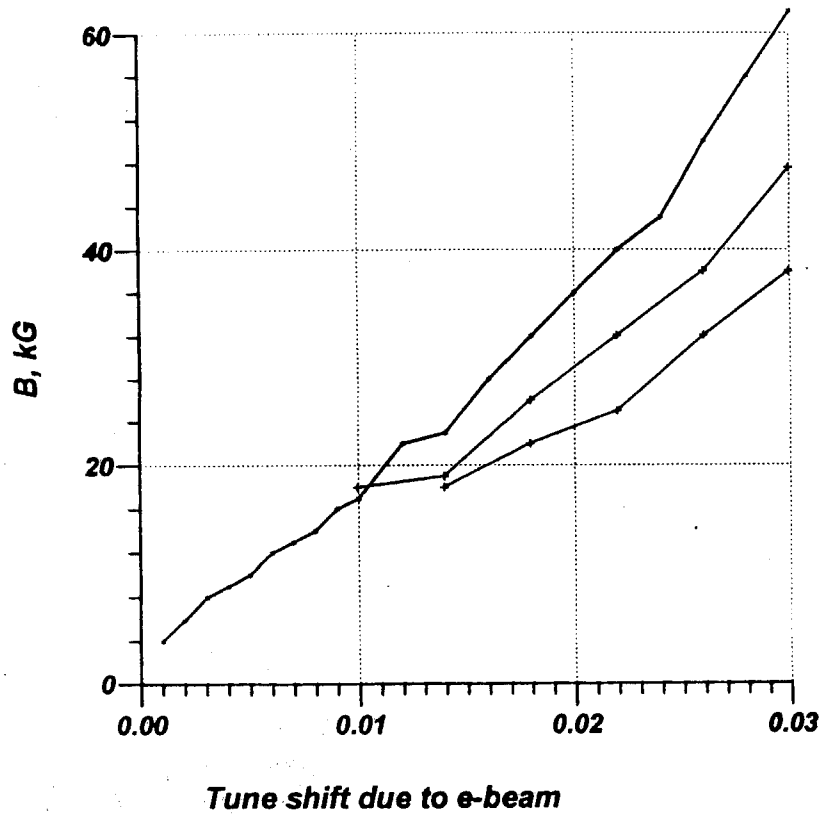

Contour plot of minimum magnetic field B[kG] required for stability of pbars with electron beam vs Tune Y and TuneX-TuneY

e-tune shift=0.01, tune spread=0.002, synchr.tune=0.0012, N=6e10, rms size=0.7mm

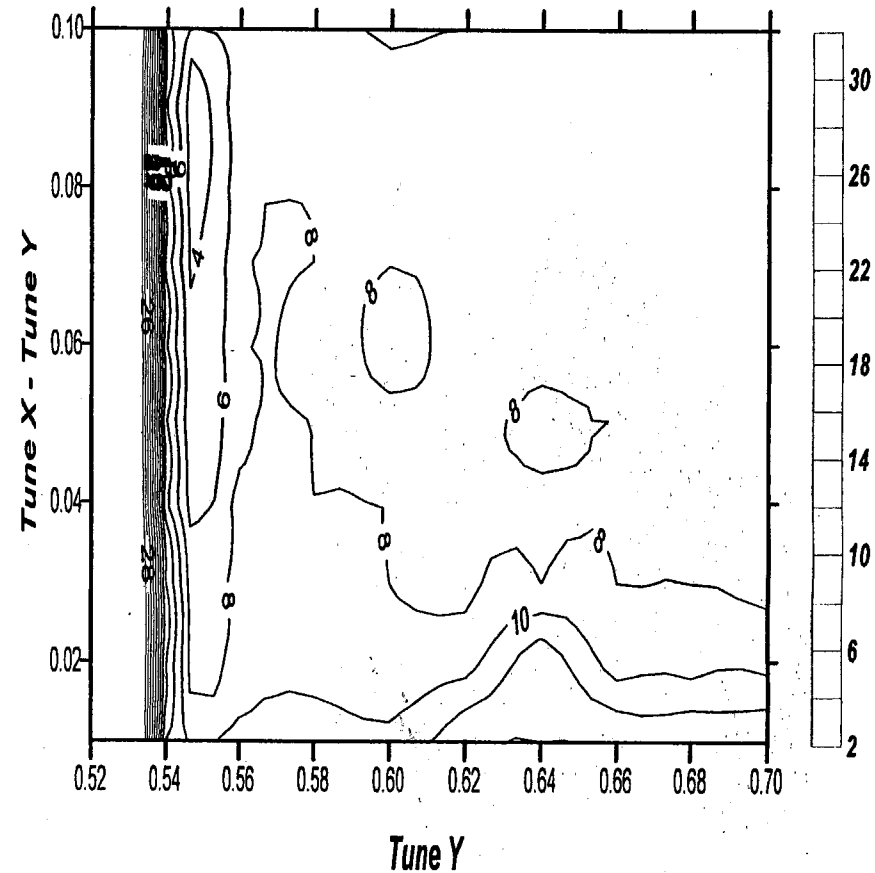

Minimum magnetic field required for pbar stability vs tune spread

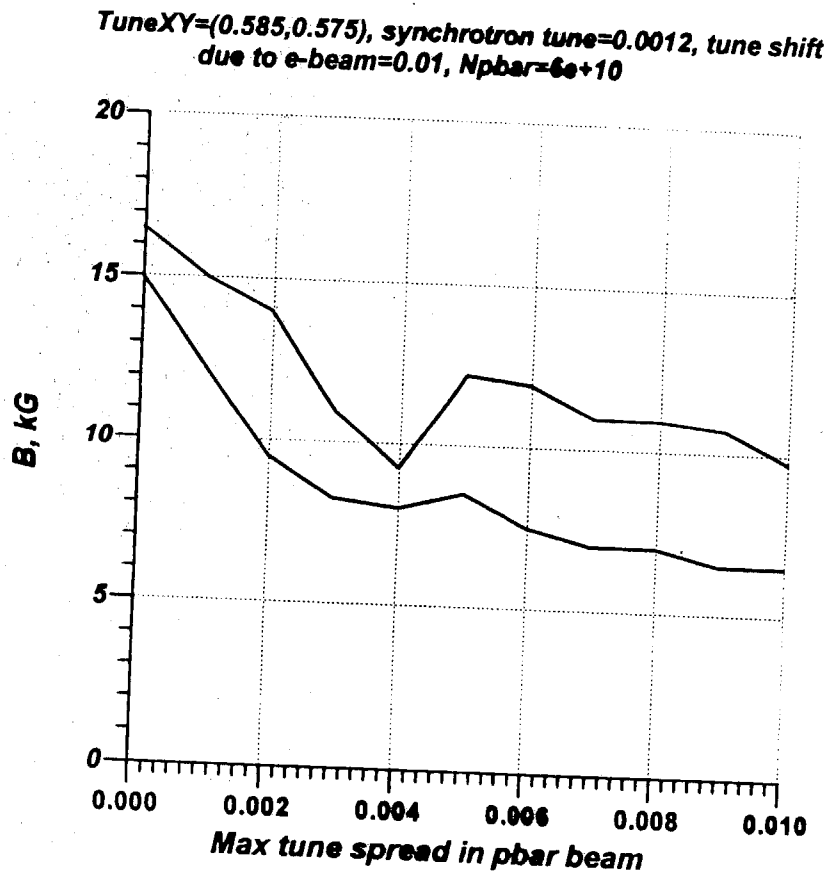

Effect of betatron tune spread on pbar spectra of soherent horizontal motion, near threshold due to electron beam

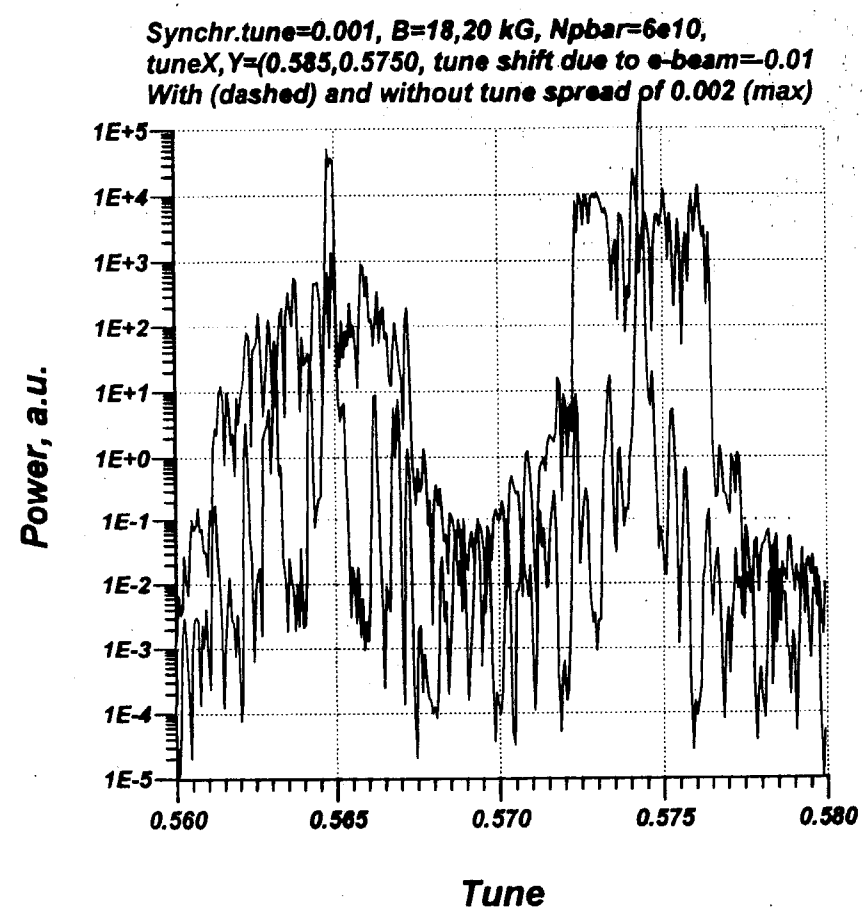

Contour plot of minimum solenoid field B[kG] required for pbars stability with e-beam vs pbar tune spread and e-beam intensity (e-tune shift)

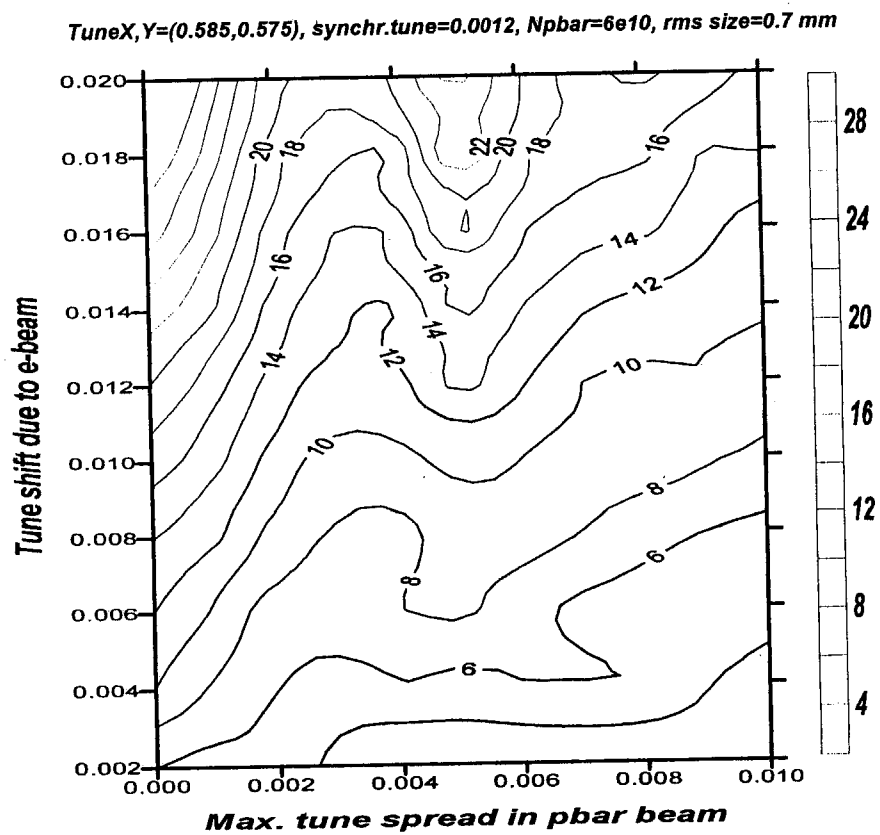

CONCLUSIONS

A.Burov THEORY

$$B_{thr} = const. \frac{\Delta\nu_e \cdot N_{\bar{p}}}{\sigma_p^2 \sqrt{\nu_s |\nu_x}}$$

- $B_{thr} \sim \frac{1}{\sqrt{\nu_s}}$ ..... AGREE
- $B_{thr} \sim \Delta\nu_e$ ..... AGREE
- $B_{thr} \sim N_{\bar{p}}/\sigma_{\bar{p}}^2$ ..... AGREE
- $B_{thr} \sim \frac{1}{\sqrt{|\nu_x - \nu_y|}}$ ..... AGREE
- B_{thr} does not depend on longitudinal parameters ..... AGREE
- B_{thr} depends on tunes ν_x, ν_y (resonances) ..... N/A
- B_{thr} falls with tune spread ..... (AGREE)
- below ~~with~~ B_{thr}, TMCI occures ~~at~~ y-plane if $\nu_y < \nu_x$ and $0.5 < \nu_x, \nu_y$ ..... N/A
- Electron Compressor at Tevatron needs $B^{MAX} \lesssim$

Comments:

Factors which may ease the TMCI (lower necessary solenoid field)

1. decoherence due to non-linear kicks (both electron and pbar beams)

2. in scheme with two E-Compressors

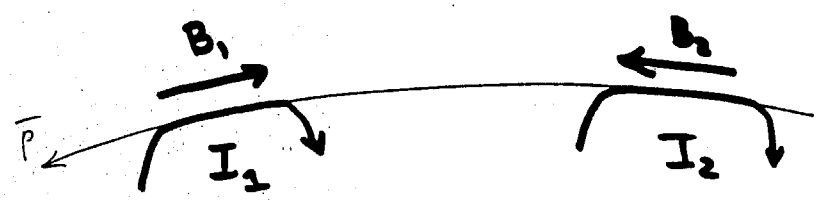

There is room for compensation of "skew" wake components

$$W^{skew} \sim I_1 \cdot \frac{K_1}{B_1} - \frac{I_2}{B_2} \cdot K_2$$

constants K_1, K_2 - depend on $\beta_1, \beta_2, \psi_1, \psi_2$

Head-Tail Instability in Storage Rings

$$N_p^{th} = (\text{Const}) \cdot \frac{E/e \cdot \nu_s}{\mathrm{Im}\langle Z_\perp \beta_\perp \rangle}$$

Tevatron: $Z_\perp^{protons} \sim 8 \ \frac{M\Omega}{m}$ (inj)
threshold

$Z_\perp^{\bar{p}} \sim 50 \ \frac{M\Omega}{m}$ (inj)

E-beam impedance

$$Z_\perp^e \propto \sqrt{\nu_s} / B$$

Q's :

Meshkov:	May a feedback to counteract the TMCI?
Shiltsev:	In practice – no: it is a head-tail effect and the necessary frequency band is huge, several GHz, besides a lot of power to correct 1 TeV pbars.
Meshkov:	I mean feedback for positioning of e-beam?
Shiltsev:	Good idea! Electrons can be well affected by comparatively small fields.
Meshkov:	How strong is coupling due to your solenoids?
Shiltsev:	Two 4T 2m long solenoids result in about 0.001 difference resonance strength. It is only few times less the natural Tevatron coupling.
Meshkov:	A scheme with two antiparallel solenoids and two beams may solve you wake and coupling problems.

#14

Beam-Beam Compensation Workshop

12-13 Feb. 1998, Fermilab

On Electron Beam Set-up for Beam-Beam Compensation in Tevatron

Vladimir Shiltsev

February 11, 1998

1 Electron Current Fluctuation

Fluctuations of the electron current from turn to turn cause time variable quadrupole kicks which lead to a transverse emittance growth of the antiproton bunches. In "the electron lens" [1, 2] the current has to be modulated rather fast although periodically, and thus, the issue of how stable is the current at one-turn scale may be of a great importance.

Emittance growth rate due to fluctuations of a gradient δG of a lens with length l is given by [3]:

$$\frac{d\varepsilon}{dt} = f_0^2 \frac{\varepsilon}{16} (\frac{el\beta_0}{Pc})^2 \sum_{n=-\infty}^{\infty} S_{\delta G}(f_0|2\nu - n|), \qquad (1)$$

where f_0 is the revolution frequency, β_0 is beta function at the lens location, Pc is the antiproton kinetic energy, ν is the machine tune, and $S_{\delta G}(f)$ is the power spectral density (PSD) of the gradient fluctuations. The PSD we use is defined for positive frequencies f. One can see that only some particular frequencies contribute into the emittance growth, the lowest of them is twice the betatron frequency $2\Delta\nu f_0$. If one assumes that the current ripple is a "white noise" with a constant PSD $S_{\delta G}$, then, the rms value of the ripple δG relates to the PSD as

$$\delta G^2 = (1/2) f_0 S_{\delta G},$$

and therefore, taking into account that there are two electron beams[1] on the pbar orbit, one gets:

$$\frac{d\varepsilon}{dt} = f_0 \frac{\varepsilon}{16} ((\frac{\beta_1}{F_1})^2 + (\frac{\beta_2}{F_2})^2)(\frac{\delta J_e}{J_e})^2 = 2\pi^2 f_0 \varepsilon (\Delta\nu_1^2 + \Delta\nu_2^2)(\frac{\delta J_e}{J_e})^2, \qquad (2)$$

[1] with presumably uncorrelated current fluctuations

where $F_{1,2}$ is focal lengths of two electron beam, $\delta J_e / J_e$ is the rms value of relative current fluctuation, $\Delta\nu_{1,2}$ is the value of tune shift produced by electron lenses 1 and 2 respectively (proportional to the current) and we used relation of $\Delta\nu = (1/4\pi)\beta_0/F$.

From Eq.(2) one immediately gets the emittance evolution equation:

$$\varepsilon(t) = \varepsilon_0 \exp(t/\tau_e), \qquad (3)$$

where characteristic growth time is equal to

$$\tau_e = \frac{1}{4\pi^2 f_0 (\Delta\nu_1{}^2 + \Delta\nu_2{}^2)(\frac{\delta J_e}{J_e})^2}. \qquad (4)$$

The growth time is different for different bunches, e.g. τ_e is smaller for the bunches which experience larger currents J_e and, therefore, tune shifts $\Delta\nu$. These bunches (named PACMAN bunches) are usually located near the gaps (see bunches 33, 53, 86, 106 in Fig.). Let us take for example bunch number 33 with $\Delta\nu = 0.01$ and $\Delta\nu_2 = 0.002$, then, requirement of

$$\tau_e > 10\ hrs$$

concludes in $\frac{\delta J_e}{J_e} < 0.53 \cdot 10^{-3}$. If one assumes constant distribution function of the ripple [2], then the value above corresponds to peak-to-peak current fluctuations of

$$\frac{\Delta J_e}{J_e} \approx 1.8 \cdot 10^{-3}. \qquad (5)$$

For non-PACMAN bunches (inside the batch) similar requirement

[2] for such distribution the rms value is $1/\sqrt{12}$ of the peak-to peak value

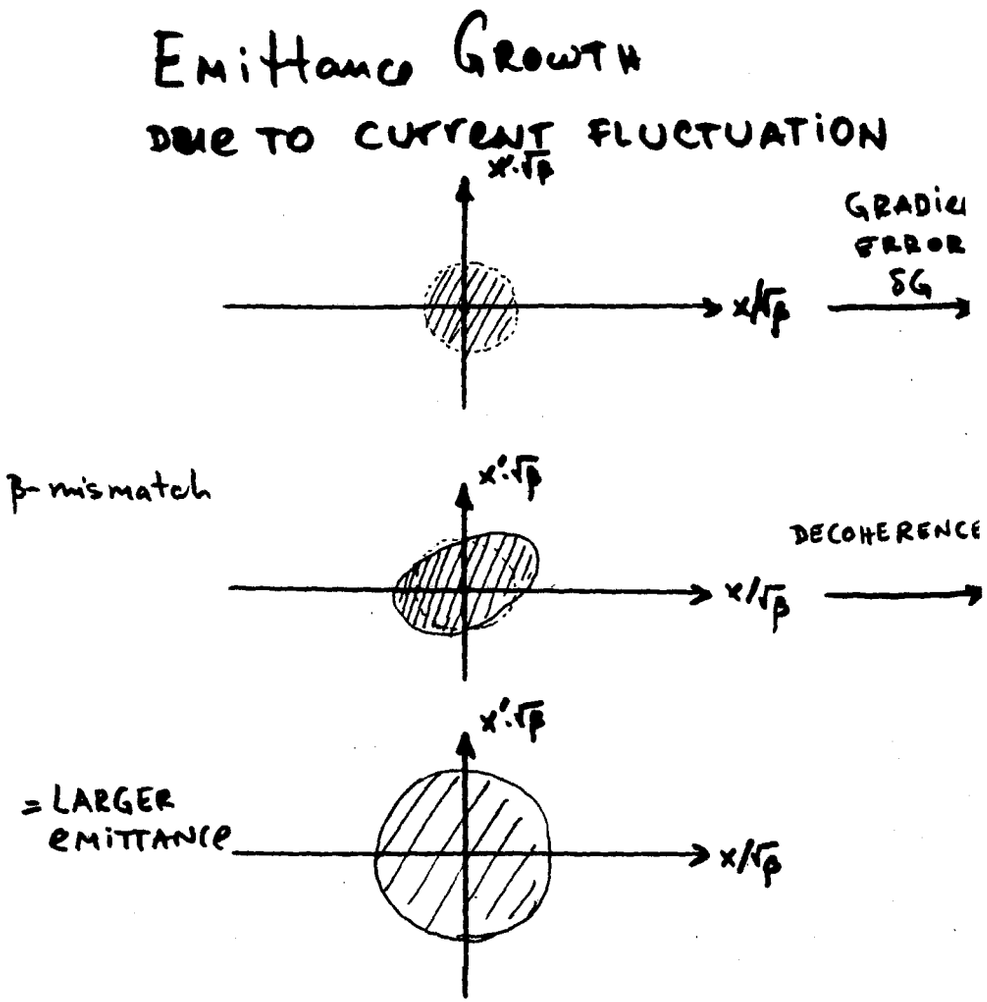

For the bunches in the middle of the bunch train, the requirement is about 0.24 μm.

The obtained values are several orders of magnitude ~~less~~ larger than vibrations of the Tevatron quadrupoles at high frequencies, e.g. accordingly to [6], rms amplitude of the Tevatron quadrupole magnet at frequency of 450 Hz is about 2 nm=0.002 μm, and the amplitude rapidly goes down with increase of frequency.

If the electron beam and the antiproton beam are not properly aligned with respect to each other and they collide off-center with displacement equal to ΔX, then the electron current ripple at betatron frequencies causes dipole kicks on antiprotons and can also lead to the transverse emittance growth. The tolerance can be easy estimated from Eq.(10) as:

$$\frac{\Delta J_e}{J_e}\Delta X \approx \delta X. \tag{11}$$

Making estimate for $\Delta X = 0.25\sigma_{\bar{p}} = 0.15$ mm, one gets the rms current ripple tolerance for the PACMAN bunches

$$\frac{\Delta J_e}{J_e} < 1.1 \cdot 10^{-3},$$

or about 0.37% peak-to-peak, and about $1.6 \cdot 10^{-3}$ (0.52 % peak-to-peak) for non-PACMAN bunches. These requirements are somewhat loose in comparison with the quadrupole kicks effect (see above in this Section), although depend on the straightness of the electron beam in the interaction region which is determined by the solenoid field quality.

is somewhat less stringent

$$\frac{\Delta J_e}{J_e} < 3.2 \cdot 10^{-3}.$$

Let us estimate the amplitude of the current fluctuations. A theory predicts that the rms Schottky noise of current J in a frequency band of Δf is equal to

$$\delta J^2 = 2 \cdot e \cdot J \cdot \Delta f,$$

thus

$$(\frac{\delta J}{J})_{Schottky} = \sqrt{\frac{2e\Delta f}{J}}. \quad (6)$$

Let's take $J \approx 2$A and $\Delta f \approx f_0 = 1/T_{Tevatron} = 47.7$ kHz, that yields:

$$(\frac{\delta J}{J})_{Schottky} \approx 10^{-7},$$

- it is much less than our requirements. Therefore, as we expect to have no valuable intrinsic source of the current noise, the current stability will require stable voltage U of the (modulated) power supply which controls the electron gun current[3]:

$$(\frac{\delta U}{U}) = \frac{2}{3}(\frac{\delta J}{J}) < 10^{-3}. \quad (7)$$

[3] taking into account Child's law $J = P \cdot U^{3/2}$

2 Transverse e-beam motion

Transverse motion of the electron beam may also cause direct antiproton emittance growth. Indeed, if the electron beam displacement is equal to δX, then the dipole kick experienced by antiprotons is $\delta\theta = \delta X/F$, where F is the focal length of the defocusing electron lens. Coherent $\bar{p}$ betatron oscillations occur and after some decoherence time they conclude in the antiproton emittance growth. The emittance grows *linearly* in time and its growth rate is equal to [4]:

$$\frac{d\varepsilon}{dt} = \frac{f_0^2}{4} \sum_{sources} \frac{\beta}{F^2} \sum_{n=-\infty}^{\infty} S_{\delta X}(f_0|\nu - n|). \quad (8)$$

Note, that now the frequencies of interest $f_0|\nu - n|$ starts from the betatron frequency of the Tevatron $\Delta\nu f_0 \approx 20$ kHz.

Using the same transformations as above, one gets for two electron lenses:

$$\frac{d\varepsilon}{dt} = 8\pi^2 f_0 \delta X^2 (\frac{\Delta\nu_1^2}{\beta_1} + \frac{\Delta\nu_2^2}{\beta_2}), \quad (9)$$

where δX now stands for the rms electron beam vibration amplitude.

Let us apply constrain on the emittance growth rate to be less than $\varepsilon/10$ hours, $\varepsilon = 3.3$ mm·mrad/$\gamma_{\bar{p}}$=$3.3 \cdot 10^{-9}$m. Then, for the PACMAN bunches we get requirement on the rms electron beam turn-to-turn position stability

$$\delta X \leq 0.16\,\mu m. \quad (10)$$

3 Solenoid Field Quality

Strong solenoid magnetic field B of the "electron lens" – of the order of several Tesla – concludes that the electrons perform very small but fast transverse oscillations (Larmour motion) around the magnetic field lines. Therefore, deviation of $\vec{B}$ from a straight line will cause off-center collisions of the pbar and electron beams. In the regime of "electron compressor" [1] - essentially non-linear electron lens - that may cause uncontrolled non-linear components of the forces. To avoid the effect, one needs the field lines not to deviate from (straight) pbar orbit more than some part of the transverse pbar beam size $\sigma_{\bar{p}}$. The rms pbar size depends on the beta-function value at the electron beam section, which is typically of the order of $\beta = 100$ m, that yields $\sigma_{\bar{p}} \approx 0.8$ mm. If one requires the solenoid field straightness of about 25%, than it is equivalent to $\Delta X = 0.2$ mm, or the transverse field component of the order of

$$\frac{\Delta B_\perp}{B} \sim \frac{\Delta X}{L} \sim \frac{0.2mm}{2m} = 10^{-4}.$$

This is comparable with the field quality in numerous electron cooling devices.

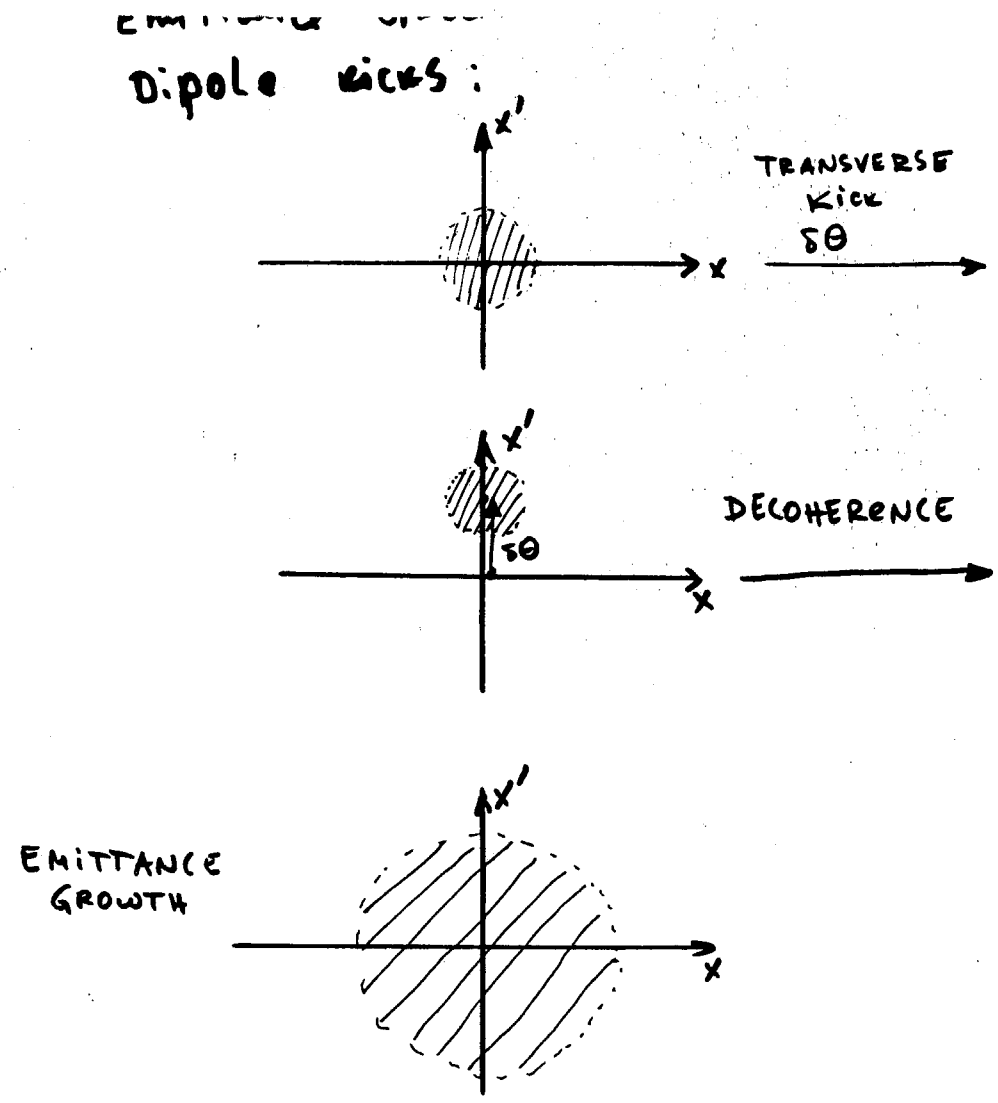

3 Solenoid Field Quality

Strong solenoid magnetic field B of the "electron lens" – of the order of several Tesla – concludes that the electrons perform very small but fast transverse oscillations (Larmour motion) around the magnetic field lines. Therefore, deviation of $\vec{B}$ from a straight line will cause off-center collisions of the pbar and electron beams. In the regime of "electron compressor" [1] - essentially non-linear electron lens - that may cause uncontrolled non-linear components of the forces. To avoid the effect, one needs the field lines not to deviate from (straight) pbar orbit more than some part of the transverse pbar beam size $\sigma_{\bar{p}}$. The rms pbar size depends on the beta-function value at the electron beam section, which is typically of the order of $\beta = 100$ m, that yields $\sigma_{\bar{p}} \approx 0.8$ mm. If one requires the solenoid field straightness of about 25%, than it is equivalent to $\Delta X = 0.2$ mm, or the transverse field component of the order of

$$\frac{\Delta B_\perp}{B} \sim \frac{\Delta X}{L} \sim \frac{0.2mm}{2m} = 10^{-4}.$$

This is comparable with the field quality in numerous electron cooling devices.

4 Electron current modulation

Now we consider the time structure of the quadrupole kick produced by electron beam. The operation of the electron lens look very similar to a traveling wave kicker [5].

Now we consider the time structure of the defocusing kick (or the tune shift) produced by the traveling wave kicker. Fig.1 demonstrates the effect of a step-like current modulation with the pulse duration of t_p (presented at the upper plot) on the antiproton bunches. Let us denote $t = 0$ the moment when the front of the electron pulse enters the interaction section. As the antiproton beam passes through the oncoming electron current pulse, the maximum deflection will be seen by test particles which at $t = 0$ are distanced by $2(1+\beta_e)l/\beta_e$ from the input end of the device. We will call the corresponding time value of $\tau_g = 2(1+\beta_e)l/c\beta_e$ as "kick growth time". The maximum kick lasts over time interval of $t_f = t_p - \tau_g$ which is supposed to be synchronized with the bunch arrival (see lower diagram in Fig.1). Behind that bunch, the kick amplitude vanishes over the growth time. Analytical expression for the tune shift is as follows:

$$\Delta\nu(t) \propto \frac{1}{2}\int_{t_s}^{t} J(t')dt', \quad t_s = -t+2\max(0, t-(1+\beta_e)l/c\beta_e). \quad (12)$$

Let the required flat top of the pbar kick be about t_f =5 ns, and the required "no-impact time" to be the same $t_n = 5$ ns; then, summarizing all times in Fig.1, the condition of $264\,ns > t_f + 2L(1+\beta_e)/c\beta_e + t_n$ must be satisfied in order to have no impact on preceding and following bunches. That gives $\beta_e > 0.08$ or kinetic energy of the electrons $U > 1.6$kV. I.e., if one needs to modulate the elec-

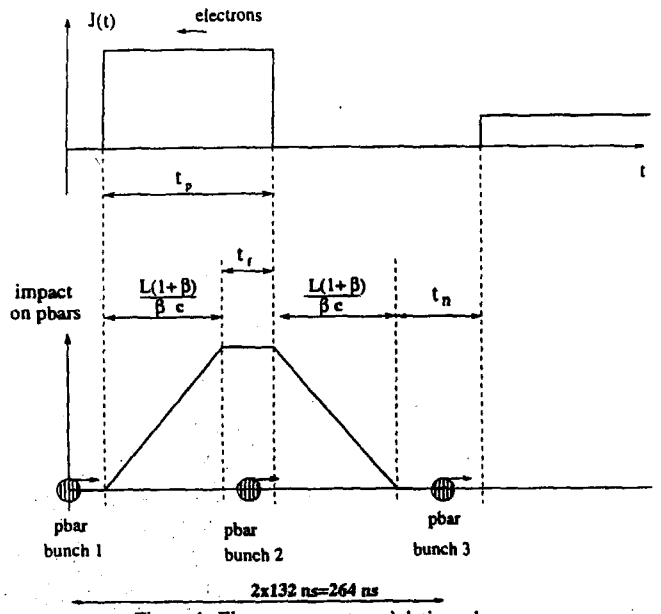

Figure 1: Electron current modulation scheme.

tron current in order to equalize the bunch-by-bunch tune shift, then the electrons have to be fast enough to provide different quadrupole kicks on different bunches. We choose β_e of the order of 0.2 that is far beyond the requirement.

One can make two remarks: firstly, if the current pulse duration is less than the growth time $t_p < \tau_g = 2(1+\beta_e)l/c\beta_e$, then the electron beam does not work in full strength; secondly, if the bunch spacing in the ring is equal to τ, then the electron current pulse duration must be less than $t_p < 2\tau - 2(1+\beta_e)l/c\beta_e$ otherwise neighbor bunches

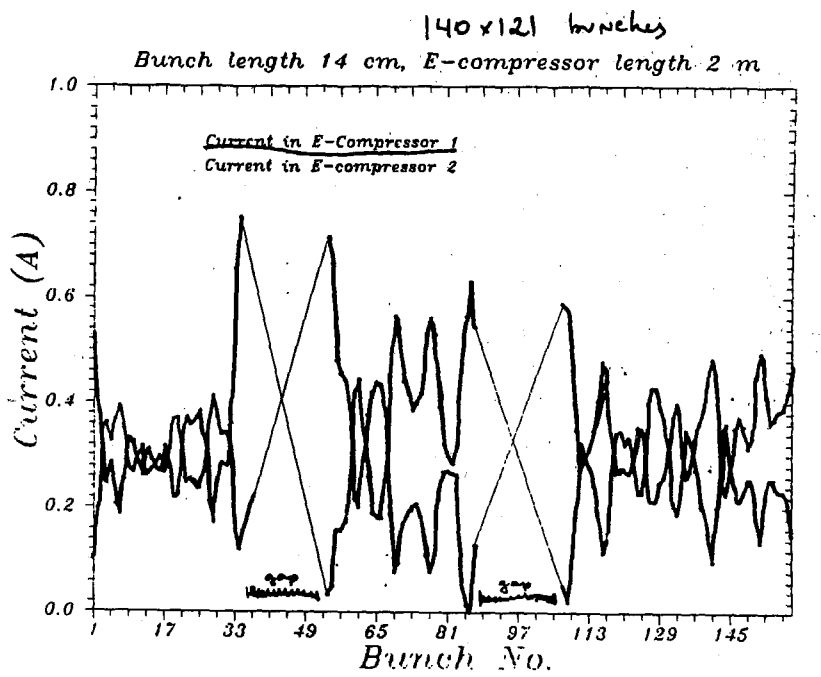

Figure 121

will be defocused too. As the result, one can conclude, that the rectangular pulse duration of $t_p = \tau_g$ corresponds to the maximum device's strength. The length of the electron beam has to be less than $L < c\beta_e\tau/2(1+\beta_e)$ because the current pulse shape can not be exactly rectangular, besides that, as we mentioned above, some flat top of the kick is required.

Making numerical example for the TEV33 with $\tau = 132$ ns and $\beta_e = 0.2$, we choose $L = 2$ m (that satisfies condition of $\tau_g = 2(1+\beta_e)L/c\beta_e = 80$ ns $< \tau$) and the requirements on the pulse length is $t_p \leq 264 - 80 = 184$ ns. In fact, as the pulse shape of the current modulation can not be exactly rectangular, than the one should require the pulse FWHA to be somewhat smaller (but still longer than τ_g), e.g. 100-120 ns.

References

[1] V.Shiltsev and D.Finley, "Electron Compression of the Beam-Beam Footprint in the Tevatron", FNAL-TM-2008 (1997).

[2] V.Shiltsev, "Electron Lens to Compensate Bunch-to-Bunch Tune Spread in TEV33", FNAL-TM-2031 (1997).

[3] G.V.Stupakov, "Emittance Growth Caused by Sextupole Vibrations in the SSC", SSCL-575 (1992).

[4] V.Lebedev, *et.al*, "Emittance Growth Due to Noise and Its Suppression with the Feedback System in Large Hadron Colliders", *Particle Accelerators*, vol.44 (1994), p.147.

[5] B.I.Grishanov, *et.al*, "Very Fast Kicker with High Repetition Rate for Accelerator Applications", *NIM A396* (1997), p.28.

[6] B.Baklakov, *et.al*, "Seismic Studies For Fermilab Future Collider Projects", FERMILAB-Conf-97/383 (1997).

Q's!

Bagley: How strong should be stray field to excite the e-beam motion of dX=0.16 micron?

Shiltsev: dB/B is about dX/L. If L=2m and B=3 T, then dB=3 mG or E=1V/cm. Again, this is at frequencies of 10-50 kHz. In the set-up, we must take care of such fields.

Meshkov: You may use a feedback for e-beam stabilization.

Danilov: Also, wake fields (e.g. resistive wall) from intensive proton beam can be of importance, although protons are separated from the pbar and electron beams.

Meshkov: To prevent "twinkle" effect due to the cathode spots, the gun must work in space charge limited regime.

M. Liege

Electron Beam Distortions due to Interaction with Antiprotons

Alexandre Zinchenko
Joint Institute for Nuclear Research, Dubna, Russia

Mini-Workshop on Beam-Beam Compensation
Fermilab
February 12-13, 1998 (Friday, 13th)

---

1) ZBEAM - a charge tracing code.

The motion of charges in the laboratory frame in some external electric and magnetic fields and in the presence of some additional moving electric charges can be described by the equation

$$m\frac{d^2\vec{r}}{dt^2} = q(\vec{E} + [\vec{v} \times \vec{B}] + \sum_{i=1}^{n} \vec{E}_i + \sum_{i=1}^{n}[\vec{v} \times \vec{B}_i]).$$

there m, q and $\vec{v}$ are the particle mass, electric charge and velocity, $\vec{E}$ and $\vec{B}$ are external electric and magnetic fields, $\vec{E}_i$ and $\vec{B}_i$ are the electric and magnetic fields of a bunch "macroparticle":

$$\vec{E}_i = \frac{q_i(Z)\vec{r}}{2\pi\epsilon_0 r^2}, \qquad \vec{B}_i = \frac{1}{c^2}[\vec{v} \times \vec{E}_i].$$

Tracking of a particle is achieved by integrating the equation of motion over successive small time steps.

2) Parameters of Tevatron:
Antiproton bunch: σ_r = 0.9 mm, σ_z = 30 cm, $N_{beam} = 6 \cdot 10^{10}$
Electron beam: r = 0.9 mm, E = 10 keV, I = 1.5 A

3) No external magnetic field.

4) External magnetic field.

5) Elliptic bunch: σ_x = 0.61 mm, σ_y = 0.31 mm.

Comment:

Zinchenko: I'd like also to attract your attention, that in our SSC compensation proposal, we considered two solenoids anticollinear fields – it gave us automatic coupling compensation.

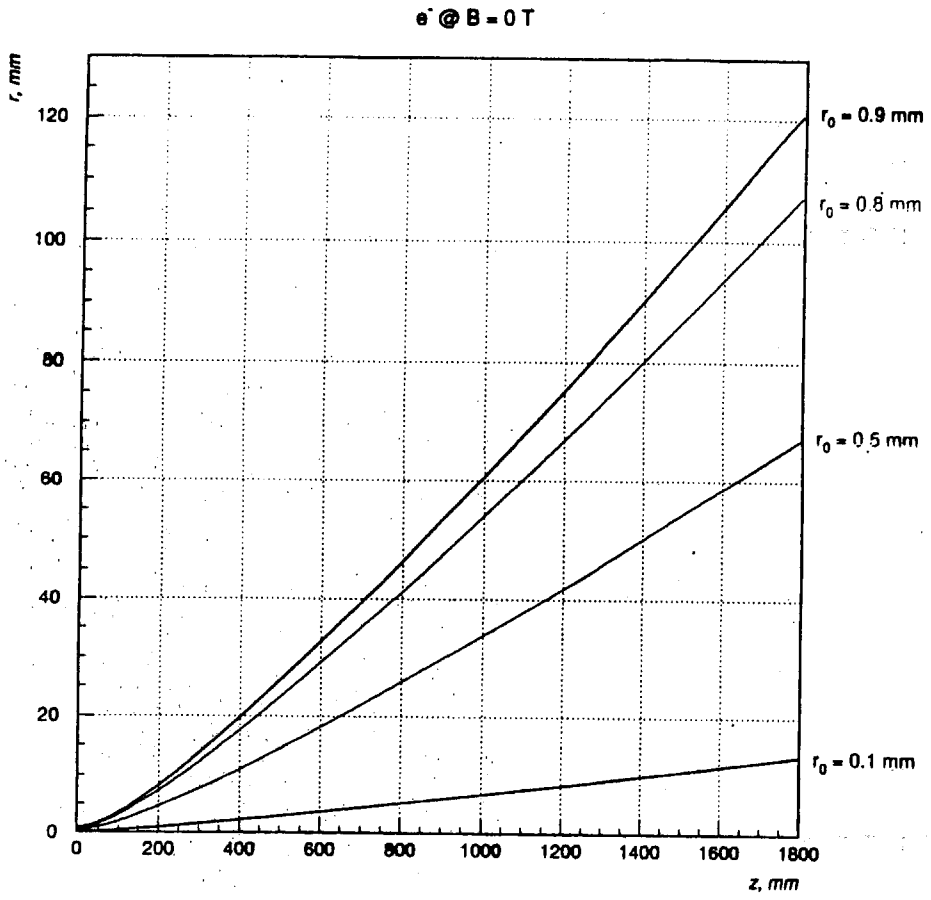
e⁻ @ B = 0 T
r, mm
z, mm
r0 = 0.9 mm
r0 = 0.8 mm
r0 = 0.5 mm
r0 = 0.1 mm
0
20
40
60
80
100
120
0
200
400
600
800
1000
1200
1400
1600
1800

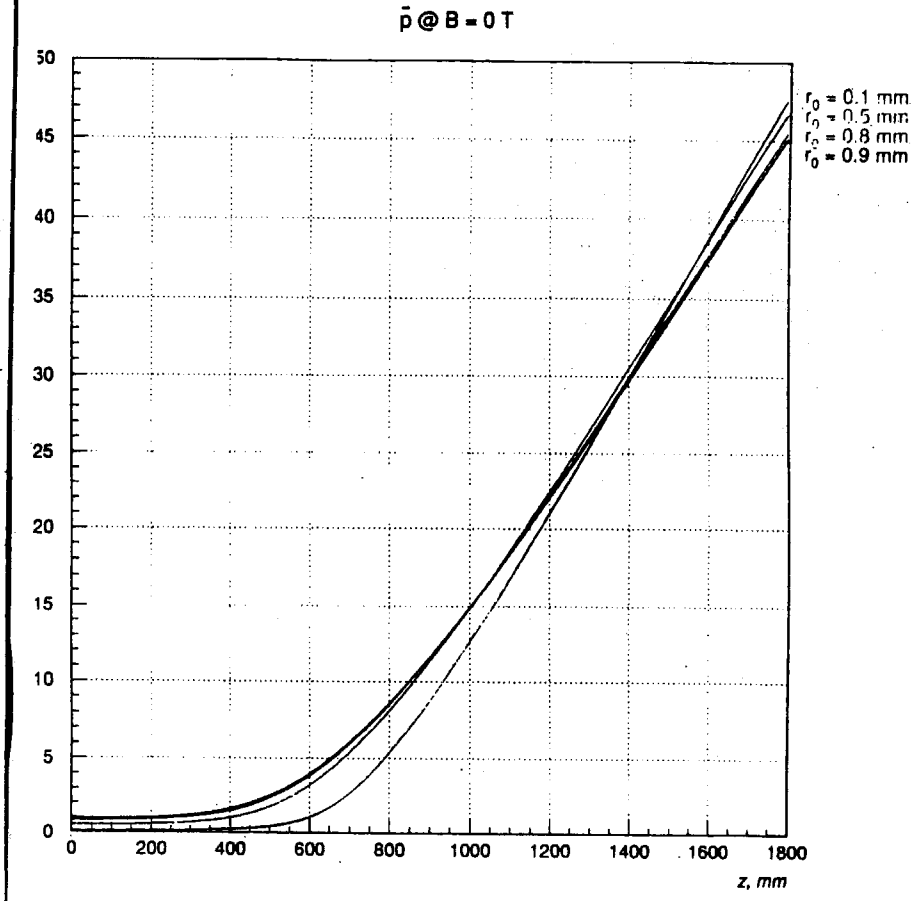
p̄ @ B = 0 T
z, mm
r0 = 0.1 mm
r0 = 0.5 mm
r0 = 0.8 mm
r0 = 0.9 mm
0
5
10
15
20
25
30
35
40
45
50
0
200
400
600
800
1000
1200
1400
1600
1800

$e + \bar{p}$

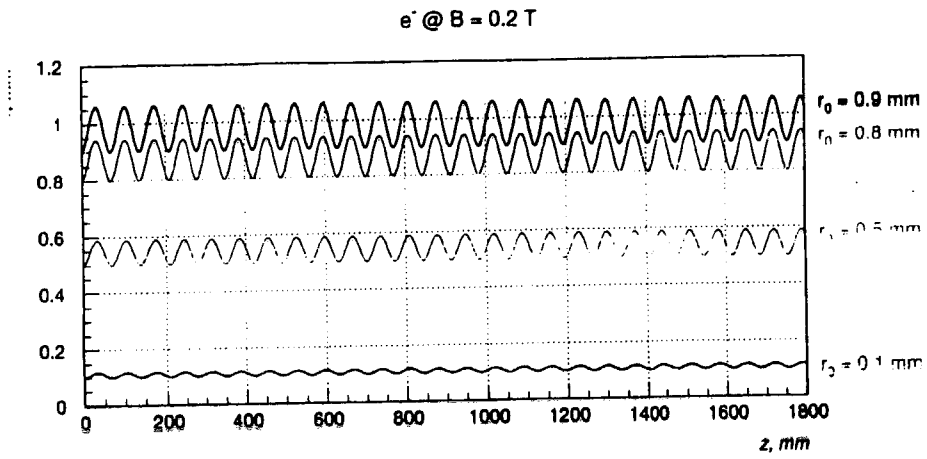
e⁻ @ B = 0.2 T
r0 = 0.9 mm
r0 = 0.8 mm
r0 = 0.5 mm
r0 = 0.1 mm
z, mm

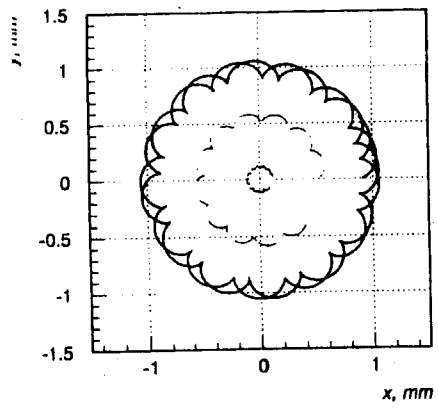
x, mm

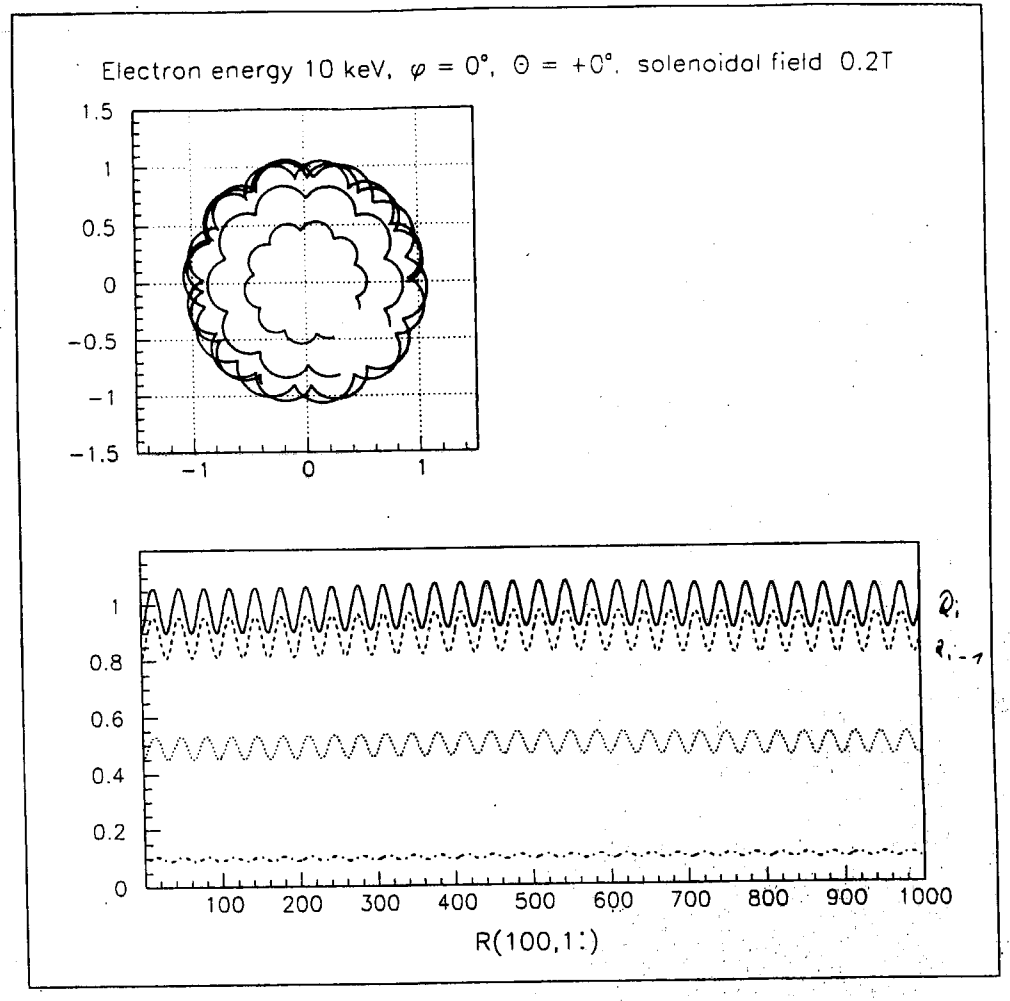
Electron energy 10 keV, φ = 0°, Θ = +0°, solenoidal field 0.2T
R(100,1:)

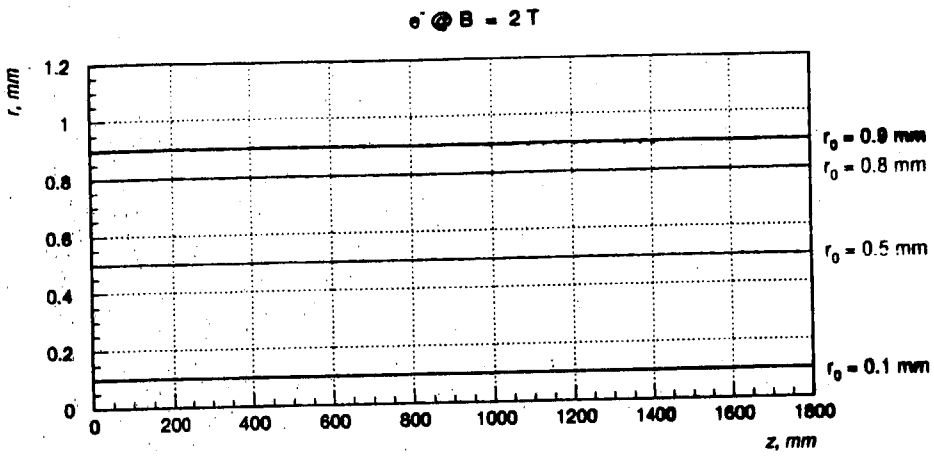
e⁻ @ B = 2 T
r, mm
z, mm
r0 = 0.9 mm
r0 = 0.8 mm
r0 = 0.5 mm
r0 = 0.1 mm

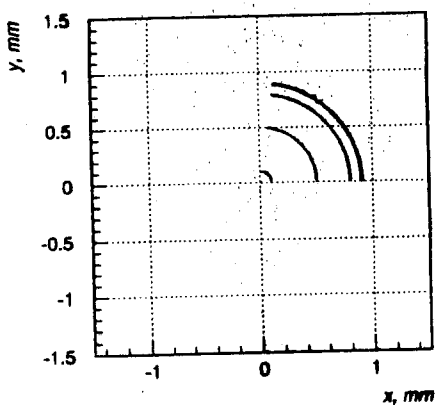
y, mm
x, mm

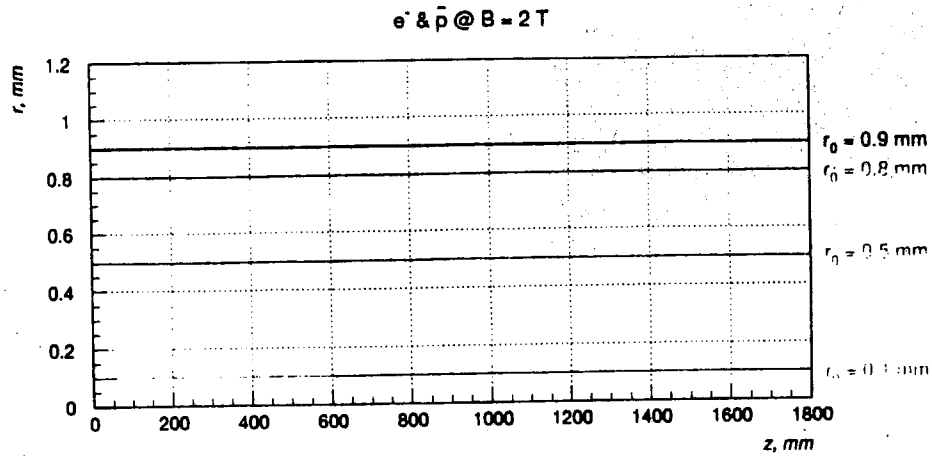
e⁻ & p̄ @ B = 2 T
r, mm
z, mm
r0 = 0.9 mm
r0 = 0.8 mm
r0 = 0.5 mm

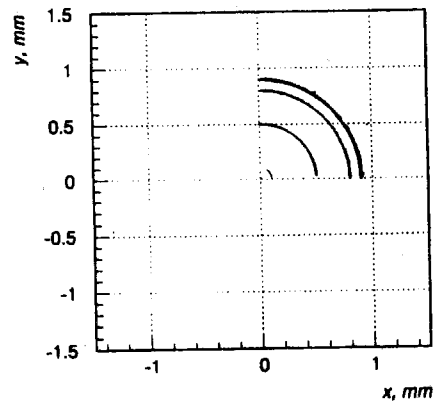
y, mm
x, mm

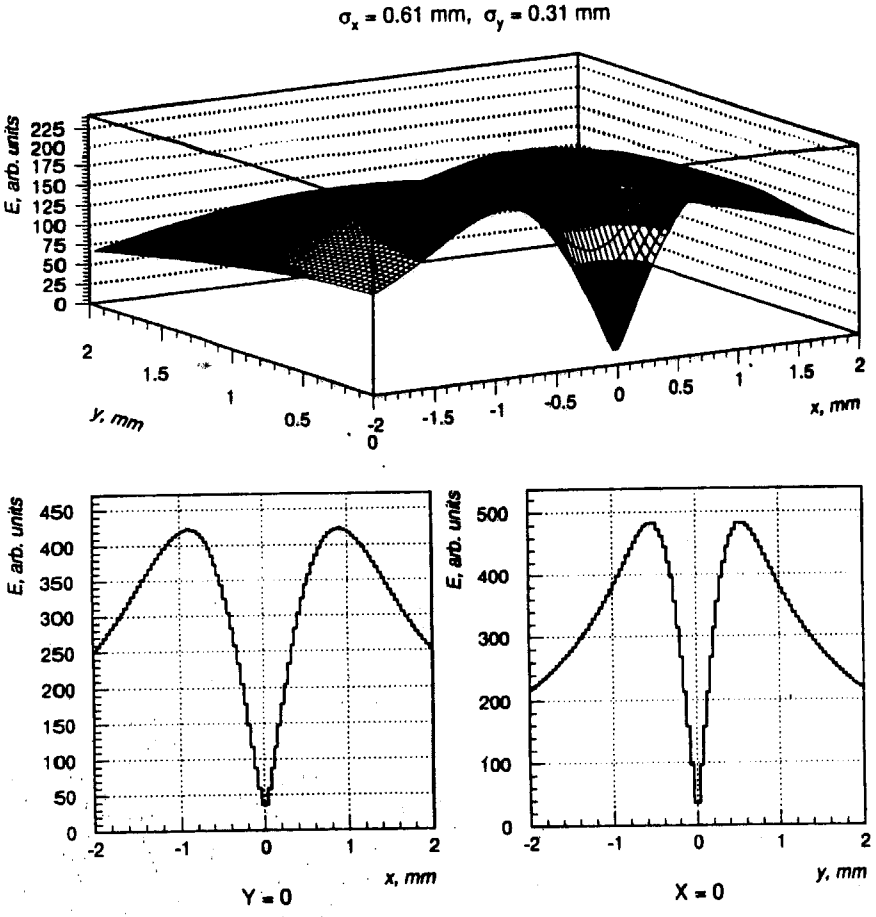
σx = 0.61 mm, σy = 0.31 mm
E, arb. units
y, mm
x, mm
Y = 0
X = 0

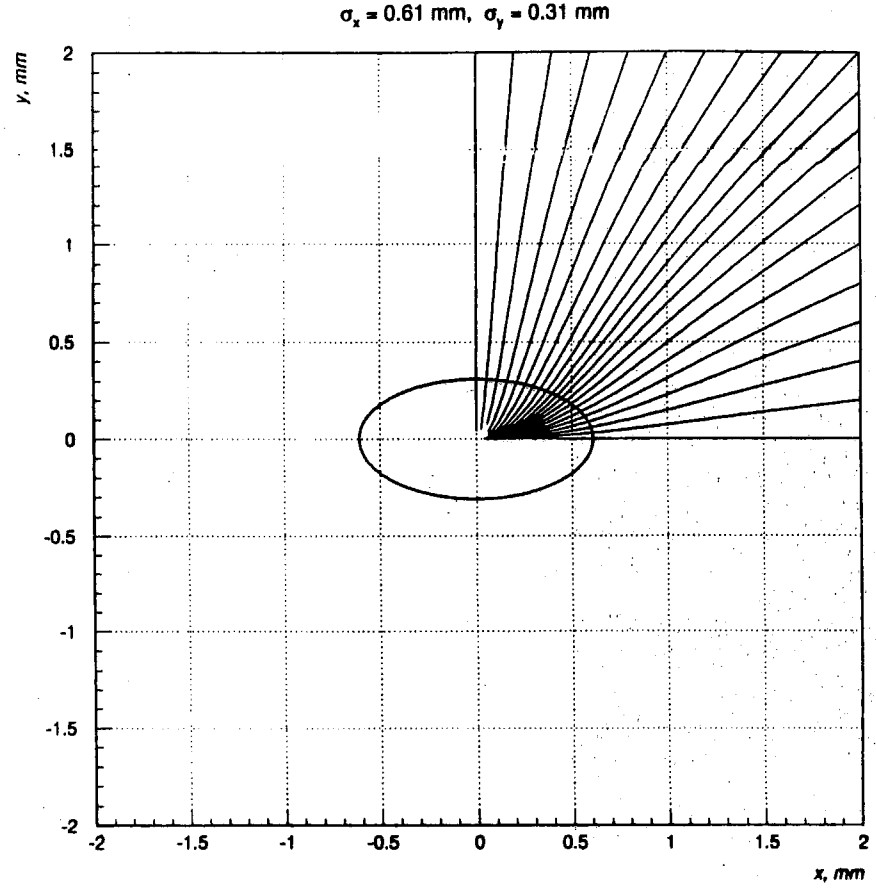
σx = 0.61 mm, σy = 0.31 mm
y, mm
x, mm

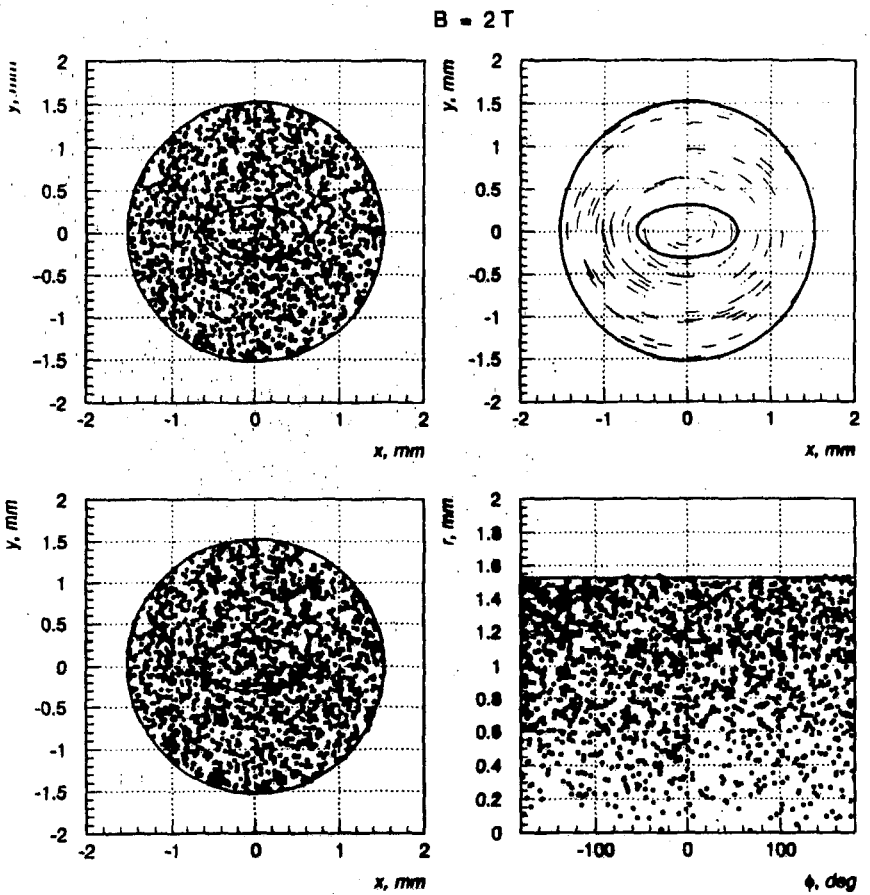
B = 2T
y, mm
x, mm
r, mm
ϕ, deg

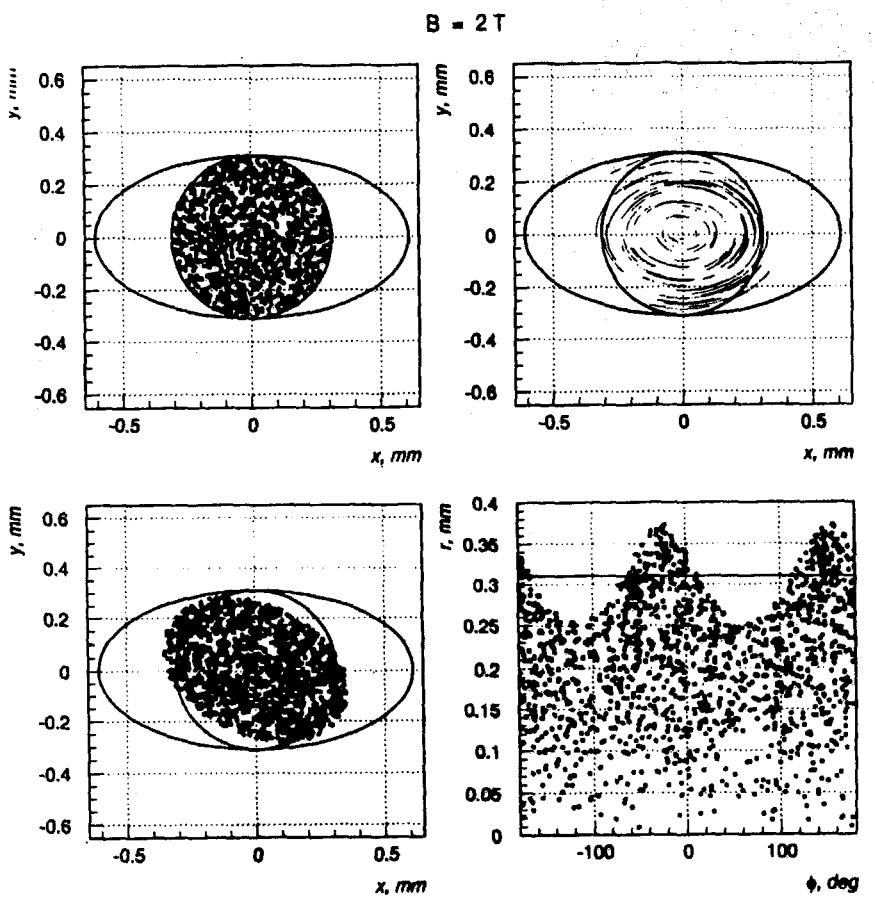
B = 2T
y, mm
x, mm
r, mm
ϕ, deg

Beam-Beam Compensation Workshop
Fermilab, Feb. 12-13, 1998

Vladimir SHILTSEV

Simple Model of Electron Beam Distortion due to Pbar Space Charge

Content:

1. Model and assumptions
2. Basic formulas and estimates
3. Numerical simulations

charge density distribution function for electrons

$$\rho_e = \rho_e(x, y, z, t)$$

Continuity equation:

$$\frac{\partial \rho}{\partial t} + \mathrm{div}(\vec{v}\rho) = 0$$

Equation of motion:

$$m_e \frac{d\vec{v}}{dt} = e\vec{E} + e\frac{\vec{v}}{c} \times \vec{B}$$

fields $\vec{E}$ - space charge [self + $\bar{p}$]

$\vec{B} = \vec{H} + \vec{B}_0$ - space current [self + $\bar{p}$] + solenoid field

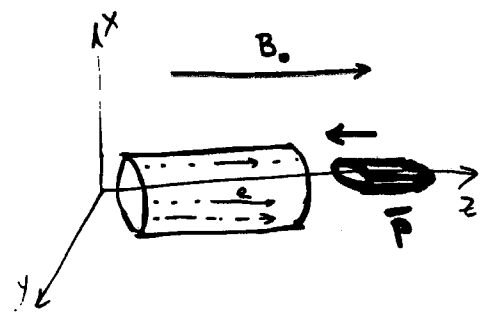

$$\begin{pmatrix} \vec{E} \\ \vec{H} \end{pmatrix} = \begin{pmatrix} E_x & E_y & 0 \\ H_x & H_y & 0 \end{pmatrix}$$

$$\vec{B}_0 = (0, 0, B)$$

The problem and assumptions:

1. electron beam is initially round $\rho(t=0)=\rho_0(r)$, $r^2=x^2+y^2$
2. $\bar{p}$-beam is elliptical $\rho_{\bar{p}}=\rho(x,y)\cdot f(t)$
3. they collide "head-on"
4. electron beam distribution slightly changes

$$\rho_e=\rho_0(r)+\delta\rho(x,y)\ ,\ \delta\rho \ll \rho_0$$

5. neglect Larmour motion of electrons
   1) it's fast —
   2) does not change ρ_0-symmetry —
   3) it's small — Zynchenko

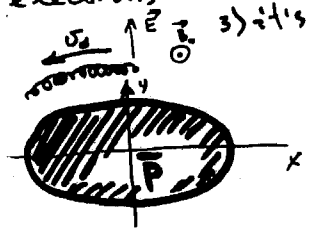

drift motion only $\vec{v}_d = c\,\dfrac{\vec{E}\times\vec{B}_0}{B_0^2}$

$$\frac{\partial\rho}{\partial t}+\mathrm{div}(\rho\vec{v}_d)=\frac{\partial\rho}{\partial t}+\vec{v}_d\cdot\vec{\nabla}\rho_0+\rho\cdot\underbrace{\mathrm{div}\,\vec{v}_d}_{=0}=0$$

$$\mathrm{div}\,\vec{v}_d=\frac{\partial v_x}{\partial x}+\frac{\partial v_y}{\partial y}=\left(\frac{\partial E_x}{\partial y}-\frac{\partial E_y}{\partial x}\right)\cdot\frac{c}{B}=c\,\frac{(\mathrm{rot}\,\vec{E})_z}{B}=0$$

$$(\mathrm{rot}\,\vec{E})_z=-\frac{1}{c}\frac{\partial H_z}{\partial t}=0$$

$$\vec{\nabla}\rho_0=\frac{\vec{r}}{r}\cdot\frac{d\rho_0(r)}{dr}=2\vec{r}\cdot\frac{d\rho_0(r^2)}{d(r^2)}$$

$$\vec{E}=e\cdot\frac{dN_{\bar{p}}}{dz}\cdot\left(-\vec{\nabla}\mathcal{U}\right)\ ,\ \text{potential } \mathcal{U}$$ ← Montague '79, Augustin '16

$$\mathcal{U}(x,y)=\int_0^\infty dq\,\frac{1-e^{-\frac{x^2}{2\sigma_x^2(1+qR)}-\frac{y^2}{2\sigma_y^2(1+q/R)}}}{\sqrt{(1+qR)(1+q/R)}}\ ,\ q=\frac{\sigma_y}{\sigma_x}$$

Now, scalar product $P=\vec{v}_d\cdot\vec{\nabla}\rho=c\,\dfrac{\vec{E}\times\vec{B}_0}{B^2}\cdot\vec{\nabla}\rho=\dfrac{2c}{B^2}\dfrac{d\rho}{d(r^2)}\cdot[\vec{E}\times\vec{B}]$

$$P=\frac{(1+\beta)\cdot c\cdot 2e}{B}\cdot\frac{dN_{\bar{p}}}{dz}\cdot\frac{d\rho_0}{d(r^2)}\cdot\frac{xy(\sigma_y^2-\sigma_x^2)}{\sigma_x^2\sigma_y^2}\cdot\underbrace{\int_0^\infty dq\,\frac{e^{-\frac{x^2}{2\sigma_x^2(1+qR)}-\frac{y^2}{2\sigma_y^2(1+q/R)}}}{(1+qR)^{3/2}(1+q/R)^{3/2}}}_{I(x,y)}$$

Thus, one gets

$$\frac{\partial\rho}{\partial t}+P=\frac{d\rho}{dz}\cdot c(1+\beta)+P=0\ ,\ \text{or}$$

$$\delta\rho_e\left(x,y,t=\frac{z}{(1+\beta)c}\right)=\frac{2e}{B}\cdot\int_{-\infty}^{z}dN_{\bar{p}}\cdot\frac{d\rho_0(r^2)}{d(r^2)}\cdot\underbrace{\frac{xy\cdot I(x,y)\cdot(\sigma_x^2-\sigma_y^2)}{\sigma_x^2\sigma_y^2}}$$

Estimation: $\sim N_{\bar{p}}$ $\quad \sim \rho_0/a_e^2 \simeq \dfrac{\rho_0}{\sigma_x^2}$ $\quad \sim I_{max}\simeq 0.4$

Therefore $\dfrac{\delta\rho_e}{\rho_0}\sim\dfrac{eN_{\bar{p}}}{Ba_e^2}\simeq\dfrac{3}{B[\mathrm{kG}]}\to 5\%$ if $B=60\,\mathrm{kG}$, $N_{\bar{p}}=6\cdot10^{10}$, $a_e=1\,\mathrm{mm}$

NUMerical simul. → $\dfrac{0.5}{B[\mathrm{kG}]}\sim 1\%$ if

Non-disturbed e-beam charge ditribution

$$\rho_0(r) = \frac{1}{1+\left(\frac{r}{r_0}\right)^{2\mu}}, \quad \mu = 3$$

$r_0 = \sigma_x$ of $\bar{p}$

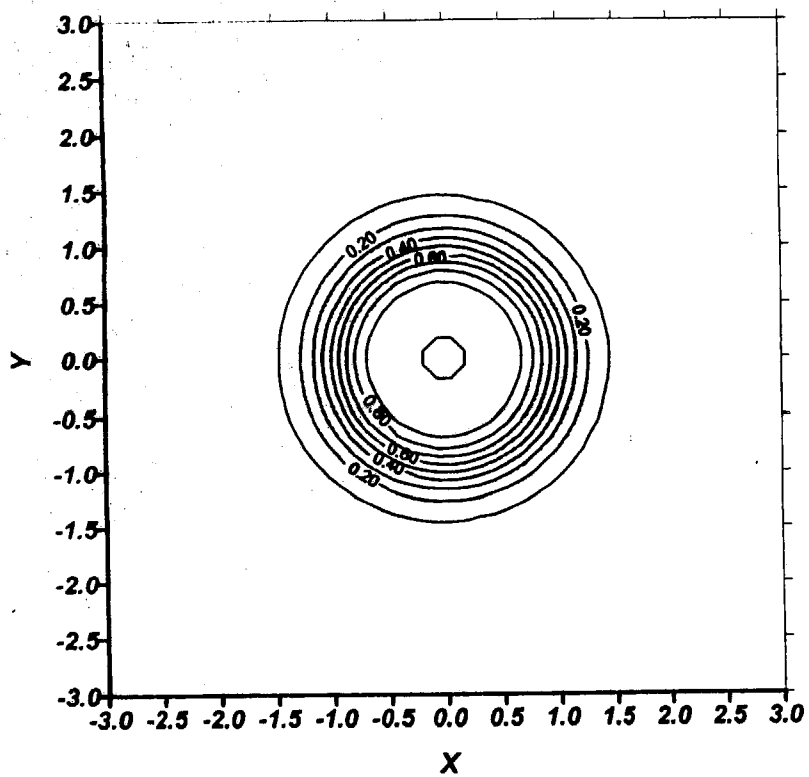

Charge density in pbar beam with aspect ratio = 2

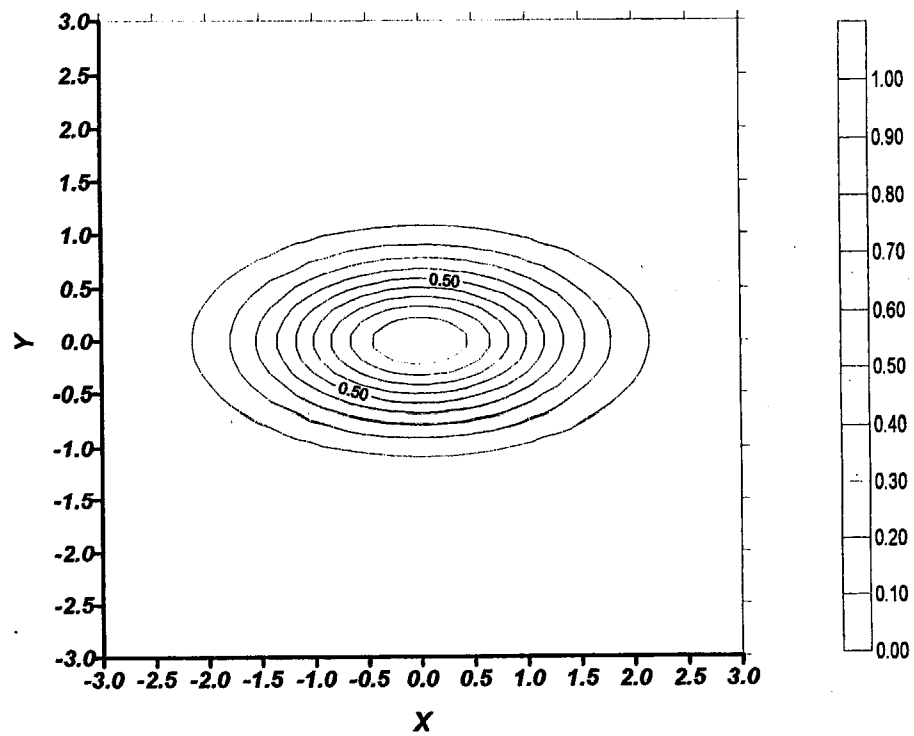

Distortion of electron beam current distribution due to elliptical pbar beam

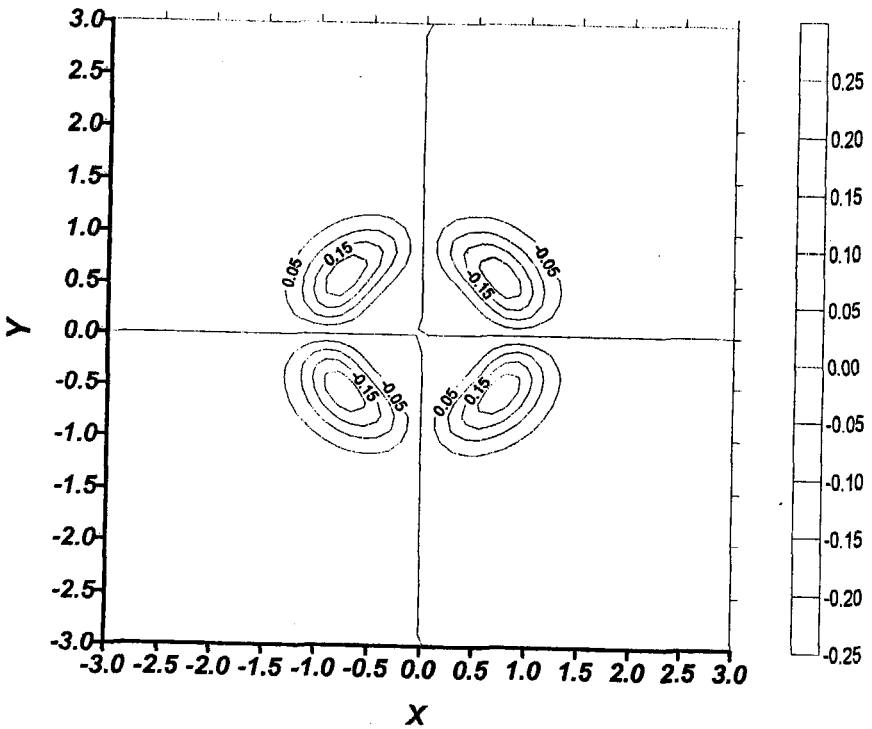

Electron beam charge distribution after passage of elliptical pbar beam

pbar aspect ratio(sigmaX/sigmaY)=2, Npbar=6e+10, solenoid field B=4 k

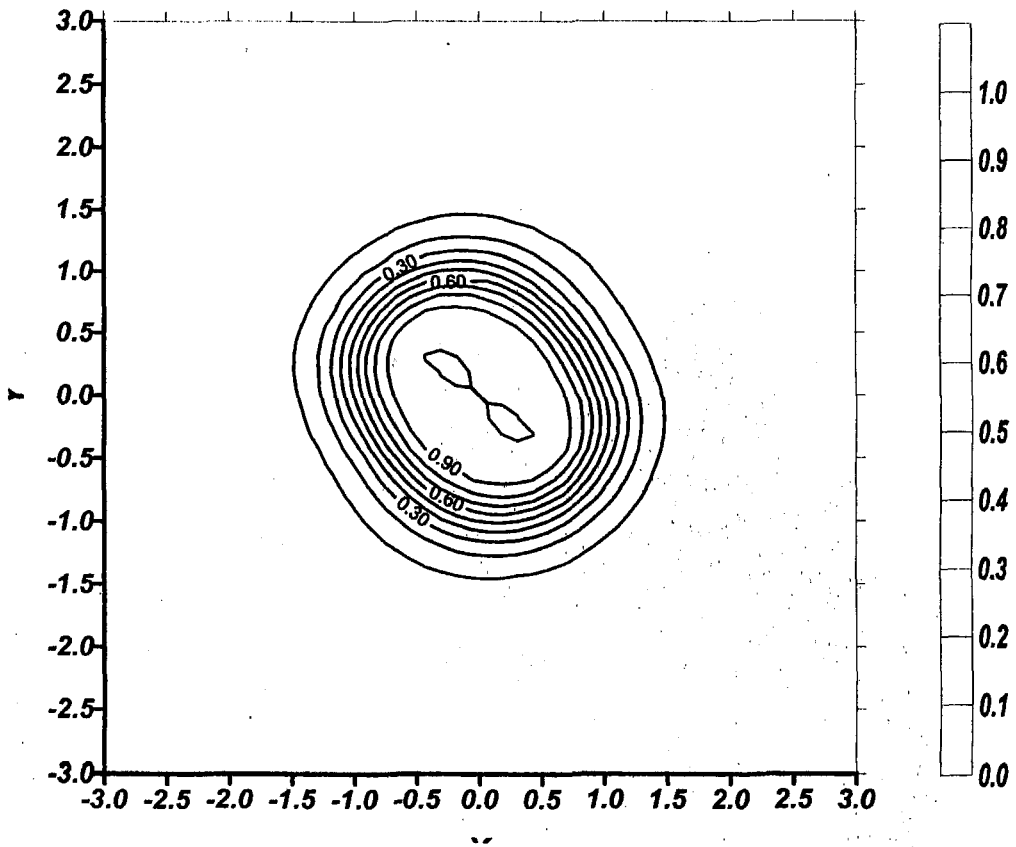

Dependence of skew distortion of electron charge distribution along Gaussion pbar bunch

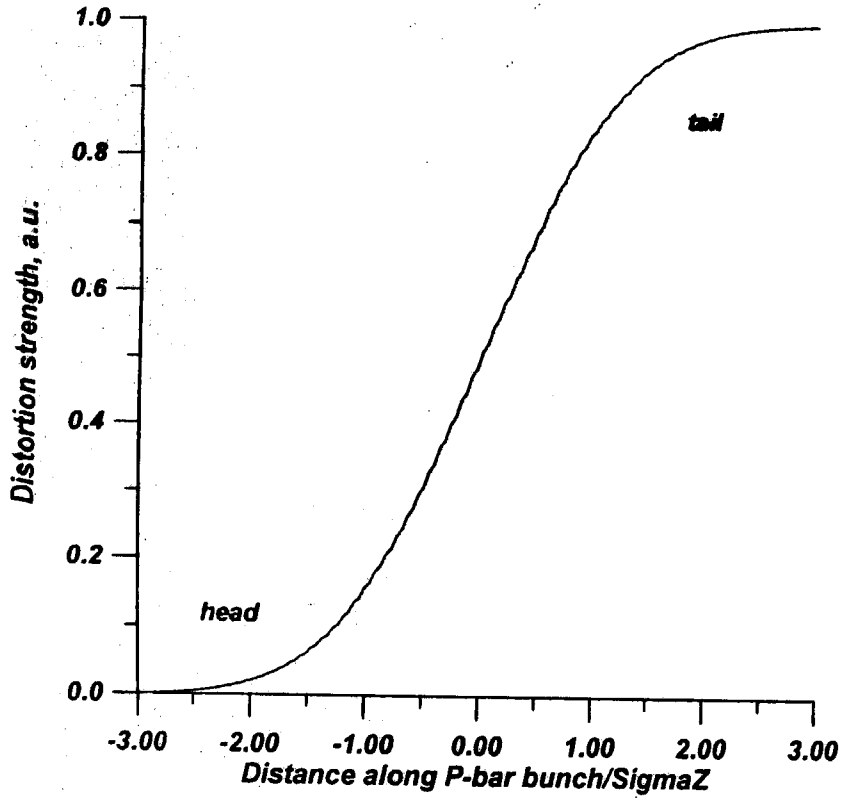

Consequences of the Distortion:

nothing – for head – $\delta\rho = 0$

skew fields in the tail $\delta\rho = x y \cdot C(x,y)$.

$$\Delta U = \frac{1}{r}\frac{\partial}{\partial r}\left(r\frac{\partial}{\partial r}U\right) + \frac{1}{r^2}\frac{\partial^2 U}{\partial \theta^2} = -4\pi C \cdot x \cdot y = -2\pi C \cdot r^2 \cdot \sin(2\theta)$$

$x = r \cdot \cos\theta$

$y = r \cdot \sin\theta$

$$U_{skew} = \frac{\pi}{6} \cdot C \cdot r^2 \cdot x \cdot y \longrightarrow \frac{\partial^2 U}{\partial x \partial y} = \frac{\pi}{2} \cdot C \cdot r^2$$

Coupling shift:

$$\varkappa = \frac{\sqrt{\beta_x \beta_y}\, e^{i(\psi_x - \psi_y)}}{4\pi} \left\langle \frac{\partial^2 U}{\partial x \partial y} \right\rangle = \frac{\sqrt{\beta_x \beta_y}\, e^{i(\psi_x - \psi_y)}}{8} \cdot C$$

For estimates: take into account

$$\Delta\nu = \frac{\beta}{4\pi} \left\langle \frac{\partial^2 U_0}{\partial r^2} \right\rangle$$

$$U_{skew} \sim U_0 \cdot \frac{0.5\, N_{\bar{p}}/10^{10}}{B[kG]}$$

$$\beta_x \sim \beta_y \sim \beta$$

see Fig.

$$\varkappa \approx \Delta\nu \cdot \frac{0.5\left[10^{-10} \cdot N_{\bar{p}}\right]}{B[kG]} \cdot \langle S(x,y) \rangle$$

averaged over betatron motion

$$\varkappa \sim 10^{-2} \cdot \frac{3}{60} \cdot 0.5 \simeq 2 \cdot 10^{-4}$$

Skew coefficient S(x,y) due to distorted electron charge distribution

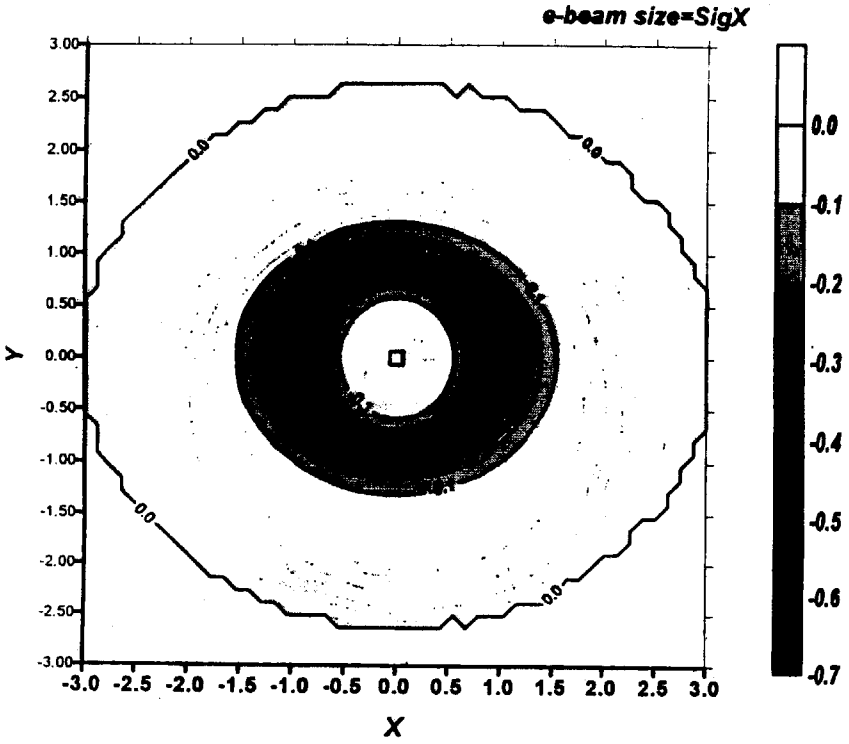

Non-disturbed e-beam charge ditribution

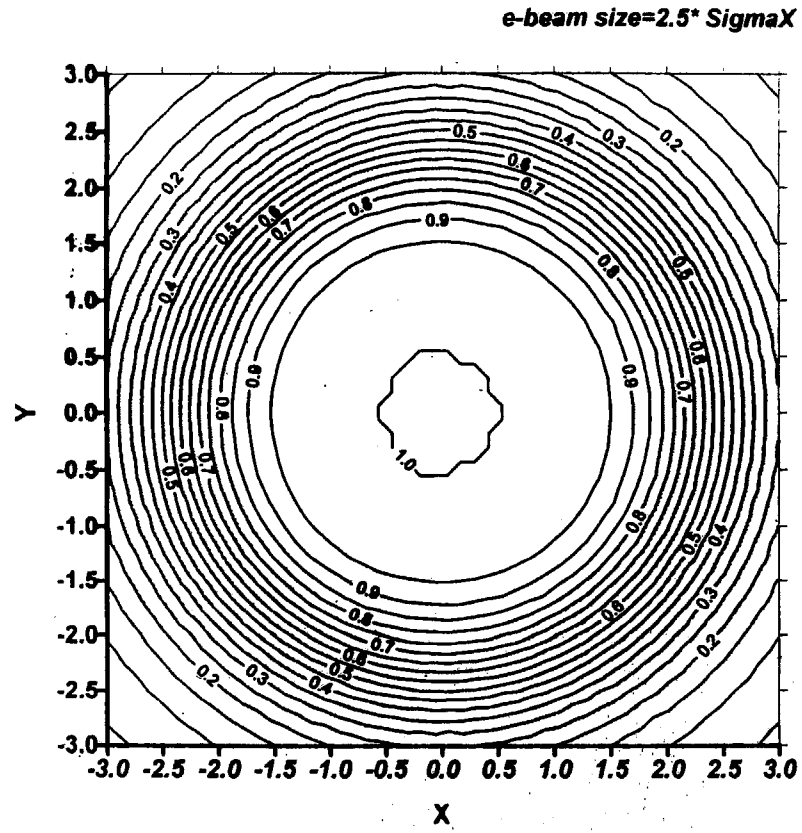

Coupling shift~$\overline{S(x,y)}$*0.5*Npbar[1e10]/B[kG]*dTune

Distortion of electron beam current distribution due to elliptical pbar beam

e-beam size=2.5*SigmaX

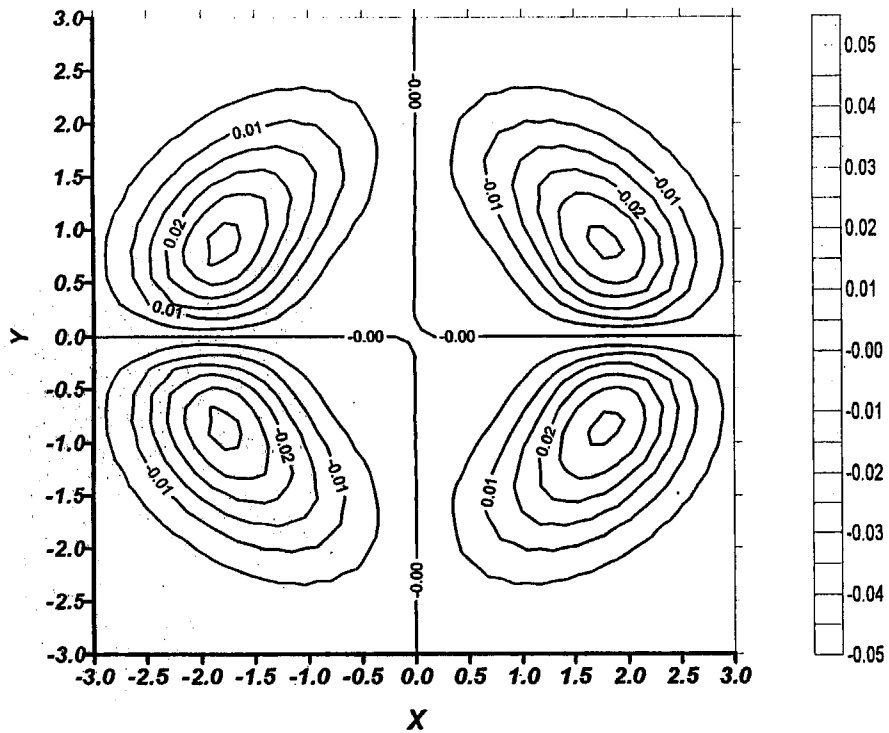

Electron beam charge distribution after passage of elliptical pbar beam

pbar aspect ratio(sigmaX/sigmaY)=2, Npbar=6e+10, solenoid field B=40 kG

e-beam size=2.5*SigmaX

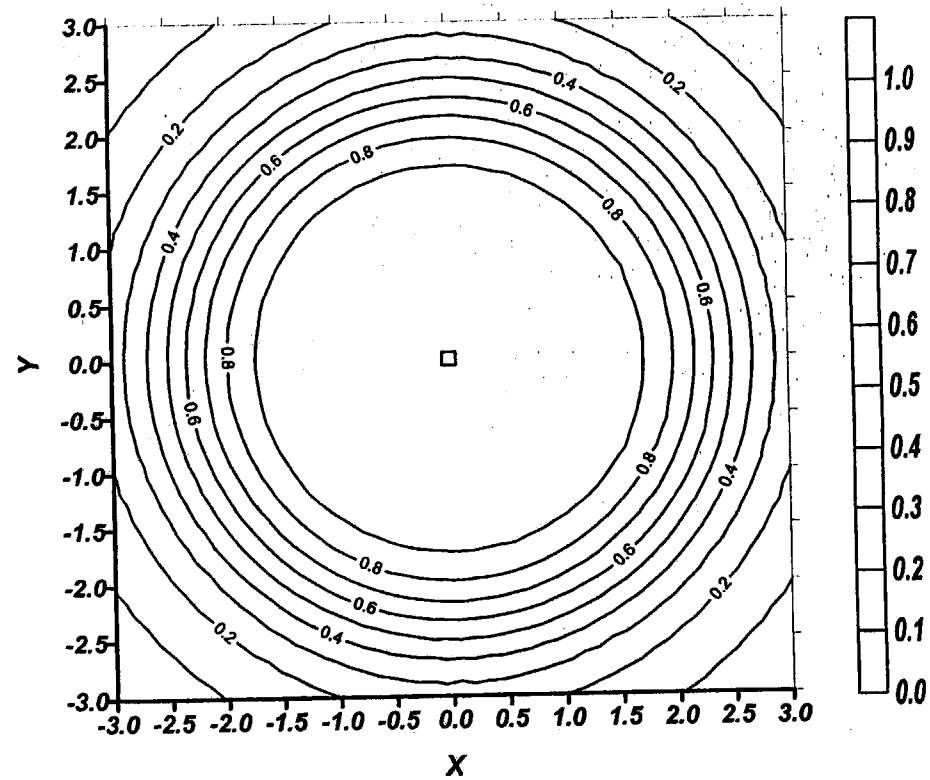

Skew coefficient S(x,y) due to distorted electron charge distribution

e-beam size=2.5*SigX

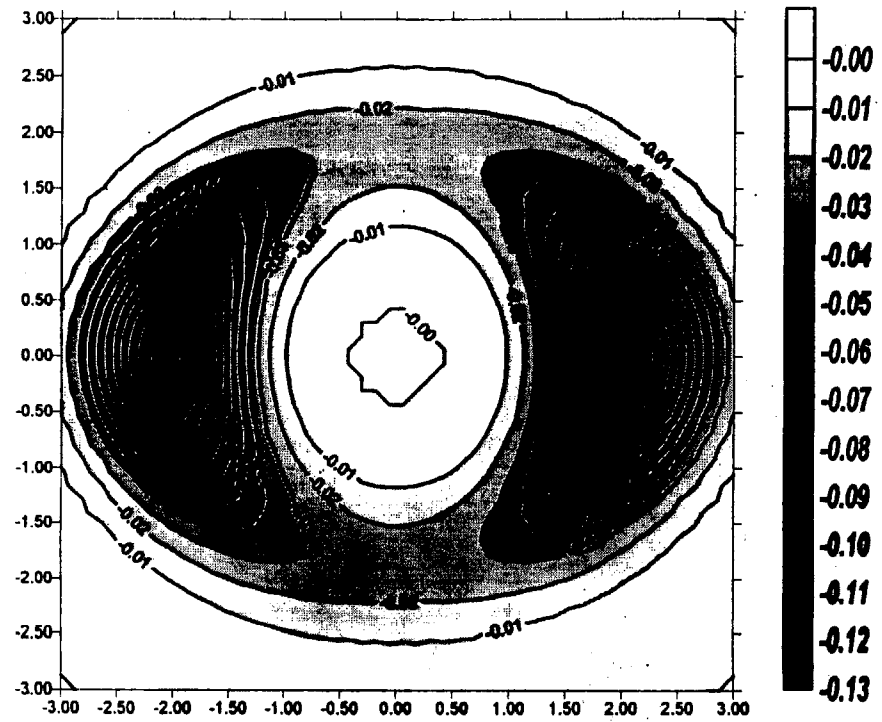

Coupling shift S(x,y)*0.5*Npbar[1e10]/B[kG]*dTune

ELECTRON BEAM STABILITY WITH RESIDUAL IONS

Andrey SERY

Mini-Workshop
on Beam-Beam Compensation in Tevatron
February 12- 13, 1998, Fermilab

Abstract

Stability of the electron beam is essential to provide reliable operation of the "electron compressor". Residual ions produced in ionization of residual gas by electron beam may cause beam distortion via so called drift instability. Therefore the residual ion density should be controlled in order to maintain safe operational condition. The mechanism of the drift instability is discussed and estimations of the acceptable ion density are given. The layout of cleaning electrodes that can sufficiently decrease the ion density is discussed.

This report is based mainly on experience obtained in investigations on the installations of **electron cooling EPOKHA and MOSOL** performed in the **Novosibirsk Institute of Nuclear Physics.**

The persons involved in the studies were

G. Budker, A. Burov, N. Dikansky, V. Kudelainen, V. Lebedev, I. Meshkov, V. Parkhomchuk, D. Pestrikov, A. Sery, A. Sharapa, A. Shemiakin, V. Shiltsev, A. Skrinsky, B. Sukhina, ... and many other

Some of these people are here now and I would like to acknowledge many useful discussions with them.

Well known, not new information for most of you. The purpose is to recall the problem and give numeric values in our parameters.

Talk's milestones

- Where the ions come from
  - Ionization of residual gas
- Why the ions can become locked in the electron beam
  - Potential well of the electron beam
  - When ions are useful
- Why ions can be a problem
  - Drift instability
  - Basic equations of ion and electron beam drift motion
  - Amplification coefficient of beam motion amplitude down along the beam
  - Absolute stability of the system
  - Parasitic beam end → beam head feedback as the reason for instability
  - Estimations of acceptable ion density Estimations of acceptable vacuum
- How ions can be removed from the beam
  - Problem of residual electrons
  - Cleaning electrode's layout
- Conclusion

Where the ions come from

Ionization of residual gas by electrons produce ions with the following rate:

$$\frac{dn_i}{dt} = \sigma_{\text{ioniz}} n_e v_e n_0$$

where σ_{ioniz} ionization cross section, n_e electron beam density, $v_e = c\beta_e$ electron velocity, n_0 residual gas density.

For $\beta_e = 0.2$ (10 kV) total cross section (including initial, second, etc. ionization) is $\sigma_{\text{ioniz}} \approx 2 \cdot 10^{-17}$ cm^2.
At room temperature $n_0 \approx 3.2 \cdot 10^{16} P(Torr)$ cm^{-3}.

Useful quantity is the "time of compensation"

$$\tau_c = \frac{1}{\sigma_{\text{ioniz}} v_e n_0}$$

Approximately $\tau_c \approx 2.5 \cdot 10^{-10}/P(Torr)$ s.

For example if $P = 10^{-10}$ Torr then $\tau_c \approx 2.5$ s.

Why the ions can become locked in the electron beam

Potential well of the electron beam prevents ions to get out of beam in transverse direction.

Potential at the axis $U_e = \pi a^2 e n_e (1 + 2\ln b/a)$ where a, b – radius of electron beam (step like density profile) and vacuum chamber, n_e – electron beam density.

Approximately $U_e \approx 30 J_e[\mathrm{A}]/\beta_e(1 + 2\ln(b/a))[\mathrm{V}]$ For example if $J_e = 2$ A, $\beta_e = 0.2$, $a = 0.1$ cm, $b = 3$ cm then $U_e \approx 2300$ V.

When the ions may be useful

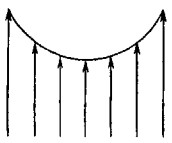

This space charge of electron beam result in difference of electron velocities in the beam cross section. For *electron cooling* this may result in decreasing of cooling decrements. Electron beam space charge change dynamics of particles being colled. Compensation of the electron beam space charge by use of residual ions will help here. Special electrostatic electrodes can be used to store the ions.

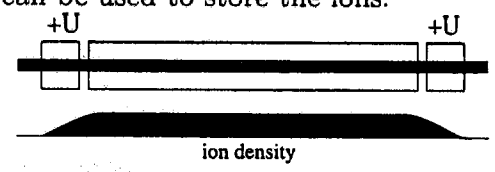

Electrodes of a special construction should be used in order to avoid storing of secondary electrons. See below.

Why ions can be a problem

"Drift instability" is the main reason that can limit the beam current in presence of ions.

Basic equations of ion and electron beam drift motion

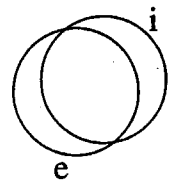

Motion of the charge density centers of the ion and electron beams in dipole approximation.

This may give only a rough estimation if $n_i \neq n_e$ since the electric field is far from uniform in this case.

It is convenient to use $\xi_i = x_i + iy_i$ and $\xi_e = x_e + iy_e$. Then

$$\ddot{\xi}_i = -i\Omega_i\dot{\xi}_i - \gamma\dot{\xi}_i + \omega_i^2(\xi_e - \xi_i)$$

$$\dot{\xi}_e + v_e\frac{d\xi_e}{dz} = -i\frac{n_i}{n_e}\Omega_d(\xi_e - \xi_i)$$

Here the ion motion is characterized by $\Omega_i = eZ_iH/(M_ic)$ – Larmor ion frequency and $\omega_i^2 = 2\pi n_e e^2 Z_i/M_i$ – plasma ion frequency, while the electrons assumed to be "magnetized", i.e. they make only drift transverse motion with $v_\perp = cE/H$ or with drift frequency $\Omega_d = \omega_i^2/\Omega_i = 2\pi n_e ec/H$.

γ – dissipation.

$\Omega_i \approx 0.96\cdot 10^7 H(kG)Z_i/A_i\ \mathrm{s}^{-1}$, $\omega_i \approx 0.75\cdot 10^8/a(mm)\sqrt{J_e(A)/\beta_e\ Z_i/A_i}$

$\Omega_d \approx 0.59\cdot 10^9 J_e(A)/H(kG)/\beta_e/a^2(mm)\ \mathrm{s}^{-1}$

For example, if $H = 3kG$, $J_e = 2A$, $\beta_e = 0.2$, $a = 1mm$, $Z_i/A_i = 1/10$

$\Omega_i \approx 2.9\cdot 10^6 s^{-1}$, $\omega_i \approx 0.75\cdot 10^8 s^{-1}$, $\Omega_d \approx 1.9\cdot 10^9 s^{-1}$

i.e. Larmor motion of ions can be neglected up to $H \sim$ a few Tesla.

Amplification coefficient

If $\xi \propto e^{ikz-i\omega t}$ then

$$k = \frac{\omega}{v_e} - \frac{\Omega_d}{v_e}\frac{n_i}{n_e}\left(1 - \frac{\omega_i^2}{(\omega_i^2 - \omega^2 + \omega\Omega_i - i\gamma\omega)}\right)$$

The system is **absolutely stable** if there is nonzero dissipation. There is **no instability**, just amplification down along the beam. Amplification coefficient $K = \exp(L\,\mathrm{Im}(k))$, maximum at resonance frequency $\omega_\perp = \Omega_i/2 - \sqrt{\Omega_i^2/4 + \omega_i^2}$

$$K_{\max} = \exp\left(-\frac{\Omega_d L}{v_e}\frac{n_i}{n_e}\frac{\omega_i^2}{\gamma\omega_\perp}\right)$$

In practice a **feedback** from the beam end to the beam beginning can exist. If the feedback coefficient η is big enough, the system may become **unstable**. The system is stable if

$$K_{\max}\eta < 1 \quad \text{or} \quad \frac{\Omega_d L}{v_e}\frac{n_i}{n_e}\frac{\omega_i^2}{\gamma|\omega_\perp|}\frac{1}{\ln(1/\eta)} < 1$$

The feedback can be produced for example by electrons reflected from the collector or by ionization electrons. For the reflected electrons simply $\eta \approx n_{\mathrm{refl}}/n_e$

Landau damping on ions

The stability threshold depends on damping $\gamma|\omega_\perp|/\omega_i^2$ (that is $\approx \gamma/\omega_i$ when $\omega_i \gg \Omega_i$).

Damping due to ion-ion collision could be significant if the ion temperature would be very low (a few K°).

The only significant source of damping is Landau damping. Landau damping exists if there is particles with the same frequency as the wave. The wave frequency and the ion frequency are equal in our case so damping will work.

Simple estimation gives $\gamma/\omega_i \approx 1$ in our case.

Estimation of Landau decrement. Suppose we have a wave with field E_w so that ions have amplitude a, i.e. $E_w \approx aE_0 n_i/n_e$. Single ion get the energy $\Delta W/\Delta t \approx eE_w a\omega_i$. Total energy of the wave is $W \approx E_w^2 a^2$. Thus the decrement is $\gamma \approx a^2 n_i \Delta W/\Delta t/W \approx 1$.

Estimations of acceptable ion density

Finally, the stability condition is

$$\frac{\Omega_d L}{v_e}\frac{n_i}{n_e}\frac{1}{\ln(1/\eta)} < 1 \quad \text{or} \quad \frac{n_i}{n_e} j_e < \frac{v_e^2 H \ln(1/\eta)}{2\pi L c}$$

where j_e is the electron current density. The feedback is hard to measure or predict, but it gives very slow dependence. Possible range $\ln(1/\eta) \sim 2 \div 8$.

Practically achieved at EPOKHA (at 35 kV) and MOSOL (at 450 V) installations at Novosibirsk INP values are

$$j_e < \frac{v_e^2 H}{2Lc} \quad \div \quad \frac{v_e^2 H}{3.8Lc}$$

Thus, the theory and practice very well correspond to each other.

Taking a conservative case we estimate the **acceptable ion density** for the "electron compressor"

$$\frac{n_i}{n_e} < \frac{v_e^2 H}{4Lcj_e} \approx 0.8\frac{H(kG)\,\beta_e^2 a^2(mm)}{L(m)\,I_e(A)}$$

If $\beta_e = 0.2$, $H = 3$ kG, $a = 1$ mm, $I_e = 2$ A, $L = 3$ m then

$$\frac{n_i}{n_e} < 1.6 \cdot 10^{-2}$$

So the ions should be cleaned out from the electron beam.

Estimations of acceptable vacuum

If the ions are created by ionization of the residual gas and can exit only at edges where perfect cleaning electrodes are located, the ion density $n_i(x)$ is:

$$\frac{n_i(x)}{n_e} = \frac{1}{\tau_c}\left(\frac{AM_p}{2ZeU_0}\right)^{1/2}\int_0^x \frac{\sqrt{n_e}\,d\xi}{\sqrt{n(\xi) - n_i(x)}}$$

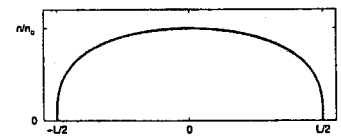

Approximate shape of the residual ion density looks like $n_i(x) \approx n_0(1 - (2x/L)^2)^{1/3}$

where $n_0 = n_e\left(\frac{\pi L}{4\tau_c\omega_i a\sqrt{(1+2\ln(b/a))/3}}\right)^{2/3}$

Estimation for $\tau_c = 2$ s, $\omega_i = 0.75 \cdot 10^8\ \mathrm{s}^{-1}$, $a = 1$ mm, $b = 15$ mm, $L = 3$ m gives $n_0/n_e \approx 0.6 \cdot 10^{-3}$. Even too good.

If we want $n_0/n_e < 1.6 \cdot 10^{-2}/\pi$ (where π is safety factor) then we should have $\tau_c > 0.08$ s, i.e. vacuum better than $P < 3 \cdot 10^{-9}$ Torr.

Ionization electrons will not store in the potential well created by ions if their temperature is high or the heating rate by the main beam is sufficient: $1/\tau_{\text{heat}} \sim d(W/U_e)/dt \approx 4L_c c r_e/(\beta_e a^2(1 + 2\ln(b/a))) \sim 20\ \mathrm{s}^{-1}$. We need $\tau_{\text{heat}} > \tau_c$. In the considered case this condition is fulfilled.

How ions can be removed from the beam

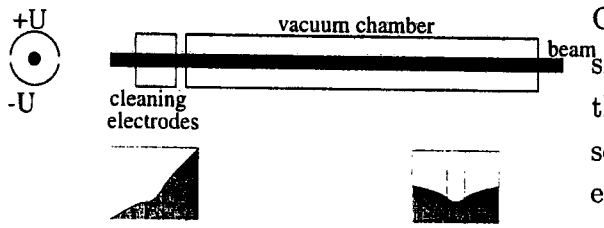

Cleaning electrodes should change the potential well so that ions can escape.

Thus $U_c = 2\pi a b e n_e = U_e \frac{b/a}{\ln(b/a)+1/2}$, where U_e is the depth of the potential well.

If $J_e = 2$ A, $\beta_e = 0.2$, $a = 0.1$ cm, $b = 3$ cm then $U_e \approx 2.3$ kV and $U_c \approx 17.7$ kV.

The voltage U_c is enough to clean out only very slow ions. In practice one should apply $U_c + \Delta U(2b/L_c)$ where L_c is the length of electrodes and ΔU is the energy that ions may have.

If the ions was created in the place where the electron beam radius $\hat{a}$ was bigger than nominal a then $\Delta U = U_e \ln(\hat{a}/a)$. We may have $\Delta U \sim 6$ kV.

So, the electrodes with $L_c \approx 20$ cm and voltage ± 20 kV will give sufficient cleaning of ions.

The electrons reflected from collector at full energy will shift by 0.6 cm by this field, thus they cannot be removed by these electrodes for one pass.

Problem of residual electrons

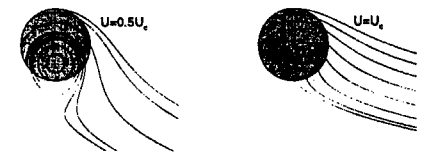

In such configuration with split cleaning electrodes the ionization electrons, that cannot leave beam since they are highly magnetized, will also escape from the beam drifting along equipotential lines.

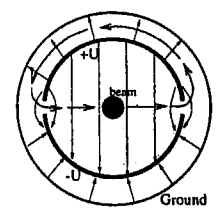

However these electrons may become trapped and store in vicinity of the electrodes until their charge will change significantly the distribution of potentials.

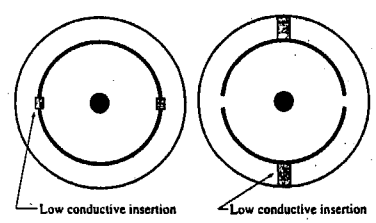

To avoid this problem one can use insertions made from low conductive material (for example semiconductor glass or ceramics covered by a conductive layer).

Conclusion

Ionization ions produced by the electron beam of electron compressor should be carefully cleaned out in order to avoid drift instability.

If the parameters are the following: beam current $J_e = 2$ A, electron velocity $\beta_e = 0.2$, electron beam radius $a = 0.1$ cm, vacuum chamber radius $b = 3$ cm, magnetic field $H = 3$ kG, then the ion density should be better than $n_i/n_e < 5 \cdot 10^{-3}$, vacuum better than $P < 3 \cdot 10^{-9}$ Torr. Special cleaning electrodes with length $L_c \approx 20$ cm and voltage ± 20 kV will provide sufficient cleaning of ions.

Meshkov: Did you take into account that ions can easily go along the electron beam and be absorbed in collector or cathode?

Sery: Yes, I did.

Meshkov: Protons will pass nearby – may they help with ion clearing?

Sery: Good point! An electric field due to highly populated proton bunch should repel ions, though protons are some cm away. It must be studied carefully – for example, the timing has to be taken into account: proton bunch arrives 64ns after pbar one.

Meshkov: It may happen that ions may not be absorbed while passing once through the clearing electrode.

Sery: This effect sets a limit on minimum electrode length. If it is long enough, the probability of "missing" the ion will be small.

Experience with Electron Guns for Medium Energy Electron cooling

S. Nagaitsev
FNAL

February 13, 1998

E-Cool experience relevant to electron beam compressor

- Generation of electron beam with a given current and transverse size
  - -- segmented cathode
  - -- negatively-biased control electrode
- Operation of electron gun and collector
  - -- current recuperation
  - -- stability

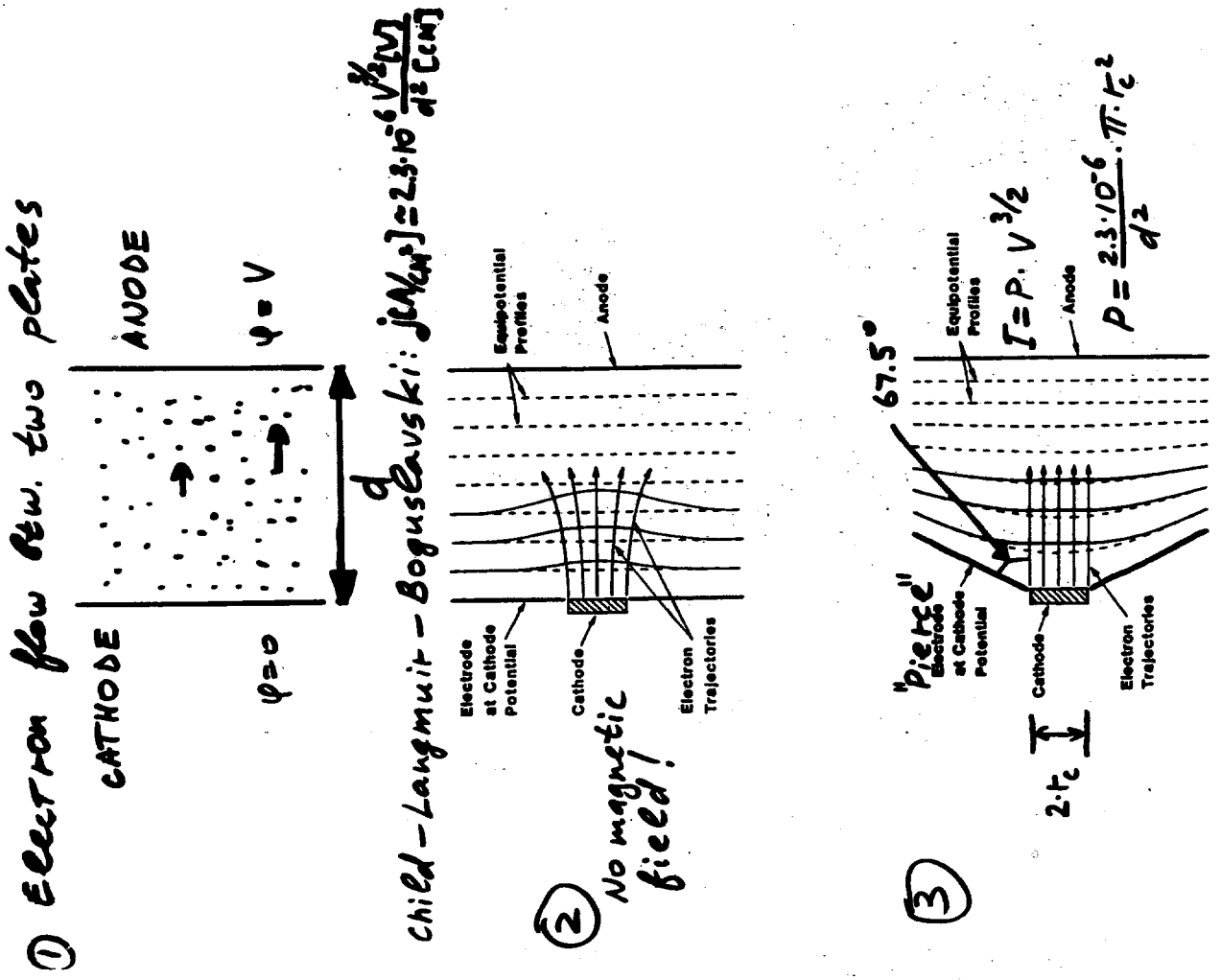

Specific features of e-cool gun

- Good current density uniformity
- Extremely low losses (< 10^{-4})
- Well "behaved" beam for all beam currents (0 - 0.5 A)
- Absence of longitudinal magnetic field

1. Need to extract beam →
→ THUS "ANODE HOLE"

2. NEED TO CONTROL BEAM CURRENT →
→ THUS ONE OR MORE CONTROL ELECTRODES (GRIDS)

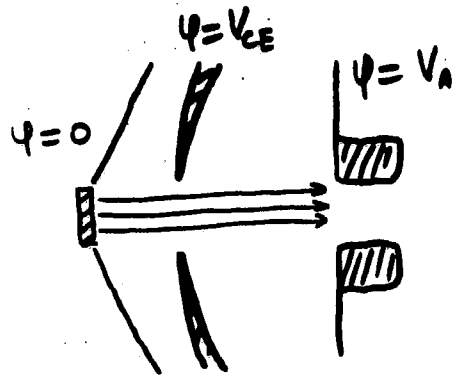

$V_{CE} < 0$ – GUN IS CLOSED

$0 \leq V_{CE} \leq V_A$ – VARIABLE CURRENT

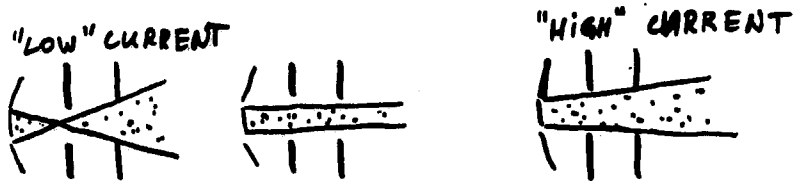

FOR A GUN WITH ONE C.E.

"LOW" $\simeq$ 0.1 "HIGH"

HOW to maintain PARALLEL ELECTRON BEAM FOR ALL CURRENTS?

1. FRED MILLS (FNAL) (+ NEC) 1987
SEGMENTED CATHODE

2. FNAL + INP 1996
GUN WITH A NEGATIVELY-BIASED CONTROL ELECTRODE

3.

Segmented CATHODE GUN

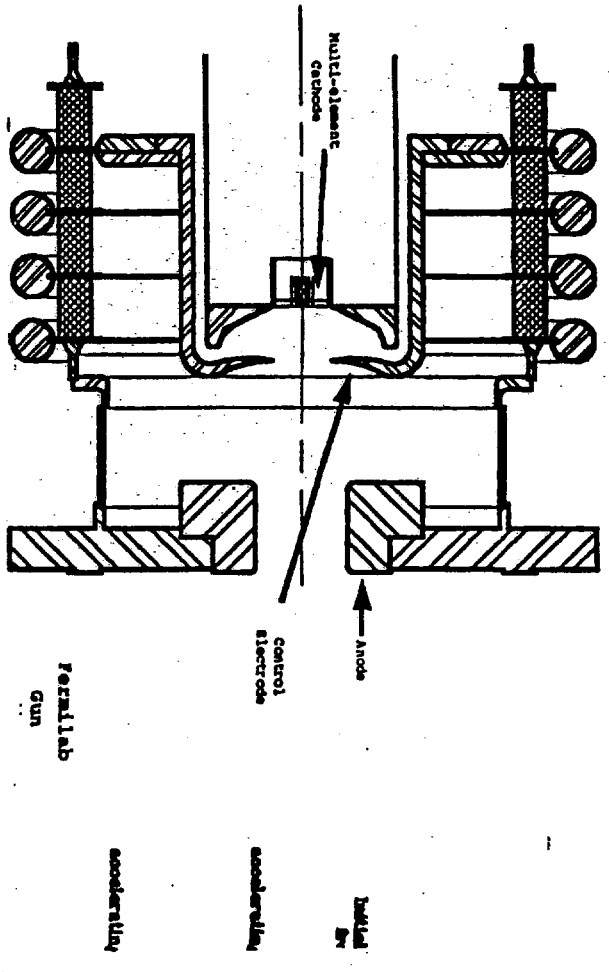

CATHODE

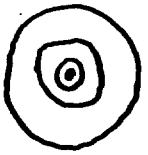

#1 0.01" OD
#2 0.02" ID — 0.12" OD
#3 0.13" ID — 0.315" OD
#4 0.325" ID — 0.75" OD

$V_A = 50\,kV$ $I_c \simeq 2.5\,A$

$P \simeq 0.22\,\mu Perv$

HORIZ. BEAM PROFILE by "FLYING WIRE"

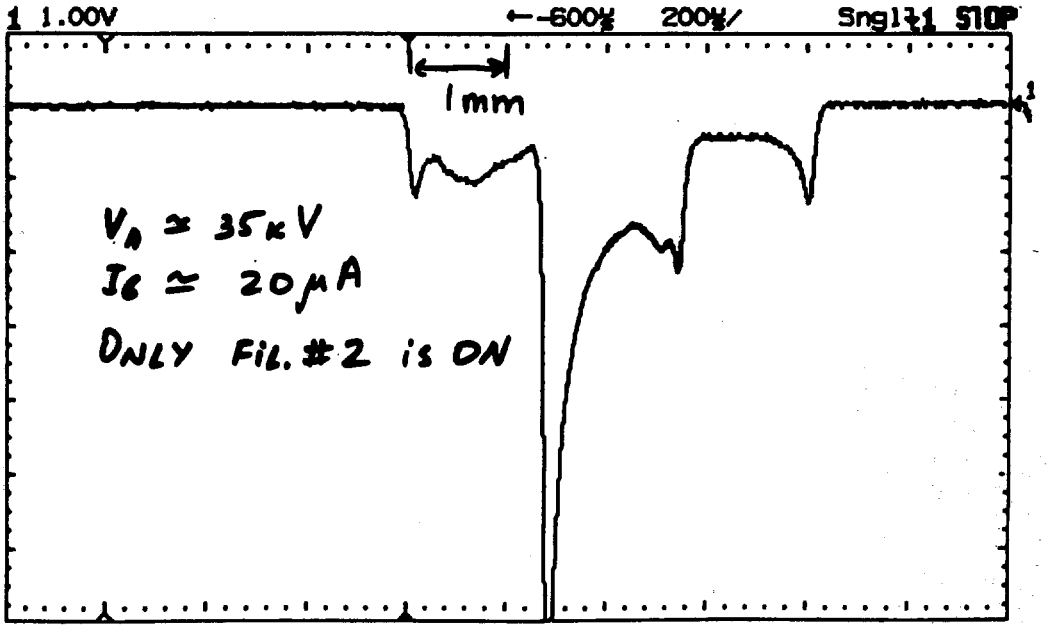

We were unable to obtain emission from ONE FILAMENT WHILE keeping others non-emitting

FIL A = 0 V
FIL B = 9.8 V
FIL C = 0 V

Gun with a negatively-biased control electrode

Idea:
change emitting area of the CATHODE WITHOUT CHANGING THE current density

DESIGN: (INP, 1996)

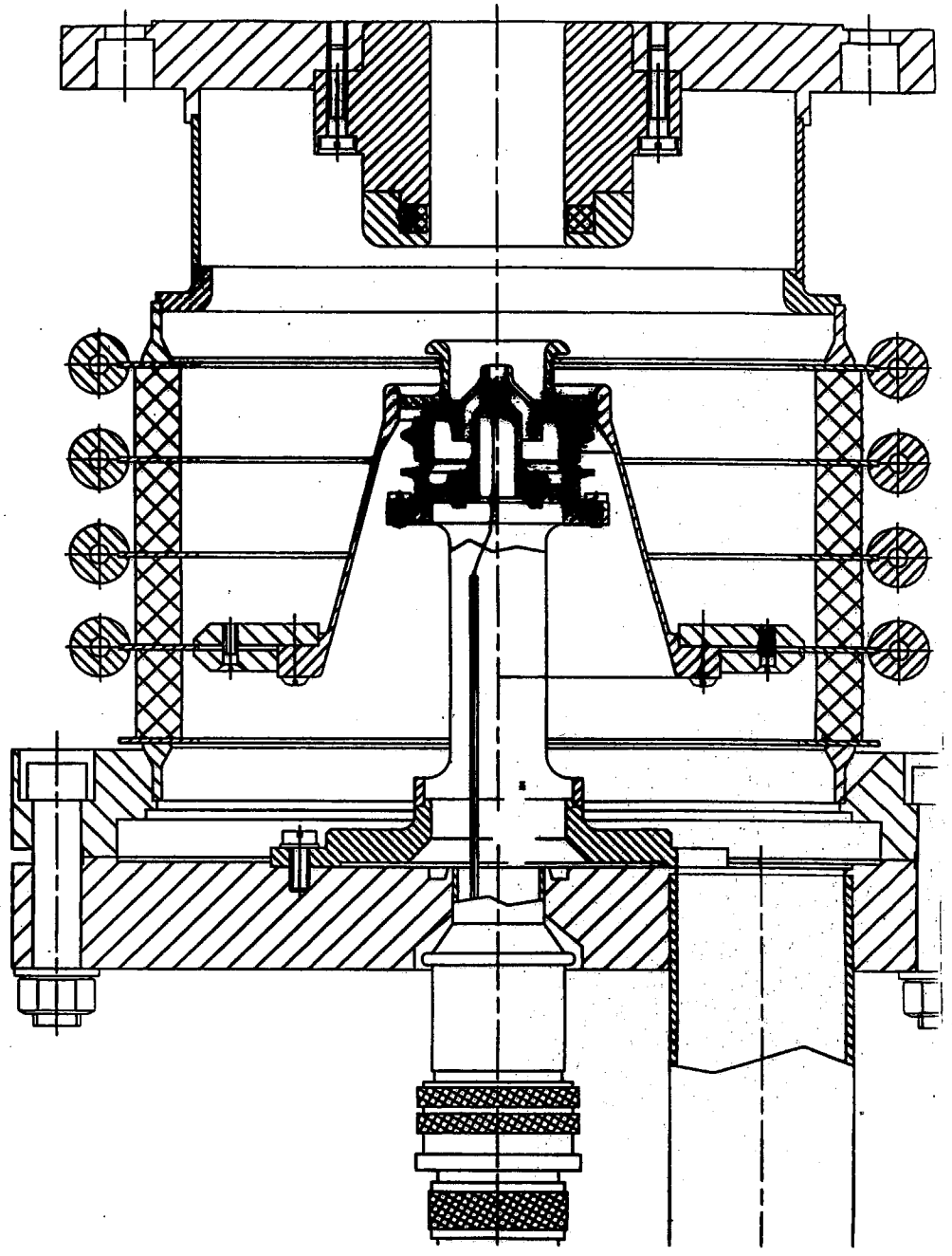

GUN SIMULATION

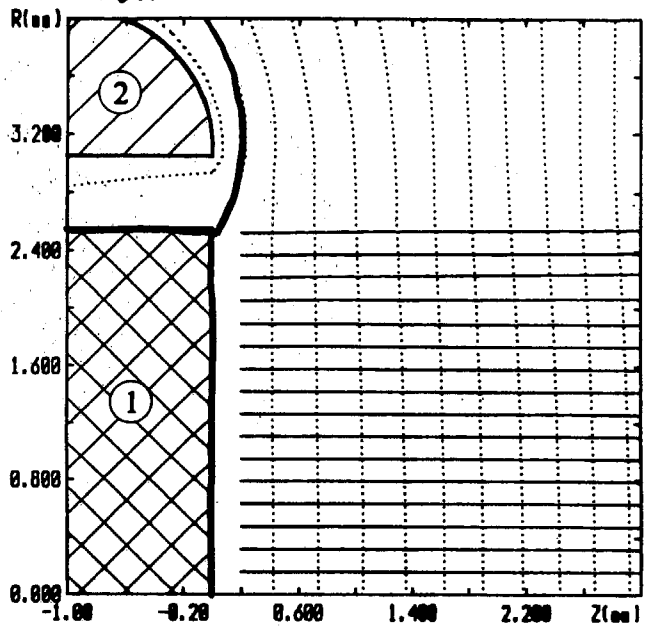

1- CATHODE (0V)
2- CONTROL ELECTRODE(-300V)

$I_G \simeq 0.5\,A$

Dotted lines - equipotentials, spaced at 200V

Fig. 36

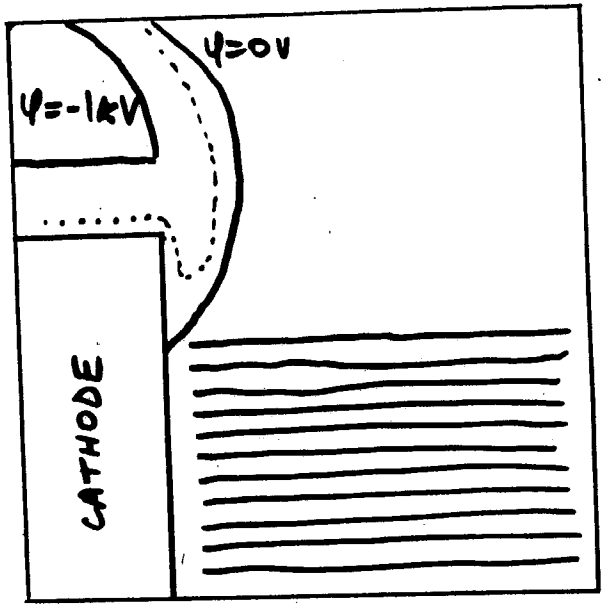

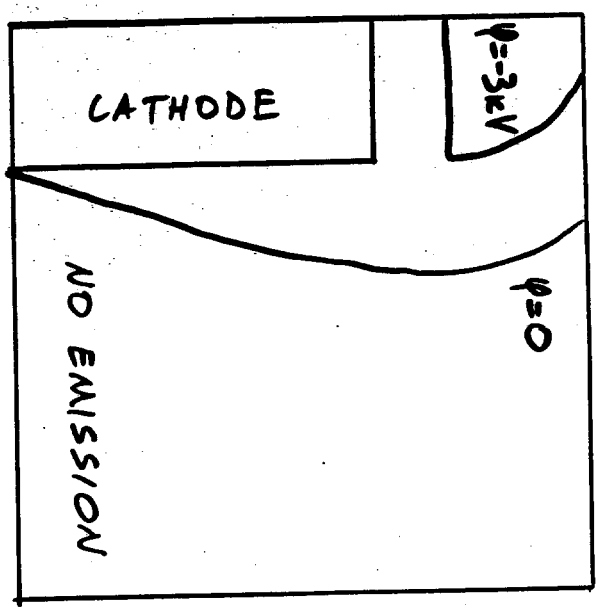

Electron gun with negatively-biased control electrode

- Provides constant density beam with variable size
- Suppresses emission from the cathode's side surface

NOTES ON HIGH PERVEANCE GUNS

Example: 2A, 10kV ⇒ $P = 2\,\mu$Perv

RECALL: $P \simeq \frac{2.3 \cdot 10^{-6}}{d^2} \pi r_c^2$

High perveance requires that $d \simeq r_c$

But....

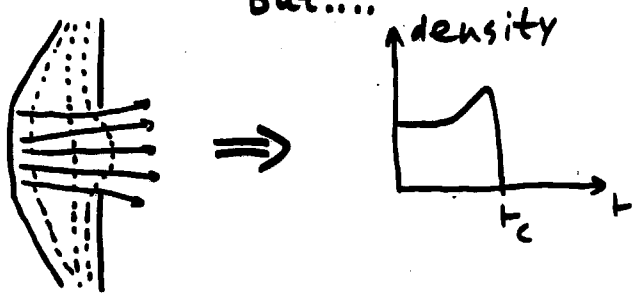

A solution

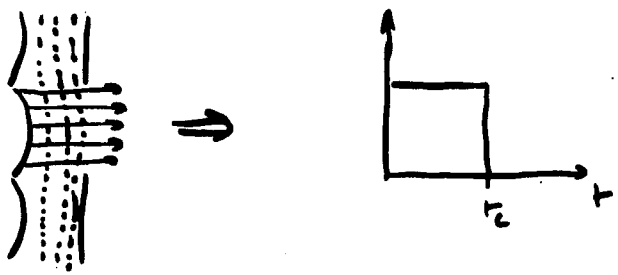

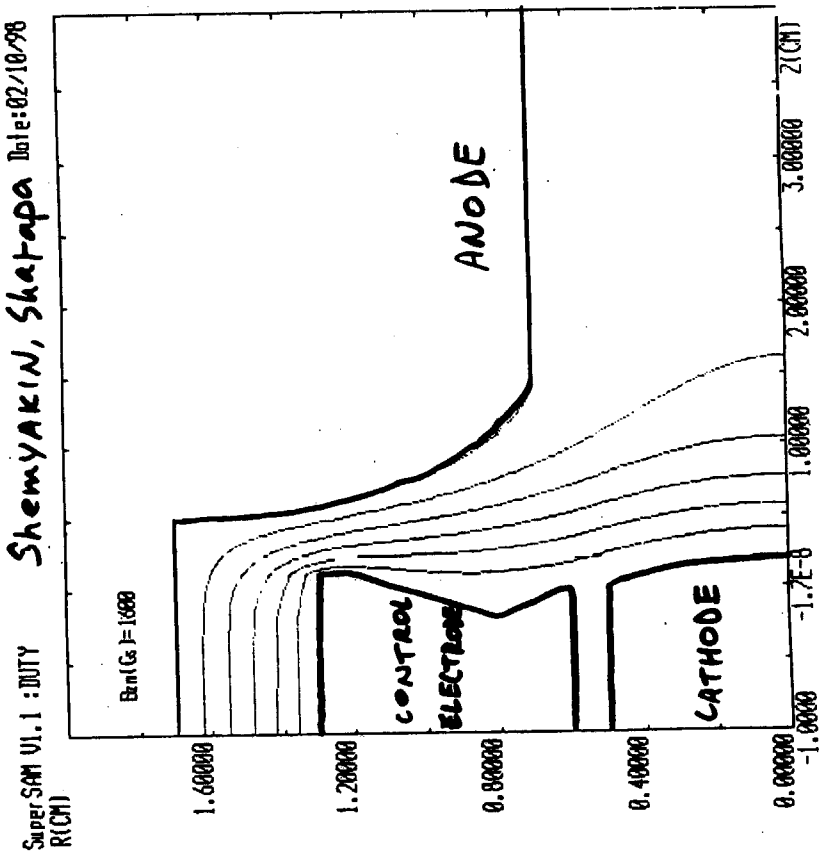

2A, 10kV, $r_c = 0.5$ cm
B = 1.6 kG

Perveance and current density are affected by: (among other things)

Long term: (1000–10000hrs)

1. CATHODE TEMPERATURE (THRU THERMAL MOTION)

2. TIME (THRU DEPLETION OF CATHODE PORES)

⋮

Short term:

1. Presence of IONS (THRU CHARGE NEUTRALIZATION and CATHODE BOMBARDMENT)

CHOICE OF CATHODE SIZE

$4\ A/cm^2 \rightarrow \sim 3000$ hrs

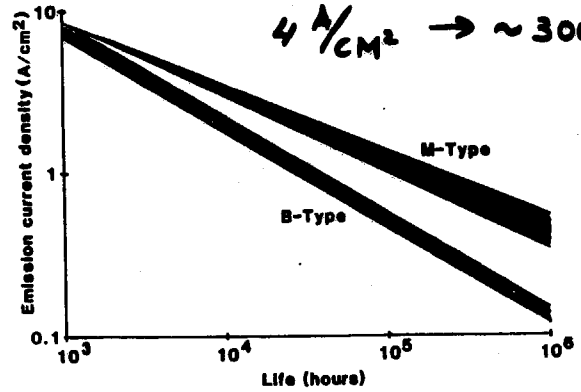

Figure 5.27 Operating Current Densities that Can be Expected as a Function of Desired Cathode Life

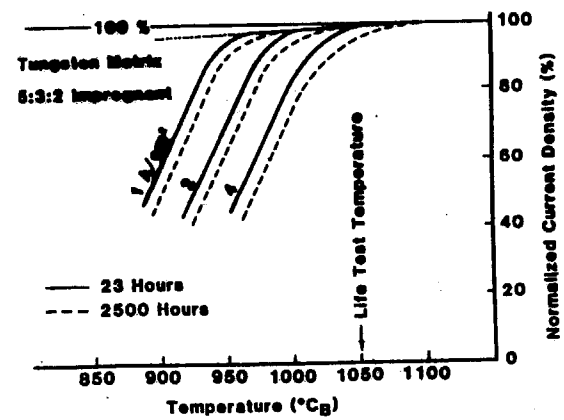

Figure 5.25 Miram Plot for Standard Cathode

(From M.C. Green, Technical Report RADC-TR-81-211, July 1981.)

Current density $\leq 4\,A/cm^2$

Thus CATHODE DIAM. is ~ 1 cm
FOR 0.5-5A GUN

NEED BEAM size $r_b \sim 1$ MM

⇓

Adiabatic compression

⇓

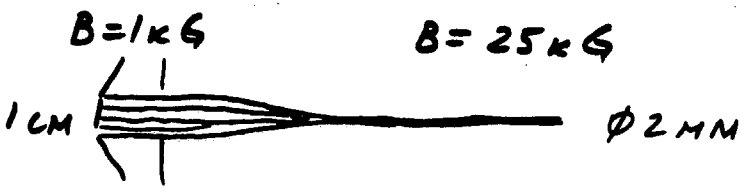

Small beam size → DEEP POTENTIAL WELL → NON-UNIFORM velocity distribution → NON-UNIFORM CURRENT DENSITY

BEAM current stability

Need $\frac{\Delta I}{I} \leq 10^{-3}$ over $\Delta T \simeq 21\,\mu s$

But modulation needed ~ 130 μs

ELECTRON BEAM LENGTH ~ 3M
TIME OF FLIGHT ($\beta \simeq 0.2$) 50 ns

Use feedback, but CANNOT REGULATE FOR THE FIRST $\Delta\tau \simeq 50$ ns

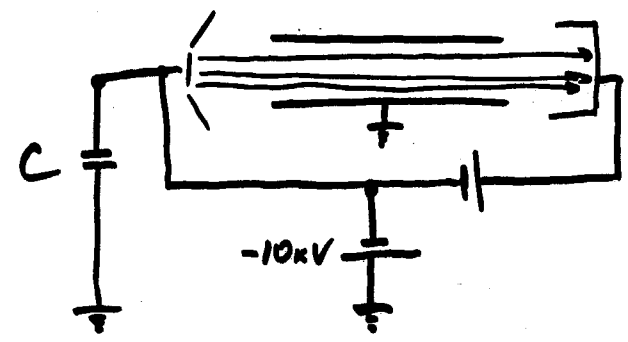

$\frac{\Delta V}{V} \sim 10^{-3} \Rightarrow \Delta V \simeq 10\,V$

$C \geq \frac{I\,\Delta\tau}{\Delta V} = \frac{2A \cdot 50ns}{10V} = 10\,nF$ OK

Q's:

Shiltsev:	Is possible to compress electron beam significantly before the anode hole? E.g. with means of special electrodes.
Nagaitsev:	In principle, yes.
Shiltsev:	How far we can go with lowering magnetic field at the cathode? Say, will be 300 G field enough for e-gun operation? It may allow higher adiabatic compression degree.
Nagaitsev:	Minimum cathode field depends on the e-current and energy. For your parameters an ideal field is somewhere between 500 and 1000 G. 300 G is near margin and needs special consideration.

Workshop on Beam-Beam Effect Compensation
Fermilab, February 12-13, 1998

"Generation of Intense Stationary Electron Beam with Controlled Parameters"

I.Meshkov, A.Sidorin, E.Syresin
JINR, Dubna, Russia

1. General schematics of the "compensator"
2. The electric field of an intense electron beam
3. Electron gun immersed in longitudinal magnetic field
4. Gun optics control
5. Electron energy recuperation
6. How to maintain one component electron beam
7. Beam shape transformation

meshkov@nu.jinr.ru

1967-1970 The elaboration of the first electron cooling device EPOKhA - Russian abbreviation from Electron Beam for Cooling of Antiprotons (I.Meshkov, R.Salimov, A.Skrinsky)

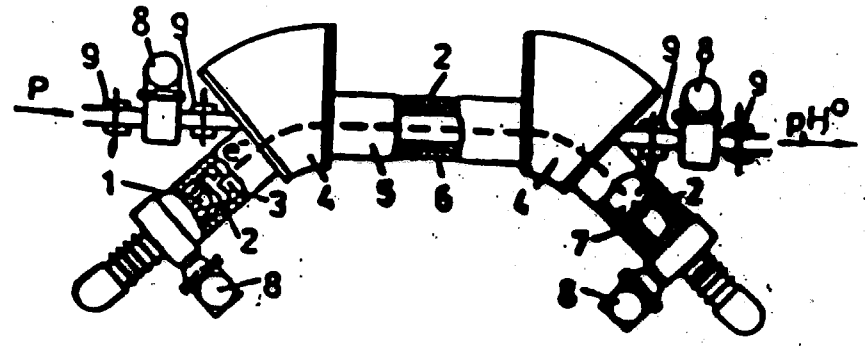

Schematic diagram of the EPOKHA setup:
1 - electron gun, 2 - straight solenoids, 3 - anodes of electron gun, 4 - toroidal solenoids, 5 - cooling section, 6 - vacuum chamber, 7 - electron beam collector, 8 - vacuum pumps, 9 - dipoles, correcting the proton trajectory *(pp')*, H^0 - yield of hydrogen atoms

The main features of the electron cooling device:
- **an intense electron beam immersed in longitudinal magnetic field (a successful solution!),**
- **a special electron gun optics - so called resonant optics,**
- **the electron energy recuperation,**

Coaxial geome

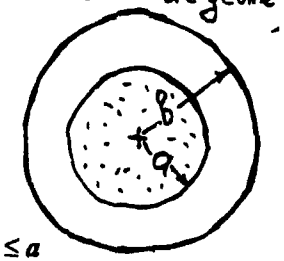

The electric field of an intense electron beam

1. Uniform density of the electron beam

The beam potential:

$$\varphi(r) = \frac{I}{v_0} \times \begin{cases} 1 + 2\ln\frac{b}{a} - \frac{r^2}{a^2}, & 0 \le r \le a \\ 2\ln\frac{b}{r}, & a \le r \le b \end{cases}$$

The beam electric field

$$\underline{E^{o}_{linear}(r)} = \frac{I}{v_0} \begin{cases} \frac{r}{a}, & 0 \le r \le a \\ \frac{a}{r}, & a \le r \le b \end{cases}$$

The beam magnetic field: $B_\theta = \beta E_r$

a, b **- the radii of the beam and of the chamber**

$v_0 = \sqrt{\frac{-2eU}{m}}$ **- the electron velocity**

$U<0$ **- the gun cathod potential** $\beta = \frac{v_0}{c}$

<u>Notice</u>: the potential difference between the beam axis and its boundary is equal to

$$\Delta U = \frac{I}{v_0} \quad \Rightarrow \quad \boxed{\Delta U_{[V]} = \frac{30 I_{[A]}}{\beta}}$$

<u>An example</u>: U**=10 kV,** I**=3A,** ΔU**=450 V**

2. The second order approximation

$$\Delta\varphi = -4\pi\rho,$$

$$\rho = \frac{J}{v(r)} = J\sqrt{\frac{m}{-2e(U-\varphi(r))}} \approx \frac{J}{v_0}\left(1 + \frac{\varphi(r)}{2U} - \frac{3}{4}\frac{\varphi^2(r)}{U^2}\right),$$

$e>0$ - absolute value of electron charge

It gives:

$$\varphi(r) \approx \frac{I}{v_0} \begin{cases} 1 + 2\ln\frac{b}{a} - \left[1 + \frac{\alpha}{2}\left(1 + 2\ln\frac{b}{a}\right)\right]\left(1 - \frac{\alpha}{8}\frac{r^2}{a^2}\right)\frac{r^2}{a^2} + C, & 0 \le r \le a \\ 2\left[1 + \frac{\alpha}{4}\left(1 + 4\ln\frac{b}{a}\right)\right]\ln\frac{b}{r}, & a \le r \le b \end{cases}$$

$$\boxed{\alpha = \frac{I}{v_0 U} = \sqrt{\frac{m}{-2e}} \cdot P_{beam} = 1.5 \cdot 10^{-2}\,\mu P,}$$

P_{beam} **- the beam perveance,** $\mu P_{[\mu A/V^{3/2}]} = 10^6 P_{[A/V^{3/2}]}$, $\mu P \sim 1\,\mu A/V^{3/2}$

$$C = \frac{\alpha}{8}\left(5 + 20\ln\frac{b}{a} + 16\ln^2\frac{b}{a}\right)$$

$$\mu P_{max} \approx \frac{15\,\mu A/V^{3/2}}{1 + 2\ln b/a}$$

$$\boxed{E(r) \approx \frac{2I}{v_0} \begin{cases} \left[1 + \alpha\left(\frac{1}{2} - \frac{r^2}{4a^2} + \ln\frac{b}{a}\right)\right]\frac{r}{a^2}, & 0 \le r \le a \\ \left[1 + \alpha\left(\frac{1}{4} + \ln\frac{b}{a}\right)\right]\frac{1}{r}, & a \le r \le b \end{cases}}$$

$\vec{B} = [\vec{\beta} \times \vec{E}]$,

$\vec{\beta} = \vec{v}_0/c$

$$\left|\frac{E_{nonlinear}}{E_{linear}}\right| = \frac{\alpha}{4}\frac{r}{a^2} \le \frac{\alpha}{4} = 3.8 \cdot 10^{-3}\,\mu P$$

<u>An example</u>: U**=10 kV, I=1.5A** $\Rightarrow$ μP**=1.5 μA/V3/2**

$$\left|\frac{E_{nonlinear}}{E_{linear}}\right| \le 5.7 \cdot 10^{-3}$$

Cylindrical electron beam in coaxial tube

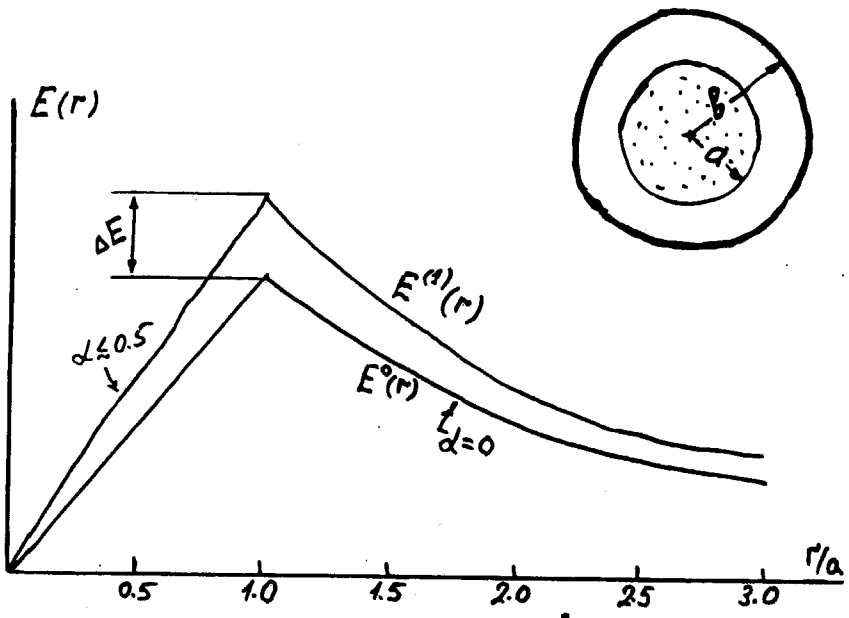

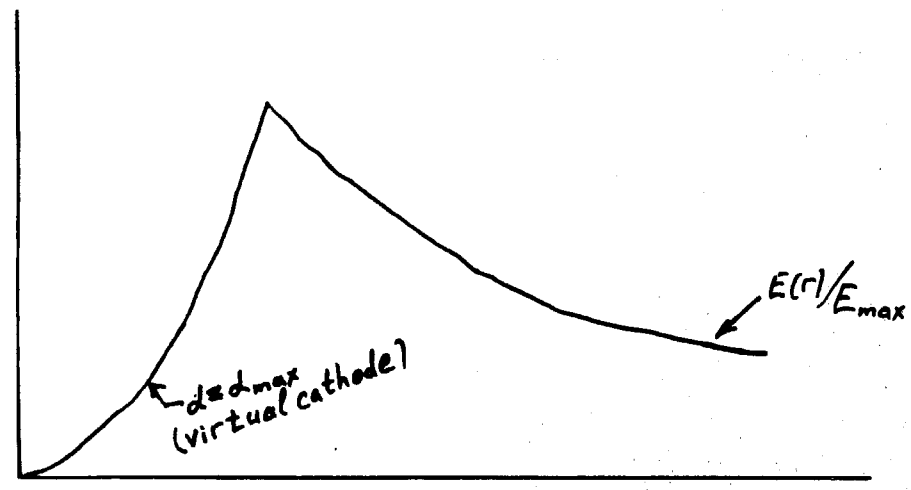

$$\Delta E = \frac{2I}{v_0 a}\cdot\alpha\left(\frac{1}{4}+\ln\frac{b}{a}\right) = \frac{2}{U}\left(\frac{I}{v_0}\right)^2\cdot\frac{1}{a}\left(\frac{1}{4}+\ln\frac{b}{a}\right)$$

What can be varied?

U - electron energy $\Rightarrow v_0$
I - electron beam current

If we can vary independently v_0 & I,
we can change $\Rightarrow$ E-field value
$\Rightarrow \alpha - E(r)$ dependence

Therefore we need a specific e-gun!

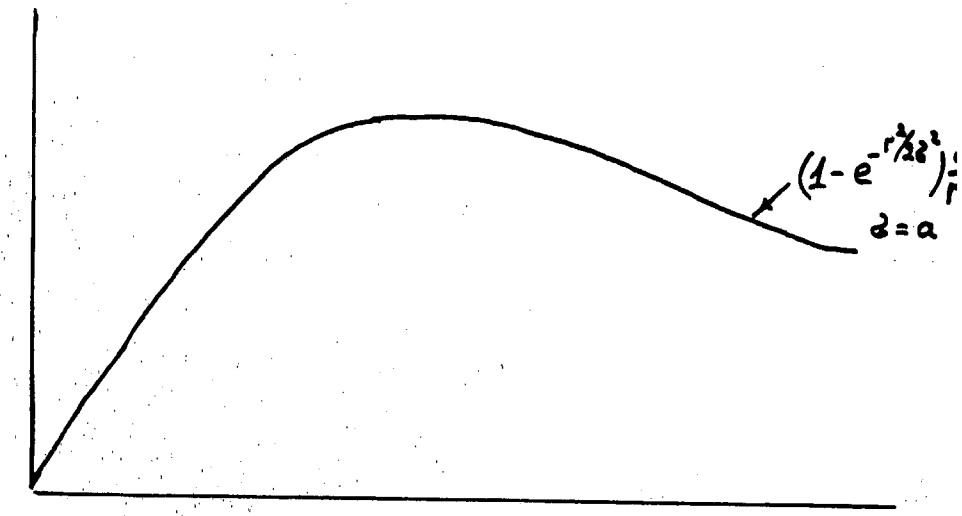
$(1-e^{-r^2/2\sigma^2})/r$
$\sigma = a$

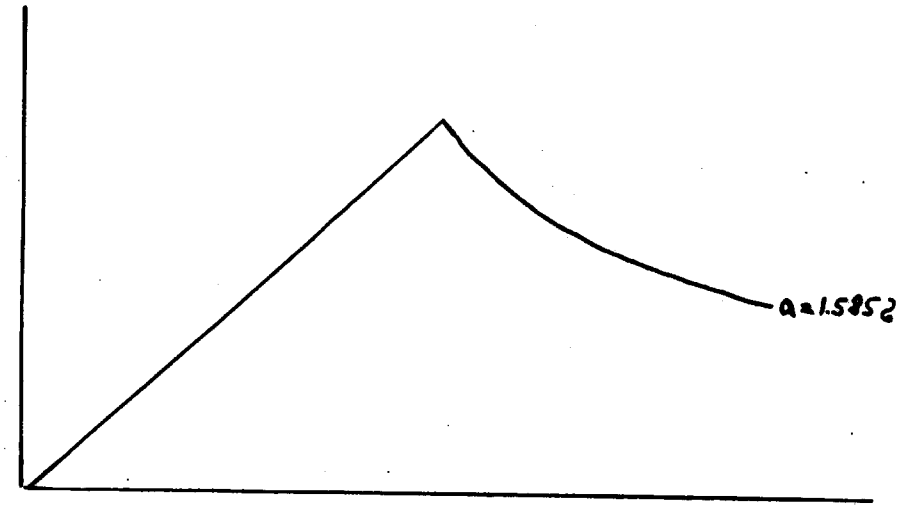
$a = 1.585\sigma$

An effect of non-coaxiality

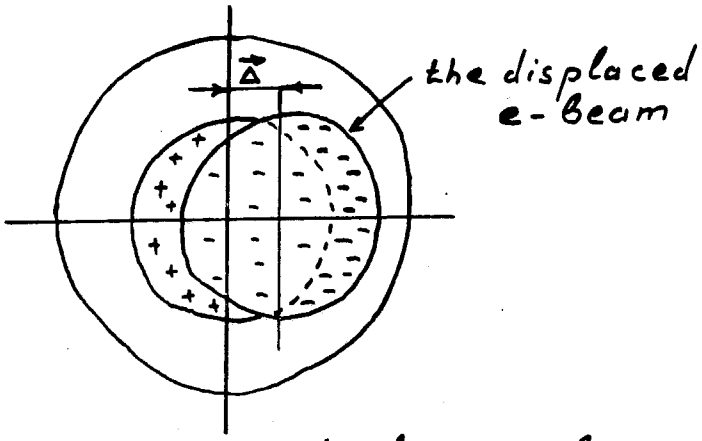

The displaced electron beam can be presented as superposition of 3 beams:

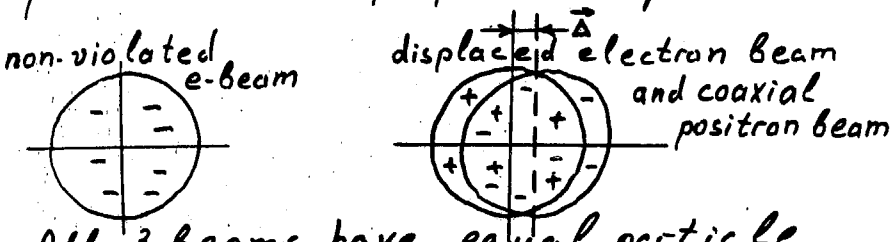

All 3 beams have equal particle density!

$$\vec{E}_\Sigma(\vec{r}) = \vec{E}_1(\vec{r}_1) + \vec{E}_2(\vec{r}_2) + \vec{E}_0(\vec{r}) =$$

$$= \frac{2I}{v_0 a^2}(\vec{r}_1 - \vec{r}_2) + \vec{E}_0(\vec{r}) = \frac{2I}{v_0 a^2}\cdot\vec{\Delta} + \vec{E}_0(\vec{r})$$

Thus, we have superposition of the „ideal" field and an uniform „error"-field.

The „electron lens" works! → However, e-beam rotates around the chamber axis!

The Novosibirsk resonant optics

(V.Kudelainen, I.Meshkov, R.Salimov, Sov.Journ.of Tech.Phys., v.41 (1970)p.2294)

The idea - a multianode gun with quasilinear distribution of $F_s(s)$:

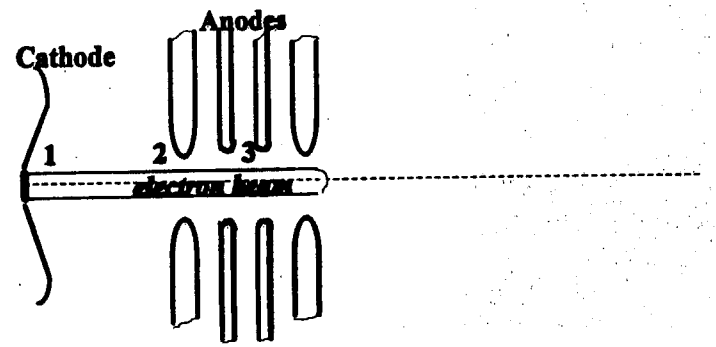

The distribution of the electric field force

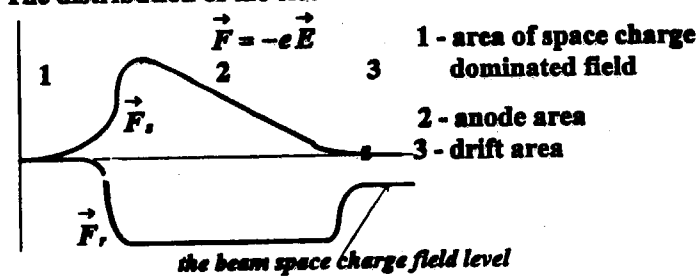

Beam current modulation is restricted!

$$P_{Beam} = P_{gun} \sim 0.2\,\mu A/V^{3/2}$$

The resonant optics conditions

In a longitudinal magnetic field and a radial electric one (an axially symmetric optics) the electron gets transverse momentum

$$\Delta p_r = \frac{e}{m}\cdot\int_0^L E_r(s)\cdot e^{i\varphi(s)}\frac{ds}{v(s)},$$
$$\varphi(s) = \frac{eB}{mc}\cdot\frac{s}{v(s)} = \frac{s}{\rho_L(s)}. \qquad (2.27)$$

When $E_r(s) \approx Const$, the integral in (2.27) is close to *zero*, if the anodes area length

$$L = n\pi(\rho_L(s))_{av}, \qquad (2.28)$$

or, more precisely,

$$\int_0^L e^{i\varphi(s)}\frac{ds}{v(s)} = 0. \qquad (2.29)$$

The function $v(s)$ is slow function of the coordinate s and integral in (2.29) can be brought close to zero by variation of the gun parameters and magnetic field magnitude.

The practical realization of resonant optics scheme was performed in NAP-M electron cooling device *EPOKHA* (*Budker INP, Novosibirsk*) and later in ICE and LEAR (CERN), Test Ring (FNAL) and in many ion coolers of the second generation.

The adiabatic optics

If the distribution of radial electric field in the anode area is a smooth function of s, the integral in the equation (2.27) is close to *zero*, even when a resonant condition is not respected. Such a case takes place, when

$$\frac{dE_r}{ds} \ll \frac{E_r(s)}{\rho_L(s)}, \qquad (2.30)$$

and

$$L \gg (\rho_L)_{av}. \qquad (2.31)$$

$L \sim \phi$ – gun electrodes apertu

(Ya.Derbenev, I.Meshkov, CERN 77-08 (1977))

The gun satisfying these conditions has a specific optics
(See I.Meshkov et al, NIM A311 (1992) p.462)

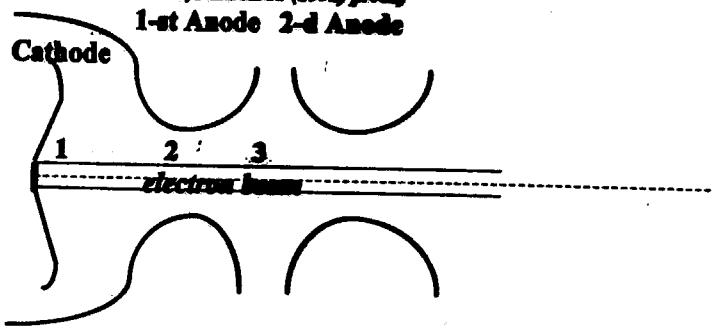

The distribution of the electric field force $\vec{F} = -e\vec{E}$

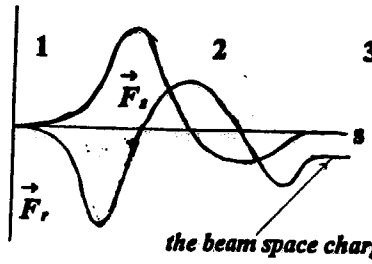

1 - area of space charge dominated field

2 - anode area

3 - drift area

The variable current gun for the LEAR electron cooler (1994)

(NIM A 355 (1995) 208)

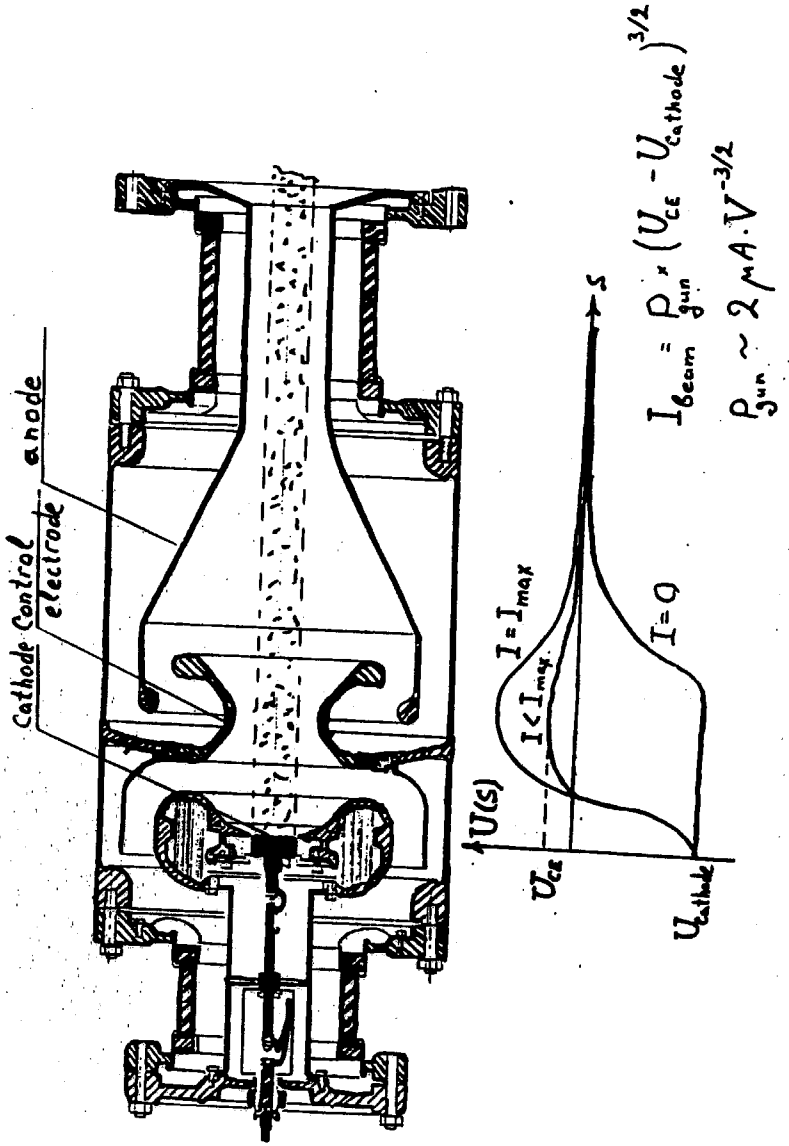

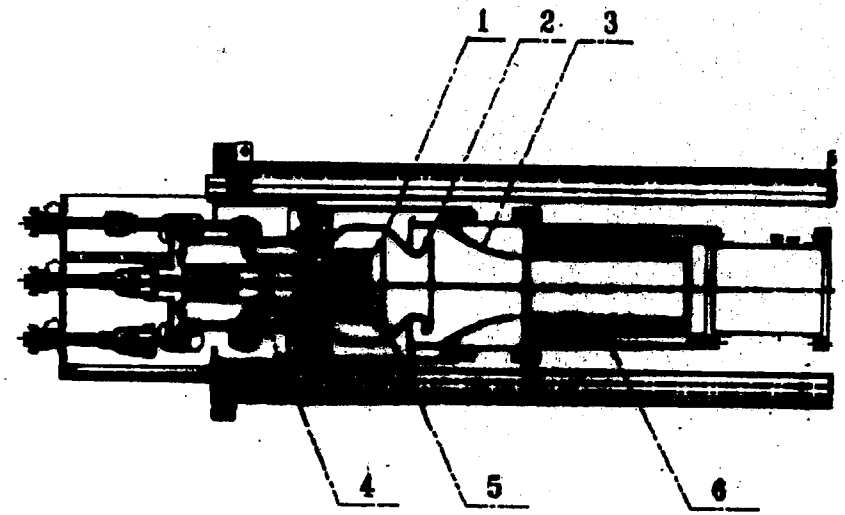

The electron gun of the LEAR electron cooler
1-focusing electrode, 2- steering electrode ("grid"), 3 – anode, 4 – high voltage isolator, 5 – cathode, 6 – NEG – pump.

The electron gun parameters

Electron energy, keV	2.3	7	20	30
Beam current, A	0.5	2.9	2.8	2.6
Beam perveance, $\mu A/V^{3/2}$	5	5	1.0	0.5
Beam diameter, mm	50	50	50	50
Steering electrode potential, kV	+8.1	+25.6	+11.5	+1.7

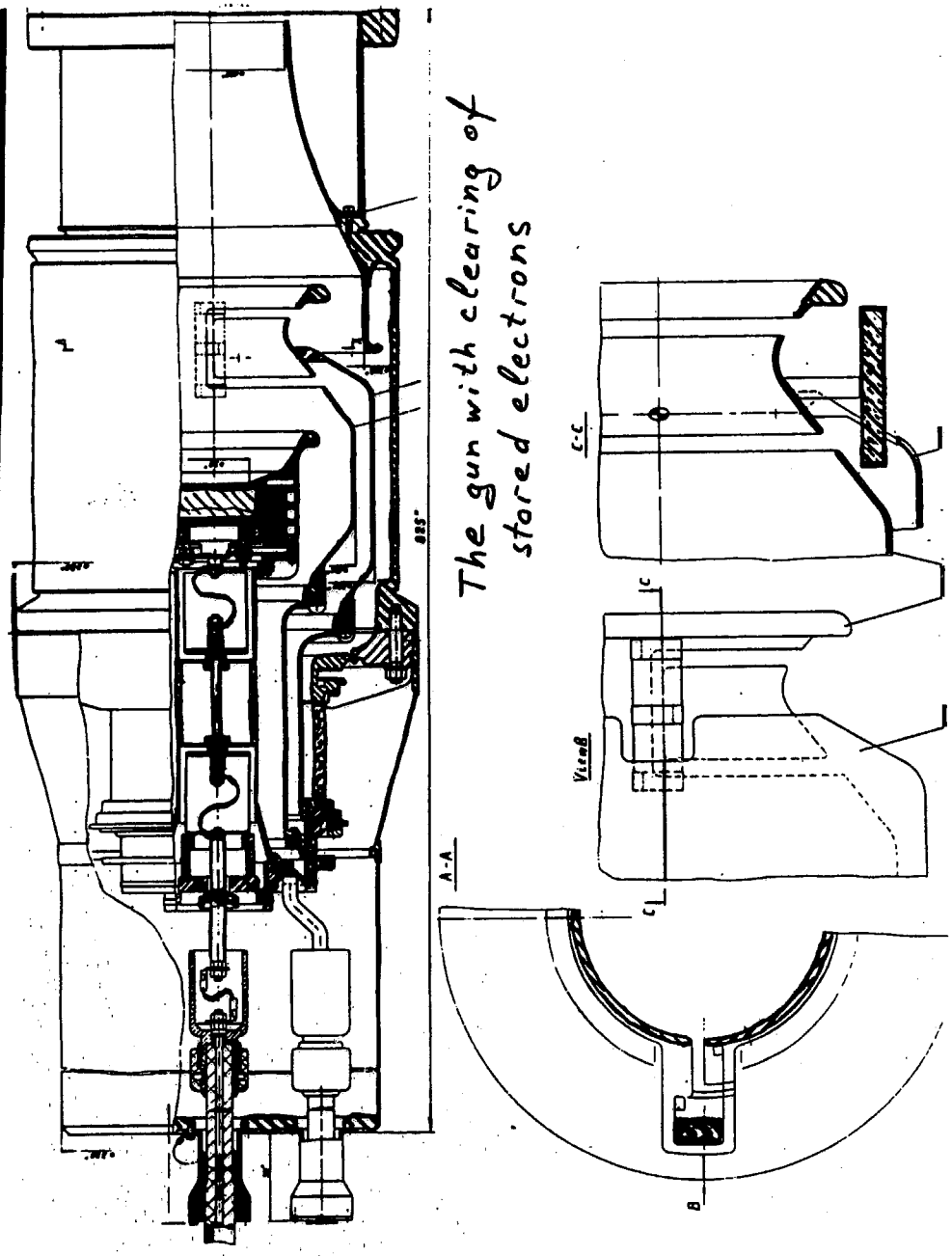

High perveance three electrode gun with clearing electrode

a)

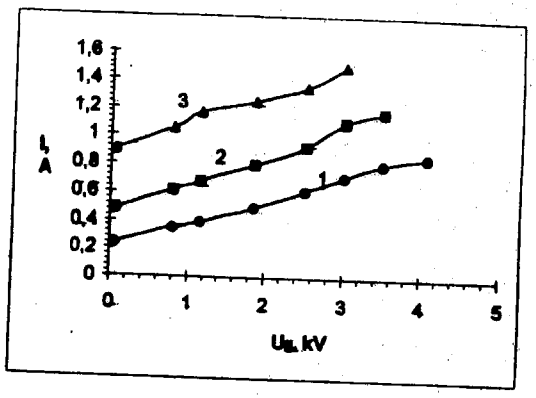

b)

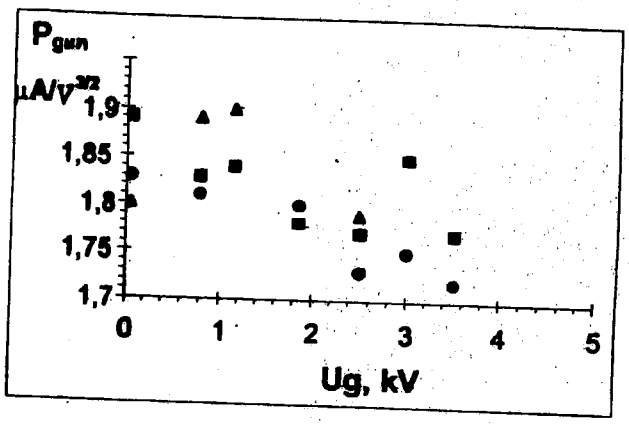

The dependence of beam current (à) and the gun perveance (b) on the steering electrode voltage: 1-U_g=2,5 kV (1); 4 kV (2); 6 kV(3).

The beam perveance P_b=6,5 μA/$V^{3/2}$ at electron energy of 2,5 keV (beam current 830 mÀ).

$P_{beam} \sim P_{max}$!

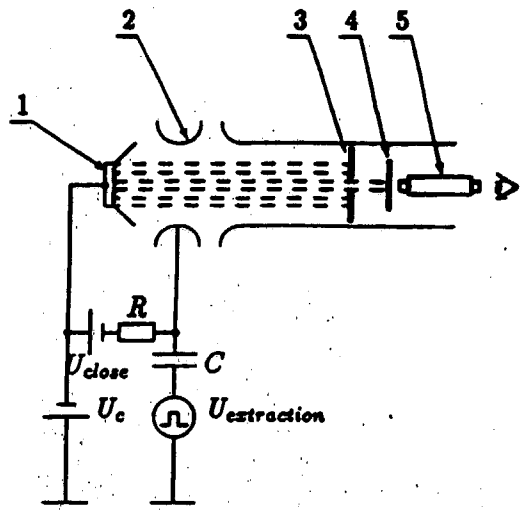

The scheme of the optical analyser

1 - gun cathode, 2 - 1-st anode, 3 - cutting diaphragm, 4 - luminescent screen, 5 - microscope.

The optical analysis of the electron beam transverse temperature

(See V.Golubev, I.Meshkov, V.Pollakov et al, Proc. of the Workshop on Beam Cooling and Related Topics, Montreux, 1993, p.159)

The method is based on the measurement of the transverse size of the thin beam cut from an intense electron beam with a pin hole diaphragm and propagating in a longitudinal magnetic field

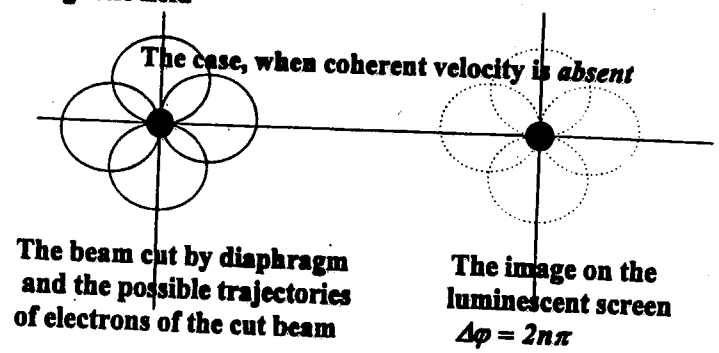

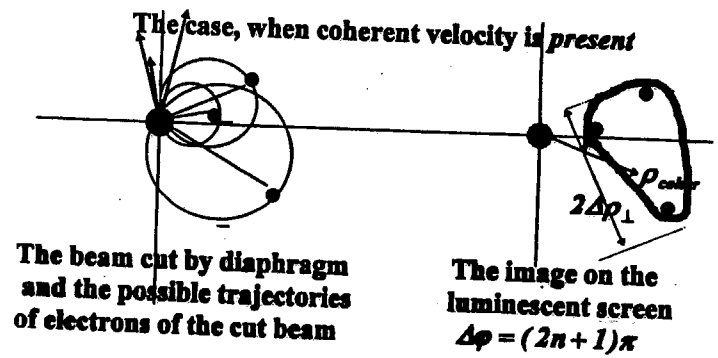

One can measure the coherent velocity of the cut electron beam

$$v_{coherent} = eB\rho_{coher} / \gamma mc \qquad (2.37)$$

and the electron velocity spread

$$\Delta v = eB\Delta\rho_\perp / \gamma mc \ . \qquad (2.38)$$

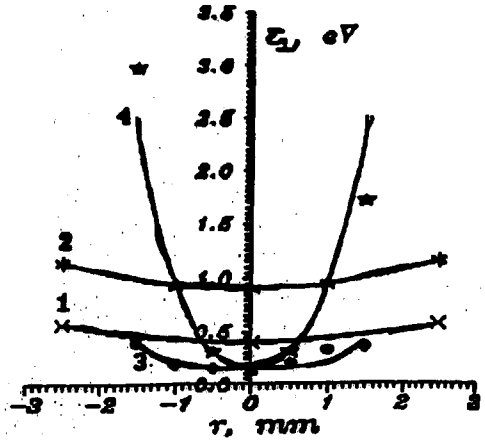

The dependence of the electron transverse energy on radial coordinate of electron for two different guns

(see details in the referred report)

1,2 - "the LEAR gun":

$E_e = 5.7\ keV, B = 600\ G, I_{beam-} = 1\ A(1)$ *and* $1.5\ A(2)$

3,4 - "the CAPT gun":

$E_e = 6.9\ keV, B = 450\ G, I_{beam-} = 0.3\ A(3)$ *and* $0.5\ A(4)$

The method resolution is limited by the resolution of the measurement of the cut beam image size δ_{res}:

$$\rho_{coher} \sim 2\Delta\rho_\perp \geq \delta_{res} \quad . \qquad (2.39)$$

The electron beam angular spread corresponding to δ_{res}, is

$$\delta\Theta = \frac{\delta p_\perp}{p} = \frac{\delta_{res} eB}{pc} = \frac{\delta_{res}}{\rho_L} \quad . \qquad (2.40)$$

$$\delta T_\perp = \frac{(\delta p_\perp)}{2m} = (\delta\Theta)^2 \beta^2\gamma^2 mc^2 / 2, \qquad (2.41)$$

$$(\delta T_\perp)_{eV} = 0.25\beta^2\gamma^2(\delta\Theta)^2_{mrad}$$

A numerical example:

E_e =272 keV

B = 1 kG

ρ_L = 1.976 cm

For $\delta_{res} \sim 0.02$ mm

one has $\delta\Theta$ = 1 mrad

$\delta T_\perp$ = 0.34 eV

The measurements of the electron transverse energy

$$\varepsilon_\perp = \varepsilon_0 \theta^2(r),$$

ε_0 - the kinetic energy of electrons,

$$\Delta\varepsilon_\perp = \varepsilon_\perp(R) - \varepsilon_\perp(0),$$

R-the beam radius,

$\varepsilon_\perp(0)$ = 0.5 – 1 eV

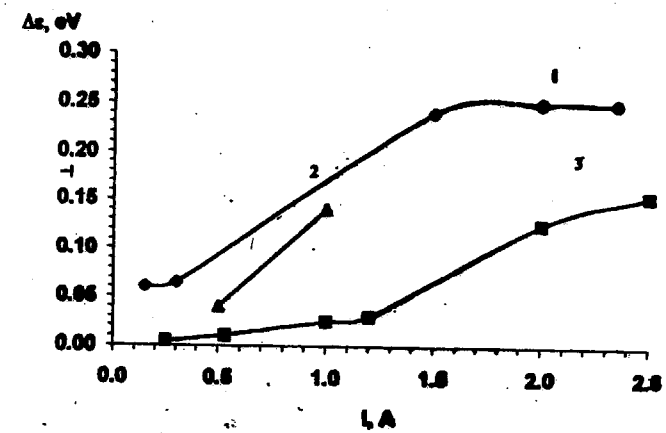

The dependence of the transverse energy difference for axial and boundary electrons on the beam current for the LEAR gun

B=600 G

Experiment: 1-ε_0 = 5.7 keV, 2 - ε_0 = 13 keV; Calculations: 3 ε_0 = 5.7 keV.

preprint

2.6. The electron beam collection and the electron energy recovery

In electron coolers the [illegible] of two parts:

1) high efficient collection of electrons to avoid a significant bombardment of [illegible] to [illegible] energy and [illegible]

2) an effective [illegible] energy - it reduces [illegible] (vacuum [illegible] the task to [illegible] problem of HVPS (see section [illegible])

The electron collector design is defined by the specific character of the energy spectrum of secondary electrons escaping the collector surface:

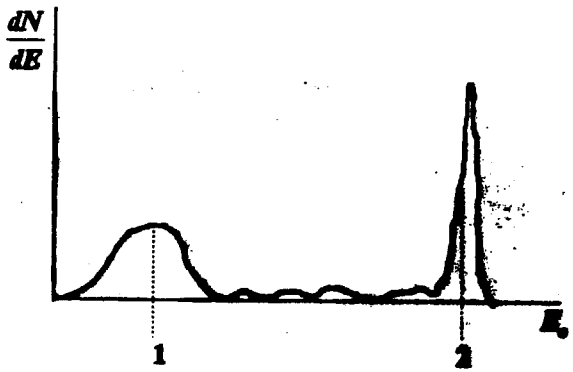

1 - the really secondary electrons, or the slow ones,
2 - the reflected electrons, or the fast ones,

The slow electron energy is of order of

$$0 < E_{slow} < 100\ eV$$

and for the fast ones

$$0.9 \cdot E_{Coll} \le E_{fast} \le E_{Coll}\ ,$$

where $E_{Coll} = e(U_{Coll} - U_{Cathode})$ - the kinetic energy of the primary electrons, reaching the collector surface, U_{Coll} - the collector potential. The slow electrons dominate in the secondary electron flux - their part is of order of

$$\Delta_{slow} \sim 98\%.$$

The part of fast electrons is of order of

$$\Delta_{fast} \sim 1\text{-}2\%.$$

The secondary emission coefficient varies significantly with primary electron energy and depends on collector material and the material surface purification. When the primary electron energy lays in the range 1-5 keV, the integral coefficient is about 0.5 for copper and 0.3 for titanium. However, in real conditions of "technical" vacuum, when cleaning is limited, the influence of adsorbed carbon oxides is large and real emission coefficient is of order of 1.0 - 1.5.

The collection efficiency

To collect electrons in full energy spectrum one has to use special design with electron traps at the collector entrance - the electrostatic and the magnetic ones.

The electrostatic trap is formed usually with an additional electrode (see collector scheme below), whose potential is lower than the collector one - so called *suppressor* (or *repeller*). Usually the suppressor potential is slightly higher of the cathode one. In this case the primary electrons are able to enter the collector space, while the secondary electrons are closed by potential barrier.

The barrier works effectively for electrons, whose energy at the collector surface do not exceed

$$E_{second} \le e(U_{min} - U_{Coll}) ,$$

where U_{min} is the minimal value of the potential inside the collector:

$$U_{Suppressor} < U_{min} < U_{Coll} .$$

Usually all three magnitudes are negative and $|U_{min}| > |U_{Coll}|$. (see plot $U(s)$ below).

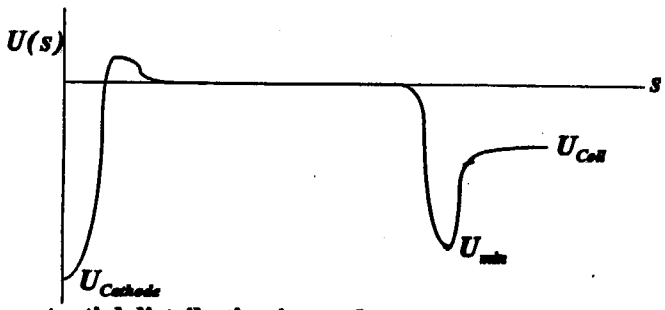

The potential distribution in an electron cooler with electron energy recuperation

In presence of the electron beam space charge the electric field distribution is even more complicated -the area of closed potential shell appears (see computer simulations result below).

The magnetic trap is formed if an efficient shielding of the collector is provided and the magnetic field vanishes abruptly at the collector entrance.

The magnetic trap stops secondary electron, like in any magnetic mirror, at the point, where electron longitudinal velocity drops to zero according two equations - the energy and the adiabatic invariant conservation:

$$\frac{m(v_\perp^2 + v_\parallel^2)}{2} = E_{second} + (-e)\cdot(U_{Coll} - U_{min}) ,$$

$$\frac{m v_\perp^2}{B} = Inv .$$

Introducing the angle

$$\Theta = arctg(v_\perp / v_\parallel)_{Coll} ,$$

which characterizes the direction of secondary electron relatively the magnetic field at the collector surface, one obtains the criterion of the secondary electron trapping:

$$\sin^2\Theta \ge \min\left\{ \begin{array}{c} \dfrac{B_{Coll}}{B(min)} \cdot \dfrac{U_{Coll} - U_{min}}{U_{Coll} - U_{Cathode}} \\ \dfrac{B_{Coll}}{B_{max}} \end{array} \right\} ,$$

where B_{Coll}, $B(min)$ and B_{max} are the magnetic field values at the collector surface, at the point of U_{min} and at the point, where $B(s)$ reaches its maximum (some additional coils can be used to enlarge it).

The magnetic trap is necessary to stop fast electrons. The slow ones are reflected usually by electrostatic barrier (trap) with very high efficiency.

A numerical example:

$U_{Cathode} = -20$ kV $\quad B_{max} = 2.0$ kG

$U_{Coll} = -19$ kV $\quad B(min) = 0.4$ kG

$U_{Suppressor} = -19.8$ kV $\quad B_0 = 1.0$ kG

$U_{min} = -19.5$ kV $\quad B_{Coll} = 60$ G

For such values $\Theta_{min} = min\{0.075, 0.03\}$. therefore, the magnetic trap works here due to existence of the significant value of B_{max}, and the part of fast electrons escaping the collector is of order of

$$\delta \sim (\Delta\Omega)_\Theta / 2\pi \sim \Theta^2 / 2\pi$$

In our example it gives $\delta \approx 7 \cdot 10^{-5}$., and full contribution of the fast electron in the flux of electrons escaping the collector (the *current losses)* is about

$$\eta_{fast} = \delta \cdot \Delta_{fast} \sim 10^{-6} .$$

Therefore, the main contribution in the current losses is due to slow electrons (and also because of their prevailing amount). In practice some essential problems are met when beam intensity is high: space charge regime with a chance of virtual cathode forming. The collection efficiency achieved in best conditions with intense beams is of order of

$$\eta \sim 10^{-5} + 10^{-4}$$

The electron energy recuperation

The second problem of electron beam collection is collector potential. Its reducing leads sooner or later to the forming of the virtual cathode preventing electrons to enter the collector. One can characterize the minimal collector potential with the collector perveance:

$$I_{beam} = P_{Coll} \cdot (\Delta U_{Coll})^{3/2} , \quad \Delta U_{Coll} = U_{Coll} - U_{Cathode} .$$

Mostly the collectors of the Faradey cup type are used in electron coolers (like presented here). They have relatively low perveance:

$$P_{Coll} \sim 12\ \mu A / V^{3/2},$$

which permits to collect a beam of the current of 4A at the collector potential $\Delta U_{Coll} = 4.8\ kV$. This is rather high value, however such a collector has simple design and very high electron collection efficiency, which makes it a convenient tool.

Few sophisticated schemes proposed for more efficient recuperation of electron energy were tested successfully in test bench experiments, however they are not used yet in electron coolers.

The problem of low collector perveance relates probably namely to the necessity of high collection efficiency: when one needs to provide very low current losses, even small fraction of reflected electrons is intolerable. Such a fraction can consist of electrons, whose longitudinal velocity (relatively to the collector decelerating field) is decreased due to some optics aberrations, which redistribute electron energy between the transverse and longitudinal velocity components. Then the decrease of the potential inside the collector can lead to the reflection of such electrons even before the virtual cathode is formed. As result, it limits the reducing of the collector potential.

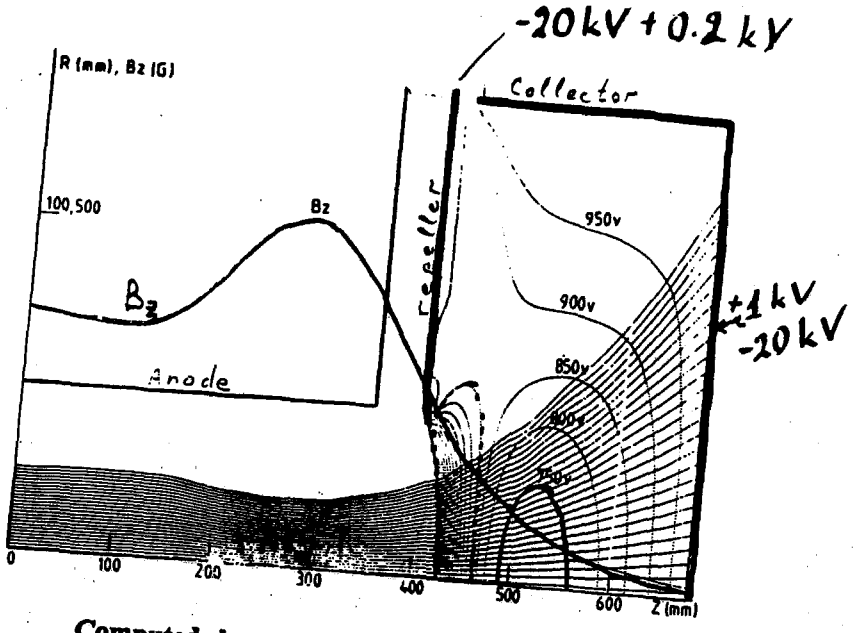

Computed electron trajectories with the collector and repeller setting respectively at 1 kV and 200 V. The electron beam energy is 20 keV and the magnetic field strength is 500 G. I_e = 1.5 A

Recent idea ⟹ $B_\perp$ at the collector surface

Recuperation of intense electron beams

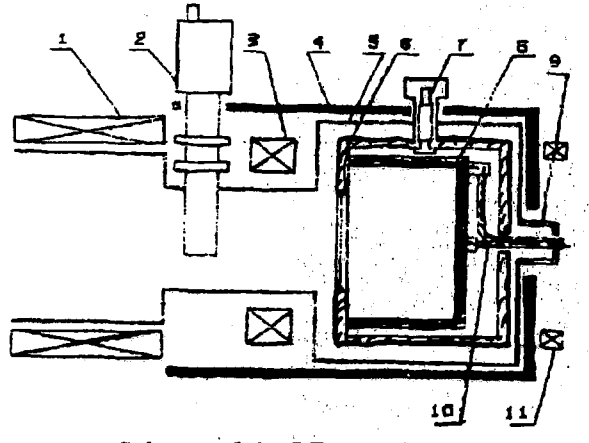

Scheme of the LEAR collector

1 -solenoid; 2 – vacuum valve; 3 – collector coil; 4 – magnetic shielding; 5 – vacuum chamber; 6 – suppressor (repeller) electrode; 7 - insulator; 8 - collector; 9 – vacuum insulator; 10 – water cooling system; 11 –compensating collector coil.

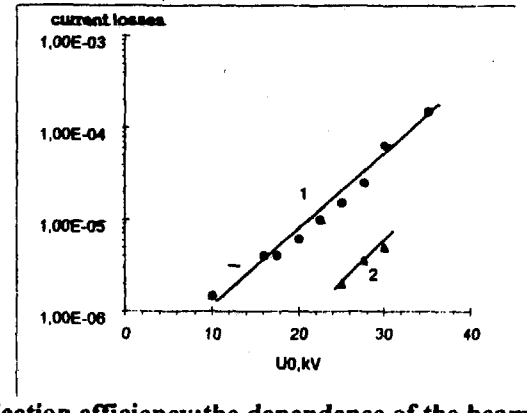

The collection efficiency:the dependence of the beam current losses on the cathode voltage.

Beam perveance 0.52 $\mu A/A^{3/2}$; B = 516 G, B_{max} = 1050 G;

1) P=5×10^{-8} ÷ 6.7×10^{-7} Torr. ; 2) P=1.5×10^{-8} Torr.

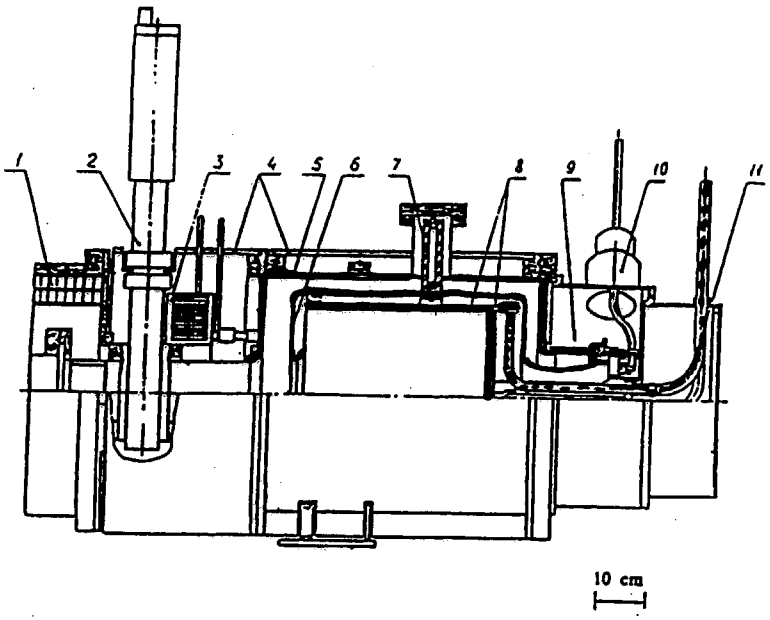

The collector scheme for the LEAR electron cooler (CAPT of Budker INP) 1992

1 - solenoid, 2 - vacuum valve, 3 - compensation coil,
4 - magnetic shielding, [redacted],
7 - supporting insulator, [redacted],
10 - feed through, 11 - water cooling tubes.

Clearing of ions with the shaker

(PAC-95, Dallas,1995
NIM A, 391, v.1, p.110, 1997)

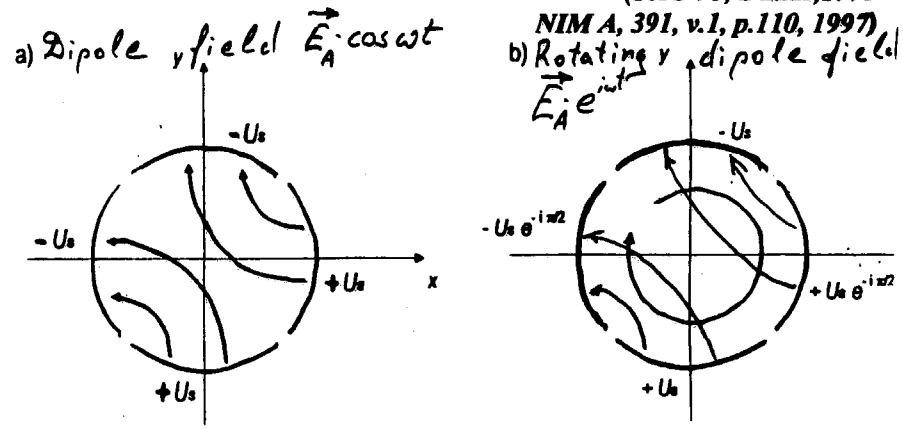

The shaker scheme

$E_\perp = E_s \sin\omega_s t$ – **transverse harmonic electric field ;**

$\omega_{shaker} \cong \omega_{inc} = 2\pi \times (200 - 400\ \text{kHz})$ – **ion incoherent oscillation frequency .**

Diffusion Ion heating

$$\left(\frac{M\omega_s^2 a^2}{2}\right)^2 \approx (ZeE_s a)^2 \frac{\tau_{ion}}{\tau_{//}}$$

***a*-beam radius,** τ_{ion} **- ionisation time,** $\tau_{//}$ **- time of ion longitudinal oscillations.**

$$U_s = 2E_s b \approx \frac{M\omega_s^2 ab}{Ze}\left(\frac{\tau_{//}}{\tau_{ion}}\right)^{1/2}$$

b – shaker electrode radius.

$U_s \approx 2 - 20$**V at pressure** 10^{-11}**-**10^{-9} **Torr**

Stabilisation of the neutralised electron beam with the shaker

LEAR experiment

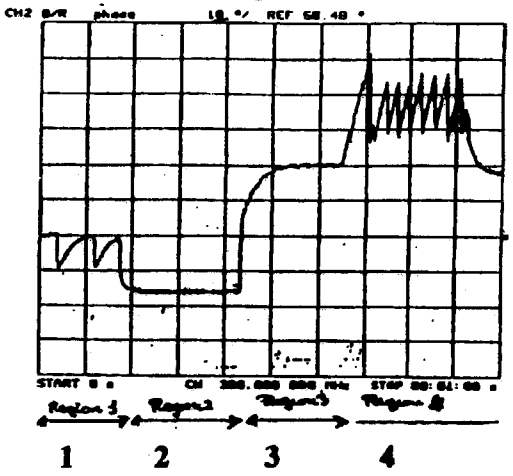

TQF-signal (LEAR).
1-traps and shaker –off, 2-traps-off, shaker on, 3- traps and shaker –on, 4-traps-on, shaker –off

Clearing of electrons.

(NIM A, 391, v.1, p.110, 1997)

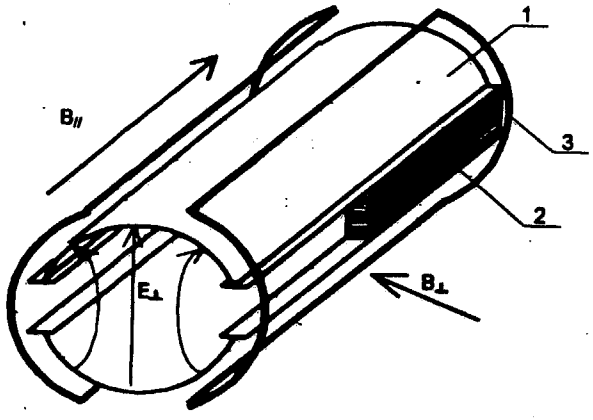

Scheme of clearing electrodes:
1-clearing electrodes, 2 - "conductive" glass, 3 - coils of transverse magnetic field

$B_\perp = cE_\perp / v_e$ **–transverse magnetic field**

$$\Delta = \left(\frac{E_\perp}{v_e B_{//}} \pm \frac{B_\perp}{B_{//}} \right)$$ **- the displasement of an electron inside clearing electrode during a single pass**

"-"-primary beam electrons,
"+"-secondary electrons, reflected from collector.

Trajectories of primary and secondary electrons inside clearing electrodes.

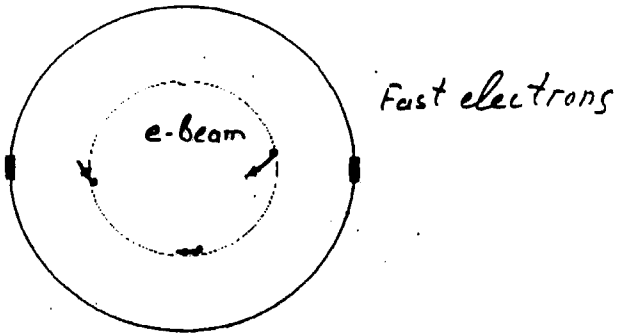

Trajectory of primary electrons inside clearing electrodes during a single pass through them.

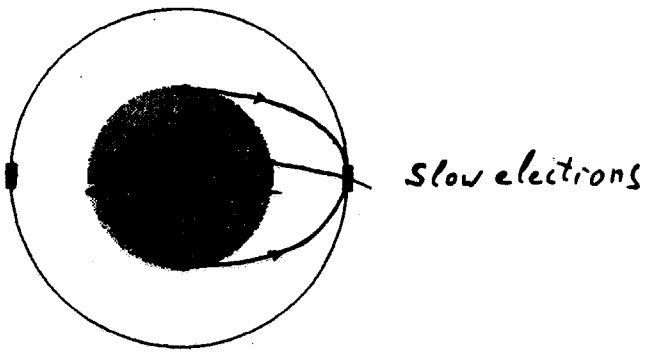

Trajectory of secondary electrons reflected from collector inside clearing electrode during one pass trough them.

The transformation of the shape of a magnetized electron beam

1. The goal: controled beam shape enables to compensate ΔQ with desirable precision

1a. The method of different β-functions:

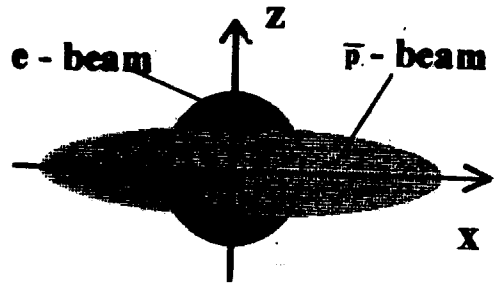

$\beta_x > \beta_z$ **- focusing by z-direction**
- weak focusing by x-direction

Disadvantage: non-independent influence by x- and z- degrees of freedom

$$\langle J_e \rangle = \frac{I_e}{S_{\bar{p}}}$$

1b. The method of e-beam shape transformation

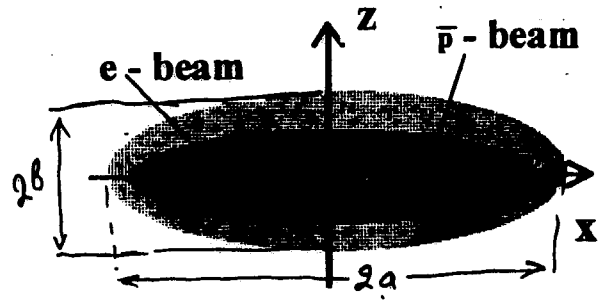

Electron beam effects like one-dimensional lens (so-called "cylindrical" lens)

Advantage: effect only on chosen degree of freedom (z-direction in the present example)

Disadvantage: the e-beam rotation $\rightarrow \frac{d\varphi}{dt} \propto \frac{I}{abB}$

2. Solenoid of the variable cross-section

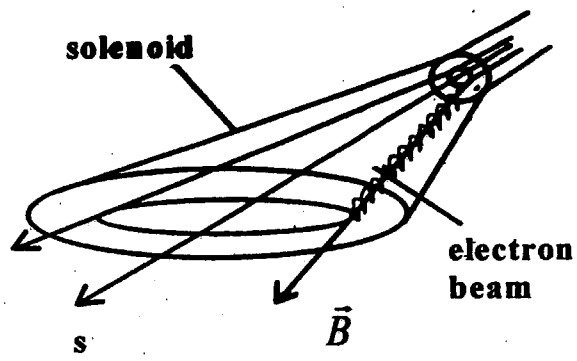

Disadvantage: fixed beam cross-section sizes

3. Crossed longitudinal and quadrupole magnetic fields

Panofsky's lens

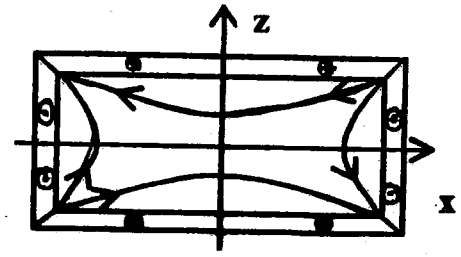

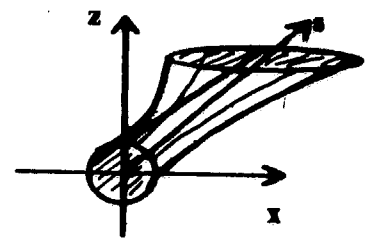

Beam shape transformation

$$z(s) = z_0 e^{-Gs/B}$$

$$x(s) = x_0 e^{Gs/B}$$

An advantage: the possibility to regulate the beam shape by changing of G.

Which e-gun do we need?

1. 3-electrode gun ⟹ independent regulation of beam current and electron energy

2. An intense e-beam with decelaration:
   - space charge influence on e-beam density
   - reduced density in area near beam axis

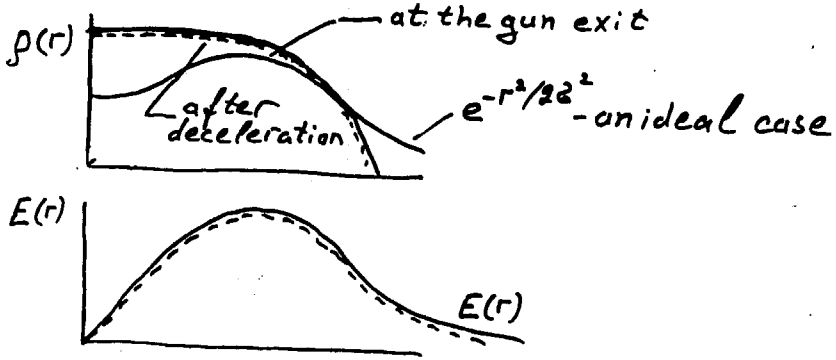

The reason: to generate an electron beam with gaussian density distribution is a hard task!

3. Sectioned cathode? The problems:
   - emission limited regime → current stability
   - different potentials of the cathode sections → „slipping instability" of e-beam

4. Electron beam compression → Yes!
   By B-field compression.

In a gun for e-cooling we need
$J(r) = \text{Const}$,
for the „Compensator" → $J(0) < J(a/2)$ and $J(a/2) > J(a)$

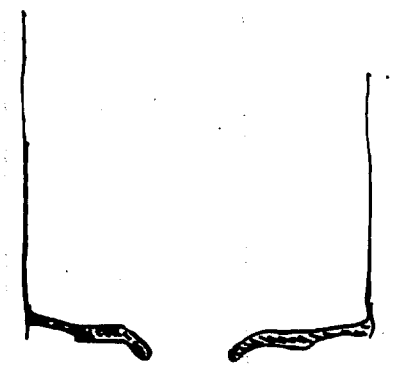

Q's:

Meshkov:	We also can measure current fluctuation spectrum in the gun comparable with what you need for e-compressor parameters which is currently under operation in Dubna. The same for cathode spots – we have everything to observe them there.

Electron Cooling at Medium Energies

Beam temperature definition:

$$T_{\mathrm{PRF}} = m_{\mathrm{particle}}\, v_{\mathrm{PRF}}^2$$

$$\frac{m_{\mathrm{electron}}}{m_{\mathrm{proton}}} = \frac{1}{1836}$$

Thermodynamical limit of electron cooling:

$$T_{\mathrm{particle}} = T_{\mathrm{electron}}$$

hence:

$$\frac{v_{\mathrm{proton}}}{v_{\mathrm{electron}}} = \frac{1}{43}$$

and:

$$\frac{\epsilon_{\mathrm{protons}}}{\epsilon_{\mathrm{electrons}}} = \frac{1}{1836}$$

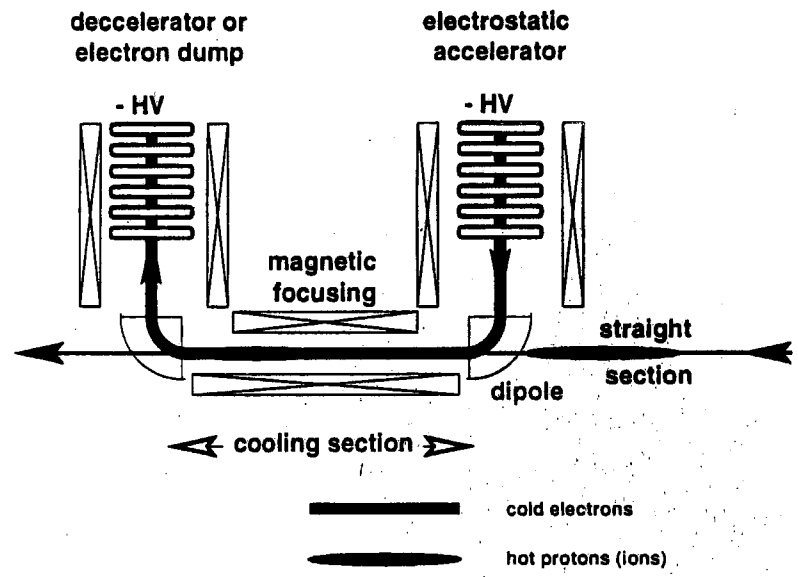

EXAMPLE: parameters of the ESR - cooler at GSI

E	= 50 - 370 MeV/u	E_e	= 27 - 200 keV
L_{ring}	= 108.36 m	L_{cool}	= 2.5 m
		I_e	= 50 - 500 mA
		B	= 0.07 - 0.15 T
$^{197}_{79}$Au		τ_{cool}	~ 10 ms

Beam Parameters for Cooling in PETRA

		protons		$Q_e = 3$ nC, $I_e = 0.8$ A electrons	
		PETRA 20 GeV	PETRA 15 GeV	Injector 10 MeV	Injector 7.5 MeV
ϵ_N	[m]	$4 * 10^{-6}$	$4 * 10^{-6}$	$4 * 10^{-6}$	$4 * 10^{-6}$
$\frac{\Delta E}{E}$				$5 * 10^{-4}$	$5 * 10^{-4}$
$\frac{\Delta p}{p}$		$4 * 10^{-4}$	$4 * 10^{-4}$		
T_{trans}	[eV]	367	277	0.582	0.582
T_{long}	[eV]	150	150	0.128	0.128
θ_{trans}		$5.0 * 10^{-5}$	$5.8 * 10^{-5}$	$5.3 * 10^{-5}$	$7.1 * 10^{-5}$
$v_{PRF,trans}$	[m/s]	$1.9 * 10^5$	$1.6 * 10^5$	$3.2 * 10^5$	$3.2 * 10^5$
$v_{PRF,long}$	[m/s]	$1.2 * 10^5$	$1.2 * 10^5$	$1.5 * 10^5$	$1.5 * 10^5$

Cooling Time Estimation in PETRA

$$\tau_{long} = \frac{\beta^4 \gamma^6 J_A \theta_{trans}{}^2 \theta_{long}}{6\pi\, c r_p\, L_C\, \eta\, J_e} \frac{A}{Z^2}$$

$$\tau_{trans} = \frac{\beta^4 \gamma^5 J_A \theta_{trans}{}^3}{6\pi\, c r_p\, L_C\, \eta\, J_e} \frac{A}{Z^2}$$

with:

$$J_A = \frac{mc^3}{e}$$

$$J_e = \frac{ecN_e}{(2\pi)^{3/2}\sigma_x\sigma_y\sigma_z}$$

$$\theta_{trans} = \sqrt{\frac{2\epsilon_N}{\beta_{cool}\gamma}}$$

$$\theta_{long} = \sqrt{2}\frac{\sigma_E}{\gamma^2}$$

Example: protons and heavy ions in PETRA

PETRA	protons	gold, A=197, Z=76
L_C	10	
β_{cool}	200 m	
σ_E	5 10^{-4}	
σ_z	0.5 m	
η	$\frac{50}{2304}$	
γ	18	
I_e	0.72 A / 1.20 A $\Longleftrightarrow$ Q_e = 3 nC / 5 nC	
τ_{trans}	20 min. / 12 min.	41 s / 25 s
τ_{long}	15 min. / 9 min.	30 s / 18 s

Electron Cooling in PETRA

K. Balewski, R. Brinkmann, K. Flöttmann, N. Holtkamp,
M. Schmitz, G.-A. Voss, P. Wesolowski,
DESY

D. Yeremian,
SLAC

Novosibirsk, Darmstadt, Jülich

Why Electron Cooling?

Principle of Electron Cooling

Cooling with a Bunched Electron Beam

Cooling Time Estimation in PETRA

Electron Recirculator for PETRA

First Developments of Electron - Injector
Tracking Using PARMELA

Summary and Outlook

Why Electron Cooling?

Specific luminosity

$$\mathrm{L_{spec}} = \frac{1}{2\,\pi\,e^2 f_0}\,\frac{1}{\sqrt{\epsilon_{\mathrm{px}}\beta_{\mathrm{px}} + \sigma_{\mathrm{ex}}{}^2}\sqrt{\epsilon_{\mathrm{py}}\beta_{\mathrm{py}} + \sigma_{\mathrm{ey}}{}^2}}$$

$$\epsilon_{\mathrm{px}} \rightarrow \frac{1}{2}\,\epsilon_{\mathrm{px}}\,, \qquad \epsilon_{\mathrm{py}} \rightarrow \frac{1}{2}\,\epsilon_{\mathrm{py}}$$

$$\Downarrow$$

$$\mathrm{L_{spec}} \rightarrow \frac{4}{3}\,\mathrm{L_{spec}}$$

Electron Cooling at Medium Energies

Beam temperature definition:

$$T_{\mathrm{PRF}} = m_{\mathrm{particle}}\ v_{\mathrm{PRF}}^2$$

$$\frac{m_{\mathrm{electron}}}{m_{\mathrm{proton}}} = \frac{1}{1836}$$

Thermodynamical limit of electron cooling:

$$T_{\mathrm{particle}} = T_{\mathrm{electron}}$$

hence:

$$\frac{v_{\mathrm{proton}}}{v_{\mathrm{electron}}} = \frac{1}{43}$$

and:

$$\frac{\epsilon_{\mathrm{protons}}}{\epsilon_{\mathrm{electrons}}} = \frac{1}{1836}$$

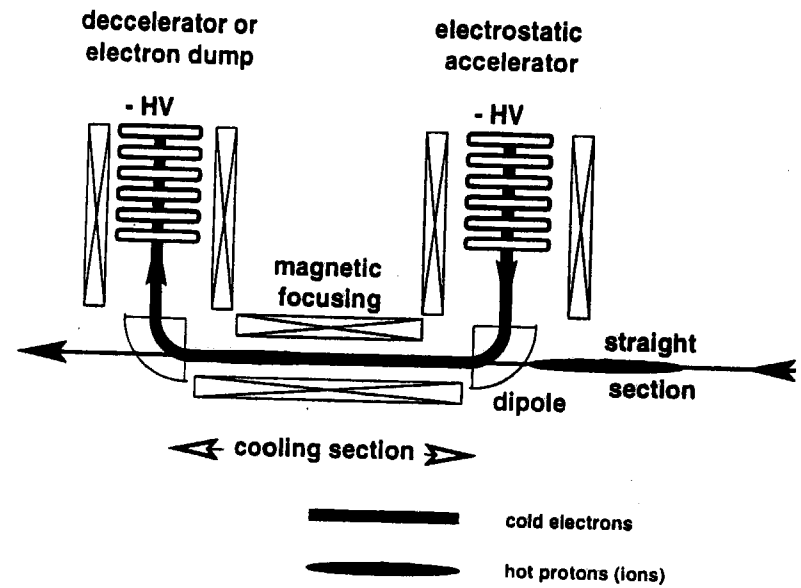

EXAMPLE: parameters of the ESR - cooler at GSI

E	= 50 - 370 MeV/u	E_e	= 27 - 200 keV
L_{ring}	= 108.36 m	L_{cool}	= 2.5 m
		I_e	= 50 - 500 mA
		B	= 0.07 - 0.15 T
$^{197}_{79}$Au		τ_{cool}	~ 10 ms

Electron Cooling at High Energies

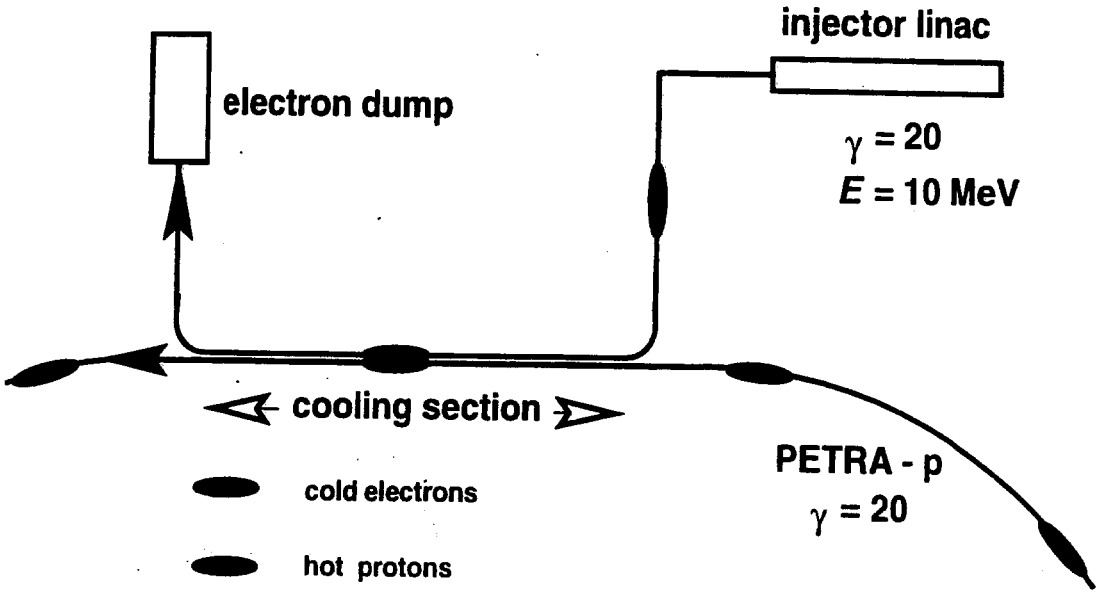

Beam Power Estimation

for a continuous dc electron beam:

$$P_{\text{beam}} = U\,I = 10\,\text{MV} * 0.72\,\text{A} = 7.2\,\text{MW}$$

for a bunched electron beam (cw - mode):

$$P_{\text{beam}} = U\,Q_e/\tau_{\text{bunch-bunch}} = 10\,\text{MV} * 3\text{nC}/96\,\text{ns} = 0.31\,\text{MW}$$

for a pulsed injector:
(10 Hz, 30 μs Puls, duty cycle = 3 10^{-4}):

$$P_{\text{beam}} = 100\,\text{W}$$

Electron Cooling in PETRA

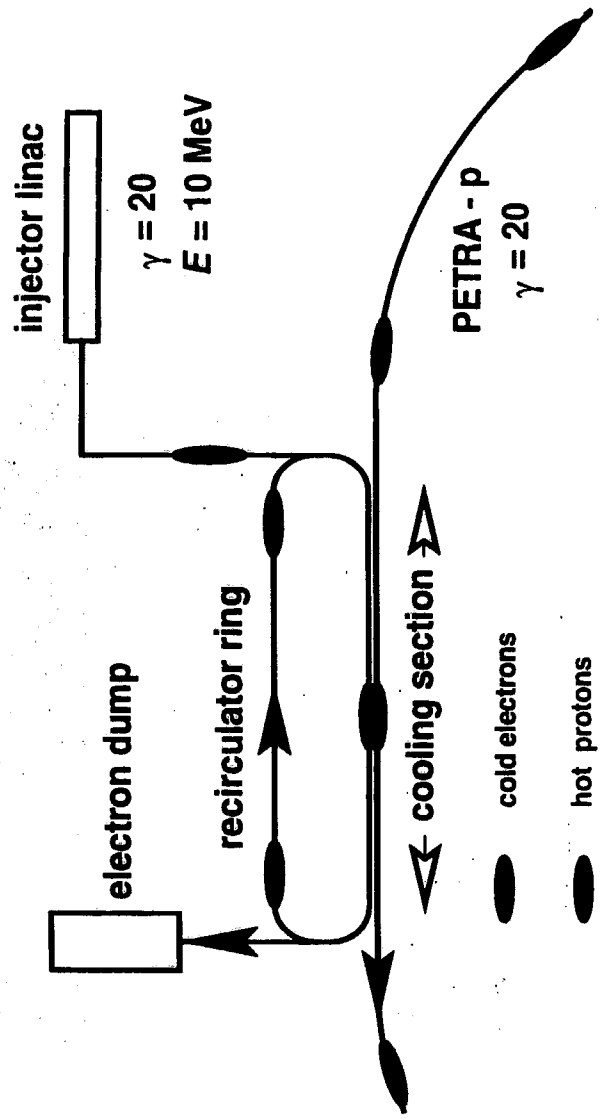

Bruyères-le-Châtel

ELSA Parameter

1 Cell @ 144MHz
10cm Gap, E=2.5MeV
average gradient: 25MV/m
pulse length ~30ps FWHM
Q = 5nC
trans. emittance <5π mrad mm
rep. rate 10Hz
ΔE ~ 50KeV
Long. emittance ~ 150 KeV mm

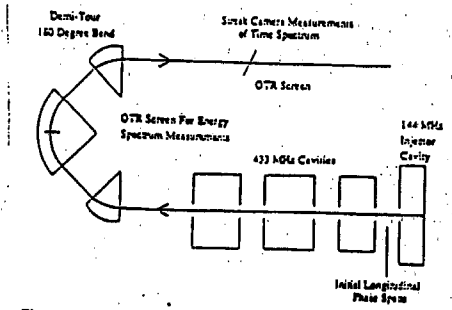

Fig. 1 Experimental layout of the ELSA accelerator for the longitudinal emittance measurements.

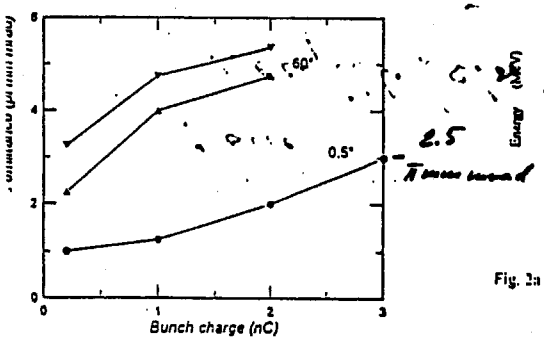

g. 1. Transverse rms emittance as a function of the bunch arge with the old drive laser injection at 60° (triangles) and der normal incidence (circles). The bunch fwhm width varies m 20 ps at low charge to 27 ps at 3 nC.

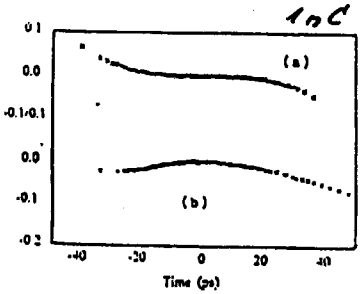

Fig. 2a Longitudinal phase spaces of the electron beam at the injector cavity exit (a) and after acceleration and transport around the non-isochronous demi-tour (b). The phase of the 433 MHz RF cavities is adjusted or minimum energy spread. $\Theta_{433} = 90°$.

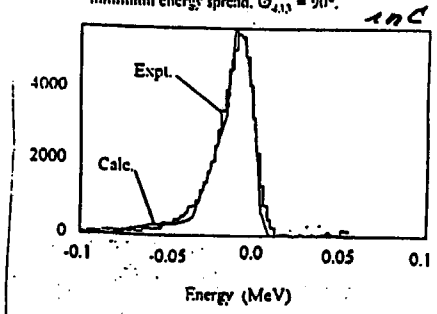

Fig. 2b Comparison of the experimental and fitted electron beam spectra. The fitted spectrum is calculated by performing the projection of the final phase space shown in Fig. 2a onto the energy axis.

Parameters of the ELSA - FEL RF-gun

1 NC - cell 144 MHz
3 SC - cells 433 MHz

Average gradient = 25 MV / m

Repetition frequency = 10 Hz

Q_e = 5 nC $\Longleftrightarrow$ I_e = 1.2 A (if matched to PETRA bunches)

$\epsilon_N < 5\,\pi$ mm mrad

$\epsilon_z \simeq 190$ keV mm

$\Delta E \simeq 50$ keV

Design Requirements for the Injector

Q_e = 3–5 nC
$\epsilon_N < 5\,\pi$ mm mrad

$\epsilon_z \simeq 2.5\ 10^{-4}$ m @ 10 MeV
$\epsilon_z \simeq 2.5\ 10^{3}$ keV mm

$\frac{\Delta E}{E}\,\sigma_z < 10^{-4}$ m

<u>for:</u>

$\sigma_z \simeq 17$ mm

$\Downarrow$

$\Delta E \simeq 63$ keV

Scheme of the Electron Injector and First Simulation - Results

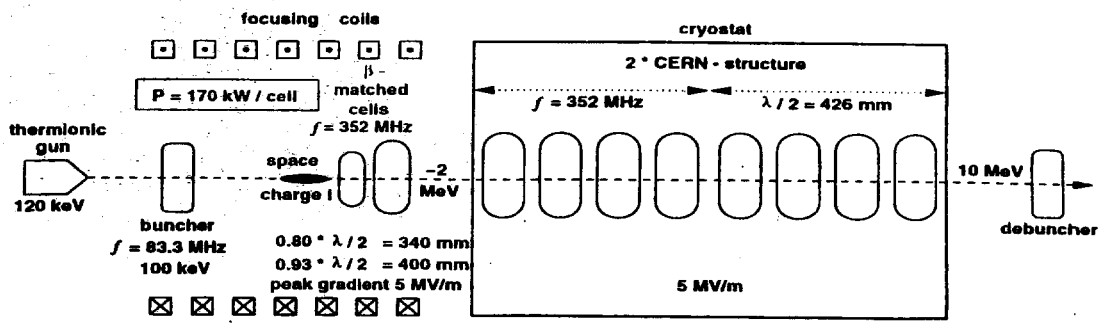

	developed	actually developing	
PARMELA - simulation for Q = 3 nC:			
ε_N π mm mrad	2.6	[redacted]	10.0
σ_z mm	260 (FW)	[redacted]	14.7
ΔE keV	0.55	4.3	62.0
$\sigma_{x,y}$ mm		[redacted]	

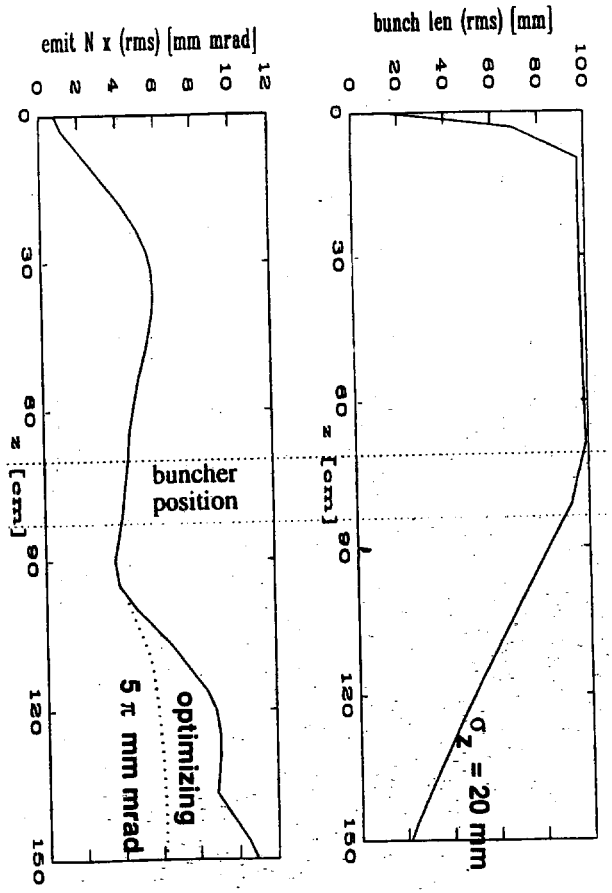

Fig. Electron Gun (D.a.)

Что делать ?

What To Do?

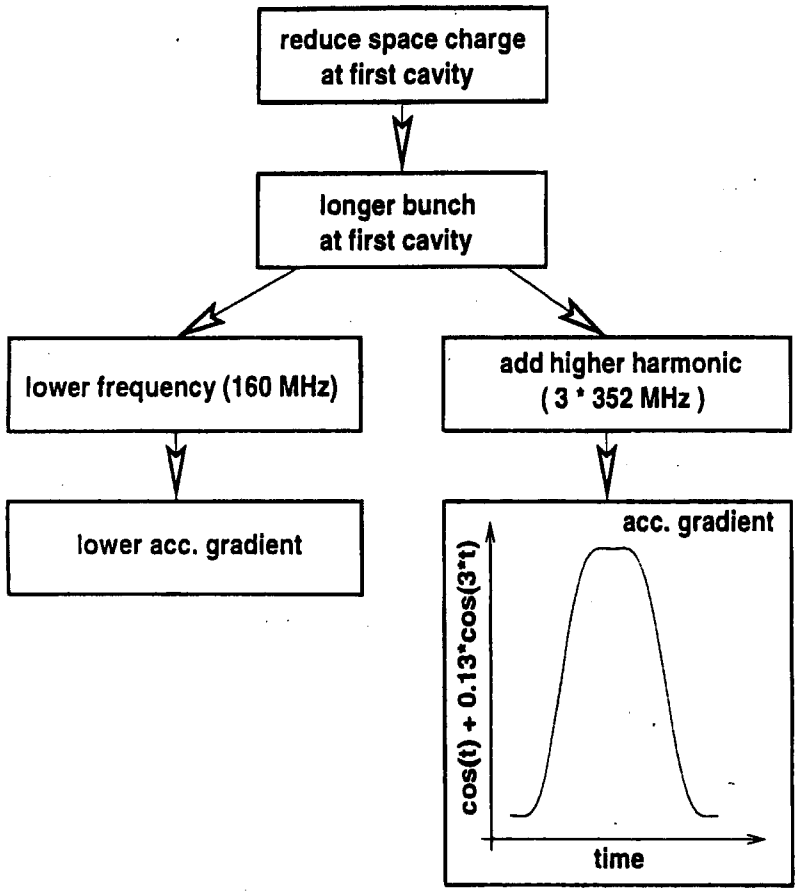

Summary and Outlook

Cooling times in PETRA:
for protons: 12 / 9 minutes for 5 nC
for heavy ions: much less than 1 minute

Reduction of electron beam power using of a bunched beam and further drastic reduction by a recirculator

First simulations of electron injector gave $\epsilon_N = 10\ \pi$ mm mrad

Electron cooling is interesting for luminosity enhancement in HERA, even if complex at high energies. Specially attractive for heavy ions.

Q's:

Shiltsev: In re-circulation scheme the e-beam lives for some thousands of turns while having low γ while interacting with protons(ions). It may cause two-beam coherent instability. Are there any estimates of the effect?

Wesolowsky: This effect has not been carefully considered yet.

Nagaitsev: Dut to high peak current, the electron beam space charge tune shift will be probably of the order of 1. Don't you think it's dangerous?

Wesolowsky: The ring design value of the self space charge tune shift is about 0.3, and currently we think it must not deteriorate its operation.

Beam-Beam Compensation Workshop
Fermilab, Feb. 12-13, 1998

Vladimir SHILTSEV

Particle Loss Diagnostics for PACMAN-Effect in Tevatron'33

Content:

1. The need of bunch-by-bunch BLM
2. PIN-diode BLMs and the set-up
3. Tevatron (fixed target) losses at time scale of:
   - 10 min
   - 1 min
   - 1 sec
   - 10 ms
   - 21 us
   - 1 us
   - 100 ns
4. The system for TEV'33

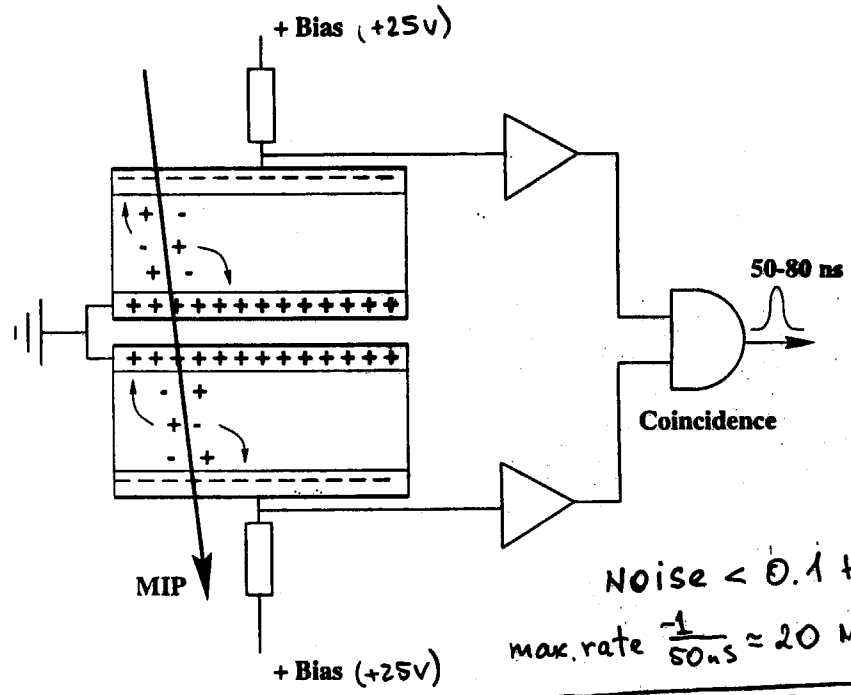

Noise < 0.1 Hz

max. rate $\frac{1}{50\,ns} \simeq 20$ MHz

Dyn. range: $> 2 \cdot 10^8$

This studies: max rate ~ 100 kHz

Efficiency: ~ 0.35 $\frac{\text{counts}}{\text{MIP}}$

Rad. resistance: 200 MRad (report

This studies ~ 1000 rad

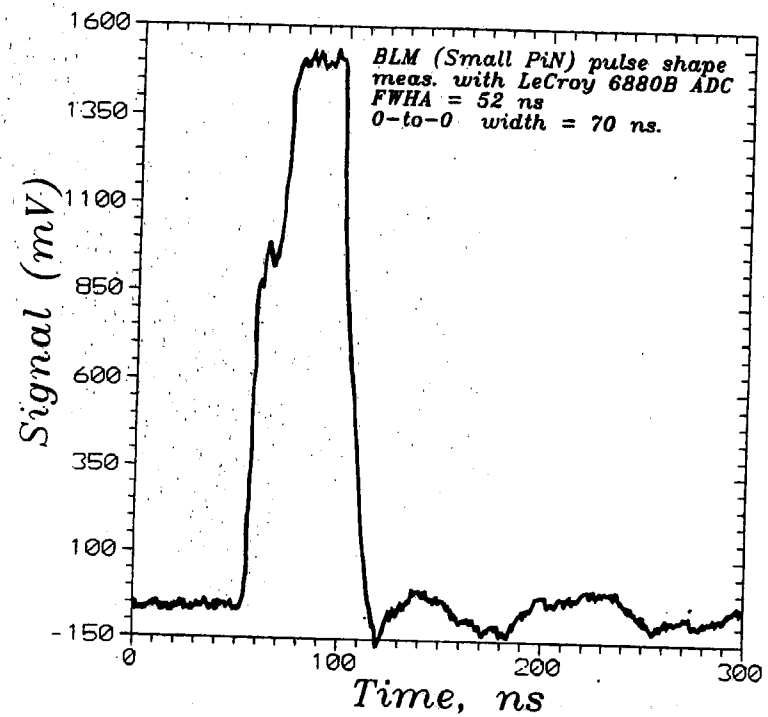
BLM (Small PiN) pulse shape
meas. with LeCroy 6880B ADC
FWHA = 52 ns
0-to-0 width = 70 ns.
Signal (mV)
Time, ns
1600
1350
1100
850
600
350
100
-150
0
100
200
300

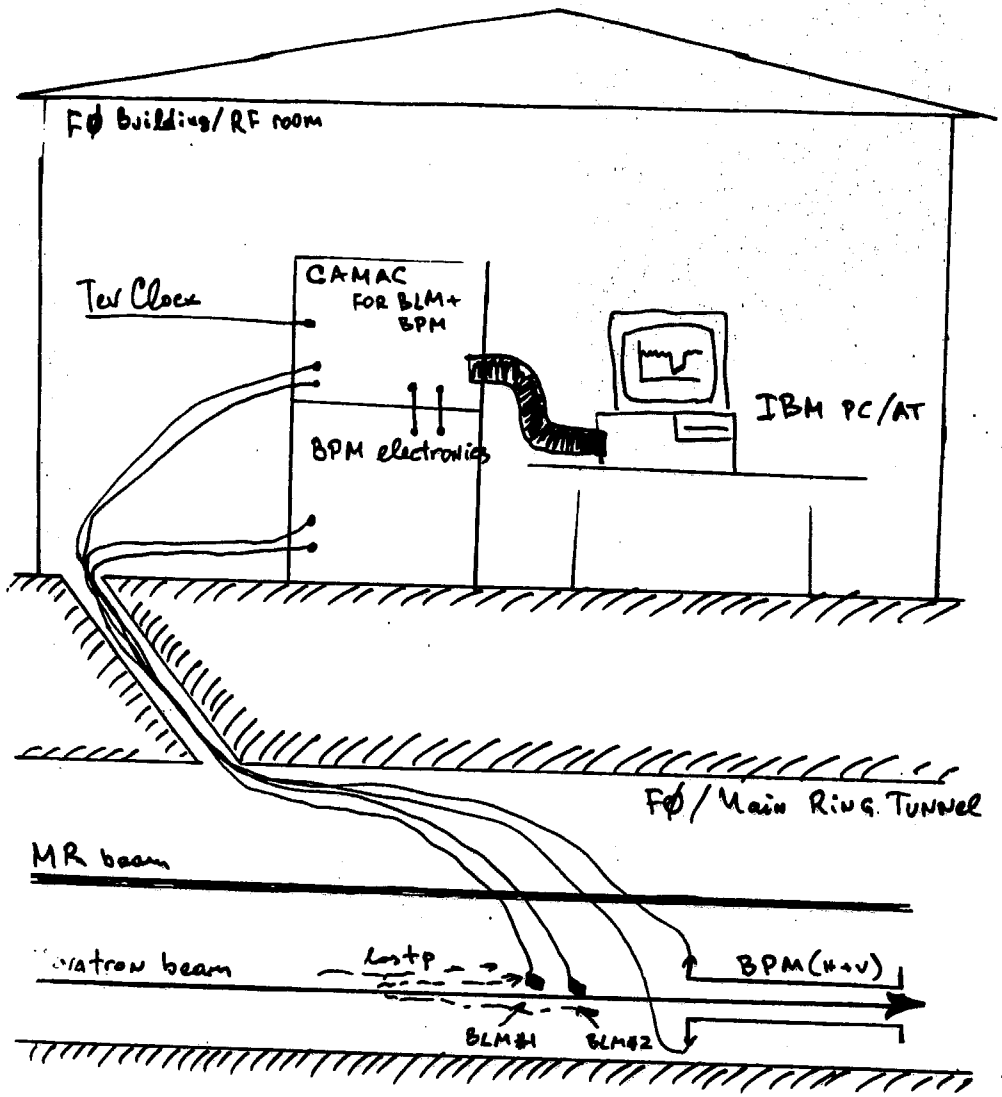
FØ building/RF room
Tev Clock
CAMAC
FOR BLM+
BPM
BPM electronics
IBM PC/AT
FØ/Main Ring Tunnel
MR beam
Tevatron beam
lost p
BPM(H+V)
BLM#1
BLM#2

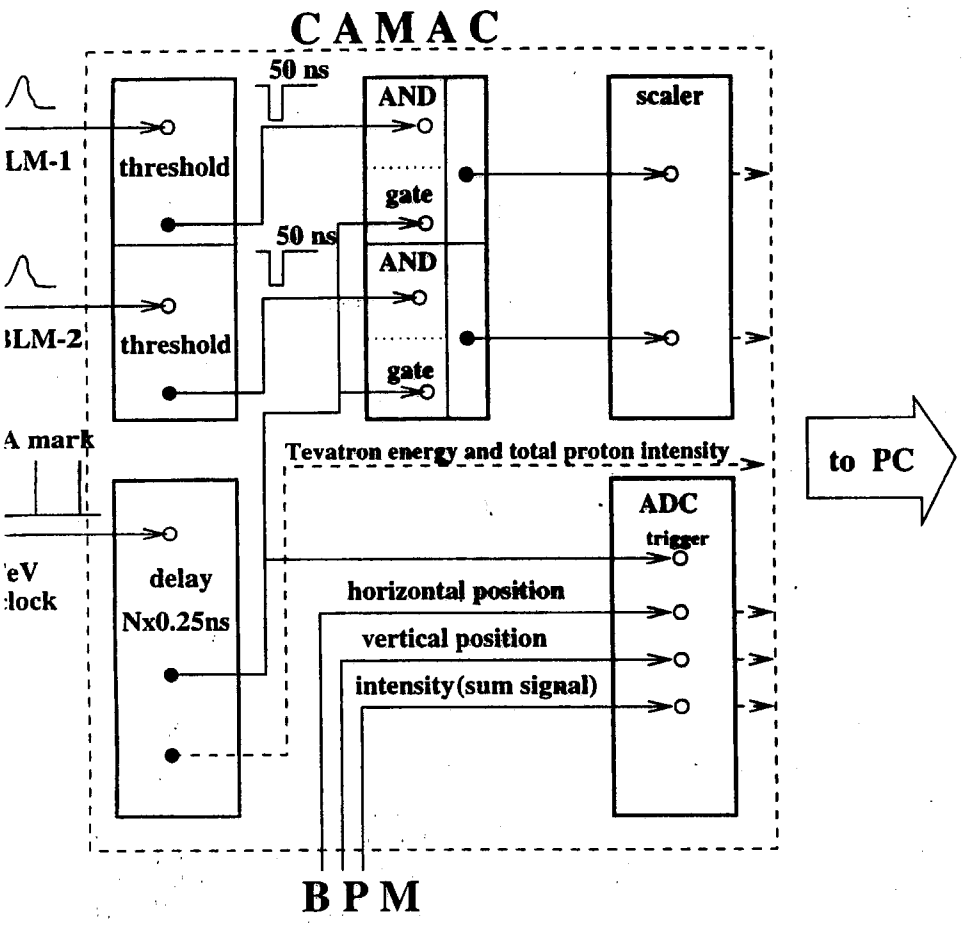
CAMAC
50 ns
AND
scaler
LM-1
threshold
gate
50 ns
AND
LM-2
threshold
gate
A mark
Tevatron energy and total proton intensity
to PC
ADC
trigger
eV
lock
delay
Nx0.25ns
horizontal position
vertical position
intensity(sum signal)
BPM

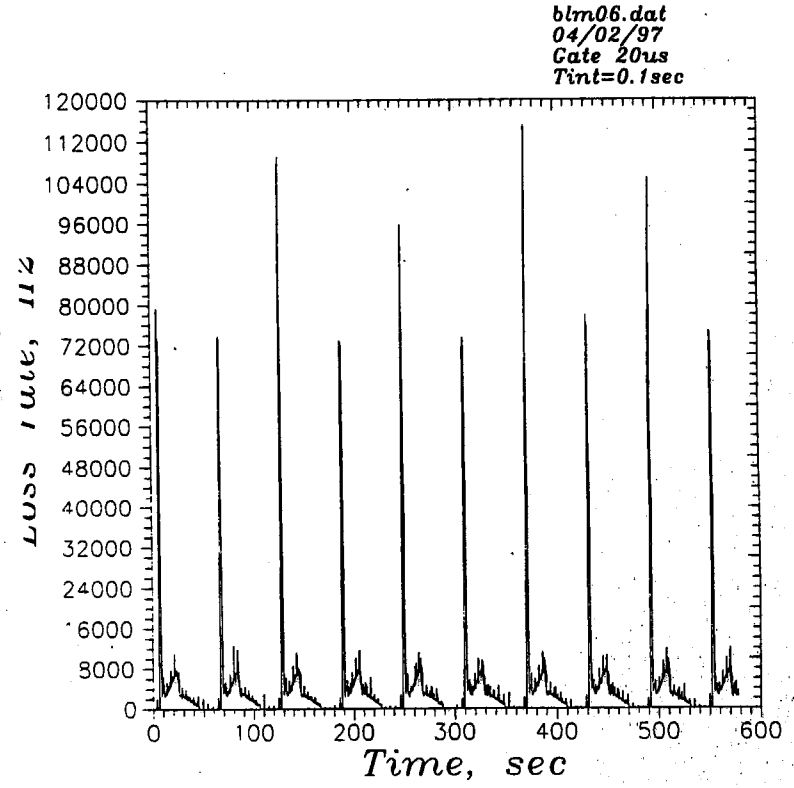
blm06.dat
04/02/97
Gate 20us
Tint=0.1sec
120000
112000
104000
96000
88000
80000
72000
64000
56000
48000
40000
32000
24000
16000
8000
0
0
100
200
300
400
500
600
Time, sec

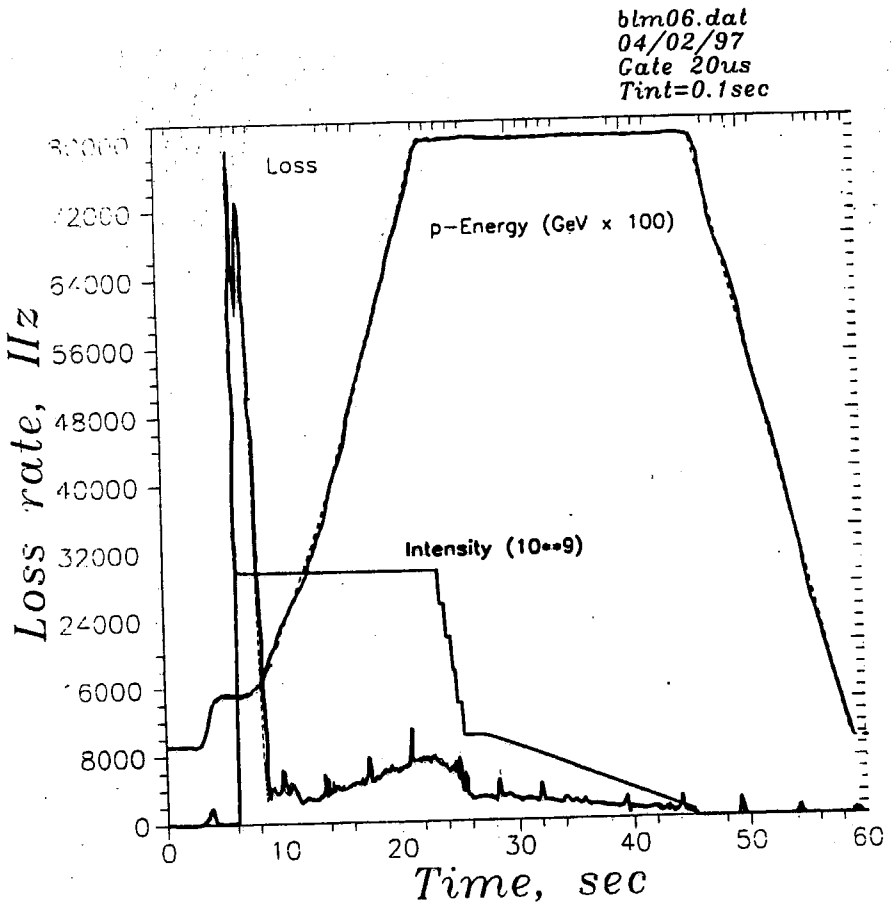
blm06.dat
04/02/97
Gate 20us
Tint=0.1sec
Loss
p-Energy (GeV x 100)
Intensity (10**9)
Loss rate, Hz
Time, sec

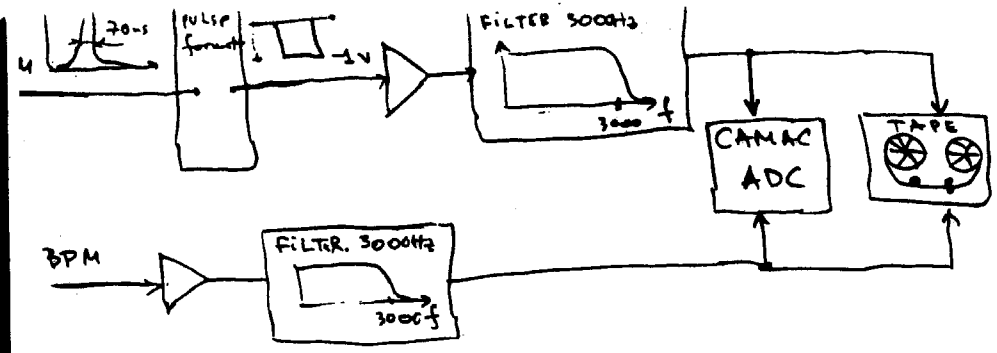
FILTER 300kHz
CAMAC
ADC
TAPE
BPM
FILTER. 300kHz

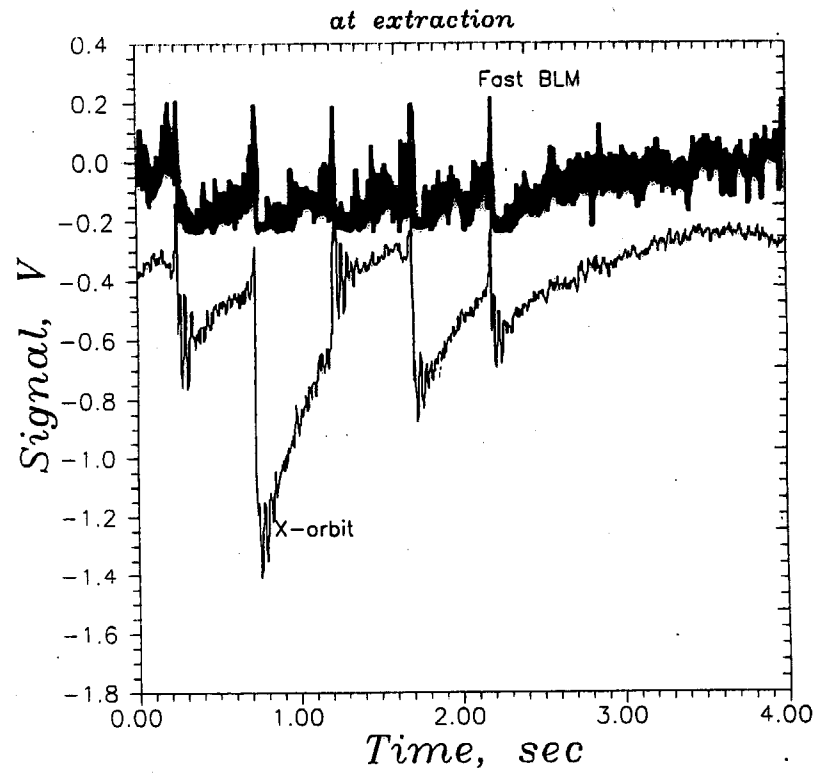
at extraction
Fast BLM
X-orbit
Signal, V
Time, sec

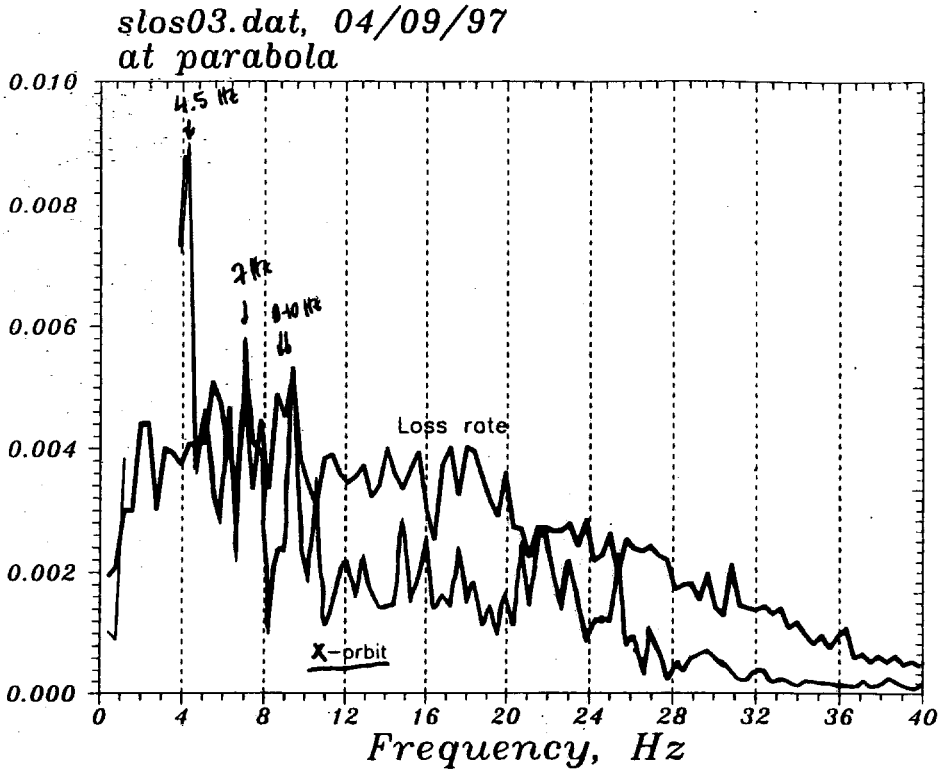
slos03.dat, 04/09/97
at parabola
4.5 Hz
7 Hz
8-10 Hz
Loss rate
X-prbit
0.010
0.008
0.006
0.004
0.002
0.000
0
4
8
12
16
20
24
28
32
36
40
Frequency, Hz

slos03

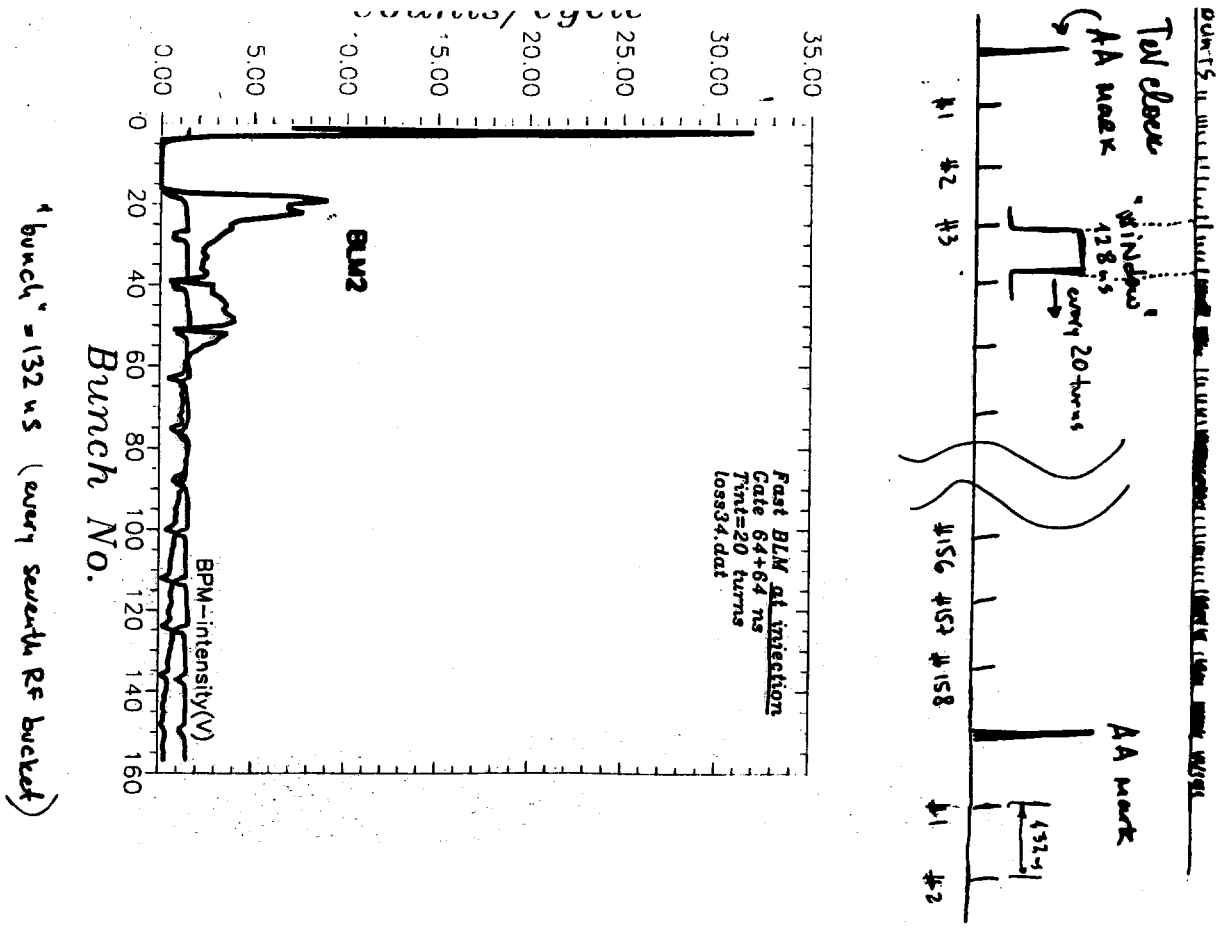
Tev clock
AA mark
"Window"
128 ns
every 20-turns
#1
#2
#3
#156
#157
#158
AA mark
132 ns
#1
#2
Fast BLM at injection
Gate 64+64 ns
Tint=20 turns
loss34.dat
BLM2
BPM-intensity(V)
35.00
30.00
25.00
20.00
15.00
10.00
5.00
0.00
0
20
40
60
80
100
120
140
160
Bunch No.
"bunch" = 132 ns (every seventh RF bucket)

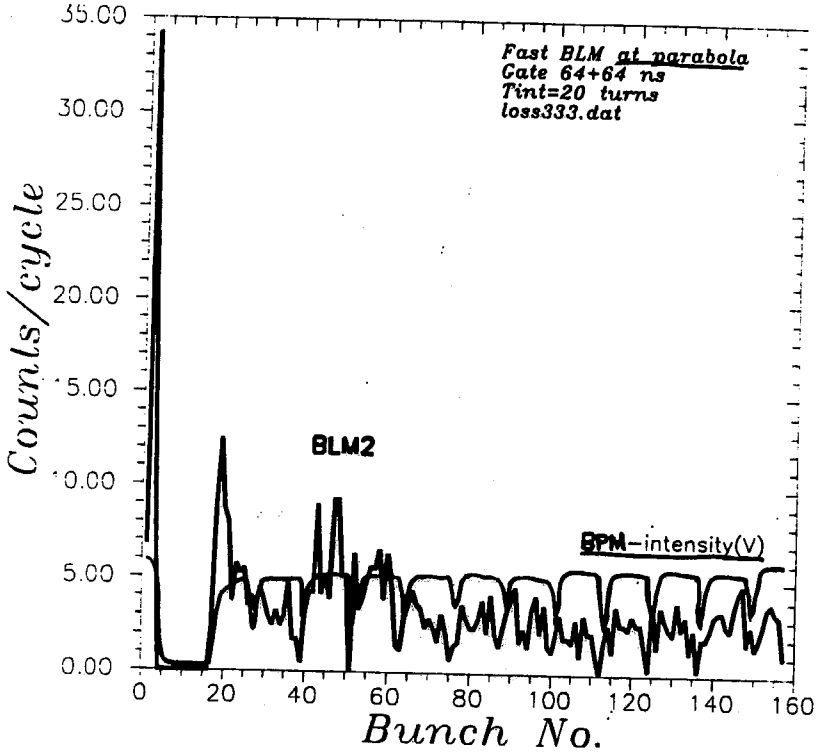
Fast BLM at parabola
Gate 64+64 ns
Tint=20 turns
loss333.dat
BLM2
BPM-intensity(V)
Counts/cycle
Bunch No.
35.00
30.00
25.00
20.00
15.00
10.00
5.00
0.00
0
20
40
60
80
100
120
140
160

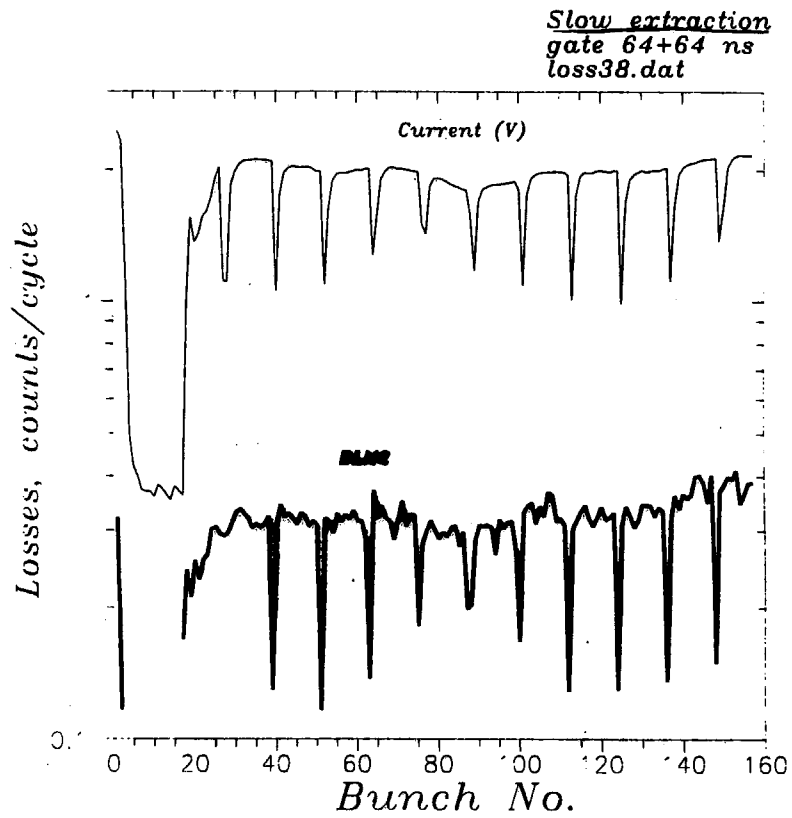
Slow extraction
gate 64+64 ns
loss38.dat
Current (V)
Losses, counts/cycle
Bunch No.
0
20
40
60
80
100
120
140
160

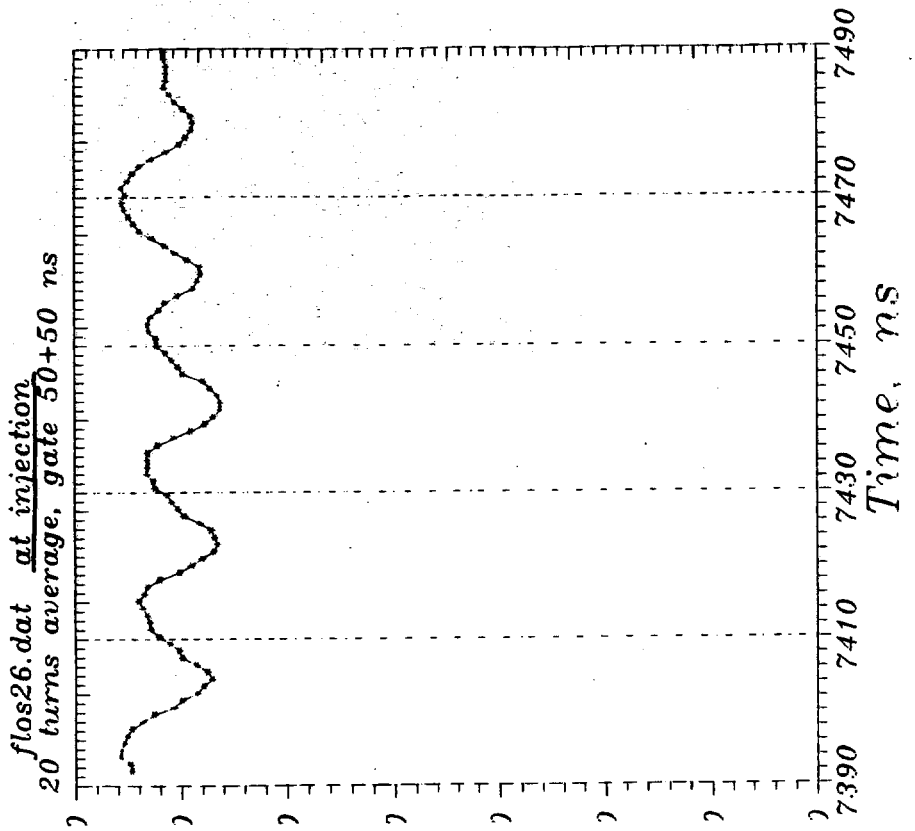
flos26.dat at injection
20 turns average, gate 50+50 ns
7390
7410
7430
7450
7470
7490
Time, ns

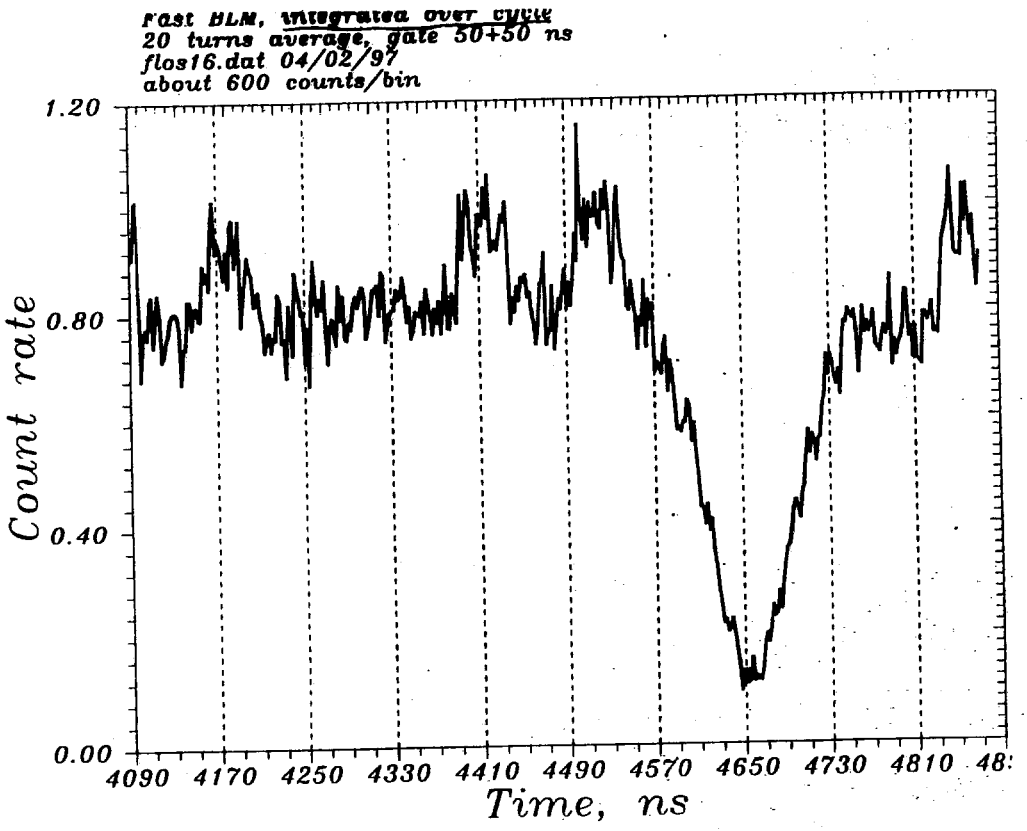
Fast BLM, integrated over cycle
20 turns average, gate 50+50 ns
flos16.dat 04/02/97
about 600 counts/bin
Count rate
0.00
0.40
0.80
1.20
4090
4170
4250
4330
4410
4490
4570
4650
4730
4810
Time, ns

FLOS16S.ps

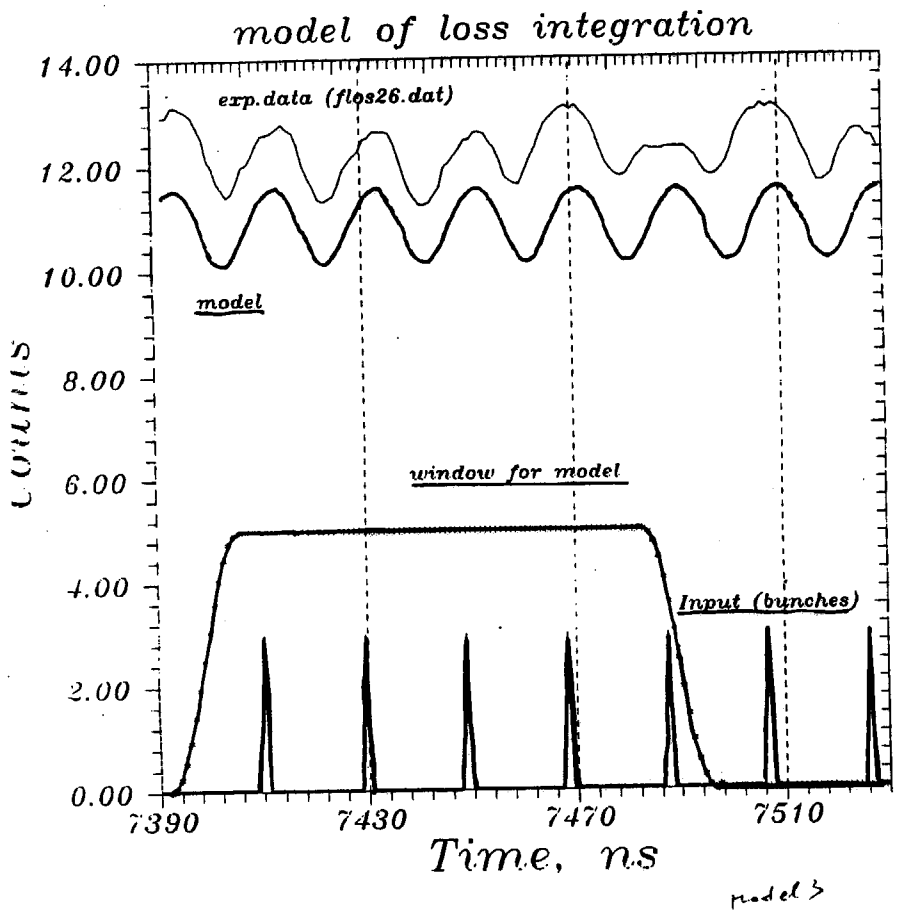

model 3

ND = 15
ND = 40

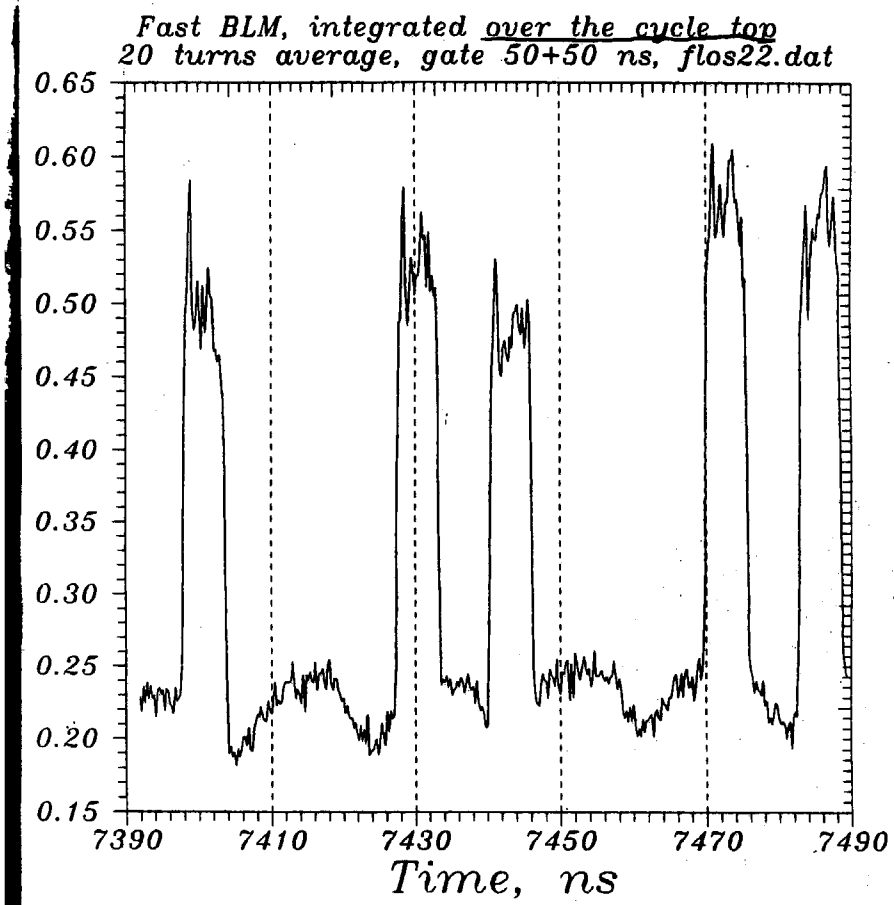

Fast BLM System for Run II - TEV33

(further work)

Goals: ① monitoring of bunch-by-bunch losses with 396 ns and 132 ns bunch spacing; both protons and antiprotons

② incorporate Fast-BLM data in control network, make it available for operators/physicists + store the loss history turn-to-turn (N turns) last

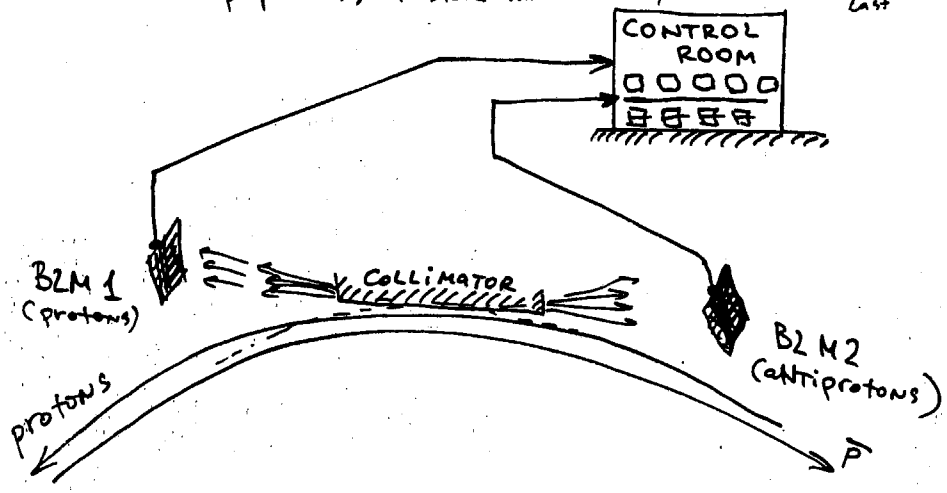

Places to install:

1) 1...4 collimators
2) injection/extraction
3) experiments (BØ, BØ, CØ)
4) arcs?
5) ?

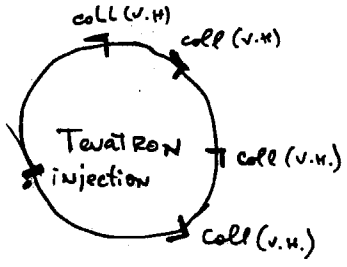

three possible arrangements:

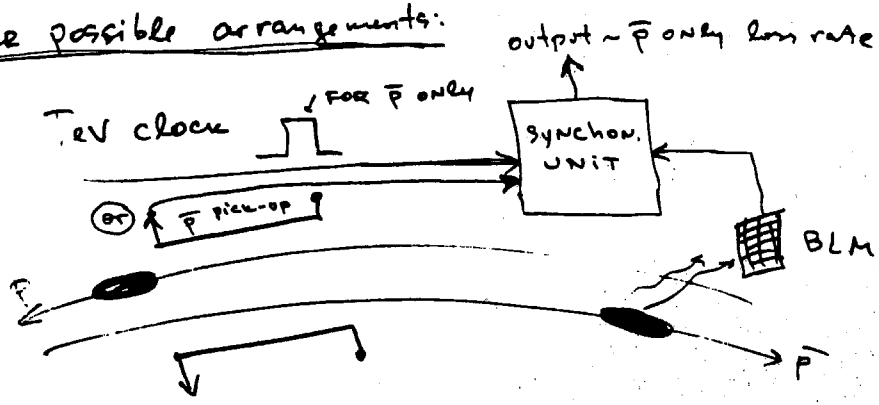

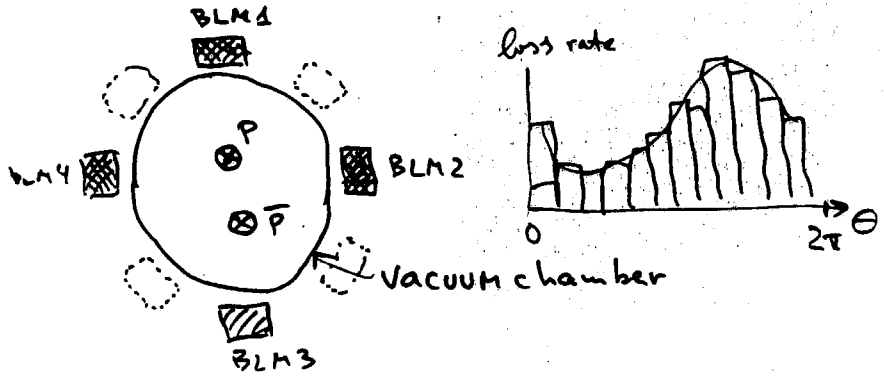

I. On-line diffusion meter (in halo)

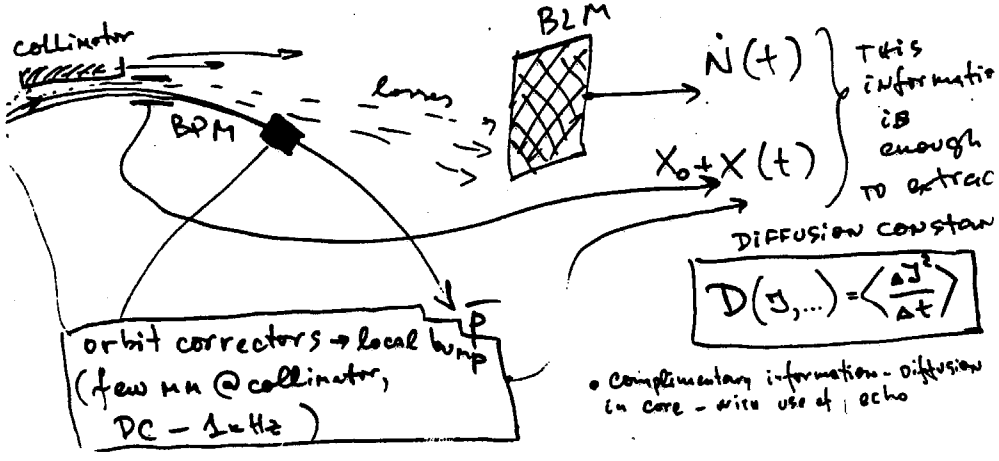

• complimentary information - diffusion in core - with use of echo

Andrei SERY

Fermilab/BINP-Protvino

Particle Losses in Tevatron Due to Electron Beam

Particle losses due to Electron Beam

Sasha Drozhdin, Andrey Sery

It is easy to see that the problem does not exist:

El. beam with $J_e = 2A$, $a = 1mm$, $\beta_e = 0.2$

$\longrightarrow$ $n_e \approx 6.6 \cdot 10^{10}$ cm^{-3}

If $L = 3m$ then the SAME amount of electrons (per m) will have residual gas with pressure

$$P \approx 0.5 \cdot 10^{-10} \text{ Torr}$$

distributed along the whole Tevatron ring.

I.e. contribution of electron compressor to the average vacuum is $\sim 0.5 \cdot 10^{-10}$ Torr (or even smaller since no strong interactions from e-beam)

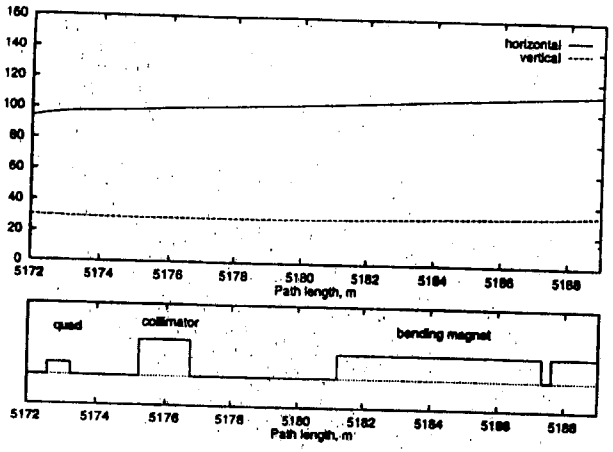

Figure 12: β functions in the F48 collimators.

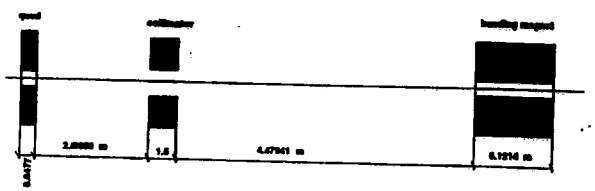

Figure 13: Collimators location in the F48 region.

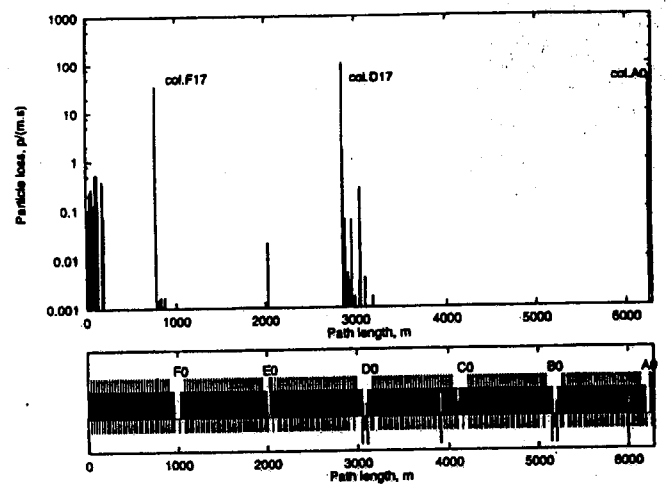

Figure 1: Scattered antiprotons loss at interaction with electron beam. Tevatron magnet quench level at 1 TeV is equal to 3.e+08 p/(m.s).

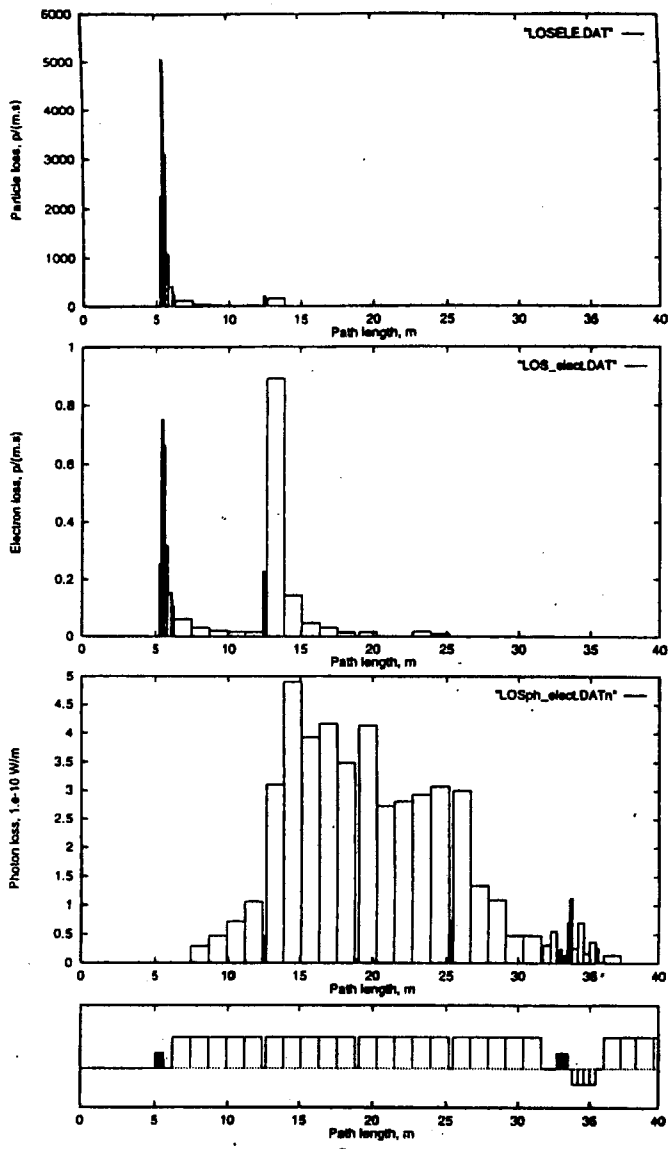

2

igure 2: Scattered electrons loss at interaction with antiproton beam: particle number er meter per second (top), energy loss normalized by 1 TeV particle (middle), and

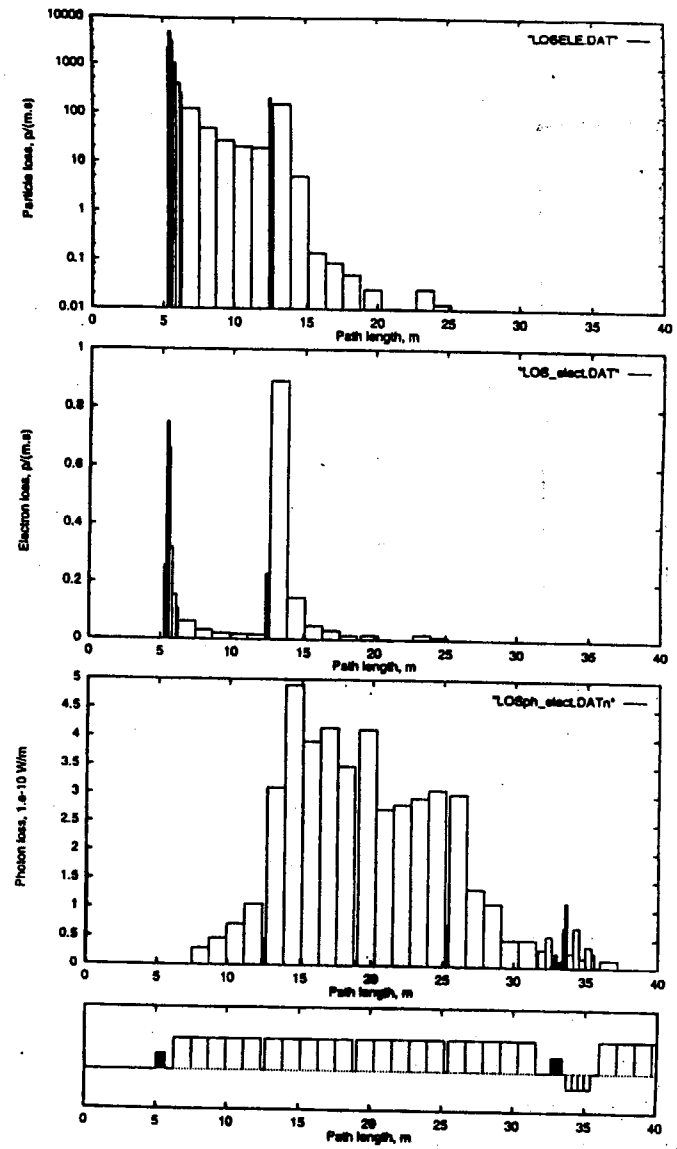

3

Figure 3: Scattered electrons loss at interaction with antiproton beam: particle number per meter per second (top), energy loss normalized by 1 TeV particle (middle), and

Comment:

Shiltsev:	Does somebody need 1TeV electrons from the E-compressor with few Hz rate? (not a question)

Report on Mini-Workshop on "Beam-Beam Compensation in the Tevatron"

to appear in *The Beam Dynamics Newsletter*

Vladimir Shiltsev shiltsev@fnal.gov FNAL, MS221, PO Box 500
Batavia, IL, 60510, USA

A Mini-Workshop on Beam-Beam Compensation in the Tevatron was held at Fermilab on February 12-13, 1998. It was the second in a series of the FNAL Mini-Workshops devoted to advanced accelerator techniques to improve the Tevatron collider performance; the previous one was "Round Beams and Related Concepts in Beam Dynamics" (FNAL, December 1996) [1]. The purpose of the Mini-Workshop was to assay the current understanding of compensation of the beam-beam effects in Tevatron with use of low-energy, high-current electron beam, relevant accelerator technology, along with other novel techniques of the compensation and previous attempts. About 30 scientists representing seven institutions from four countries (FNAL, SLAC, BNL, Novosibirsk, CERN, and Dubna) were in attendance with 21 talks presented. The event gave firm ground for wider collaboration on experimental test of the compensation at the Tevatron collider. If there are any questions concerning the Workshop or its Proceedings [2] which are published with limited circulation, contact V.Shiltsev (shiltsev@fnal.gov), or visit our Web page **http://www-bd.fnal.gov/lug/tev33/ebeam_comp/ebeam_comp.html**.

The cited proceedings for the Mini-Workshop are mostly copies of transparencies presented and compressed texts of already printed papers. The participants were very responsive and energetic in addressing the issues posed to them; nearly every concern was considered at some level and several points were resolved. Questions and answers were an essential part of the meeting and are placed in the Proceedings after each talk in a brief form.

There were no special working groups, and all talks were plenary, nevertheless, the informal format of the presentations and flexible schedule did allow enough time for discussions.

The meeting started with a welcoming address by John Marriner of the FNAL Beams Division, followed by talks which were divided in several groups according to the beam-beam compensation topics chosen by the organizer.

1 Proposals and Physics of Beam-Beam Compensation

The first day of the Workshop was devoted to the theory of the beam-beam compensation, and previous proposals and attempts. There were nine talks on:

V.Shiltsev	FNAL	Beam-Beam Compensation with Electron Beam in Tevatron
V.Danilov	INP/FNAL	Beam-Beam Tracking for Tevatron with "Electron Compressor"
R.Siemann	SLAC	Beam-Beam Interaction with Four Colliding Beams
A.Zinchenko	Dubna	Compensation Proposals for SSC and LHC
H.Riege	CERN	What Could We Gain with Beam Neutralization in LHC?
G.Stupakov	SLAC	Plasma Suppression of Beam-Beam Interaction
M.Syphers	BNL	Issues of e-p Polarimetry in RHIC
F.Zimmerman	SLAC	Beam-Beam Effects in Linear Colliders
D.Whittum	SLAC	Beam-Beam Compensation in Linear Colliders

V.Shiltsev presented an idea of compensation of beam-beam effects in the Tevatron collider with use of 1-2 Amperes 10-keV electron beam [3, 4]. Modifications of the proposal are 1) the "electron lens" with modulated current which is supposed to provide different linear defocusing forces for different antiproton bunches (spaced by 132 ns in the Tevatron'33 upgrade project) and, therefore, equalize their betatron frequencies which are not naturally equal due to proton-antiproton interaction in numerous parasitic crossings along the ring; and 2) the "electron compressor", essentially nonlinear but DC electron lens to compensate (in average) the effect of proton beam on $\bar{p}$ beam and, thus, to reduce the beam-beam footprint. The electron beam setup looks much like an electron cooler, besides electrons collide with antiprotons (proton beam is separated from the latter two). About 2-m long and 2-mm diameter electron beam to be installed in a place with large beta-function($\sim$100m), away from the main interaction points (IPs - B0 and D0). A strong longitudinal magnetic field of the order of 3 T plays a significant role in maintaining stability of both electron and antiproton beams. The R&D plans of the beam-beam compensation experiment in the Tevatron were also discussed.

Results of 3D beam-beam tracking with nonlinear "electron compressor" were reported by V.Danilov. One important conclusion was that the electron beam distribution has to be tuned to the form other than Gaussian in order to mimic bunch-length effects on beam-beam interaction previously studied by Krishnagopal and Siemann, Pestrikov, and Hirata.

An excellent historical overview of the four beam compensation $e^-e^-e^+e^+$ theory and the DCI(Orsay) experiment [5] was given by R.Siemann along with presentation of his computer simulations with Podobedov [6], which explain

coherent instabilities taking place in the system due to multi-turn memory in all the beams. Another extreme case (no memory at all) is the interaction at the IP of future e^-e^+ Linear Colliders(LCs). There the beams disruption over time of interaction will play a major role and corresponding beam-beam limits are orders of magnitudes higher than in circular colliders. F.Zimmerman and D.Whittum discussed these effects and possible gain of four-beam compensation in LCs [10].

A.Zinchenko and H.Riege reported similar beam-beam compensation proposals for the SSC and the LHC [7, 8]. G.Stupakov outlined a plasma neutralization idea of his and P.Chen [9], which looks very promising for muon colliders, while plasma causes strong deterioration of the beam lifetime in proton machines. M.Syphers overviewed a new polarimeter technique for RHIC using polarized electron beam, where coherent stability may be of similar importance to what is expected for the FNAL "electron lenses".

2 Coherent and Incoherent Effects due to Electron Beam

There were seven talks devoted to stability issues:

V.Danilov	INP/FNAL	TMCI of Tevatron p-bar Beam Interacting with Electron Current
A.Burov	INP/FNAL	Impedance of Compensating Electron Beam
V.Shiltsev	FNAL	Simulations of Head-Tail Instability in Tevatron with "Electron Compressor"
V.Shiltsev	FNAL	Requirements on Electron Beam for Beam-Beam Compensation in Tevatron
A.Zinchenko and V.Shiltsev	Dubna FNAL	Electron Beam Distortions due to Interaction with (Anti)Protons
A.Sery	INP/FNAL	Stability of Electron Beam with Ions

As mentioned above, the electron beam that interacts in the Fermilab beam-beam compensation project will go to a beam dump (collector) just after interaction with antiprotons; therefore, no long-term memory will occur in the two beam system, and the stability issues are somewhere in between the past (and somewhat discouraging) experience of the DCI and expectations for future Linear Colliders. Nevertheless, some effects may appear even in the single-pass system.

V.Danilov, A.Burov and V.Shiltsev pursued semi-analytical, theoretical [11] and numerical approaches to a "head-tail" instability caused by wide band impedance due to electron beam. The results were in good agreement to each other, and concluded in the requirement of some 3-5 T solenoid magnetic field. the $\bar{p}$ emittance growth consideration of V.Shiltsev concluded in technically challenging requirements on the electron current stability and the magnetic

field uniformity. A.Zinchenko and V.Shiltsev reported results of their studies of the electron charge distribution distortions due to oncoming elliptic antiproton beam, which were found inversely proportional to the solenoid field and quite acceptable with 3 T field. Residual ions can be easily cleared from the electron beam to the stability safe level, as estimated by A.Sery [12].

3 Electron Beam Sources, Beams Diagnostics

The last group of presentations was as follow:

S.Nagaitsev	FNAL	Experience with Electron Guns for Medium Energy Electron Cooling and Possible e-Source for "Electron Compressor"
I.Meshkov	Dubna	Generation of Intense Stationary Electron Beam with Controlled Parameters
P.Wesolowsky	DESY	Electron Cooling in PETRA
V.Shiltsev	FNAL	Particle Loss Diagnostics for PACMAN-Effect in TEV'33
A.Sery	INP/FNAL	Particle Losses due to Electron Beam

S.Nagaitsev, I.Meshkov and P.Wesolowsky presented an overview on powerful electron sources developed for the "electron cooling". The beam-beam compensation does not require a very cold electron beam, it makes the task of an electron gun design easier. Nevertheless, the requirement of the electron current distribution tuning and/or fast current modulation will require novel approaches in the design. Vast experience and good understanding of the space-charge dominated thermionic electron sources was demonstrated (see also overviews in [13], and several technical solutions were proposed for the required electron gun.

V.Shiltsev discussed pbar beam diagnostics necessary for the beam-beam compensation test, including fast PIN-diode beam loss monitors to distinguish losses from different bunches in the Tevatron [14]. Finally, A.Sery had shown that back-scattered electrons with energies up to TeV produced in the "electron compressor" will not cause any radiation problem due to very small collision cross section.

Numerous discussions at the Workshop covered many other issues of the beam-beam compensation. In addition to reviewing the plausibility of the beam-beam compensation in the Tevatron, it was the goal of the Workshop to advance understanding of the general character of the challenges to be met and to make incremental progress on design issues. In this, the Workshop was very successful.

References

[1] V.Shiltsev, "Mini-Workshop on Round Beams and Related Concepts in Beam Dynamics", *Beam Dynamics Newsletter, No.13* (April 1997), p.44.

[2] V.Shiltsev, ed., "Contributions to the Mini-Workshop on Beam-Beam Compensation", FERMILAB-Conf-98/064 (March 1998).

[3] V.Shiltsev, D.Finley, "Electron Compression" of Beam-Beam Tune Spread in the Tevatron", FERMILAB-TM-2008 (1997).

[4] V.Shiltsev, "Electron Lens" to Compensate Bunch-To-Bunch Tune Spread in TEV33", FERMILAB-TM-2031 (1997).

[5] J. Le Duff, *et. al,* "Space Charge Compensation with DCI", *Proc. 11th Int. Conf. on High Energy Accel.*, CERN (1980), p.707.

[6] B.Podobedov, R.Siemann, "Coherent Beam-Beam Interaction with Four Colliding Beams", *Phys.Rev.E, vol.52, No.3*, (1995).

[7] E.Tsyganov, A.Taratin, A.Zinchenko, "Innovations in Accelerator Technology", *Fizika Elementarnih Chastic i Atomnogo Yadra, vol.27, No.3*, (1996) p.675; see also SSCL-Preprint-519 (1993).

[8] H.Riege, "Beam Space Charge Neutralization in the Interaction Regions of LHC with Low-Energy DC Electron Beam", to appear as LHC Project Note (1998).

[9] G.Stupakov, P.Chen, "Plasma Suppression of Beam-Beam Interaction in Circular Colliders", *Phys.Rev.Lett., vol.76*, (1996), p.3715.

[10] D.Whittum, R.Siemann, "Neutral Beam Collisions at 5TeV", *Proc. 1997 IEEE PAC*, Vancouver (1997).

[11] A.Burov, "Electron Cooler Impedances", *Particle Accelerators, vol.57,* (1997), p.131.

[12] A.Burov, V.Kudelainen, V.Lebedev, V.Parkhomchuk, A.Sery, V.Shiltsev, "Experimental Studies of Compensated Electron Beam", Novosibirsk INP 89-116 (1989); translated in CERN PS 93-09 (1993).

[13] I.Meshkov, "Physics and Technique of Electron Cooling", RIKEN-AF-AC-2 (1997);
I.Meshkov, ed., *Proc. Workshop on Beam Cooling, NIM A 391, No.1* (1997).

[14] V.Shiltsev, "Fast PIN-Diode Beam Loss Monitors at Tevatron", FERMILAB-TM-2012 (1997).